

# COMPLIANT WATER WAVE ABSORBERS

by

JEROME H. MILGRAM

S.B., Massachusetts Institute of Technology

(1961)

M.S., Massachusetts Institute of Technology

(1962)

SUBMITTED IN PARTIAL FULFILLMENT

OF THE REQUIREMENTS FOR THE

DEGREE OF DOCTOR OF

PHILOSOPHY

at the

MASSACHUSETTS INSTITUTE OF

TECHNOLOGY

August, 1965

Signature of Author.....

Department of Naval Architecture and  
Marine Engineering, August 20, 1965

Certified by.....

Thesis Supervisor /

Accepted by.....

Chairman, Departmental Committee  
on Graduate Students

## COMPLIANT WATER WAVE ABSORBERS

by

Jerome H. Milgram

Submitted to the Department of Naval Architecture and Marine Engineering on August 20, 1965 in partial fulfillment of the requirement for the degree of Doctor of Philosophy.

This report comprises a detailed theoretical and experimental study of the problem of absorbing plane water waves by means of a moving boundary at one end of a channel. The non-linear problem is formulated as a sequence of linear problems by means of perturbation techniques. This formulation is carried out first for a general moving boundary and then for the specific case where the boundary is a hinged paddle above a solid wall. In order to avoid the parameter of the channel length in the theoretical work, this work is carried out for a semi-infinite tank. Solutions for the necessary wave absorber characteristics are determined by the first order (linear) theory. Second order solutions are determined when the incident wave is a plane, periodic, progressive wave. The theoretical developments are done with the neglect of surface tension, but these effects are considered in a separate chapter and they are accounted for in the computer programs used for the design of a wave absorbing system. The problem of synthesizing a wave absorbing system whose characteristics closely approximate an ideal absorber and which can be constructed readily is solved. The solution of this problem requires a computer-aided design procedure for electric filters which may be of general interest for its own sake, apart from the remainder of this work. The stability of wave absorbers is examined by a utilization of the theory of waves with complex wave numbers. It is shown that such waves can be constructed as combinations of waves with real wave numbers travelling in skew directions in the vertical plane of the channel. The absorption of wave pulses is considered. The velocity potential for a wave pulse can be represented as an integral over the normal modes of the absorbing channel if certain restrictions on the characteristics of the absorber are met. Experiments on the absorption of periodic waves and wave pulses were carried out. In addition an experiment was performed which confirms the theoretical relationship between pressure and surface elevation. This was done as part of an examination of the possibility of activating a wave absorber with a pressure signal in the future.

Thesis Supervisor: Martin A. Abkowitz

Title: Professor of Naval Architecture

## ACKNOWLEDGEMENTS

The author wishes to express his appreciation to Professor Martin A. Abkowitz, project supervisor; and Professors Erik L. Mollo-Christensen and Justin E. Kerwin, project committee members; as well as to the M.I.T. Computation Center which provided the Time-Sharing System on which the computer work was done. The author is also grateful to Block Associates, Inc. whose kind loan of some electronic apparatus facilitated the experiments, and to Mr. Raymond Johnson whose Shop at M.I.T. fabricated parts of the apparatus.

Special credit is due to Mr. Stanley Chang who did the equation lettering, and to Mr. Donald Yansen who was of great assistance in constructing the experimental apparatus and in proofreading parts of the theoretical work.

## TABLE OF CONTENTS

<u>Subject</u>	<u>Page</u>
TITLE PAGE	i
ABSTRACT	ii
ACKNOWLEDGEMENTS	iii
TABLE OF CONTENTS	iv
LIST OF FIGURES	vi
LIST OF SYMBOLS	ix
CHAPTER 1. Introduction	1
CHAPTER 2. General Formulation of the Problem	10
CHAPTER 3. Formulation of the Boundary Condition at the Wave Absorber and the Hydrodynamic Moment on the Absorber When the Absorber is a Hinged Paddle	21
CHAPTER 4. Solution of the Equations for the First-Order Waves When the Incident Wave is a Plane, Periodic, Progressive Wave	29
CHAPTER 5. Solution of the Equations for the Second-Order Waves When the Incident Wave is a Plane, Periodic Progressive Wave	39
CHAPTER 6. The Effect of Surface Tension	77
CHAPTER 7. Synthesis of a Linear Wave Absorbing System Function	81
CHAPTER 8. Oblique Waves	96
CHAPTER 9. The Stability of Linear Active Wave Absorbers	112
CHAPTER 10. Determination of the Reflection Coefficient	116
CHAPTER 11. Absorption of Wave Pulses	130
CHAPTER 12. Discussion of Theoretical and Experimental Wave Absorber Results	142

<u>Subject</u>	<u>Page</u>
CHAPTER 13. Investigation of the Relationship Between Pressure and Surface elevation	147
CHAPTER 14. Conclusions	163
REFERENCES	165
APPENDIX A. Design and Construction of the Experimental Wave Tank	166
APPENDIX B. Design of the Wave Absorbing Filter	168
APPENDIX C. Wave Height to Voltage Transducer	187
APPENDIX D. Alterations to the Chart Recorder	191
APPENDIX E. Integral Tables	194
APPENDIX F. Descriptions and Listings of Computer Programs	200
APPENDIX G. Computer-Aided Design Procedure for the synthesis of a Rational System Function Which Approximates Prescribed Frequency Characteristics	235

## LIST OF FIGURES

<u>Figure</u>	<u>Page</u>
1-1 Picture of experimental apparatus	7
1-2 Picture of details of the absorbing end of the tank	9
2-1 Diagram of the geometry for a general absorber	20
3-1 Diagram of the geometry for a hinged paddle absorber	28
3-2 The change in paddle immersion due to a change in paddle angle	28
6-1 Computer printout showing the effect of surface tension on the eigenvalues for the wave absorber problem	79
7-1 Computer printout for the synthesis of a comparatively simple wave absorbing system function	88
7-2 Computer printout for the stability study of the system function synthesized in figure 7-1	90
7-3 Computer printout for the theoretical determination of the reflection coefficients for the system function synthesized in figure 7-1.	91
7-4, 7-5, and 7-6 These figures correspond to figures 7-1, 7-2, and 7-3 respectively, where in this case a more complicated system function is considered.	92 94 95
10-1 Diagram of the experiment to measure the reflection coefficient	125
10-2 Sample record from the experiment to measure the reflection coefficient	126
10-3 Graph of theoretical and experimental reflection coefficients	127
10-4 Graphs of the experimental and theoretical system functions	128
10-5 Diagram of the experiment to measure the system function	129
11-1 Surface elevation vrs. time for a wave pulse in a channel with an absorber	140

<u>Figure</u>	<u>Page</u>
11-2 Surface elevation vrs. time for a wave pulse in in a channel with a 10 degree sloping beach	141
11-3 Surface elevation vrs. time for a wave pulse in a channel terminated with a solid wall	141
13-1 Diagram of the experiment to measure the relationship between pressure and wave height	152
13-2 to 13-10 Graphs of the results of the experiment to measure the relationship between pressure and wave height	154 to 162
A-1 Scale drawing of the wave tank	167
B-1 Representation of an operational amplifier	168
B-2 Simple amplifier circuit	169
B-3 General linear circuit activated by an operational amplifier	171
B-4 Diagram of the wave absorbing system	184
B-5 Picture of the gearing between motor, paddle, and feedback potentiometer	185
B-6 Circuitry around the feedback amplifier	173
B-7 Pole-zero plot for the system function used in the experiments	186
B-8 and B-99 Parts of the circuitry used to achieve the desired system function	177
B-10 through B-13 Parts of the circuitry needed to achieve a more complicated system function than the one which was constructed	181 182 183
C-1 Schematic diagram of the circuit for the Wave Height to Voltage Transducer	190
D-1 Schematic diagram showing alterations to the paper chart recorder used to attain a high frequency rolloff in the response of the recorder	192

<u>Figure</u>		<u>Page</u>
D-2	Amplitude frequency response for the altered paper chart recorder	193
G-1 and G-2	Sample computer outputs for the computer-aided design scheme for synthesizing electric filters	249 to 253

## LIST OF SYMBOLS

- $\nabla$  - Gradient
- $\nabla^2$  - Laplacian
- x,y - rectangular axis
- h - depth of water channel
- g - acceleration due to gravity
- $\rho$  - density of the fluid
- $\eta$  - surface elevation
- $\vec{V}$  - velocity
- $\phi$  - velocity potential
- t - time
- T - surface tension
- $\xi$  - horizontal position of the wave absorber
- $V_n$  - component of velocity normal to the absorber at the absorber
- $\epsilon$  - perturbation parameter; also used as a small positive number in Chapter 11
- p - depth of the pivot for a hinged paddle absorber
- P - pressure
- $\theta$  - paddle angle, also used to represent wave obliqueness angle in Chapter 8
- $\Delta$  - change in paddle immersion
- $M_h$  - hydrodynamic moment on the absorber
- B - amplitude of sinusoidal paddle motion
- $\omega$  - radian frequency
- l - distance from absorber to end wall of the channel
- $\alpha, \nu, f$  - eigenvalues (In Chapter 8,  $\alpha = fh$ )
- A, B, N, D, G (with subscripts only), R (with subscripts only) - coefficients
- $H_m$  - ratio of first order moment to first order angle of the paddle
- $H_h$  - ratio of first order complex paddle angle to first order complex amplitude of the wave height a distance d from the paddle

nh(as subscripts) - non-homogenous

h(as subscript) - homogenous

L - linear operator as defined

K - curvature

R - radius of curvature

$S = \sigma + i\omega$  - type of complex frequency usually used by electrical engineers

$\xi$  - phase angle

## I INTRODUCTION AND READING GUIDE

This introductory chapter is intended to serve as a guide to the reader as well as to introduce the chapters which follow. Therefore, the bulk of this chapter comprises a compendium of the remainder of this report, chapter by chapter.

The study reported here concerns the absorption of waves by means of some kind of device which moves in some manner that is controlled by the wave incident upon it. At the outset of this work it was thought that the absorber would work by moving in response to the force exerted on it by the incident wave; thus the title "Compliant Water Wave Absorbers." However, the wave absorber which was eventually built and tested was actuated by a signal derived from the surface elevation at a fixed point near the absorber. The only previous work done in this field which the author has been able to find is by Baumann (1). In Baumann's work an absorbing paddle is connected to a mass, a spring and a magnetic damper. The various constants were experimentally varied in order to achieve complete absorption at one frequency. For Baumann's absorber, the bandwidth for which the reflection coefficient was less than 10 percent was about five percent of an octave. The absorber reported on here has a bandwidth for which the reflection coefficient was less than 5 percent of two octaves. Furthermore, the method described herein can be used for any desired bandwidth.

In addition to the direct results of the study of the wave absorbing problem, the experimental work reported here gives further confirmation of the validity of the linearized water wave theory. Some previous work in this field was done by Ursell, Dean and Yu (2) in their very careful study

of "Forced Small Amplitude Water Waves."

Since wave absorbers can be used in tanks with a wide variety of lengths it is desirable that the tank length not be a parameter in the theoretical work. Therefore the theoretical work is based on a semi-infinite tank. When waves which are shorter than one tank length are considered the error in the theoretical reflection coefficient caused by the finite length is negligible. The solution to the initial value problem in a finite tank will be very different from the solution in an infinite tank although the method of solution and the proof of the existence of a solution is almost identical in the two cases. The finite tank is subject to a type of instability which is not present in a semi-infinite tank. However, if an absorber is stable in a semi-infinite tank, it is also stable in a finite tank provided that it has a reflection coefficient less than unity at low frequencies and the coefficient does not rise too rapidly with frequency.

In chapter two a general formulation is carried out for an arbitrary type of absorber (piston, paddle, etc.). The validity of a perturbation series is assumed and equations and boundary conditions for the first and second order potentials are derived. The development is necessarily very similar to other perturbation expansions in this field and need not be read by the reader who is already familiar with such expansions or is not interested in them. Chapter three carries out the necessary perturbation expansions and determines the first and second order boundary conditions for the case where the wave absorber is a paddle hinged at its bottom a distance  $P$  below the free surface, with a solid wall between the bottom of

the paddle and the bottom of the tank. Expressions for the first and second order hydrodynamic moments on the paddle are also derived in chapter three.

In chapter four the solution of the first order equations subject to first order boundary conditions for a sinusoidal incident wave is carried out. The problem is reduced to four separate self-adjoint Sturm-Liouville problems and the solution is given by the resulting eigenfunction series. The coefficients of the series are evaluated for the case where the absorber is a hinged paddle. The linear system function from paddle angle to force is determined such that there be no reflected wave. Similarly the linear system function from surface elevation at a fixed point to paddle angle is determined. Since the first order theory is linear, the system having the correct response will absorb a finite sum of sinusoidal waves.

The solution for the second order problem when the incident wave is a plane, periodic progressive wave is carried out in chapter five. The problem is cast in the form of a non-homogeneous linear boundary value problem in which the non-homogeneous terms are non-linear combinations of the known first order solutions. Because of these terms, a second order absorbing system will not absorb an arbitrary finite sum of plane periodic, progressive waves.

In the vicinity of the absorber the first order solution contains a wave having a horizontal sinusoidal dependence and a sequence of waves having a vertical sinusoidal dependence. The second order wave resulting from the non-linear interaction of the wave with a horizontal sinusoidal dependence and one of the other waves is interesting. It has a sinusoidal

dependence in a direction which is neither horizontal nor vertical, but rather in a direction which is oblique with respect to the horizontal-vertical frame of reference. The derivation of the second order solution is very long and the resulting expressions are complicated. Therefore, the reading of chapter five is not recommended unless the reader has a similar problem, wants to design a second order absorber or has a particular interest in the non-linear interaction described above.

Chapter six shows that the effect of surface tension is negligibly small for the wave frequencies an absorber would usually encounter. The expressions needed to include surface tension effects in the linear theory are determined.

If a wave absorbing system is to be useful, its system function must be a good approximation of that system function which results in complete absorption. The synthesis of a system function which can be built and has the above characteristics is carried out in chapter seven for the hinged paddle type absorber according to linear (first order) theory. In order to carry out this synthesis, it was necessary to devise a computer-aided design scheme for synthesizing the system function of an electronic filter. This scheme is of interest apart from the remainder of this report and is reported briefly in chapter seven and in detail in appendix g.

In chapter eight the theory of oblique waves in a semi-infinite tank is carried out and it is shown that these waves can be represented by the same expressions as more usual waves, except that the wave numbers in the representation are complex for oblique waves. When oblique waves satisfy a homogeneous free surface condition, it is shown that the frequency must be complex which results in the fact that the wave amplitude increases or

decreases with time. Such waves must be used in a consideration of the stability of a wave absorbing system with respect to negative going waves; this being the topic of chapter nine. Normal modes with complex frequencies must be used for the solution to the initial value problem in a finite tank, but theoretical problems in a finite tank are not considered in this report. Chapters eight and nine constitute a study of the stability of a servomechanism in which the feedback is provided by a hydrodynamic element (the region of the tank between the paddle and the wave measuring probe).

If the wave absorbing system had the exact system function calculated in chapter four, there would be no reflected wave according to linear theory. Since the synthesized system function differs from the exact system function there will be a reflected wave in theory, the reflection coefficient varying with frequency. When an experimental system is built its system function will vary slightly from the synthesized function resulting in a different set of reflection coefficients. The above topics are considered in chapter ten. Also, the results of experiments with the absorber are reported in chapter ten. In most instances the difference between measured and theoretical reflection coefficients was about 1 percent.

The solution to the initial value problem for the semi-infinite tank is considered in chapter eleven. A set of conditions on the behavior of the absorbing system function sufficient for the validity of a given representation of the solution are determined. Some interesting qualitative experiments on the absorption of wave pulses were carried out and are reported in chapter eleven. A discussion of theoretical and experimental wave absorber results constitutes chapter twelve.

An interesting possibility is to actuate a wave absorber by a signal derived from a measurement of the pressure at a tap in the tank wall. In order to confirm the theoretical relationship between pressure and surface elevation an extensive series of experiments was performed. These experiments do indeed confirm the theoretical relationship. The investigation of this relationship is reported in chapter thirteen.

Appendix A contains a brief description of the experimental wave tank as well as a scale drawing of the tank. Appendix B considers the design of the actual electric circuits needed to achieve the synthesized wave absorber system function. These are active electric circuits, being activated by operational amplifiers. Appendix B contains a short description of the operational usage of operational amplifiers for the reader who is unfamiliar with these devices. The design of two synthesized system functions is carried out, the more complicated circuit having a lower reflection coefficient than the simpler circuit of the two. The simpler circuit was built and tested in the experimental work.

Appendix C contains a description of the wave measuring probe and its associated circuitry. This wave measuring device performed very well over a wide range of wave heights and even gave excellent results for waves which were less than  $1/20$  of an inch in height.

Appendix D describes the alterations which were made to the paper chart recorder used in the experiments in order that it would filter out high frequency noise.

Appendix E is a table of the integrals needed in chapters four and five. Appendix F contains brief descriptions of the most important computer

programs used in this work. It is not intended that these descriptions be sufficient to inform the reader how to use the programs, but rather that they are intended to serve as a reference to one who is somewhat familiar with the programs. An exception to this is the computer program IMERG which is described in detail in appendix G. This program, which is used to synthesize electric filters for prescribed magnitude and phase characteristics may be of considerable general interest for its own sake.

The following figures in this chapter show the experimental apparatus.

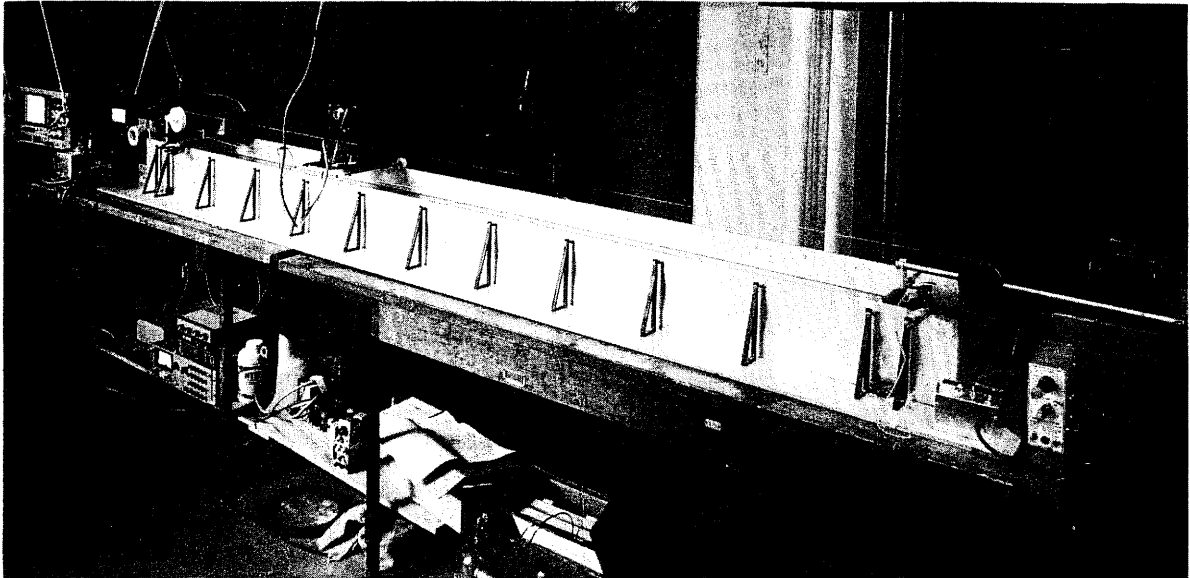


FIGURE 1-1 Overall view of experimental apparatus. At right hand end is the wavemaker and the wavemaker control as well as the towcord motor and its control. The apparatus at the left hand end is labeled in the succeeding figures.

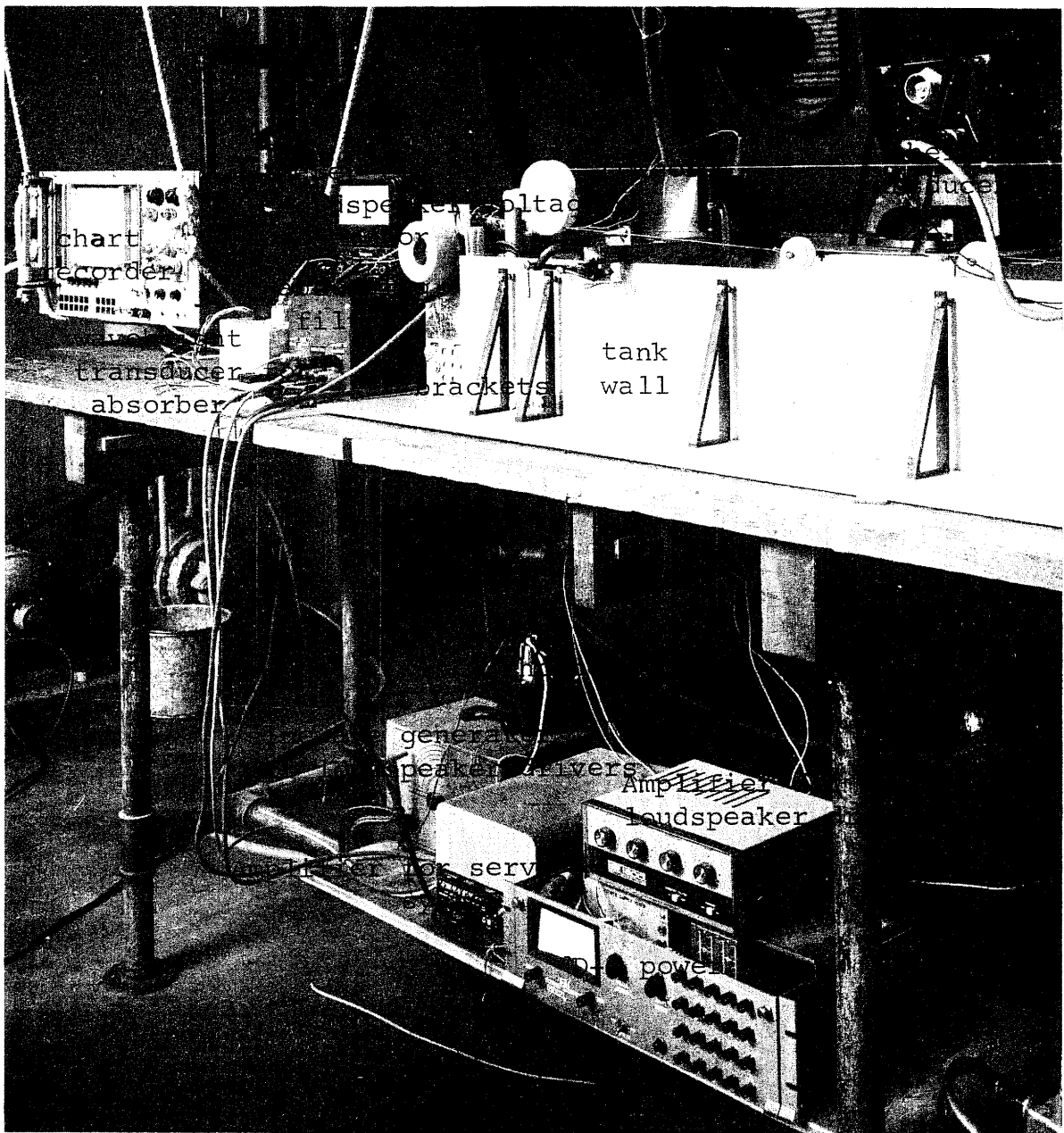


FIGURE 1-2a Detailed view of apparatus at absorbing end of the wave tank. The various components are labeled on the next page.

## GENERAL FORMULATION OF THE PROBLEM

The geometry of the problem is based on a "semi-infinite" tank containing a fluid of mean depth,  $h$ , as shown in Figure 2-1. Two-dimensional plane progressive surface waves, propagating from left to right in Figure 1 are to be absorbed. A fixed two-dimensional coordinate system is used with the  $x$ -axis horizontal and positive to the right.  $x = 0$  corresponds to a plane which will be the limiting position of a wave absorbing device as the wave amplitude tends to zero.  $x = l$  corresponds to the right-hand end wall of the tank shown in Figure 2-1. The  $y$  axis is vertical and positive upwards.  $y = 0$  corresponds to the "still water line" and  $y = -h$  corresponds to the bottom of the tank. The surface position is denoted by  $\eta(x, t)$ .

The fluid flow is assumed to be frictionless and irrotational so that:

$$\vec{v} = \nabla \phi \quad (2-1)$$

$$\nabla^2 \phi = 0 \quad (2-2)$$

The boundary conditions are:

1. There can be no component of flow normal to the bottom of the tank at the bottom of the tank:

$$\left. \frac{\partial \phi}{\partial y} \right|_{y=-h} = 0 \quad (2-3)$$

2. Fluid particles which are on the free surface at any time, are on the surface at all times (this is equivalent to requiring that the component of fluid velocity normal to the surface, when measured in a reference frame attached to the surface, be zero):

$$(\phi_y - \eta_t - \phi_x \eta_x) \Big|_{y=\eta} = 0 \quad (2-4)$$

This is known as the kinematic free surface condition.

3. Newton's Laws and therefore, Bernoulli's equation, applies to particles on the free surface upon which the pressure is assumed to be constant:

$$\left[ \phi_t + \frac{1}{2}(\phi_x^2 + \phi_y^2) + g\eta \right] \Big|_{y=\eta} = 0 \quad (2-5)$$

This is known as the dynamic free surface condition.

4. Considering the horizontal position of the wave absorber to be  $\xi(y,t)$ ;  $V_n$  the component of velocity of the absorber normal

to the absorber itself must be equal to  $\phi_n \Big|_{x=\xi}$ , the component

of fluid velocity normal to the absorber, at the absorber:

$$V_n(y,t) = \phi_n \Big|_{x=\xi} \quad (2-6)$$

5. At the end wall of the tank, the horizontal component of fluid velocity must be zero:

$$\phi_x|_{x=l} = 0 \quad (2-7)$$

The problem will now be formulated by means of a perturbation theory in which it is assumed that the following series are valid:

$$\phi(x, y, t) = \epsilon \phi^{(1)}(x, y, t) + \epsilon^2 \phi^{(2)}(x, y, t) + \dots \quad (2-8)$$

$$\eta(x, t) = \epsilon \eta^{(1)}(x, t) + \epsilon^2 \eta^{(2)}(x, t) + \dots \quad (2-9)$$

$$\xi(y, t) = \epsilon \xi^{(1)}(y, t) + \epsilon^2 \xi^{(2)}(y, t) + \dots \quad (2-10)$$

It is not known a priori whether or not the mathematical problem being considered yields solutions for  $\phi$ ,  $\eta$  and  $\xi$  which are analytic in  $\epsilon$  in the neighborhood of  $\epsilon = 0$ ; and even if the expansions were valid the "radius of convergence" of the series would be unknown. However, because of the success of this technique in similar problems, it will be carried out here and the theoretical results then compared with experimental results. Equations for quantities of order (1) and (2) will be determined.

By using the perturbation series for  $\phi$ , Laplace's equation (2-2) becomes

$$\epsilon \nabla^2 \phi^{(1)} + \epsilon^2 \nabla^2 \phi^{(2)} + \dots = 0 \quad (2-11)$$

For  $\phi$  to be analytic in  $\epsilon$  in the neighborhood of  $\epsilon = 0$  the coefficient of each power of  $\epsilon$  in eq. (2-11) must be zero.

$$\nabla^2 \phi^{(1)} = 0 \quad (2-12)$$

$$\nabla^2 \phi^{(2)} = 0 \quad (2-13)$$

$\phi$  is a harmonic function of  $x$  and  $y$  throughout the fluid so  $\phi_x$  and  $\phi_y$  can be expanded in power series in  $y$  about  $y = 0$ . The existence of a power series in  $y$  for  $\phi_t$  is assumed.

The various series expansions for terms needed in the boundary conditions at the free surface are:

$$\phi_y|_{y=\eta} = \phi_y|_{y=0} + \eta \phi_{yy}|_{y=0} + \dots \quad (2-14)$$

$$\phi_t|_{y=\eta} = \phi_t|_{y=0} + \eta \phi_{ty}|_{y=0} + \dots \quad (2-15)$$

Substitution of the perturbation series expansions into equation (2-15) results in:

$$\phi_t|_{y=\eta} = \epsilon \phi_t^{(1)}|_{y=0} + \epsilon^2 (\phi_t^{(2)} + \eta^{(1)} \phi_{ty}^{(1)})|_{y=0} + \dots \quad (2-16)$$

$$\frac{1}{2}(\phi_x^2 + \phi_y^2)|_{y=\eta} = \frac{\epsilon^2}{2}(\phi_x^{(1)2} + \phi_y^{(1)2}) + \dots \quad (2-17)$$

$$g\eta = \epsilon g\eta^{(1)} + \epsilon^2 g\eta^{(2)} + \dots \quad (2-18)$$

Substitution of the preceding expressions into the dynamic free surface condition gives:

$$\begin{aligned} & \epsilon [\phi_t^{(1)}|_{y=0} + g\eta^{(1)}] \\ & + \epsilon^2 [(\phi_t^{(2)} + \eta^{(1)} \phi_{ty}^{(1)} + \frac{1}{2} \phi_x^{(1)2} + \frac{1}{2} \phi_y^{(1)2})|_{y=0} + g\eta^{(2)}] = 0 \end{aligned} \quad (2-19)$$

As in the case of Laplace's equation, the coefficient of each power of  $\epsilon$  must be zero giving:

$$\phi_{\epsilon}^{(1)}|_{y=0} + g\eta^{(1)} = 0 \quad (2-20)$$

$$\phi_{\epsilon}^{(2)}|_{y=0} + \eta^{(1)} \phi_{\epsilon y}^{(1)}|_{y=0} + \frac{1}{2}(\phi_x^{(1)2} + \phi_y^{(1)2})|_{y=0} + g\eta^{(2)} = 0 \quad (2-21)$$

Insertion of the series expansions for the various terms in the free surface kinematic condition along with the assumed requirement of analyticity in  $\epsilon$  around  $\epsilon = 0$  gives:

$$\eta_{\epsilon}^{(1)} - \phi_y^{(1)}|_{y=0} = 0 \quad (2-22)$$

$$\eta_{\epsilon}^{(2)} + \eta_x^{(1)} \phi_x^{(1)}|_{y=0} - \phi_y^{(2)} - \eta^{(1)} \phi_{yy}^{(1)}|_{y=0} = 0 \quad (2-23)$$

Combining equations (2-20) and (2-22) gives:

$$(\phi_{\epsilon\epsilon}^{(1)} + g\phi_y^{(1)})|_{y=0} = 0 \quad (2-24)$$

Combining equations (2-21) and (2-23) gives:

$$\begin{aligned}
 (\phi_{xx}^{(2)} + g\phi_y^{(2)}) \Big|_{y=0} &= \left[ g\phi_x^{(1)}\eta_x^{(1)} - g\phi_{yy}^{(1)}\eta^{(1)} - \phi_{ey}^{(1)}\eta_c^{(1)} \right. \\
 &\quad \left. - \phi_{ey}^{(1)}\eta^{(1)} - \phi_x^{(1)}\phi_{xc}^{(1)} - \phi_y^{(1)}\phi_{yc}^{(1)} \right] \Big|_{y=0} \quad (2-25)
 \end{aligned}$$

Substitution of equations (2-20) and (2-22) into (2-25) gives:

$$\begin{aligned}
 (\phi_{xx}^{(2)} + g\phi_y^{(2)}) \Big|_{y=0} &= \\
 & \left[ 2g\phi_x^{(1)}\eta_x^{(1)} - g\phi_{yy}^{(1)}\eta^{(1)} - 2\phi_{ey}^{(1)}\eta_c^{(1)} - \phi_{ey}^{(1)}\eta^{(1)} \right] \Big|_{y=0} \quad (2-26)
 \end{aligned}$$

Similarly the lower boundary condition becomes:

$$\phi_y^{(1)} \Big|_{y=-h} = 0 \quad (2-27)$$

and

$$\phi_y^{(2)} \Big|_{y=-h} = 0 \quad (2-28)$$

Also the boundary condition at  $x = l$  becomes:

$$\phi_x^{(1)} \Big|_{x=l} = 0 \quad (2-29)$$

and

$$\phi_x^{(2)} \Big|_{x=l} = 0 \quad (2-30)$$

It is assumed that the wave absorber motion can be expanded as:

$$V_n(y,t) = \epsilon V_n^{(1)}(y,t) + \epsilon^2 V_n^{(2)}(y,t) + \dots \quad (2-31)$$

and since  $\phi$  is a harmonic function, it is known that

$$\phi_n \Big|_{x=\xi} = \phi_n \Big|_{x=0} + \xi \phi_{nx} \Big|_{x=0} + \dots \quad (2-32)$$

Thus the boundary condition at the absorber, equation (2-6), becomes:

$$\phi_n^{(1)} \Big|_{x=0} = V_n^{(1)} \quad (2-33)$$

$$\phi_n^{(2)} \Big|_{x=0} = V_n^{(2)} - \xi^{(1)} \phi_{nx}^{(1)} \Big|_{x=0} \quad (2-34)$$

For convenience the preceding equations are regrouped and renumbered:

$$\nabla^2 \phi^{(1)} = 0 \quad (2-35)$$

$$(\phi_{tt}^{(1)} + g \phi_y^{(1)}) \Big|_{y=0} = 0 \quad (2-36)$$

$$\phi_y^{(1)} \Big|_{y=-h} = 0 \quad (2-37)$$

$$\phi_x^{(1)} \Big|_{x=l} = 0 \quad (2-38)$$

$$\phi_n^{(1)} \Big|_{x=0} = V_n^{(1)} \quad (2-39)$$

$$\nabla^2 \phi^{(2)} = 0 \quad (2-40)$$

$$\begin{aligned} (\phi_{tt}^{(2)} + g\phi_y^{(2)}) \Big|_{y=0} = \\ (2g\phi_x^{(1)}\eta^{(1)} - g\phi_{yy}^{(1)}\eta^{(1)} - 2\eta_c^{(1)}\phi_{ty}^{(1)} - \eta^{(1)}\phi_{tty}^{(1)}) \Big|_{y=0} \end{aligned} \quad (2-41)$$

$$\phi_x^{(2)} \Big|_{x=L} = 0 \quad (2-42)$$

$$\phi_x^{(2)} \Big|_{x=0} = \gamma_x^{(2)} - \xi^{(1)} \phi_{xz}^{(1)} \Big|_{x=0} \quad (2-43)$$

The perturbation expansion yields a homogeneous boundary value problem, equations (2-35) through (2-39), for the first order quantities  $\phi^{(1)}$ ,  $\eta^{(1)}$  and  $\xi^{(1)}$ ; and a non-homogeneous boundary value problem, equations (2-40) through (2-43), for the second-order quantities  $\phi^{(2)}$ ,  $\eta^{(2)}$  and  $\xi^{(2)}$ . The non-homogeneous terms are quantities involving first-order quantities. Similarly, if the third-order problem were formulated, the non-homogeneous terms would contain first and second order quantities, and so forth. By sequentially solving first, second, third... order equations, the solution to the problem can be obtained if the perturbation series converge. In order to carry out the above scheme the general form of the absorber motion must be known. For the specific

example solved in the following chapters and upon which experiments were performed, the absorber is a paddle hinged at a distance  $p$  beneath the calm free surface position with a solid wall between the bottom of the paddle and the bottom of the tank.

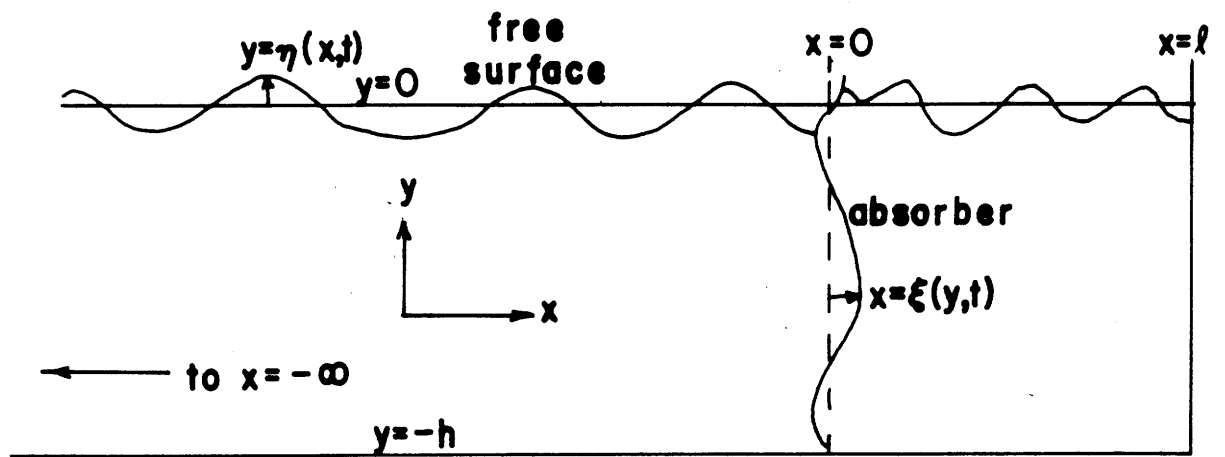


FIGURE 2-1 Diagram of general wave absorber geometry.

FORMULATION OF THE BOUNDARY CONDITION AT THE WAVE ABSORBER  
AND THE HYDRODYNAMIC MOMENT ON THE ABSORBER  
WHEN THE ABSORBER IS A HINGED PADDLE

Consider a wave absorbing paddle hinged a distance  $\beta$  below the free surface and a solid vertical wall between the bottom of the tank and the paddle hinge at  $x = 0$  as shown in Figure 3-1. The paddle angle  $\theta$  is considered to be positive when the paddle lies in the region  $0 < x < l$ .  $\theta(t)$  is to be chosen such that there is no energy radiating reflected wave.

Let,

$$\theta(t) = \epsilon \theta^{(1)}(t) + \epsilon^2 \theta^{(2)}(t) + \dots \quad (3-1)$$

The paddle position is  $\xi(y, t)$

$$\xi(y, t) = \begin{cases} (y - \beta) \tan \theta & y \geq -\beta \\ 0 & y < -\beta \end{cases} \quad (3-2)$$

The normal velocity of the paddle is  $V_n$

$$V_n(y, t) = \begin{cases} \frac{(y + \beta)}{\cos \theta} \theta_t & y \geq -\beta \\ 0 & y < -\beta \end{cases} \quad (3-3)$$

Expanding  $\frac{1}{\cos \theta}$  in a Maclaurin series in  $\theta$  and use of equation (3-1)

in equation (3-3) gives:

$$V_n(y, t) = \begin{cases} \epsilon(y+h) \theta_t^{(1)} + \epsilon^2(y+h) \theta_t^{(2)} + \dots & y \geq -\beta \\ 0 & y < -\beta \end{cases} \quad (3-4)$$

$$\phi_n = \phi_x \frac{dx}{dn} + \phi_y \frac{dy}{dn} \quad (3-5)$$

Figure (3-2) shows that:

$$\frac{dx}{dn} = \begin{cases} \cos \theta & y \geq -\beta \\ 1 & y < -\beta \end{cases} \quad (3-6)$$

and

$$\frac{dy}{dn} = \begin{cases} -\sin \theta & y \geq -\beta \\ 0 & y < -\beta \end{cases} \quad (3-7)$$

Use of the Maclaurin series in  $\theta$  for  $\sin \theta$  and  $\cos \theta$ , and equations

(3-1) through (3-5) gives:

$$\phi_n \Big|_{x=0} = \begin{cases} \epsilon \phi_x^{(1)} \Big|_{x=0} + \epsilon^2 (\phi_x^{(2)} - \theta^{(1)} \phi_y^{(1)}) & y \geq -\beta \\ \epsilon \phi_x^{(1)} \Big|_{x=0} + \epsilon^2 \phi_x^{(2)} & y < -\beta \end{cases} \quad (3-8)$$

$$\phi_n^{(1)} \Big|_{x=0} = \phi_x^{(1)} \Big|_{x=0} \quad (3-9)$$

$$\phi_n^{(2)} \Big|_{x=0} = \begin{cases} \phi_n^{(2)} \Big|_{x=0} - \theta^{(2)} \phi_y^{(2)} \Big|_{x=0} & y \geq -\beta \\ \phi_n^{(2)} \Big|_{x=0} & y < -\beta \end{cases} \quad (3-10)$$

$$V_n^{(1)} = \begin{cases} (y+\beta) \theta_t^{(1)} & y \geq -\beta \\ 0 & y < -\beta \end{cases} \quad (3-11)$$

$$V_n^{(2)} = \begin{cases} (y+\beta) \theta_t^{(2)} & y \geq -\beta \\ 0 & y < -\beta \end{cases} \quad (3-12)$$

$$\xi^{(2)} = \begin{cases} (y+k) \theta^{(2)} & y \geq -\beta \\ 0 & y < -\beta \end{cases} \quad (3-13)$$

$$\phi_{nx}^{(2)} \Big|_{x=0} = \phi_{nx}^{(1)} \Big|_{x=0} \quad (3-14)$$

Substitution of equations (3-9) and (3-11) into (2-39) gives

$$\phi_n^{(2)} \Big|_{x=0} = \begin{cases} (y+\beta) \theta_t^{(2)} & y \geq -\beta \\ 0 & y < -\beta \end{cases} \quad (3-15)$$

Substitution of (3-11), (3-12), (3-13) and (3-14) into (2-43) gives

$$\phi_x^{(2)} \Big|_{x=0} = \begin{cases} (y+\beta) \theta_c^{(2)} + (\theta^{(2)} \phi_y^{(2)} - (y+\beta) \theta^{(2)} \phi_{xx}^{(2)}) \Big|_{x=0} & y \geq -\beta \\ 0 & y < -\beta \end{cases} \quad (3-16)$$

The pressure is denoted by  $p(x, y, t)$  and the value this function takes on the negative  $x$  face of the paddle is called  $P_1(y, t)$  and its value on the positive  $x$  face of the paddle is called  $P_2(y, t)$ .

The moment exerted by the fluid on the paddle, which is taken as positive when the paddle is pushed toward positive values of  $x$ , is denoted by  $M_h(t)$ .

$$M_h(t) = \int_{-\beta}^a \frac{(y+\beta)}{\cos^2 \theta} [P_1(y, t) - P_2(y, t)] dy \quad (3-17)$$

The pressure is related to the velocity potential by Bernoulli's equation:

$$\frac{p}{\rho} = -\phi_c - \frac{1}{2} (\phi_x^2 + \phi_y^2) - gy \quad (3-18)$$

It is assumed that a perturbation series for the pressure exists.

$$p = -\rho gy + \epsilon p^{(1)} + \epsilon^2 p^{(2)} + \dots \quad (3-19)$$

$\rho$  designates either  $\rho_1$  or  $\rho_2$ .

$\phi$  is a harmonic function of  $x$  and  $y$  as is  $\phi_t$  for a periodic wave.

Therefore the following expansion for  $\rho$  is valid.

$$\rho(y,t) = \rho(x,y,t)|_{x=0} + \rho(x,y,t)\xi|_{x=0} \quad (3-20)$$

Substitutions of the various perturbation series into equation (3-18), evaluating the resulting equations at  $x = \xi = (y+h)\theta$  and imposing analyticity in  $\epsilon$  at  $\epsilon = 0$  gives the following equations.

$$\rho^{(1)}(y,t) = -\rho\phi_t|_{x=0} \quad (3-21)$$

$$\rho^{(2)}(y,t) = -\frac{\rho}{2}(\phi_x^{(1)2} + \phi_y^{(1)2})|_{x=0} - \rho\phi_t^{(1)}|_{x=0} \quad (3-22)$$

Using the above expressions as well as the Maclaurin series for  $\cos^2\theta$  gives the following equations for  $M_h^{(1)}$  and  $M_h^{(2)}$

$$M_k^{(2)}(t) = \int_{-p}^0 -(y+p) \rho [\phi_c^{(2)}|_{x=0-} - \phi_c^{(2)}|_{x=0+}] dy \quad (3-23)$$

$$M_k^{(2)}(t) = -\rho \int_{-p}^0 (y+p) \left[ (\phi_x^{(2)} + \phi_y^{(2)} + \phi_c^{(2)})|_{x=0-} - (\phi_x^{(2)} + \phi_y^{(2)} + \phi_c^{(2)})|_{x=0+} \right] dy \quad (3-24)$$

A quantity which will prove useful to know is the change in immersion of the negative x face of the paddle as the paddle moves in waves. This quantity is called  $\Delta$ . The perturbation series for  $\Delta$  will now be determined, using Figure(3-2) as a guide.

$$\text{total paddle immersion} = [p + \eta(x_p)] \cos \theta \quad (3-25)$$

$$x_p = [p + \eta(x_p)] \tan \theta \quad (3-26)$$

$$\Delta = \left\{ p + \epsilon \eta^{(1)}|_{x=0} + \epsilon^2 \eta^{(2)}|_{x=0} + \epsilon^2 \frac{d\eta^{(1)}}{dx} \Big|_{x=0} p \theta^{(1)} \right\} (1 + \frac{\theta^{(1)2}}{2} \epsilon^2) - p \quad (3-27)$$

$$\Delta^{(1)} = \eta^{(1)}|_{x=0} \quad (3-28)$$

$$\Delta^{(2)} = \eta^{(2)} \Big|_{x_0} + \rho \frac{\theta^{(2)^2}}{2} + \rho \theta^{(2)} \frac{\partial \eta^{(2)}}{\partial x}$$

(3-29)

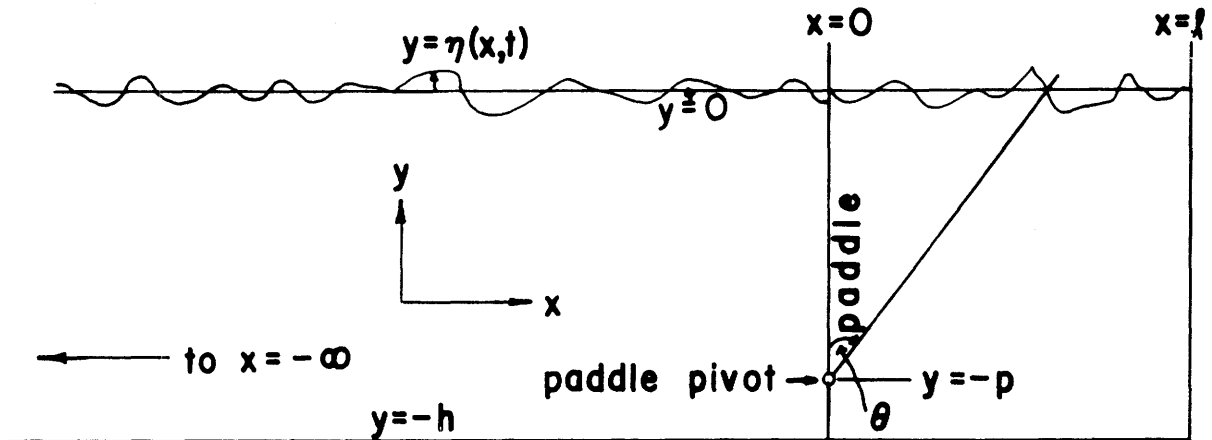


FIGURE 3-1 Diagram of wave absorber geometry when the absorber is a hinged paddle.

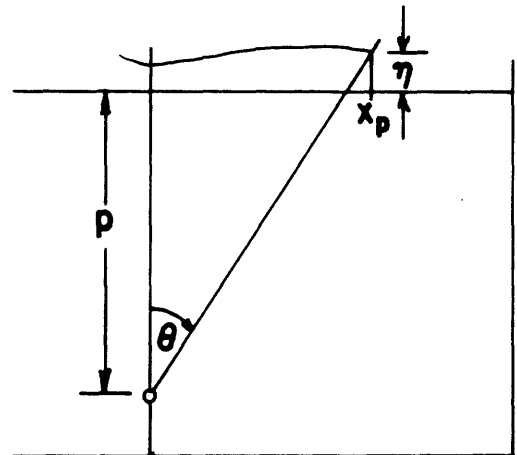


FIGURE 3-2 Diagram showing how the immersed length of an absorbing paddle changes when the paddle angle is changed.

## CHAPTER 4

### SOLUTION OF THE EQUATIONS FOR THE FIRST-ORDER WAVES WHEN THE INCIDENT WAVE IS A PLANE, PERIODIC, PROGRESSIVE WAVE

#### Introduction

The first-order potential  $\phi^{(1)}$  must satisfy equations (2-35) through (2-39). The case considered here is that of a hinged paddle wave absorber so the boundary condition at the absorber is given by equation (3-15). The first-order potential of a plane, progressive, periodic wave has a sinusoidal time dependence so it is anticipated that the paddle angle necessary to have no reflected energy radiating wave will also have a sinusoidal time dependence.

Let

$$\theta^{(1)}(t) = B e^{-i\omega t} \quad (4-1)$$

The physical variable  $\theta^{(1)}$  is given by the real part of the above equation. Complex notation is used only as a matter of convenience. Since the equation and boundary conditions satisfied by the first-order potential are linear, the use of complex variables can and will be carried through the calculations. In order to obtain an equation for a physical quantity at any stage in the following development, it is only necessary to take the real part of the equation under consideration. The solution for the first-order potential is sought in the form of a series, each term of which satisfies equations (2-35) through (2-38) and is separable in the sense that it is the product of three functions, one of  $x$ , one of  $y$ , and one of  $t$ . Such a solution to the sinusoidal problem will be found

subsequently and it will be complete in the sense that the function to which the series converges satisfies equation (3-15). Each of the terms in the series is to be of the form:

$$\phi_e(x, y, t) = F(x) G(y) e^{\pm i\omega t} \quad (4-2)$$

In order that  $\phi_e$  satisfy Laplace's equation (Equation 2-35), F and G must satisfy:

$$\frac{F''}{F} = \alpha^2 \quad (4-3)$$

$$-\frac{G''}{G} = \alpha^2 \quad (4-4)$$

F and G are subjected to the following boundary conditions:

$$G' = 0 \quad \text{at} \quad y = -h \quad (4-5)$$

$$-\omega^2 G + g G' = 0 \quad \text{at} \quad y = 0 \quad (4-6)$$

$$F' < \infty \quad \text{at} \quad x = -\infty \quad (4-7)$$

$$F' = 0 \quad \text{at} \quad x = l \quad (4-8)$$

It is also required that the complete solution for  $\phi^{(1)}$  satisfy equation (3-15).

Since there is a specified boundary condition at  $x = 0$ , the problem becomes two problems, one for the potential for  $-\infty < x \leq 0$  and one for  $0 \leq x \leq l$ .

The problem has thus been recast into four Sturm-Liouville problems, one for F and one for G in each of the regions  $-\infty < x \leq 0$ , and  $0 \leq x \leq l$ . The solution to equation (4-4) is:

$$G(y) = C_1 e^{i\alpha y} + C_2 e^{-i\alpha y} \quad (4-9)$$

To satisfy equation (4-5):

$$C_1 = C_2 e^{2i\alpha h} \quad (4-10)$$

For real values of  $\alpha$  equation (4-6) is satisfied if:

$$\omega^2 = -\alpha g \tan \alpha h \quad (4-11)$$

To consider imaginary values of  $\alpha$ , let:

$$\alpha = i\alpha_0 \quad (4-12)$$

where  $\alpha_0$  is real. In this case, equation (4-6) is satisfied if:

$$\omega^2 = \alpha_0 g \tanh \alpha_0 h \quad (4-13)$$

Equation (4-11) yields an infinite number of eigenvalues and equation (4-13) yields a single positive eigenvalue and a single negative eigenvalue. The solutions to equations (4-11) and (4-13) are both positive and negative. For every solution  $+\alpha$  there is one  $-\alpha$ . However, each of these two eigenvalues has the same eigenfunction so no loss of generality occurs in considering all the eigenvalues to be positive.

The Potential in the Region  $-\infty < x \leq 0$

The complete solution for  $\phi^{(1)}$  in the region  $-\infty < x \leq 0$  is:

$$\begin{aligned} \phi^{(1)} = & A \cosh \alpha_0(y+h) e^{i(\alpha_0 x - \omega t)} + A' \cosh \alpha_0(y+h) e^{i(\alpha_0 x + \omega t)} \\ & + \sum_{n=1}^{\infty} A_n \cos \alpha_n(y+h) e^{\alpha_n x} e^{-i\omega t} \end{aligned} \quad (4-14)$$

$$\begin{aligned} \phi_x \Big|_{x=0} = & i\alpha_0 A \cosh \alpha_0(y+h) e^{-i\omega t} \\ & + i\alpha_0 A' \cosh \alpha_0(y+h) e^{i\omega t} \\ & + \sum_{n=1}^{\infty} \alpha_n A_n \cos \alpha_n(y+h) e^{-i\omega t} \end{aligned} \quad (4-15)$$

Differentiation of equation (4-1) yields:

$$\theta_t^{(1)} = -i\omega B^{(1)} e^{-i\omega t} \quad (4-16)$$

Substitution of equations (4-15) and (4-16) into equation (3-15) gives:

$$\begin{aligned} i\alpha_0 A \cosh \alpha_0(y+h) e^{-i\omega t} + i\alpha_0 A' \cosh \alpha_0(y+h) e^{i\omega t} \\ + \sum_{n=1}^{\infty} \alpha_n A_n \cos \alpha_n(y+h) e^{-i\omega t} = \begin{cases} -i\omega B_2(y+\rho) e^{-i\omega t} & y \geq -\rho \\ 0 & y < -\rho \end{cases} \end{aligned} \quad (4-17)$$

The term in equation (4-14) whose coefficient is A represents the first-order potential of the incident wave. The term whose coefficient is A' represents the first-order potential of the reflected wave. For there

to be no first-order reflected wave,  $A'$  must be zero. The relationship between  $A$ ,  $A'$  and  $B^{(1)}$  is established by multiplying equation (4-17) by  $\cosh \alpha_0 (y + h)$  and integrating the resulting equation from  $y = -h$  to  $y = 0$ .

This provides the desired relationship because the function  $\cosh \alpha_0 (y + h)$  is orthogonal to  $\cos \alpha_n (y + h)$  for  $n = 1, 2, \dots$  over the interval  $y = -h$  to  $y = 0$ . This fact can be seen from direct substitution or observing that  $\cosh \alpha_0 (y + h)$  and  $\cos \alpha_0 (y + h)$  are each eigenfunctions of the problem for  $G$ , but belong to different eigenvalues.

Values of the following integrals are needed:

$$\int_1^{(2)} = \int_{-h}^0 \cosh^2 \alpha_0 (y+h) dy = \frac{h}{2} \left[ 1 + \frac{1}{2\alpha_0 h} \sinh 2\alpha_0 h \right] \quad (4-18)$$

$$\int_2^{(2)} = \int_{-p}^0 (y+p) \cosh \alpha_0 (y+h) dy = \frac{p}{\alpha_0} \sinh \alpha_0 h + \frac{1}{\alpha_0^2} (\cosh \alpha_0 (h-p) - \cosh \alpha_0 h) \quad (4-19)$$

Hence,

$$\begin{aligned} & i\alpha_0 A \frac{h}{2} \left[ 1 + \frac{1}{2\alpha_0 h} \sinh 2\alpha_0 h \right] e^{-i\omega t} \\ & + i\alpha_0 A' \frac{h}{2} \left[ 1 + \frac{1}{2\alpha_0 h} \sinh 2\alpha_0 h \right] e^{i\omega t} \\ & + i\omega B^{(2)} \left[ \frac{p}{\alpha_0} \sinh \alpha_0 h + \frac{1}{\alpha_0^2} (\cosh \alpha_0 (h-p) - \cosh \alpha_0 h) \right] e^{-i\omega t} \\ & = 0 \end{aligned} \quad (4-20)$$

The requirement that  $A'$  be equal to zero gives the relationship between  $A$  and  $B^{(1)}$ .

$$\begin{aligned}
B^{(1)} &= -\frac{\alpha_0}{\omega} \frac{I_1}{I_2} A \\
&= -A \frac{\alpha_0 k (1 + \frac{1}{2\alpha_0 k} \sinh 2\alpha_0 k)}{2\omega \left[ \frac{\rho}{\alpha_0} \sinh \alpha_0 k + \frac{1}{\alpha_0^2} (\cosh \alpha_0 (k-p) - \cosh \alpha_0 k) \right]} \quad (4-21)
\end{aligned}$$

In order to fix the phase of the incident wave, A is taken as a real, positive number. Then, equation (4-21) shows that  $B^{(1)}$  is real. Therefore the first and fourth terms in equation (4-17) have a time dependence of the form  $\sin \omega t$  and the second term is zero. For the equation to be valid for all time, all the terms in the sum must have a time dependence of the form  $\sin \omega t$ . This implies that all the  $A_n$ 's are imaginary.

Let

$$A_n = i b_n \quad (4-22)$$

where the  $b_n$ 's are real.

In order to determine the  $b_n$ 's, multiply equation (4-17) by  $\cos \alpha_n (y+h)$  and integrate from  $y = -h$  to  $y = 0$ .  $\cos \alpha_n (y+h)$  and  $\cos \alpha_m (y+h)$  are orthogonal over the interval if  $m \neq n$ . Values of the following integrals are needed:

$$\int_{-h}^0 \cos^2 \alpha_n (y+h) dy = \frac{1}{2} \left[ \frac{1}{2\alpha_n} \sinh 2\alpha_n h + h \right] \quad (4-23)$$

$$\begin{aligned}
 I_{+n}^{(2)} &= \int_{-p}^0 (y+p) \cos \alpha_n (y+k) dy \\
 &= \frac{p}{\alpha_n} \sin \alpha_n k + \frac{1}{\alpha_n^2} [\cos \alpha_n k - \cos \alpha_n (k-p)]
 \end{aligned} \tag{4-24}$$

Thus,

$$\begin{aligned}
 b_n &= -\frac{\omega}{\alpha_n} \frac{I_{+n}^{(2)}}{I_{-n}^{(1)}} B^{(2)} \\
 &= -2\omega B^{(2)} \frac{\alpha_n p \sin \alpha_n k + \cos \alpha_n k - \cos \alpha_n (k-p)}{\alpha_n^2 \left( \frac{1}{2\alpha_n} \sin 2\alpha_n k + k \right)}
 \end{aligned} \tag{4-25}$$

The Potential in the Region  $0 \leq x \leq l$

By proceeding just as in the case  $-\infty < x \leq 0$ , the same eigenvalues are obtained here. This occurs because the Sturm-Liouville problem for  $G$  determines the eigenvalues and this problem is the same in the two regions  $-\infty < x \leq 0$  and  $0 \leq x \leq l$ . The boundary condition at  $x = l$  (equation 4-8) implies complete reflection at  $x = l$  so that the  $x$  dependence of the eigenfunctions must be of the form  $\cosh \alpha(x - l)$ . Inasmuch as  $B^{(1)}$  is real, equation (3-15) shows that  $\phi_x$  must have a time dependence of the form  $\sin \omega t$ . Therefore, the complete solution for  $\phi^{(1)}$  in the region  $0 \leq x \leq l$  is:

$$\phi^{(1)} = N_0 \cosh \alpha_0 (y+k) \cos \alpha_0 (x-l) \sin \omega t + \sum_{n=1}^{\infty} N_n \cos \alpha_n (y+k) \cosh \alpha_n (x-l) \sin \omega t \tag{4-26}$$

$$\phi_n^{(2)} \Big|_{x=0} = \alpha_0 N_0 \cosh \alpha_0 (y+h) \sin \alpha_0 l \sin \omega t$$

$$- \sum_{n=1}^{\infty} \alpha_n N_n \cos \alpha_n (y+h) \sinh \alpha_n l \sin \omega t \quad (4-27)$$

Substitution of equations (4-1) and (4-27) into equation (3-15) gives:

$$\begin{aligned} & \alpha_0 N_0 \cosh \alpha_0 (y+h) \sin \alpha_0 l - \sum_{n=1}^{\infty} \alpha_n N_n \cos \alpha_n (y+h) \sinh \alpha_n l \\ & = \begin{cases} (y+\beta) \omega B^{(1)} & y \geq -\beta \\ 0 & y < -\beta \end{cases} \quad (4-28) \end{aligned}$$

The condition that  $B^{(1)}$  is real has been used in obtaining the above equation. The relationship between  $N_0$  and  $B^{(1)}$  is obtained by multiplying equation (4-28) by  $\cosh \alpha_0 (y+h)$  and integrating from  $y = -h$  to  $y = 0$ .

$$\begin{aligned} N_0 &= \frac{\omega B^{(1)}}{\alpha_0 \sin \alpha_0 l} \frac{I_2^{(1)}}{I_1^{(1)}} \\ &= \frac{\omega}{\alpha_0} B^{(1)} \frac{\frac{h}{\alpha_0} \sinh \alpha_0 h + \frac{1}{\alpha_0^2} (\cosh \alpha_0 (h-\beta) - \cosh \alpha_0 h)}{\frac{h}{2} (1 + \frac{1}{2\alpha_0 h} \sinh 2\alpha_0 h) \sin \alpha_0 l} \quad (4-29) \end{aligned}$$

The relationship between  $N_n$  and  $B^{(1)}$  is obtained by multiplying equation (4-28) by  $\cos \alpha_n (y+h)$  and integrating from  $y = -h$  to  $y = 0$ .

$$N_n = - \frac{\omega}{\alpha_n \sinh \alpha_n l} B^{(1)} \frac{\tilde{L}_{4n}}{\tilde{r}^{(1)}} =$$

$$- \frac{2\omega}{\alpha_n} B^{(1)} \frac{\left[ \frac{\rho}{2\alpha_n} \sin \alpha_n h + \frac{1}{2\alpha_n} (\cos \alpha_n h - \cos \alpha_n (h-\rho)) \right]}{\left( \frac{1}{2\alpha_n} \sin 2\alpha_n h + h \right) \sinh \alpha_n l} \quad (4-30)$$

The first order moment on the paddle is obtained by substituting the expression for  $\phi^{(1)}$  into equation (3-23).

$$M_k^{(1)}(\omega) = \rho \left[ (i\omega A + \omega N_0 \cos \alpha_0 l) \tilde{L}_2^{(1)} \right. \\ \left. + \sum_{n=1}^{\infty} (i\omega A_n + \omega N_n \cosh(\alpha_n l)) \tilde{L}_{4n}^{(1)} \right] \quad (4-31)$$

The ratio of the complex amplitude of the first-order moment to the first-order complex amplitude of the paddle angle is the linear frequency response function from motion to moment and is called  $H_m(-\omega)$

The minus sign in  $H(-\omega)$  occurs because the time dependence of the incident wave is  $e^{-i\omega t}$ .

$$H_m(-\omega) = \frac{\rho}{B^{(1)}} \left[ (i\omega A + \omega N_0 \cos \alpha_0 l) \tilde{L}_2^{(1)} \right. \\ \left. + \sum_{n=1}^{\infty} (i\omega A_n + \omega N_n \cosh \alpha_n l) \tilde{L}_{4n}^{(1)} \right] \quad (4-32)$$

It is important to realize that the frequency response is based on a driving function of the form  $e^{-i\omega t}$ . This means that  $i$  represents a phase lag, not a phase lead.

The ratio of the first order complex amplitude of the paddle angle to the first order complex amplitude of the wave height measured a distance  $x$  from the paddle is called  $H_h(-\omega)$

$$H_h(-\omega) = \frac{\theta}{\eta^{(1)}|_{x=d}} \quad (4-33)$$

The wave height can be obtained from equation (4-14) by use of the fact that  $A' = 0$  and the kinematic boundary condition

$$\phi_y^{(1)} = \eta_c^{(1)} \quad (2-22)$$

This gives

$$\eta^{(1)} = -\frac{\alpha_0 k}{i\omega} \sinh \alpha_0 k e^{i(\alpha_0 x - \omega t)} + \sum_{n=1}^{\infty} \frac{\alpha_n d_n}{i\omega} \sin \alpha_n k e^{\alpha_n x} e^{-i\omega t} \quad (4-34)$$

Then,

$$H_h(-\omega) = \frac{B}{i \frac{\alpha_0 k}{\omega} \sinh \alpha_0 k e^{-i\alpha_0 d} - \sum_{n=1}^{\infty} i \frac{\alpha_n d_n}{\omega} \sin \alpha_n k e^{-\alpha_n d}} \quad (4-35)$$

CHAPTER 5

SOLUTION OF THE EQUATIONS FOR THE SECOND-ORDER WAVES WHEN THE INCIDENT  
IS A PLANE, PERIODIC, PROGRESSIVE WAVE

Waves in the Region  $-\infty < x \leq 0$

When the incident wave is a plane, periodic, progressive wave with circular wave number  $\alpha_0$  and frequency  $\omega$  and there is no first order energy radiating reflected wave, the first order potential is:

$$\begin{aligned} \phi^{(1)} = & A \cosh \alpha_0 (y+h) \cos(\alpha_0 x - \omega t) \\ & + \sum_{n=1}^{\infty} b_n \cos \alpha_n (y+h) e^{\alpha_n x} \sin \omega t \end{aligned} \quad (5-1)$$

and the first order surface elevation is:

$$\begin{aligned} \eta^{(1)} = & -\frac{\omega}{g} A \cosh \alpha_0 h \sin(\alpha_0 x - \omega t) \\ & - \frac{\omega}{g} \sum_{n=1}^{\infty} b_n \cos \alpha_n h e^{\alpha_n x} \cos \omega t \end{aligned} \quad (5-2)$$

The above equations as well as the relations between A,  $\omega$ , the  $\alpha$ 's and the b's are determined in the preceding chapter.

A solution to equation (2-40) is now sought in the form:

$$\phi^{(2)} = \phi_{nh}^{(2)} + \phi_h^{(2)} \quad (5-3)$$

where nh stands for non-homogeneous and h stands for homogeneous.

The individual equations to be satisfied by the two parts of  $\phi^{(2)}$  are.

$$\left( \phi_{nh_{cc}}^{(2)} + g \phi_{nh_{yy}}^{(2)} \right) \Big|_{y=0} =$$

$$\left( 2g \phi_z^{(2)} \eta_x^{(2)} - g \phi_{yy}^{(2)} \eta^{(2)} - 2\eta_c^{(2)} \phi_{cy}^{(2)} - \eta^{(2)} \phi_{cyy}^{(2)} \right) \Big|_{y=0} \quad (5-5)$$

$$\phi_{nh_{yy}}^{(2)} \Big|_{y=-h} = 0 \quad (5-6)$$

$$\nabla^2 \phi_h^{(2)} = 0 \quad (5-7)$$

$$\left( \phi_{h_{cc}}^{(2)} + g \phi_{h_{yy}}^{(2)} \right) \Big|_{y=0} = 0 \quad (5-8)$$

$$\phi_{h_{yy}}^{(2)} \Big|_{y=-h} = 0 \quad (5-9)$$

$$\left( \phi_{nh_x}^{(2)} + \phi_{hx}^{(2)} \right) \Big|_{x=0} = \begin{cases} (y+\beta) \phi_c^{(2)} + \theta^{(2)} \phi_y^{(2)} - (y+\beta) \theta^{(2)} \phi_{zx} & y > -\beta \\ 0 & y < -\beta \end{cases} \quad (5-10)$$

If  $\phi_{nh}^{(2)}$  and  $\phi_h^{(2)}$  satisfy the above set of equations, then their sum, which is  $\phi^{(2)}$  satisfies equations (2-40) through (2-43).

The following is a list of expressions needed in expressing the right-hand side of equation (5-5):

$$\eta^{(2)} = -\frac{\omega}{g} A \cosh \alpha_0 h \sin(\alpha_0 x - \omega t) - \frac{\omega}{g} \sum_{n=1}^{\infty} b_n \cos \alpha_n h e^{\alpha_n x} \cos \omega t \quad (5-2)$$

$$\phi_z^{(2)} \Big|_{y=0} = -\alpha_0 A \cosh \alpha_0 h \sin(\alpha_0 x - \omega t) + \sin \omega t \sum_{n=1}^{\infty} \alpha_n b_n \cos \alpha_n (y+h) e^{\alpha_n x} \quad (5-11)$$

$$\phi_{yy}|_{y=0} = \alpha_0^2 A \cosh \alpha_0 h \cos(\alpha_0 x - \omega t) - \sin \omega t \sum_{n=1}^{\infty} \alpha_n^2 b_n \cos \alpha_n (y+h) e^{\alpha_n x}$$

$$\phi_{xy}|_{y=0} = \omega \alpha_0 A \cosh \alpha_0 h \cos(\alpha_0 x - \omega t) - \sum_{n=1}^{\infty} \omega \alpha_n b_n \sin \alpha_n h e^{\alpha_n x} \cos \omega t \quad (5-12)$$

$$\phi_{xxy}|_{y=0} = -\omega^2 \alpha_0 A \sinh \alpha_0 (y+h) \cos(\alpha_0 x - \omega t) + \sin \omega t \sum_{n=1}^{\infty} \omega^2 \alpha_n b_n \sin \alpha_n (y+h) e^{\alpha_n x} \quad (5-13)$$

$$\eta_x = -\frac{\alpha_0 \omega}{g} A \cosh \alpha_0 h \cos(\alpha_0 x - \omega t) - \cos \omega t \sum_{n=1}^{\infty} \frac{\omega}{g} \alpha_n b_n \cos \alpha_n h e^{\alpha_n x} \quad (5-14)$$

$$\eta_c = \frac{\omega^2}{g} A \cosh \alpha_0 h \cos(\alpha_0 x - \omega t) + \frac{\omega^2}{g} \sum_{n=1}^{\infty} b_n \cos \alpha_n h e^{\alpha_n x} \sin \omega t \quad (5-15)$$

To simplify the writing of expressions let:

$$A \cosh \alpha_0 h = C_0 \quad (5-17)$$

$$A \sinh \alpha_0 h = S_0 \quad (5-18)$$

$$\cos(\alpha_0 x - \omega t) = C \quad (5-19)$$

$$\sin(\alpha_0 x - \omega t) = S \quad (5-20)$$

$$b_n e^{\alpha_n x} \cos \alpha_n h = C_n \quad (5-21)$$

$$b_n e^{\alpha_n x} \sin \alpha_n h = S_n \quad (5-22)$$

$$\cos \omega t = C_\omega \quad (5-23)$$

$$\sin \omega t = S_\omega \quad (5-24)$$

With this notation, equation (5-2) and equations (5-11) through (5-16 )

become:

$$\eta^{(2)} = -\frac{\omega}{g} C_0 S - C_\omega \sum_{n=1}^{\infty} \frac{\omega}{g} C_n \quad (5-25)$$

$$\phi_x^{(2)} \Big|_{y=0} = -\alpha_0 C_0 S - S_\omega \sum_{n=1}^{\infty} \alpha_n C_n \quad (5-26)$$

$$\phi_{yy} \Big|_{y=0} = \alpha_0^2 C_0 C - S_\omega \sum_{n=1}^{\infty} \alpha_n^2 C_n \quad (5-27)$$

$$\phi_{xy} \Big|_{y=0} = \omega \alpha_0 S_0 S - \omega C_\omega \sum_{n=1}^{\infty} \alpha_n S_n \quad (5-28)$$

$$\phi_{tt} \Big|_{y=0} = -\omega^2 \alpha_0 S_0 C + S_\omega \sum_{n=1}^{\infty} \omega^2 \alpha_n S_n \quad (5-29)$$

$$\eta_x^{(2)} = -\frac{\alpha_0 \omega}{g} C_0 C - C_\omega \sum_{n=1}^{\infty} \frac{\omega}{g} \alpha_n C_n \quad (5-30)$$

$$\eta_t^{(2)} = \frac{\omega^2}{g} C_0 C + \frac{\omega^2}{g} S_\omega \sum_{n=1}^{\infty} C_n \quad (5-31)$$

Substitution of equations (5-25 ) through (5-31) into equation (5-5)

gives:

$$\begin{aligned} (\phi_{nh_{xx}}^{(2)} + g \phi_{nh_{yy}}^{(2)}) \Big|_{y=0} &= 3\alpha_0^2 \omega C_0^2 S C - 3\frac{\omega^3 \alpha_0}{g} C_0 S_0 S C \\ &+ 2\omega \alpha_0 C_0 \sum_{n=1}^{\infty} \alpha_n C_n [S_\omega C_\omega - C_\omega S_\omega] + \alpha_0^2 \omega C_0 C C_\omega \sum_{n=1}^{\infty} C_n - \frac{\omega^3 \alpha_0}{g} S_0 \sum_{n=1}^{\infty} C_n [2SS_\omega + CC_\omega] \\ &- \omega C_0 S S_\omega \sum_{n=1}^{\infty} \alpha_n^2 C_n + \frac{\omega^3}{g} C_0 \sum_{n=1}^{\infty} \alpha_n S_n [2CC_\omega + SS_\omega] - 2\omega C_\omega S_\omega \sum_{n=1}^{\infty} \sum_{m=1}^{\infty} \alpha_m \alpha_n C_m C_n \\ &- \omega S_\omega C_\omega \sum_{m=1}^{\infty} \sum_{n=1}^{\infty} \alpha_m^2 C_m C_n + 3\frac{\omega^3}{g} S_\omega C_\omega \sum_{m=1}^{\infty} \sum_{n=1}^{\infty} \alpha_n S_n C_m \end{aligned} \quad (5-32)$$

$$\text{Let } \phi_{nh}^{(2)} = \sum_{i=1}^3 \phi_{nh_i}^{(2)} \quad (5-33)$$

such that, with the operator  $\left[ \frac{\partial^2}{\partial x^2} + g \frac{\partial}{\partial y} \right] \Big|_{y=0}$  denoted by L,

$$L\phi_{nh_1}^{(2)} = 3\alpha_0^2 \omega C_0^2 SC - 3 \frac{\omega^3 \alpha_0}{g} C_0 S_0 SC \quad (5-34)$$

$$\begin{aligned} L\phi_{nh_2}^{(2)} = & 2\omega \alpha_0 C_0 \sum_{n=1}^{\infty} \alpha_n C_n (SC\omega - CS\omega) + \alpha_0^2 \omega C_0 CC\omega \sum_{n=1}^{\infty} C_n \\ & - \frac{\omega^3 \alpha_0}{g} S_0 \sum_{n=1}^{\infty} C_n (2SS\omega + CC\omega) - \omega C_0 SS\omega \sum_{n=1}^{\infty} \alpha_n^2 C_n \\ & + \frac{\omega^3}{g} C_0 \sum_{n=1}^{\infty} \alpha_n S_n [2CC\omega + SS\omega] \end{aligned} \quad (5-35)$$

$$\begin{aligned} L\phi_{nh_3}^{(2)} = & C_0 S_0 \omega \left[ -2\omega \sum_{m=1}^{\infty} \sum_{n=1}^{\infty} \alpha_m \alpha_n C_m C_n \right. \\ & \left. - \omega \sum_{m=1}^{\infty} \sum_{n=1}^{\infty} \alpha_m^2 C_m C_n + \frac{3\omega^3}{g} \sum_{m=1}^{\infty} \sum_{n=1}^{\infty} \alpha_m S_m C_n \right] \end{aligned} \quad (5-36)$$

Next the  $\phi_{nh_i}^{(2)}$ 's are determined such that

$$\nabla^2 \phi_{nh_i}^{(2)} = 0 \quad (5-37)$$

equations (5-34) through (5-36) are satisfied and,

$$\frac{\partial}{\partial y} \phi_{nh_i}^{(2)} \Big|_{y=-h} = 0 \quad (5-38)$$

Let

$$\phi_{nh_1}^{(2)} = A_1 \cosh 2\alpha_0(y+h) \sin(2\alpha_0 x - 2\omega t) \quad (5-39)$$

This function satisfies equations (5-37) and (5-38). In order that it also satisfies the non-homogeneous boundary condition (5-34),

$$A_1 = \frac{\frac{3}{4} A^2 \alpha_0^2 \omega (1 + \cosh 2\alpha_0 h) - \frac{3}{4} A^2 \left(\frac{\omega^3 \alpha_0}{g}\right) \sinh 2\alpha_0 h}{-4\omega^2 \cosh 2\alpha_0 h + 2\alpha_0 g \sinh 2\alpha_0 h} \quad (5-40)$$

For convenience, an equation in complex variables whose real part is equation (5-35) will be considered. In this equation, the real part of  $\phi_{nh_2}^{(2)}$  will represent the  $\phi_{nh_2}^{(2)}$  of equation (5-35). In all succeeding complex equations, this will be the case. In order to see that the real part of the complex equation is equation (5-35), the following identities will be needed.

$$CC_\omega = \mathcal{R}_e \left[ \frac{1}{2} (e^{i(\alpha_0 x - 2\omega t)} + e^{i\alpha_0 x}) \right] \quad (5-41)$$

$$SS_\omega = \mathcal{R}_e \left[ \frac{1}{2} (e^{i(\alpha_0 x - 2\omega t)} - e^{i\alpha_0 x}) \right] \quad (5-42)$$

$$2SS_\omega + CC_\omega = \mathcal{R}_e \left[ \frac{3}{2} e^{i(\alpha_0 x - 2\omega t)} - \frac{1}{2} e^{i\alpha_0 x} \right] \quad (5-43)$$

$$2CC_\omega + SS_\omega = \mathcal{R}_e \left[ \frac{3}{2} e^{i(\alpha_0 x - 2\omega t)} + \frac{1}{2} e^{i\alpha_0 x} \right] \quad (5-44)$$

$$SC_\omega - CS_\omega = \mathcal{R}_e \left[ -ie^{i(\alpha_0 x - 2\omega t)} \right] \quad (5-45)$$

The complex equation to be considered is:

$$\begin{aligned} \mathcal{Q}_{n_2}^{(2)} = \sum_{n=1}^{\infty} A b_n e^{\alpha_n x} \left\{ -2i\omega \alpha_0 \alpha_n \cosh \alpha_n h \cos \alpha_n h e^{i(\alpha_0 x - 2\omega t)} \right. \\ \left. + \frac{1}{2} \alpha_0^2 \omega \cosh \alpha_n h \cos \alpha_n h (e^{i(\alpha_0 x - 2\omega t)} + e^{i\alpha_0 x}) \right. \\ \left. - \frac{\omega^3 \alpha_0}{g} \sinh \alpha_n h \cos \alpha_n h \left( \frac{3}{2} e^{i(\alpha_0 x - 2\omega t)} - \frac{1}{2} e^{i\alpha_0 x} \right) \right. \\ \left. - \frac{1}{2} \omega \alpha_n^2 \cosh \alpha_n h \cos \alpha_n h (e^{i(\alpha_0 x - 2\omega t)} - e^{i\alpha_0 x}) \right. \\ \left. + \frac{\omega^3}{g} \alpha_n \cosh \alpha_n h \sin \alpha_n h \left( \frac{3}{2} e^{i(\alpha_0 x - 2\omega t)} + \frac{1}{2} e^{i\alpha_0 x} \right) \right\} \end{aligned} \quad (5-46)$$

Let

$$\begin{aligned} D_{S_n} = \frac{1}{2} \alpha_0^2 \omega \cosh \alpha_n h \cos \alpha_n h + \frac{\omega^3 \alpha_0}{2g} \sinh \alpha_n h \cos \alpha_n h \\ + \frac{\omega \alpha_n^2}{2} \cosh \alpha_n h \cos \alpha_n h + \frac{\omega^3 \alpha_n}{2g} \cosh \alpha_n h \sin \alpha_n h \end{aligned} \quad (5-47)$$

and

$$\begin{aligned}
D_{J_n} = & -2i\omega\alpha_0\alpha_n \cosh\alpha_0 h \cos\alpha_n h + \frac{\alpha_0^2\omega}{2} \cosh\alpha_0 h \cos\alpha_n h \\
& - \frac{3}{2} \frac{\omega^3\alpha_0}{g^2} \sinh\alpha_0 h \cos\alpha_n h \\
& - \frac{\omega\alpha_n^2}{2} \cosh\alpha_0 h \cos\alpha_n h + \frac{\omega^3\alpha_n}{2g} \cosh\alpha_0 h \sin\alpha_n h
\end{aligned} \tag{5-48}$$

Then equation (5-46) can be written as:

$$\phi_{nh_2}^{(2)} = \sum_{n=1}^{\infty} A_n b_n \left[ D_{S_n} e^{x(i\alpha_0 + \alpha_n)} + D_{J_n} e^{x(i\alpha_0 + \alpha_n) - i2\omega t} \right] \tag{5-49}$$

The solution to equation (5-37) which satisfies the boundary conditions (5-38) and (5-49) is a series, each term of which is the sum of two oblique travelling waves (see Chapter 8) plus a steady component with a spatial dependence similar to that of the travelling waves. It is assumed that the series converges uniformly. Equation (5-49) shows that the time dependence of the oblique waves must be sinusoidal with radian frequency  $2\omega$ .

Let

$$\begin{aligned}
\phi_{nh_2}^{(2)} = & \sum_{n=1}^{\infty} \left\{ A_{21n} e^{x(i\alpha_0' \cos\theta_n + \alpha_0' \sin\theta_n) + y(-i\alpha_0' \sin\theta_n + \alpha_0' \cos\theta_n) - i2\omega t} \right. \\
& + A_{22n} e^{x(i\alpha_0' \cos\theta_n + \alpha_0' \sin\theta_n) + y(i\alpha_0' \sin\theta_n - \alpha_0' \cos\theta_n) - i2\omega t} \\
& + A_{23n} e^{x(i\alpha_0' \cos\theta_n + \alpha_0' \sin\theta_n) + y(-i\alpha_0' \sin\theta_n + \alpha_0' \cos\theta_n)} \\
& \left. + A_{24n} e^{x(i\alpha_0' \cos\theta_n + \alpha_0' \sin\theta_n) + y(i\alpha_0' \sin\theta_n - \alpha_0' \cos\theta_n)} \right\}
\end{aligned} \tag{5-50}$$

$\theta$  is the obliqueness angle

It has been anticipated that  $\theta$  will depend on  $n$ .

Let

$$-i\alpha'_0 \sin \theta_n + \alpha'_0 \cos \theta_n = \bar{F}_n \quad (5-51)$$

$$i\alpha'_0 \cos \theta_n + \alpha'_0 \sin \theta_n = i\bar{F}_n \quad (5-52)$$

Use of equations (5-51) and (5-52) in equation (5-50) gives:

$$\begin{aligned} \Phi_{nh_2}^{(2)} = \sum_{n=1}^{\infty} \left[ A_{21n} e^{i\bar{F}_n x + \bar{F}_n y - 2i\omega t} + A_{22n} e^{i\bar{F}_n x - \bar{F}_n y - 2i\omega t} \right. \\ \left. + A_{23n} e^{i\bar{F}_n x + \bar{F}_n y} + A_{24n} e^{i\bar{F}_n x - \bar{F}_n y} \right] \quad (5-53) \end{aligned}$$

$$\begin{aligned} \mathcal{L}\Phi_{nh_2}^{(2)} = \sum_{n=1}^{\infty} \left[ (-4\omega^2 + g\bar{F}_n) A_{21n} e^{i\bar{F}_n x - 2i\omega t} \right. \\ \left. + (-4\omega^2 - g\bar{F}_n) A_{22n} e^{i\bar{F}_n x - 2i\omega t} \right. \\ \left. + g\bar{F}_n A_{23n} e^{i\bar{F}_n x} - g\bar{F}_n A_{24n} e^{i\bar{F}_n x} \right] \quad (5-54) \end{aligned}$$

$$\begin{aligned} \frac{\partial}{\partial y} \Phi_{nh_2}^{(2)} \Big|_{y=h} = \sum_{n=1}^{\infty} \left[ (\bar{F}_n A_{21n} e^{-\bar{F}_n h} - \bar{F}_n A_{22n} e^{\bar{F}_n h}) e^{i\bar{F}_n x - 2i\omega t} \right. \\ \left. + (\bar{F}_n A_{23n} e^{-\bar{F}_n h} - \bar{F}_n A_{24n} e^{\bar{F}_n h}) e^{i\bar{F}_n x} \right] \quad (5-55) \end{aligned}$$

Equation (5-38) is satisfied if

$$A_{21n} e^{-\bar{F}_n h} - A_{22n} e^{\bar{F}_n h} = 0 \quad (5-56)$$

and

$$A_{23n} e^{-F_n h} - A_{24n} e^{F_n h} = 0 \quad (5-57)$$

Equations (5-49) and (5-54) imply:

$$F_n = \alpha_0 - i\alpha_n \quad (5-58)$$

$$g F_n (A_{23n} - A_{24n}) = D_{5n} \quad (5-59)$$

$$(-4\omega^2 + g F_n) A_{21n} + (-4\omega^2 - g F_n) A_{22n} = D_{5n} \quad (5-60)$$

Equations (5-51) and (5-58) imply

$$\tan \theta_n = \frac{\alpha_n}{\alpha_0} \quad (5-61)$$

With  $F_n$  given by equation (5-58), equations (5-56), (5-57), (5-59) and (5-60) are four simultaneous algebraic equations whose inversion gives the values of  $A_{21n}$ ,  $A_{22n}$ ,  $A_{23n}$  and  $A_{24n}$ .

$\phi_{nh_3}^{(2)}$  will be determined in the form of a double infinite series such

that  $L$  operating on the  $mn$ 'th term of the series equals the  $mn^{4h}$  term on the right-hand side of equation (5-36) and each term of the series satisfies equation (5-37) and boundary condition (5-38). The series is assumed to converge uniformly.

Equation (5-36) is now rewritten with the substitution of the identity:

$$C_\omega S_\omega = \frac{1}{2} \sin 2\omega t \quad (5-63)$$

and the definition

$$\mathcal{L}\phi_{nh_3}^{(2)} = \sum_{m=1}^{\infty} \sum_{n=1}^{\infty} \frac{b_m b_n}{2} e^{\alpha_{mn} x} \sin 2\omega t \left[ -2\omega \alpha_m \alpha_n \cos \alpha_m h \cos \alpha_n h \right. \\ \left. - \omega \alpha_m^2 \cos \alpha_m h \cos \alpha_n h + \frac{3\omega^3}{g} \alpha_m \sin \alpha_m \cos \alpha_n h \right] \quad (5-64)$$

(5-65)

$$\text{Let } D_{mn} = \frac{b_m b_n}{2} \left[ -2\omega \alpha_m \alpha_n \cos \alpha_m h \cos \alpha_n h \right. \\ \left. - \omega \alpha_m^2 \cos \alpha_m h \cos \alpha_n h + \frac{3\omega^3}{g} \alpha_m \sin \alpha_m \cos \alpha_n h \right]$$

(5-66)

$$\mathcal{L}\phi_{nh_3}^{(2)} = \sum_{m=1}^{\infty} \sum_{n=1}^{\infty} D_{mn} e^{\alpha_{mn} x} \sin 2\omega t \quad (5-67)$$

Let

$$\phi_{nh_3}^{(2)} = \sum_{m=1}^{\infty} \sum_{n=1}^{\infty} A_{3mn} \sin 2\omega t e^{\alpha_{mn} x} \cos \alpha_{mn} (y+h) \quad (5-68)$$

This satisfies equation (5-37) and boundary condition (5-38).

Next, let L operate on equation (5-68)

$$\mathcal{L}\phi_{nh_3}^{(2)} = \sum_{m=1}^{\infty} \sum_{n=1}^{\infty} A_{3mn} \sin 2\omega t e^{\alpha_{mn}x} (-4\omega^2 \cos \alpha_{mn}h - g\alpha_{mn} \sin \alpha_{mn}h) \quad (5-69)$$

Thus the boundary condition (5-36) is satisfied if:

$$A_{3mn} = \frac{D_{mn}}{-4\omega^2 \cos \alpha_{mn}h - g\alpha_{mn} \sin \alpha_{mn}h} \quad (5-70)$$

Equation (5-33) can now be written in more detail as:

$$\begin{aligned} \phi_{nh}^{(2)} = & A_1 \cosh 2\alpha_0(y+h) \sin(2\alpha_0x - 2\omega t) + \sum_{n=1}^{\infty} \left\{ A_{21n} e^{i\beta_n x + \beta_n y - i2\omega t} \right. \\ & + A_{22n} e^{i\beta_n x - \beta_n y - i2\omega t} + A_{23n} e^{i\beta_n x + \beta_n y} + A_{24n} e^{i\beta_n x - \beta_n y} \left. \right\} \\ & + \sum_{m=1}^{\infty} \sum_{n=1}^{\infty} A_{3mn} \sin 2\omega t e^{\alpha_{mn}x} \cos \alpha_{mn}(y+h) \end{aligned} \quad (5-71)$$

Next  $\phi_h^{(2)}$  and  $\theta^{(2)}(t)$  will be determined such that there is no reflected energy radiating second order wave.

From the form of  $\phi_{nh}^{(2)}$ , it is anticipated that  $\phi_h^{(2)}$  will have a steady part and a non-steady part with time dependence  $e^{+i2\omega t}$

$$\phi_k^{(2)} = \phi_{k_s}^{(2)}(x, y) + \phi_{k_{ns}}^{(2)}(x, y, t) \quad (5-72)$$

Seeking separable solutions for  $\phi_{hs}^{(2)}(x, y)$  and  $\phi_{hns}^{(2)}(x, y, t)$  leads to two

Sturm-Liouville problems.

For the non-steady part, the eigenfunctions have the form:

$$\phi_e = F(x) G(y) e^{\pm 2\omega t} \quad (5-73)$$

In order that each eigenfunction satisfy Laplace's equation,

$$\frac{F''}{F} = \nu^2 \qquad -\frac{G''}{G} = \nu^2 \quad (5-75)$$

The homogeneous boundary conditions (5-8) and (5-9) require that

$$G' = 0 \quad \text{at } y = -h \quad (5-76)$$

$$-4\omega^2 G + g G' = 0 \quad \text{at } y = 0 \quad (5-77)$$

To have finite velocity everywhere,

$$|F'| < \infty \quad \text{as } x \rightarrow -\infty \quad (5-78)$$

With the solutions to (5-75), the boundary conditions require that the eigenvalues satisfy:

$$4\omega^2 = \gamma_0 g \tanh \gamma_0 h \quad (5-79)$$

$$4\omega^2 = -\gamma_n g \tanh \gamma_n h \quad n > 0 \quad (5-80)$$

Then the solution for  $\phi_{ns}^{(2)}$  is:

$$\begin{aligned} \phi_{ns}^{(2)} = & Q_0 \cosh \gamma_0(y+h) e^{i(\gamma_0 x - 2\omega t)} \\ & + Q_0' \cosh \gamma_0(y+h) e^{i(\gamma_0 x + 2\omega t)} \\ & + \sum_{n=1}^{\infty} Q_n \cos \gamma_n(y+h) e^{\gamma_n x} e^{-i2\omega t} \end{aligned} \quad (5-81)$$

From Sturm-Liouville theory it is known that the infinite sum of the  $\phi_{e's}$  is complete in the sense that the series can be made to converge to any square integrable function of  $y$  at  $x = 0$ . The same is true for the derivative of the series with respect to  $x$ . For the steady part the eigenfunctions have the form:

$$\phi_e = \bar{F}(x) G(y) \quad (5-82)$$

Since the eigenfunctions are to satisfy Laplace's equation,

$$\frac{\bar{F}''}{\bar{F}} = \gamma^2 \quad (5-83)$$

$$-\frac{G''}{G} = \gamma^2 \quad (5-84)$$

The homogenous boundary conditions (5-7) and (5-8) require that:

$$G' = 0 \text{ at } y = -h \quad (5-76)$$

$$G' = 0 \text{ at } y = 0 \quad (5-85)$$

For finite velocity everywhere,

$$|F'| < \infty \text{ as } x \rightarrow -\infty \quad (5-86)$$

These boundary conditions require that the eigenvalues satisfy

$$\gamma_n = \frac{n\pi}{h} \quad (5-87)$$

with the corresponding eigenfunctions

$$\phi_{en} = e^{\frac{n\pi x}{h}} \cos \frac{n\pi y}{h} \quad (5-88)$$

The complete solution for  $\phi_{hs}^{(2)}$  is therefore:

$$\phi_{hs}^{(2)} = \sum_{n=1}^{\infty} D_n e^{\frac{n\pi x}{h}} \cos \frac{n\pi y}{h} \quad (5-89)$$

Now the form of  $\phi^{(2)}$  can be written in full detail.

$$\begin{aligned}
\Phi^{(2)} = & A_1 \cosh 2\alpha_0(y+h) \sin(2\alpha_0 x - 2\omega t) \\
& + \sum_{n=1}^{\infty} \left\{ A_{21n} e^{i\beta_n x + \beta_n y - i2\omega t} + A_{22n} e^{i\beta_n x - \beta_n y - i2\omega t} + A_{23n} e^{i\beta_n x + \beta_n y} \right. \\
& \left. + A_{24n} e^{i\beta_n x - \beta_n y} \right\} + \sum_{m=1}^{\infty} \sum_{n=1}^{\infty} A_{3mn} \sin 2\omega t e^{\alpha_{mn} x} \cos \alpha_{mn}(y+h) \\
& + Q_0 \cosh \gamma_0(y+h) e^{i(\gamma_0 x - 2\omega t)} + Q'_0 \cosh \gamma_0(y+h) e^{i(\gamma_0 x + 2\omega t)} \\
& + \sum_{n=1}^{\infty} Q_n \cos \gamma_n(y+h) e^{\gamma_n x} e^{-i2\omega t} \\
& + \sum_{n=1}^{\infty} D_n e^{\frac{n\pi x}{h}} \cos \frac{n\pi y}{h}
\end{aligned}$$

(5-90)

The Q's and D's must be chosen **such** that the second order boundary condition at  $x = 0$  (3-10) is satisfied. The functions needed in equation (3-16) are:

$$\Phi_y^{(2)} \Big|_{x=0} = \alpha_0 A \sinh \alpha_0(y+h) \cos \omega t - \sum_{n=1}^{\infty} \alpha_n b_n \sin \alpha_n(y+h) \sin \omega t \quad (5-91)$$

$$\Phi_{xx} \Big|_{x=0} = -\alpha_0^2 A \cosh \alpha_0(y+h) \cos \omega t - \sum_{n=1}^{\infty} \alpha_n^2 b_n \cos \alpha_n(y+h) \sin \omega t \quad (5-92)$$

$$\theta^{(1)} = B^{(1)} \cos \omega t \quad (5-93)$$

$$\theta^{(2)} = B^{(2)} e^{-i2\omega t} \quad (5-94)$$

Those functions which appear in products of functions must be written in real function form. Substitution of the preceding functions in equation (3-16) yields the real part of the following equation.

$$\begin{aligned} & i\gamma_0 Q_0 \cosh \gamma_0(y+h) e^{-i2\omega t} + i\gamma_0 Q_0' \cosh \gamma_0(y+h) e^{i2\omega t} \\ & + \sum_{n=1}^{\infty} \gamma_n Q_n \cos \gamma_n(y+h) e^{-i2\omega t} + \sum_{n=1}^{\infty} \frac{n\pi}{k} D_n \cos \frac{n\pi y}{k} \\ & + 2A_2 \alpha_0 \cosh 2\alpha_0(y+h) e^{-i2\omega t} \\ & + \sum \left\{ iF_n A_{21n} e^{\alpha_n y - i2\omega t} + iF_n A_{22n} e^{-\alpha_n y - i2\omega t} \right. \\ & \quad \left. + iF_n A_{23n} e^{\alpha_n y} + iF_n A_{24n} e^{-\alpha_n y} \right\} \\ & + \sum \sum i\alpha_{mn} A_{3mn} \cos \alpha_{mn}(y+h) e^{-i2\omega t} = \\ & \left. \begin{aligned} & -i2\omega(y+\beta) B^{(2)} e^{-i2\omega t} + \frac{1}{2} B^{(2)} \alpha_0 A \sinh \alpha_0(y+h) \\ & + \frac{1}{2} B^{(2)} \alpha_0 A \sinh \alpha_0(y+h) e^{-i2\omega t} + \frac{1}{2} (y+\beta) B^{(2)} \alpha_0^2 A \cosh \alpha_0(y+h) \\ & + \frac{1}{2} (y+\beta) B^{(2)} \alpha_0^2 A \cosh \alpha_0(y+h) e^{-i2\omega t} \\ & - \frac{1}{2} \sum i B^{(2)} \alpha_n b_n \sin \alpha_n(y+h) e^{-i2\omega t} \\ & - \frac{1}{2} \sum i (y+\beta) B^{(2)} \alpha_n^{(2)} b_n \cos \alpha_n(y+h) e^{-i2\omega t} \end{aligned} \right\} \quad \begin{array}{l} y \geq -\beta \\ \\ \\ \\ \\ y < -\beta \end{array} \\ & 0 \end{aligned}$$

(5-95)

Equation (5-95) implies the following two equations

$$\begin{aligned}
 & i \gamma_0 Q_0 \cosh \gamma_0 (y+h) - i \gamma_0 \bar{Q}_0' \cosh \gamma_0 (y+h) + \sum_{n=1}^{\infty} \gamma_n Q_n \cos \gamma_n (y+h) \\
 & + 2 A_2 \alpha_0 \cosh 2\alpha_0 (y+h) + \sum_{n=1}^{\infty} \left\{ F_n A_{21n} e^{F_n y} + i F_n A_{22n} e^{-F_n y} \right\} \\
 & + \sum_{m=1}^{\infty} \sum_{n=1}^{\infty} i \alpha_{mn} A_{3mn} \cos \alpha_{mn} (y+h) =
 \end{aligned}$$

$$\left\{ \begin{aligned}
 & -i 2\omega (y+\beta) B^{(2)} e^{-i2\omega t} + \frac{1}{2} B^{(3)} \alpha_0 A \sinh \alpha_0 (y+h) \\
 & + \frac{1}{2} (y+\beta) B^{(2)} \alpha_0^2 A \cosh \alpha_0 (y+h) \\
 & - \frac{1}{2} \sum_{n=1}^{\infty} i B^{(2)} \alpha_n b_n \sin \alpha_n (y+h) \\
 & - \frac{1}{2} \sum_{n=1}^{\infty} i (y+\beta) B^{(2)} \alpha_n^2 b_n \cos \alpha_n (y+h) \qquad y \geq -\beta \\
 & 0 \qquad \qquad \qquad y < -\beta
 \end{aligned} \right.$$

$$\sum_{n=1}^{\infty} \frac{n\pi}{h} D_n \cos \frac{n\pi y}{h} + \sum_{n=1}^{\infty} \left\{ i F_n A_{21n} e^{F_n y} + i F_n A_{22n} e^{-F_n y} \right\} \quad (5-96)$$

$$= \left\{ \begin{aligned}
 & \left( \frac{1}{2} B^{(2)} \alpha_0 A \sinh \alpha_0 (y+h) + \frac{1}{2} B^{(2)} \alpha_0^2 A (y+\beta) \cosh \alpha_0 (y+h) \right) \qquad y \geq -\beta \\
 & 0 \qquad \qquad \qquad y < -\beta
 \end{aligned} \right.$$

(5-97)

$\overline{Q'}$  is the complex conjugate of  $Q'$ .

The only second order energy radiating wave which would exist in the absence of a termination to the tank is given by the term containing the coefficient  $A_1$ . The first three terms on the left-hand side of equation (5-96) form a complete set of square integrable functions. The functions they are to equal will be adjusted so that  $Q_0$  and  $Q'_0$  will be zero. This adjustment will be accomplished by adjusting  $B^{(2)}$ . The value of  $B^{(2)}$  which gives the desired result is unique. This value will be determined by setting  $Q_0$  and  $Q'_0$  to zero, multiplying equation (5-96) by  $\cosh \gamma_0 (y+h)$  and integrating from  $y = -h$  to  $y = 0$ .

The following notation will be used for the various integrals:

$$I_1^{(2)} = \int_{-h}^0 (y+\beta) \cosh \gamma_0 (y+h) dy \quad (5-98)$$

$$I_2^{(2)} = \int_{-h}^0 \sinh \alpha_0 (y+h) \cosh \gamma_0 (y+h) dy \quad (5-99)$$

$$I_3^{(2)} = \int_{-h}^0 (y+\beta) \cosh \alpha_0 (y+h) \cosh \gamma_0 (y+h) dy \quad (5-100)$$

$$I_{A_n}^{(2)} = \int_{-h}^0 \sin \alpha_n (y+h) \cosh \gamma_0 (y+h) dy \quad (5-101)$$

$$\tilde{L}_{5n}^{(2)} = \int_{-p}^0 (y+p) \cos \alpha_n(y+h) \cosh \gamma_0(y+h) dy \quad (5-102)$$

$$\tilde{L}_{6n}^{(2)} = \int_{-h}^0 e^{\beta_n y} \cosh \gamma_0(y+h) dy \quad (5-103)$$

$$\tilde{L}_{7n}^{(2)} = \int_{-h}^0 e^{-\beta_n y} \cosh \gamma_0(y+h) dy \quad (5-104)$$

$$\tilde{L}_8^{(2)} = \int_{-h}^0 \cosh \alpha_0(y+h) \cosh \gamma_0(y+h) dy \quad (5-105)$$

$$\tilde{L}_{9mn}^{(2)} = \int_{-h}^0 \cos \alpha_{mn}(y+h) \cosh \gamma_0(y+h) dy \quad (5-106)$$

The evaluation of these integrals appears in appendix E

With this notation

$$\begin{aligned} B^{(2)} = & \frac{1}{i2\omega \tilde{L}_1^{(2)}} \left[ \frac{1}{2} B^{(1)} \alpha_0 A \tilde{L}_2^{(2)} + \frac{1}{2} B^{(1)} \alpha_0^2 A \tilde{L}_3^{(2)} \right. \\ & + \sum_{n=1}^{\infty} \left( -\frac{1}{2} i B^{(1)} \alpha_n b_n \tilde{L}_4^{(2)} - \frac{1}{2} i B_n \alpha_n^2 \tilde{L}_5^{(2)} - i \beta_n A_{22n} \tilde{L}_6^{(2)} - i \beta_n A_{22n} \tilde{L}_7^{(2)} \right) \\ & \left. - 2 A_1 \alpha_0 \tilde{L}_8^{(2)} - \sum_{m=1}^{\infty} \sum_{n=1}^{\infty} i A_{3mn} \alpha_{mn} \tilde{L}_{9mn}^{(2)} \right] \end{aligned}$$

(5-107)

The  $Q_n$ 's will be determined by multiplying equation (5-96) by  $\cos \gamma_n (y+h)$  and integrating from  $y = -h$  to  $y = 0$ . The values of the following integrals will be needed:

$$\int_{-h}^0 \cos \gamma_n (y+h) \cos \gamma_m (y+h) dy = 0 \quad \text{for } n \neq m \quad (5-108)$$

$$\tilde{I}_{10n}^{(2)} = \int_{-h}^0 \cos^2 \gamma_n (y+h) dy \quad (5-109)$$

$$\tilde{I}_{11n}^{(2)} = \int_{-p}^0 (y+p) \cos \gamma_n (y+h) dy \quad (5-110)$$

$$\tilde{I}_{12n}^{(2)} = \int_{-h}^0 \sinh \alpha_0 (y+h) \cos \gamma_n (y+h) dy \quad (5-111)$$

$$\tilde{I}_{13n}^{(2)} = \int_{-p}^0 (y+p) \cosh \alpha_0 (y+h) \cos \gamma_n (y+h) dy \quad (5-112)$$

$$\tilde{I}_{14nj}^{(2)} = \int_{-h}^0 \sin \alpha_j (y+h) \cos \gamma_n (y+h) dy \quad (5-113)$$

$$\tilde{I}_{15nj}^{(2)} = \int_{-p}^0 (y+p) \cos \alpha_j (y+h) \cos \gamma_n (y+h) dy \quad (5-114)$$

$$\tilde{I}_{16nj}^{(2)} = \int_{-h}^0 e^{\beta_j y} \cos \gamma_n (y+h) dy \quad (5-115)$$

$$\tilde{L}_{17n_j}^{(2)} = \int_{-h}^0 e^{-\tilde{F}_j y} \cos \gamma_n (y+h) dy \quad (5-116)$$

$$\tilde{L}_{18n}^{(2)} = \int_{-h}^0 \cosh 2\alpha_0 (y+h) \cos \gamma_n (y+h) dy \quad (5-117)$$

$$\tilde{L}_{19n_{jk}}^{(2)} = \int_{-h}^0 \cos \alpha_{jk} (y+h) \cos \gamma_n (y+h) dy \quad (5-118)$$

An expression for  $Q_n$  using the above notation follows.

$$\begin{aligned} Q_n = & \frac{1}{\gamma_n \tilde{L}_{10n}^{(2)}} \left[ -i2\omega B^{(2)} \tilde{L}_{11n}^{(2)} + \frac{1}{2} B^{(2)} \alpha_0 A \tilde{L}_{12n}^{(2)} \right. \\ & + \frac{1}{2} B^{(2)} \alpha_0^2 A \tilde{L}_{13n}^{(2)} - \sum_{j=1}^{\infty} \frac{1}{2} i B^{(2)} \alpha_j b_j \tilde{L}_{14n_j}^{(2)} \\ & - \sum_{j=1}^{\infty} \frac{1}{2} i B^{(2)} \alpha_j^2 b_j \tilde{L}_{15n_j}^{(2)} \\ & - \sum_{j=1}^{\infty} i \tilde{F}_j (A_{21j} \tilde{L}_{16n_j}^{(2)} + A_{22j} \tilde{L}_{17n_j}^{(2)}) \\ & \left. - 2A_1 \alpha_0 \tilde{L}_{18n}^{(2)} - \sum_{j=1}^{\infty} \sum_{k=1}^{\infty} i \alpha_{jk} A_{3jk} \tilde{L}_{19n_{jk}}^{(2)} \right] \quad (5-119) \end{aligned}$$

In order to determine the  $D_n$ 's equation (5-97) is multiplied by

$\cos \frac{m \pi y}{h}$  and the resulting equation integrated from  $y = -h$  to  $y = 0$ .

$$\int_{-h}^0 \cos \frac{m \pi y}{h} \cos \frac{n \pi y}{h} dy = \frac{h}{2} \delta_{mn} \quad (5-120)$$

Let

$$\tilde{L}_{20n} = \int_{-b}^0 \sinh \alpha_0 (y+h) \cos \frac{n \pi y}{h} dy \quad (5-121)$$

$$\tilde{L}_{21n} = \int_{-b}^0 (y+b) \cosh \alpha_0 (y+h) \cos \frac{n \pi y}{h} dy \quad (5-122)$$

$$\tilde{L}_{22nj} = \int_{-h}^0 e^{\tilde{F}_j y} \cos \frac{n \pi y}{h} dy \quad (5-123)$$

$$\tilde{L}_{23nj} = \int_{-h}^0 e^{-\tilde{F}_n y} \cos \frac{n \pi y}{h} dy \quad (5-124)$$

Using this notation,  $D_n$  can be expressed as follows:

$$\begin{aligned} D_n = & \frac{2}{n \pi} \left[ \frac{1}{2} B^{(2)} \alpha_0 \mathcal{A} \tilde{L}_{20n}^{(2)} + \frac{1}{2} B^{(2)} \alpha_0^2 \mathcal{A} \tilde{L}_{21n}^{(2)} \right. \\ & \left. - \sum_{j=1}^{\infty} i \tilde{F}_j \mathcal{A}_{23j} \tilde{L}_{22nj}^{(2)} - \sum_{j=1}^{\infty} i \tilde{F}_j \mathcal{A}_{24j} \tilde{L}_{23nj}^{(2)} \right] \quad (5-125) \end{aligned}$$

A listing of expressions for the various I's appears in appendix E.

Waves in the Region  $0 \leq x \leq l$

As in the previous section,  $\phi^{(2)}$  will be found in the form of a non-homogeneous part plus a homogeneous part. Equations (5-3) through (5-10) must be satisfied. In addition to these requirements, the boundary condition of no velocity normal to the wall at  $x = l$  must be satisfied.

$$\phi_x = 0 \quad \text{at } x=l \quad (5-126)$$

This homogeneous linear condition will be satisfied by making each additive term of the solution satisfy the same condition. The functions  $\phi^{(1)}$  and  $\eta^{(1)}$  are determined in Chapter 4.

$$\begin{aligned} \phi^{(2)} = & N_0 \cosh \alpha_0(y+h) \cos \alpha_0(x-l) \sin \omega t \\ & + \sum_{n=1}^{\infty} N_n \cos \alpha_n(y+h) \cosh \alpha_n(x-l) \sin \omega t \end{aligned} \quad (5-127)$$

$$\begin{aligned} \eta^{(2)} = & -\frac{\omega}{g} N_0 \cosh \alpha_0 h \cos \alpha_0(x-l) \cos \omega t \\ & - \frac{\omega}{g} \sum_{n=1}^{\infty} N_n \cos \alpha_n h \cosh \alpha_n(x-l) \cos \omega t \end{aligned} \quad (5-128)$$

The first order functions needed in equation (5-5) are listed below:

$$\begin{aligned} \phi_x^{(2)} \Big|_{y=0} = & -\alpha_0 N_0 \cosh \alpha_0 h \sin \alpha_0(x-l) \sin \omega t \\ & + \sum_{n=1}^{\infty} \alpha_n N_n \cos \alpha_n h \sinh \alpha_n(x-l) \sin \omega t \end{aligned} \quad (5-129)$$

$$\begin{aligned} \Phi_{yy}^{(2)}|_{y=0} &= \alpha_0^2 N_0 \cosh \alpha_0 h \cos \alpha_0 (x-l) \sin \omega t \\ &+ \sum_{n=1}^{\infty} -\alpha_n^2 \cos \alpha_n h \cosh \alpha_n (x-l) \sin \omega t \end{aligned}$$

(5-130)

$$\begin{aligned} \Phi_{xy}^{(2)}|_{y=0} &= \alpha_0 \omega N_0 \sinh \alpha_0 h \cos \alpha_0 (x-l) \cos \omega t \\ &- \sum_{n=1}^{\infty} \alpha_n \omega N_n \sin \alpha_n h \cosh \alpha_n (x-l) \cos \omega t \end{aligned}$$

(5-131)

$$\begin{aligned} \Phi_{tty}^{(2)}|_{y=0} &= -\omega^2 \alpha_0 N_0 \sinh \alpha_0 h \cos \alpha_0 (x-l) \sin \omega t \\ &+ \sum_{n=1}^{\infty} \omega^2 \alpha_n N_n \sin \alpha_n h \cosh \alpha_n (x-l) \sin \omega t \end{aligned}$$

(5-132)

$$\begin{aligned} \eta_x &= \frac{\omega \alpha_0}{g} N_0 \cosh \alpha_0 h \sin \alpha_0 (x-l) \cos \omega t \\ &- \frac{\omega}{g} \sum_{n=1}^{\infty} \alpha_n N_n \cos \alpha_n h \sinh \alpha_n (x-l) \end{aligned}$$

(5-133)

$$\begin{aligned} \eta_c &= \frac{\omega^2}{g} N_0 \cosh \alpha_0 h \cos \alpha_0 (x-l) \sin \omega t \\ &+ \frac{\omega^2}{g} \sum_{n=1}^{\infty} N_n \cos \alpha_n h \cosh \alpha_n (x-l) \sin \omega t \end{aligned}$$

(5-134)

A simplified notation, like that used in the previous section, will be used here. Although the symbols used mean different things in each section, their use is only intermediary and no confusion should result.

Let

$$N_0 \cosh \alpha_0 h = C_0 \quad (5-135) \quad N_0 \sinh \alpha_0 h = S_0 \quad (5-136)$$

$$\cos \alpha_0 (x-l) = C \quad (5-137) \quad \sin \alpha_0 (x-l) = S \quad (5-138)$$

$$N_n \cos \alpha_n h = C_n \quad (5-139) \quad N_n \sin \alpha_n h = S_n \quad (5-140)$$

$$\cosh \alpha_n (x-l) = Ch_n \quad (5-141) \quad \sinh \alpha_n (x-l) = Sh_n \quad (5-142)$$

$$\cos \omega t = C_\omega \quad (5-143) \quad \sin \omega t = S_\omega \quad (5-144)$$

Substitution of equations (5-129) through (5-144) into equation (5-5) gives:

$$\begin{aligned}
\phi_{nhx}^{(2)} + g \phi_{nhy}^{(2)} \Big|_{y=0} &= S_\omega C_\omega \left\{ \alpha_0^2 \omega C_0^2 (C^2 - 2S^2) - 3 \frac{\omega^3}{g} \alpha_0 S_0 C_0 C^2 \right. \\
&+ 4 \omega \alpha_0 C_0 S \sum_{n=1}^{\infty} \alpha_n C_n S h_n + \omega C_0 C (\alpha_0^2 \sum_{n=1}^{\infty} C_n C h_n - \sum_{n=1}^{\infty} \alpha_n^2 C_n C h_n) \\
&- 3 \alpha_0 \frac{\omega^3}{g} S_0 C \sum_{n=1}^{\infty} C_n C h_n + 3 \frac{\omega^3}{g} C_0 C \sum_{n=1}^{\infty} \alpha_n S_n C h_n \\
&\left. + \omega (-2 \sum_{m=1}^{\infty} \sum_{n=1}^{\infty} \alpha_m \alpha_n C_m C_n S h_m S h_n - \sum_{m=1}^{\infty} \sum_{n=1}^{\infty} \alpha_m^2 C_m C_n C h_m C h_n) \right\}
\end{aligned}$$

(5-145)

Let

$$\phi_{nh}^{(2)} = \sum_{i=1}^3 \phi_{nh_i}^{(2)} \tag{5-33}$$

$$\phi_{nh_1}^{(2)} = \alpha_0 \omega C_0 S_\omega C_\omega \left[ \alpha_0 C_0 (C^2 - 2S^2) - \frac{3\omega^2}{g} S_0 C^2 \right] \tag{5-146}$$

$$\begin{aligned}
\phi_{nh_2}^{(2)} &= \omega S_\omega C_\omega \sum_{n=1}^{\infty} \left( 4 \alpha_0 \alpha_n C_0 S C_n S h_n - \alpha_n^2 C_0 C C_n C h_n \right. \\
&\quad \left. - 3 \alpha_0 \frac{\omega^2}{g} S_0 C C_n C h_n + 3 \frac{\omega^2}{g} \alpha_n C_0 C S_n C h_n + \alpha_0^2 C_0 C C_n C h_n \right)
\end{aligned} \tag{5-147}$$

$$\phi_{nh_3}^{(2)} = -\omega S_\omega C_\omega \sum_{m=1}^{\infty} \sum_{n=1}^{\infty} \alpha_m C_m C_n (\alpha_n S h_m S h_n + \alpha_m C h_m C h_n) \tag{5-148}$$

As was done in the preceding section, the  $\phi_{nh_1}^{(2)}$ 's will be determined such

that

$$\nabla^2 \phi_{nh_1}^{(2)} = 0 \quad (5-37)$$

and

$$\frac{\partial}{\partial y} \phi_{nh_1}^{(2)} = 0 \quad (5-38)$$

In the region  $0 \leq x \leq l$ , each of the  $\phi_{nh_1}^{(2)}$ 's will also satisfy:

$$\frac{\partial}{\partial x} \phi_{nh_1}^{(2)} = 0 \text{ at } x=l \quad (5-149)$$

Let

$$\begin{aligned} \phi_{nh_1}^{(2)} = & G_{11} \cosh 2\alpha_0(y+h) \cos 2\alpha_0(x-l) \sin 2\omega t \\ & + G_{12} \sin 2\omega t \end{aligned} \quad (5-150)$$

In order that  $\phi_{nh_1}^{(2)}$  satisfy equation (5-146),

$$G_{11} = \frac{\alpha_0 \omega N_0^2 \cosh \alpha_0 h (\alpha_0 \cosh \alpha_0 h + 3 \frac{\omega^2}{g} \sinh \alpha_0 h)}{\omega^2 \cosh 2\alpha_0 h - \frac{1}{2} \alpha_0 g \sinh 2\alpha_0 h} \quad (5-151)$$

and

$$G_{12} = \frac{\alpha_0}{16\omega} N_0^2 \cosh \alpha_0 h (\alpha_0 \cosh \alpha_0 h + 3 \frac{\omega^2}{g} \sinh \alpha_0 h) \quad (5-152)$$

Equation (5-147) is the real part of the following equation:

$$\begin{aligned} \Phi_{nh_2}^{(2)} = & \frac{\omega}{4} \sin 2\omega t \sum (i4\alpha_0\alpha_n C_0 C_n - \alpha_n^2 C_0 C_n - 3\alpha_0 \frac{\omega^2}{g} S_0 C_n \\ & + 3\frac{\omega^2}{g} \alpha_n C_0 S_n + \alpha_0^2 C_0 C_n) (e^{\frac{(i\alpha_0 + \alpha_n)(x-l) + (-i\alpha_0 + \alpha_n)(y+h)}{+l}} \end{aligned} \quad (5-153)$$

Let

$$\begin{aligned} \Phi_{nh_2}^{(2)} = & \sin 2\omega t \sum G_{2n} \cdot \left[ e^{\frac{(i\alpha_0 + \alpha_n)(x-l) + (-i\alpha_0 + i\alpha_n)(y+h)}{+l}} \right. \\ & + e^{\frac{(i\alpha_0 + \alpha_n)(x-l) + (\alpha_0 - i\alpha_n)(y+h)}{+l}} + e^{\frac{(-i\alpha_0 - \alpha_n)(x-l) + (\alpha_0 - i\alpha_n)(y+h)}{+l}} \\ & \left. + e^{\frac{(i\alpha_0 - \alpha_n)(x-l) + (-\alpha_0 + i\alpha_n)(y+h)}{+l}} \right] \end{aligned} \quad (5-154)$$

This function satisfies the lower boundary condition and the boundary condition at the end wall.

Equation (5-147) is satisfied term by term if:

$$G_{2n} = \frac{\frac{\omega}{4} [-i4\alpha_0\alpha_n C_0 C_n - \alpha_n^2 C_0 C_n - 3\alpha_0 \frac{\omega^2}{g} \alpha_n C_0 S_n + \alpha_0^2 C_0 C_n]}{e^{\frac{(-\alpha_0 + i\alpha_n)h(-4\omega^2 + g(-\alpha_0 + i\alpha_n))}{+l}} + e^{\frac{(\alpha_0 - i\alpha_n)h(-4\omega^2 + g(\alpha_0 - i\alpha_n))}{+l}}} \quad (5-155)$$

Substituting the appropriate expressions for the abbreviations in equation (5-148) gives equation (5-156):

$$\begin{aligned} \Phi_{nh_3}^{(2)} = & \frac{\omega}{2} \sin 2\omega t \sum_{m=1}^{\infty} \sum_{n=1}^{\infty} \alpha_m C_m C_n \cdot \\ & (\alpha_n \sinh \alpha_m (x-l) \sinh \alpha_n (x-l) + \alpha_m \cosh \alpha_m (x-l) \cosh \alpha_n (x-l)) \end{aligned} \quad (5-156)$$

Let

$$\alpha_m + \alpha_n = \alpha_{mn} \quad (5-157)$$

$$\alpha_m - \alpha_n = \alpha'_{mn} \quad (5-158)$$

Substitution of equations (5-157) and (5-158) into (5-156) and use of the following identities gives equation (5-161)

$$\sinh A \sinh B = \frac{1}{2} (\cosh(A+B) - \cosh(A-B)) \quad (5-159)$$

$$\cosh A \cosh B = \frac{1}{2} (\cosh(A+B) + \cosh(A-B)) \quad (5-160)$$

$$\begin{aligned} \phi_{nk_3}^{(2)} = & -\frac{\omega}{4} \sin 2\omega t \sum_{m=1}^{\infty} \sum_{n=1}^{\infty} \alpha_m C_m C_n \cdot \\ & \left[ \alpha_{mn} \cosh \alpha_{mn}(x-l) + \alpha'_{mn} \cosh \alpha'_{mn}(x-l) \right] \end{aligned} \quad (5-161)$$

Let

$$\begin{aligned} \phi_{nk_3}^{(2)} = & \sin 2\omega t \sum_{m=1}^{\infty} \sum_{n=1}^{\infty} G_{32mn} \cosh \alpha_{mn}(x-l) \cos \alpha_{mn}(y+kh) \\ & + G_{32mn} \cosh \alpha'_{mn}(x-l) \cos \alpha'_{mn}(y+kh) \end{aligned} \quad (5-162)$$

This function satisfies the boundary conditions (5-38) and (5-149). For equation (5-161) to be satisfied:

$$G_{32mn} = \frac{-\omega \alpha_m C_m C_n \alpha_{mn}}{-\omega^2 \cos \alpha_{mn} h - \frac{1}{4} g \alpha_{mn} \sin \alpha_{mn} h} \quad (5-163)$$

$$G_{2lmn} = \frac{-\omega \alpha_m C_m C_n \alpha'_{mn}}{\omega^2 \cos \alpha'_{mn} h - \frac{1}{4} g \alpha'_{mn} \sin \alpha'_{mn} h} \quad (5-164)$$

The problem for  $\phi_h^{(2)}$  in the region  $0 \leq x \leq l$  is very similar to the problem for  $\phi_h^{(2)}$  in the region  $x \leq 0$ . The eigenvalues are the same, but all the eigenfunctions are standing waves for  $0 \leq x \leq l$ .

$$\begin{aligned} \phi_h^{(2)} = & R_0 \cosh \gamma_0(y+h) \cos \gamma_0(x-l) e^{-i2\omega t} \\ & + \sum_{n=1}^{\infty} R_n \cos \gamma_n(y+h) \cosh \gamma_n(x-l) e^{-i2\omega t} \end{aligned} \quad (5-165)$$

As usual the real part of the above equation gives the physical function  $\phi_h^{(2)}$ .

The set of eigenfunctions of  $\phi_h^{(2)}$  are all of the solutions to the associated Sturm-Liouville problem and therefore they are complete in the sense that the series of eigenfunctions can be made to converge to any square integrable function at  $x = 0$  as can the derivative of the solution with respect to  $x$ .

The complete solution for  $\phi_h^{(2)}$  in the region  $0 \leq x \leq l$  can now be written as follows.

$$\begin{aligned}
\phi^{(2)} = & \left\{ i G_{22} \cosh 2\alpha_0(y+h) \cos 2\alpha_0(x-l) + i G_{12} \right. \\
& + \sum_{n=1}^{\infty} G_{2n} i \left[ e^{i\beta_n(x-l) - \beta_n(y+h)} + e^{-i\beta_n(x-l) - \beta_n(y+h)} \right. \\
& \quad \left. + e^{i\beta_n(x-l) + \beta_n(y+h)} + e^{-i\beta_n(x-l) + \beta_n(y+h)} \right] \\
& + \sum_{m=1}^{\infty} \sum_{n=1}^{\infty} \left[ i G_{32mn} \cosh \alpha_{mn}(x-l) \cos \alpha_{mn}(y+h) \right. \\
& \quad \left. + i G_{32mn} \cosh \alpha'_{mn}(x+l) \cos \alpha'_{mn}(y+h) \right] \\
& + R_0 \cosh \gamma_0(y+h) \cos \gamma_0(x-l) \\
& + \sum_{n=1}^{\infty} R_n \cos \gamma_n(y+h) \cosh \gamma_n(x-l) \left. \right\} e^{-i2\omega t}
\end{aligned}$$

(166)

The problem now becomes that of determining the R's such that the boundary condition at  $x = 0$ , (5-10) is satisfied.

$$\begin{aligned}
\phi_x^{(2)} \Big|_{x=0} = & \left\{ 2i\alpha_0 G_{21} \cosh 2\alpha_0(y+h) \cos 2\alpha_0 l \right. \\
& + \sum_{n=1}^{\infty} G_{2n} \left[ -F_n e^{-iF_n l - F_n(y+h)} + F_n e^{iF_n l - F_n(y+h)} \right. \\
& \quad \left. - F_n e^{-iF_n l + F_n(y+h)} + F_n e^{iF_n l + F_n(y+h)} \right] \\
& + \sum_{m=1}^{\infty} \sum_{n=1}^{\infty} \left[ i G_{32mn} \alpha_{mn} \sinh(-\alpha_{mn} l) \cos \alpha_{mn}(y+h) \right. \\
& \quad \left. + i G_{32mn} \alpha'_{mn} \sinh(-\alpha'_{mn} l) \cos \alpha'_{mn}(y+h) \right] \\
& + \gamma_0 R_0 \cosh \gamma_0(y+h) \sin \gamma_0 l \\
& + \sum_{n=1}^{\infty} \gamma_n R_n \cos \gamma_n(y+h) \sinh(-\gamma_n l) \left. \right\} \sin 2\omega t
\end{aligned}$$

(5-167)

The known functions needed in equation (3-16) are:

$$\theta^{(2)} = B^{(2)} \cos \omega t$$

(5-93)

$$\theta_t^{(2)} = -i2\omega B^{(2)} e^{-i2\omega t}$$

(5-168)

$$\begin{aligned}
\phi_y^{(2)} \Big|_{x=0} = & \alpha_0 N_0 \sinh \alpha_0(y+h) \cos \alpha_0 l \sin \omega t \\
& - \sum_{n=1}^{\infty} \alpha_n N_n \sin \alpha_n(y+h) \cosh \alpha_n l \sin \omega t
\end{aligned}$$

(5-169)

$$\begin{aligned} \varphi_{xx}^{(5)} \Big|_{x=0} &= -\alpha_0^2 N_0 \cosh \alpha_0 (y+h) \cos \alpha_0 l \sin \omega t \\ &+ \sum_{n=1}^{\infty} \alpha_n^2 N_n \cos \alpha_n (y+h) \cosh \alpha_n l \sin \omega t \end{aligned}$$

(5-170)

Substitution of equations (5-167) through (5-170) into equation (3-16) gives the real part of the following equation:

$$\begin{aligned} &R_0 \gamma_0 \sin \gamma_0 l \cosh \gamma_0 (y+h) - \sum_{n=1}^{\infty} R_n \gamma_n \sinh \gamma_n l \cos \gamma_n (y+h) \\ &= -2i \alpha_0 G_{32} \cosh 2\alpha_0 (y+h) \cos 2\alpha_0 l \\ &\quad - \sum_{n=1}^{\infty} G_{2n} \left[ -\bar{F}_n e^{-i\bar{F}_n l - \bar{F}_n (y+h)} + \bar{F}_n e^{i\bar{F}_n l - \bar{F}_n (y+h)} \right. \\ &\quad \quad \left. - \bar{F}_n e^{-i\bar{F}_n l + \bar{F}_n (y+h)} + \bar{F}_n e^{i\bar{F}_n l + \bar{F}_n (y+h)} \right] \\ &\quad + \sum_{m=1}^{\infty} \sum_{n=1}^{\infty} \left[ i\alpha_{mn} G_{32mn} \sinh \alpha_{mn} l \cos \alpha_{mn} (y+h) \right. \\ &\quad \quad \left. + i\alpha'_{mn} G_{32mn} \sinh \alpha'_{mn} l \cos \alpha'_{mn} (y+h) \right] + i2\omega (y+h) \\ &\quad + \frac{iB^{(5)}}{2} \left[ \alpha_0 N_0 \cos \alpha_0 l \sinh \alpha_0 (y+h) - \sum_{n=1}^{\infty} \alpha_n N_n \cosh \alpha_n l \sin \alpha_n (y+h) \right] \\ &\quad - \frac{iB^{(2)}}{2} \left[ -\alpha_0^2 N_0 \cos \alpha_0 l (y+h) \cosh \alpha_0 (y+h) \right. \\ &\quad \quad \left. + \sum_{n=1}^{\infty} \alpha_n^2 N_n (y+h) \cosh \alpha_n l \cos \alpha_n (y+h) \right] \end{aligned}$$

(5-171)

To determine  $R_0$ , multiply equation (5-171) by  $\cosh \gamma_0(y+h)$  and integrate from  $y = -h$  to  $y = 0$ .

The following notations will be used.

$$\tilde{I}_{24} = \int_{-h}^0 \cosh^2 \gamma_0(y+h) dy \quad (5-172)$$

$$\tilde{I}_{25mn} = \int_{-h}^0 \cos \alpha'_{mn}(y+h) \cosh \gamma_0(y+h) dy \quad (5-173)$$

$$\tilde{I}_{26njk} = \int_{-h}^0 \cos \alpha'_{jk}(y+h) \cos \gamma_n(y+h) dy \quad (5-174)$$

$$\begin{aligned} R_0 = & \frac{1}{\gamma_0 \sin \gamma_0 l \tilde{I}_{24}} \left\{ -2i\alpha_0 G_{31} \cos 2\alpha_0 l \tilde{I}_3 \right. \\ & - \sum_{n=1}^{\infty} G_{2n} \tilde{F}_n [e^{i\tilde{F}_n l} - e^{-i\tilde{F}_n l}] [e^{-\tilde{F}_n h} \tilde{I}_{7n} + e^{\tilde{F}_n h} \tilde{I}_{6n}] \\ & - \sum_{n=1}^{\infty} \sum_{m=1}^{\infty} [i\alpha_{mn} G_{31mn} \sinh \alpha_{mn} l \tilde{I}_{9mn} + i\alpha'_{mn} G_{32mn} \sinh \alpha'_{mn} l \tilde{I}_{25mn}] \\ & - i2\omega \tilde{I}_1 + \frac{iB^{(2)}}{2} [\alpha_0 N_0 \cos \alpha_0 l \tilde{I}_2 - \sum \alpha_n N_n \cosh \alpha_n l \tilde{I}_{4n}] \\ & \left. - \frac{iB^{(2)}}{2} [-\alpha_0^2 N_0 \cos \alpha_0 l \tilde{I}_3 + \sum_{n=1}^{\infty} \alpha_n^2 N_n \cosh \alpha_n l \tilde{I}_{5n}] \right\} \end{aligned}$$

(5-175)

To determine the R n's, multiply equation (5-171) by  $\cos \nu_m(y+h)$  and integrate from  $y = -h$  to  $y = 0$ .

$$\begin{aligned}
 R_n = & \frac{1}{\gamma_n \sinh \gamma_n l \tilde{I}_{10n}} \left\{ -2i\alpha_0 G_{32} \cos 2\alpha_0 l \tilde{I}_{10n} \right. \\
 & \left. - \sum_{j=1}^{\infty} G_{2j} \left[ \tilde{F}_j e^{-\tilde{F}_j h} \tilde{I}_{17nj} + \tilde{F}_j e^{\tilde{F}_j h} \tilde{I}_{16nj} \right] \left[ e^{i\tilde{F}_j l} - e^{-i\tilde{F}_j l} \right] \right\} \\
 & + \sum_{j=1}^{\infty} \sum_{k=1}^{\infty} \left[ i\alpha_{jk} G_{32jk} \sinh \alpha_{jk} l \tilde{I}_{10nj} \right. \\
 & \quad \left. + i\alpha'_{jk} G_{32jk} \sinh \alpha'_{jk} l \tilde{I}_{26nj} \right] \\
 & - i2\omega \tilde{I}_{12n} \\
 & + \frac{iB^{(3)}}{2} \left[ \alpha_0 N_0 \cos \alpha_0 l \tilde{I}_{12n} - \sum_{j=1}^{\infty} \alpha_j N_j \cosh \alpha_j l \tilde{I}_{14nj} \right] \\
 & - \frac{iB^{(2)}}{2} \left[ -\alpha_0^2 N_0 \cos \alpha_0 l \tilde{I}_{13n} + \sum_{j=1}^{\infty} \alpha_j N_j \cosh \alpha_j l \tilde{I}_{15nj} \right]
 \end{aligned}$$

(5-176)

## Chapter 6

### THE EFFECT OF SURFACE TENSION

The theory developed in the preceding chapters does not contain the effects of surface tension. It is shown in this chapter that the effects of surface tension are negligibly small for the wave frequencies that a absorber would normally encounter.

In the presence of surface tension there is a discontinuity in the pressure across the free surface of an amount

$$(p_1 - p_2) = \mathcal{T}K \quad (6-1)$$

where  $\mathcal{T}$  is the surface tension (force/unit length) and  $K$  is the surface curvature. In the case of two dimensional waves,

$$K = \frac{1}{R} \quad (6-2)$$

$R$  being the radius of curvature of the surface.

In terms of the surface elevation  $\eta$ ,  $K$  is given by [ see Thomas (4) ]

$$K = \frac{1}{R} = \frac{\eta_{xx}}{(1 + \eta_x^2)^{3/2}} \quad (6-3)$$

Use of the perturbation series for  $\eta$  (2-9) gives:

$$K = \epsilon \eta_{xx}^{(1)} + \epsilon^2 \eta_{xx}^{(2)} + \dots \quad (6-4)$$

Only the linearized (first order) problem will be considered here for which

$$K^{(1)} = \eta^{(1)}_{xx} \quad (6-5)$$

The first order dynamic free surface condition (see chapter 2)

becomes:

$$\phi_t^{(1)} \Big|_{y=0} + g \eta^{(1)} - \frac{\bar{T}}{\rho} \eta^{(1)}_{xx} = 0 \quad (6-6)$$

The last term of equation (6-6) is the value of  $p/\rho$  on the underside of the free surface and it can be seen that this equation reduces to equation (2-20) when  $T = 0$ . Combining equation (6-6) with the first order kinematic free surface condition (2-22) gives:

$$\left( \phi_{xx}^{(1)} + g \phi_y^{(1)} - \frac{\bar{T}}{\rho} \phi_{xxy}^{(1)} \right) \Big|_{y=0} = 0 \quad (6-7)$$

The potential  $\phi^{(1)}$  must still satisfy Laplace's Equation (2-35) so the methods of solution of chapter (4) are applicable, but in this case equation (4-6) is replaced by

$$-\omega^2 G + g G' - \frac{\bar{T}}{\rho} \frac{F''(0)}{F(0)} G' = 0 \quad (6-8)$$

Equation (4-11) is replaced by:

$$\omega^2 = -\left( \alpha g + \frac{\bar{T} \alpha^3}{\rho} \right) \tanh \alpha h \quad (6-9)$$

and Equation (4-13) is replaced by:

$$\omega^2 = \left( \alpha_0 g + \frac{\mathcal{J} \alpha_0^3}{\rho} \right) \tanh \alpha_0 h \quad (6-10)$$

Thus the solutions here are similar to those of Chapter 4, the only difference being a change in the eigenvalues. For the value of  $g$  at the surface of earth (32.2 feet/second<sup>2</sup>) and the value of  $T$  for water at room temperature (0.0050 pounds/ft.) the effect of surface tension is significant only for values of  $\omega$  that are so large that the viscous attenuation of these waves obviates a wave absorber.

As an example,  $\alpha_0$  and the first nine  $\alpha_n$ 's were calculated for  $T = 0.0050$  and for  $T = 0$ ; for values of the radian frequency of 4, 8, 12, 16 and 20 radians per second. The results of these calculations appear in figure 7-1 and it can be seen that the effect of surface tension is very small for radian frequencies below 16 radians per second.

Even though the effects of surface tension are very small, they are taken into account in the following work in the design of the wave absorber for the sake of physical completeness.

```

printf .tape. 4
W 1053.6
00010 00.4167 00.3750 00.2500 01.9400 32.1600 00.0050 00.1667
00020 04.00 20.00 04.00
00030 9
00040 00.40
R .266+1.550

```

```

loadgo tten egval
W 1054.0
EXECUTION.

```

RADIAN FREQUENCY = 4.0

EIGENVALUES FOR SURFACE TENSION OF 0.0050 POUNDS/FOOT

1.13	7.38	15.00	22.56	30.11	37.66	45.20	52.75	60.29	67.83
------	------	-------	-------	-------	-------	-------	-------	-------	-------

EIGENVALUES FOR NO SURFACE TENSION

1.13	7.38	15.00	22.56	30.12	37.66	45.21	52.75	60.29	67.84
------	------	-------	-------	-------	-------	-------	-------	-------	-------

RADIAN FREQUENCY = 8.0

EIGENVALUES FOR SURFACE TENSION OF 0.0050 POUNDS/FOOT

2.54	6.86	14.75	22.40	29.99	37.55	45.11	52.66	60.20	67.74
------	------	-------	-------	-------	-------	-------	-------	-------	-------

EIGENVALUES FOR NO SURFACE TENSION

2.54	6.86	14.76	22.41	30.00	37.57	45.13	52.68	60.23	67.78
------	------	-------	-------	-------	-------	-------	-------	-------	-------

RADIAN FREQUENCY = 12.0

EIGENVALUES FOR SURFACE TENSION OF 0.0050 POUNDS/FOOT

4.66	6.00	14.34	22.12	29.77	37.37	44.95	52.51	60.06	67.60
------	------	-------	-------	-------	-------	-------	-------	-------	-------

EIGENVALUES FOR NO SURFACE TENSION

4.66	6.00	14.35	22.14	29.80	37.41	45.00	52.57	60.14	67.69
------	------	-------	-------	-------	-------	-------	-------	-------	-------

RADIAN FREQUENCY = 16.0

EIGENVALUES FOR SURFACE TENSION OF 0.0050 POUNDS/FOOT

7.94	5.14	13.81	21.75	29.48	37.13	44.73	52.31	59.87	67.41
------	------	-------	-------	-------	-------	-------	-------	-------	-------

EIGENVALUES FOR NO SURFACE TENSION

7.98	5.15	13.82	21.78	29.52	37.19	44.81	52.41	60.00	67.57
------	------	-------	-------	-------	-------	-------	-------	-------	-------

RADIAN FREQUENCY = 20.0

EIGENVALUES FOR SURFACE TENSION OF 0.0050 POUNDS/FOOT

12.29	4.62	13.25	21.31	29.13	36.83	44.47	52.06	59.63	67.18
-------	------	-------	-------	-------	-------	-------	-------	-------	-------

EIGENVALUES FOR NO SURFACE TENSION

12.44	4.62	13.27	21.35	29.19	36.92	44.58	52.21	59.82	67.42
-------	------	-------	-------	-------	-------	-------	-------	-------	-------

FIGURE 6-1 Eigenvalues for the wave absorber problem showing the effects of surface tension.

## Chapter 7

### SYNTHESIS OF A LINEAR WAVE ABSORBING SYSTEM FUNCTION

In general a compliant linear absorber will be a device whose output will be obtained as a linear operation on some input. The device to be considered in detail here gives as an output the paddle angle as a linear operation on the wave height at a distance  $d$  upstream from the paddle. The scheme used in this work is to measure the wave height by a device which produces an electric voltage proportional to the wave height. (Details of this device appear in appendix C). This voltage serves as the input to an electric filter whose output controls the paddle angle by means of a servo mechanism (details of the servo mechanism appear in appendix B). This section deals with the synthesis of the system function of the electric filter. Details of the design and construction of the electric filter appear in appendix B.

At this point, a knowledge of the usual mathematics and methods of circuit design and synthesis is assumed to be held by the reader. This information can be found in references (5) and (6). The system function of the filter  $H_e(s)$  will be sought in the form of a rational polynomial in  $S$  where

$$S = \sigma + i\omega \tag{7-1}$$

$$H_e(s) = A \frac{(s-z)(s-b)\dots ( )}{(s-q)(s-r)\dots ( )} \tag{7-2}$$

(A few pertinent facts will be given below). For details, see references 5 and 6. The frequency response for a sinusoidal excitation is  $H_e(-i\omega)$ . The frequently used convention of improperly calling this function  $H_e(-\omega)$  will be followed here. The minus sign in the arguments occur because the hydrodynamics of the wave absorber problem are based on the time function  $e^{-i\omega t}$ . The inverse fourier transform from  $\omega$  to  $t$  of  $H(\omega)$  gives the response of the filter to a unit impulse in time (dirac delta "function"). In order that this response be real all complex poles must have a conjugate pole and all complex zeros must have a conjugate zero, i.e., a zero at  $S = a$  requires that there be a zero at  $S = a^*$  unless  $a$  is real. In order that the filter be stable for zero input and not give any impulse response before the impulse occurs no poles can be in the right half of the  $S$  plane, i.e., the real parts of the positions of the poles must not be positive.

The number and positions of the poles and zeros must be chosen such that an adequate approximation to the desired frequency response is given by  $H_e(-\omega)$ . In this case the desired frequency response is  $H_h(-\omega)$ . Since it is desired to limit the reflection coefficient of the wave absorber to a few percent, it is necessary that the  $H_e(-\omega)$  approximate  $H_h(-\omega)$  to this degree of accuracy. A number of methods of choosing the number of poles and zeros and their positions have been studied and the most satisfactory one is reported in reference 7 by Linvill. He first guessed at the needed number of poles and zeros and found the logarithm of the frequency response of this system and the error between this function and

the logarithm of the desired frequency response. Logarithms were used because they afforded the convenient separation of magnitude and angle into real and imaginary parts and this facilitated Linvill's evaluation. Then the rate of change of error with changing each pole and zero position separately was determined. Next by assuming that these rates of change were approximately correct over the entire range of position change, Linvill could find a new set of positions for his poles and zeros by inverting a set of algebraic linear equations. The process was repeated again and again until either the desired accuracy was reached or the filter designer "gave up." This process involved a tremendous amount of tedious calculation. In order to ease this task, the present author wrote a computer program to carry out Linvill's method and this program was successful. However, the author has evolved another scheme which works better than the forementioned method and uses much less computer time. The first step is to guess at the number of poles and zeros and their positions as Linvill did. This information and the desired frequency response is transmitted to a computer by typewriter console or teletype. The computer determines the mean square error. Then the computer takes the first pole or zero in the input list and moves it by a slight amount in the complex plane along the direction of the real axis. The mean square error is computed. Next the pole or zero is moved by a small amount in the other direction along the direction of the real axis and the mean square error (henceforth known as MSE) is again computed. The direction in which the MSE is decreased most is determined and the pole

or zero is moved in that direction by a given amount. The MSE is again found and if it is decreased from its initial value the pole or zero is left at its new position. Otherwise the pole or zero is returned to its original position. If the pole or zero is complex this scheme is also carried out for movement in the direction of the imaginary axis. In the case of complex poles or zeros the conjugate pole or zero is moved simultaneously. Then the scheme is carried out for the next pole or zero in the input list. When this is done for all poles and zeros the new MSE is typed out so that the designer knows how the scheme is progressing. The whole process is then repeated with a smaller allowed change in pole and zero positions usually 90 percent of the previous allowed change. This process can be repeated as many times as desired.

The first step in synthesizing a system function is to compute the desired system function. This is done by the computer program BHN (Listings of all computer programs appear in appendix F). This program needs the subroutine EGVAL which determines the necessary eigenvalues. In the first block of output from BHN (see fig. 7-1) the frequency is given first and the next four columns give real and imaginary parts, size and angle of the desired frequency response. Examination of the resulting frequency response shows that over the frequency range of interest, the needed system behaves somewhat like an integrator. Also, it is desirable that the system have a zero at the origin of the S-plane to avoid any

possibility of drift. In order to get something like an integrator and a zero at the origin the signal will be prefiltered by a system having two poles on the real axis near the origin at a point  $S = -a$  and a zero at  $S = 0$ .

Then the desired frequency response for a filter cascaded with the pre-filter is determined. The sizes and angles of this frequency response are given by the columns labeled SF and ANGF in the first block of output from BHN (figures 7-1 and 7-4). Then the subroutine IMERG performs the forementioned relaxation scheme of locating the poles and zeros. The normalized mean square error is printed out after each step as was mentioned before. These values form the long vertical column of numbers in figures 7-1 and 7-4. The normalization is based on a mean square value of unity for the frequency response over the frequency range of interest. Finally the real and imaginary parts, sizes and angles of the filter output are printed.

In order to determine the reflection coefficient of the system which was synthesized, the computer program called TOT was prepared. Sample outputs from TOT appear in figures 7-3 and 7-6 where the column labeled RAD gives the radian frequency of the incident wave, RFR gives the real part of the reflected wave for a unit incident wave, RFI gives the imaginary part, SIZE gives the amplitude and ANGLE gives the angle of the reflected wave with respect to the incident wave.

The sample outputs show the synthesis of two wave absorbing filters, one being more complicated and having a lower reflection coefficient than the other. Figures 7-1, 7-2 and 7-3 show the various computer outputs for the simpler filter and Figures 7-4, 7-5, and 7-6 show the outputs for the more sophisticated filter. It is of interest to note that over the frequency range of interest the root mean square error in the absorbing filter (square root of the number labeled normalized error in the output of IMERG) is considerably greater than the reflection coefficients given by TOT. This interesting and fortunate effect occurs because the wave probe senses both the reflected as well as the incident wave so that the component of the reflected wave which is in phase with the incident wave acts as an error reducing feedback signal to the absorbing system. Another result which should be noted is that for the simpler filter waves at some frequencies above the designed range of absorption have reflection coefficients greater than unity. This appears to indicate instability at these frequencies for the finite tank in which the experiment was performed. Such an instability does not appear in the output of the computer program STABI because this program is based on a semi-infinite tank. However, the apparent instability does not appear in practice because at the frequencies for which the reflection coefficient is large, the viscous dissipation is also large; in fact the viscous dissipation is large enough so that after a wave has travelled twice the length of the tank its amplitude was diminished more than the amplification

of the "absorber" increases it. Consequently, the finite tank is stable with this filter.



H = 930.301819

REAL ZEROS  
- DUMMY VARIABLE BLOCK  
-4.996573E 01

REAL POLES  
- DUMMY VARIABLE BLOCK  
-1.069712E 01 -8.229470E 01

COMPLEX ZEROS  
REAL PART  
- DUMMY VARIABLE BLOCK  
0 0

IMAGINARY PART  
- DUMMY VARIABLE BLOCK  
0 0

COMPLEX POLES  
REAL PART  
- DUMMY VARIABLE BLOCK  
.000000E 00 -.000000E 00

IMAGINARY PART  
- DUMMY VARIABLE BLOCK  
.000000E 00 -.000000E 00

NORMALIZED ERROR= .00548

FILTER FREQUENCY RESPONSE

RAD	HPR	HPI	SIZE	ANGLE
3.0000	49.3181	12.5874	50.8991	.2499
5.0000	44.2316	18.6064	47.9858	.3982
7.0000	38.4650	22.2856	44.4545	.5251
9.0000	32.9728	24.0494	40.8115	.6302
11.0000	28.1983	24.5102	37.3617	.7155
13.0000	24.2374	24.1897	34.2431	.7844

EXIT CALLED. PM MAY BE TAKEN.  
R 18.766+7.583

Figure 7-1 (cont.) This shows the data about the computed filter.

OM REAL	OM IMAG	GR + RADIM	GI + RADIM
1.000	0.	25.07589054	-15.42179585
1.307	.541	-1.31697989	-19.83724070
1.473	.911	-6.44168437	-13.77785158
1.622	1.169	-7.33790612	-10.12782574
1.762	1.376	-7.47647679	-7.71284282
3.000	0.	-3.56994247	-.20304990
3.419	.555	-4.91426927	-3.11987484
3.707	1.122	-5.95355988	-3.94540000
3.920	1.624	-6.66202581	-3.84634888
4.099	2.049	-6.89567316	-3.48070872
5.000	0.	-5.89086449	-.81195116
5.451	.540	-5.96692514	-1.92569959
5.809	1.119	-6.13324612	-2.43364882
6.095	1.688	-6.28802925	-2.58135879
6.330	2.220	-6.40013462	-2.53345722
7.000	0.	-5.90142280	-1.20469517
7.464	.530	-5.81597275	-1.67341805
7.861	1.101	-5.80887437	-1.92076042
8.196	1.682	-5.84152359	-2.01158175
8.481	2.252	-5.88808513	-1.99722651
9.000	0.	-5.45022464	-1.24407649
9.472	.525	-5.37219346	-1.44193017
9.890	1.086	-5.34902942	-1.54492095
10.258	1.665	-5.36150360	-1.57203308
10.581	2.245	-5.39445758	-1.54309279
11.000	0	-4.93188179	-1.05389260
11.477	.521	-4.88726825	-1.12440780
11.910	1.074	-4.88082045	-1.15093270
12.300	1.647	-4.90112507	-1.13726775
12.650	2.229	-4.93909949	-1.09217687
13.000	0.	-4.44141573	-.74426333
13.481	.518	-4.42776853	-.74721396
13.924	1.065	-4.44124573	-.72949067
14.330	1.632	-4.47497344	-.68917129
14.701	2.211	-4.52333945	-.63050908
15.000	0.	-3.97625068	-.38310965
15.483	.516	-3.98753273	-.33927162
15.934	1.058	-4.01878649	-.28938930
16.352	1.619	-4.06608504	-.22626637
16.739	2.194	-4.12586093	-.15185494
17.000	0.	-3.50807658	-.00027516
17.485	.514	-3.53552851	.08568028
17.941	1.052	-3.58143699	.16410238
18.369	1.608	-3.64074391	.25064040
18.768	2.178	-3.71108606	.34426961
19.000	0.	-3.00755018	.38886477
19.487	.512	-3.03961098	.51797118
19.948	1.047	-3.09644434	.62686749
20.382	1.599	-3.16566068	.74164201
20.792	2.165	-3.24588943	.86165439

FIGURE 7-2 Results of stability calculation for filter synthesized in figure 7-1. Instability occurs at any complex frequency for which GR and GI are simultaneously zero which does not happen in the calculated frequency range.

```

printf .tape. 4
W 1230.4
00010 00.4167 00.3750 00.2500 01.9400 32.1600 00.0050 00.1667
00020 01.00 20.00 01.00
00030 6
00040 00.40
R .300+.533

```

```

printf .tape. 5
W 1230.7
00010 2 4 0 0
00020 927.228
00030 00.00 -50.45
00040 -00.40 -00.40 -10.72 -82.67
00050 00.00
00060 00.00
00070 00.00
00080 00.00
R .333+.533

```

```

loadgo tot trns rat egval
W 1231.1
EXECUTION.

```

RAD	RFR	RFI	SIZE	ANGLE	FTR SIZE	FTR ANGLE
1.000	.091	.366	.377	1.326	45.313	.895
2.000	.029	.157	.159	1.390	24.959	1.345
3.000	.015	.076	.078	1.373	16.666	1.555
4.000	.008	.030	.031	1.325	12.265	1.698
5.000	.001	.001	.001	1.137	9.536	1.809
6.000	-.007	-.017	.018	4.310	7.676	1.902
7.000	-.016	-.025	.030	4.162	6.331	1.982
8.000	-.024	-.024	.034	3.944	5.316	2.051
9.000	-.029	-.014	.032	3.578	4.527	2.112
10.000	-.028	.007	.029	2.899	3.900	2.166
11.000	-.016	.036	.040	1.980	3.393	2.214
12.000	.016	.071	.073	1.346	2.978	2.256
13.000	.076	.105	.129	.944	2.633	2.294
14.000	.171	.128	.214	.644	2.343	2.328
15.000	.312	.132	.339	.401	2.099	2.358
16.000	.514	.106	.525	.203	1.890	2.385
17.000	.811	.042	.813	.051	1.711	2.410
18.000	1.282	-.049	1.283	-.039	1.556	2.432
19.000	2.107	-.029	2.107	-.014	1.421	2.452
20.000	3.296	.860	3.407	.255	1.303	2.470

FIGURE 7-3 Results of calculation to determine reflection coefficients for filter synthesized in figure 7-1 and the frequency response of the complete filter (including the pre-filter).



H = 1.336292E 05

REAL ZEROS  
- DUMMY VARIABLE BLOCK  
    .000000E 00   -.000000E 00

REAL POLES  
- DUMMY VARIABLE BLOCK  
    -5.492040E 01   -1.050855E 02   -1.799702E 02

COMPLEX ZEROS  
  REAL PART  
- DUMMY VARIABLE BLOCK  
    4.087797E 00

  IMAGINARY PART  
- DUMMY VARIABLE BLOCK  
    1.956879E 01

COMPLEX POLES  
  REAL PART  
- DUMMY VARIABLE BLOCK  
    .000000E 00   -.000000E 00

  IMAGINARY PART  
- DUMMY VARIABLE BLOCK  
    .000000E 00   -.000000E 00

NORMALIZED ERROR= .00088

FILTER FREQUENCY RESPONSE

RAD	HPR	HPI	SIZE	ANGLE
3.0000	49.5931	8.1296	50.2551	.1625
4.0000	48.1898	10.6754	49.3581	.2180
5.0000	46.4044	13.0824	48.2132	.2748
6.0000	44.2506	15.3184	46.8270	.3333
7.0000	41.7451	17.3524	45.2080	.3939
8.0000	38.9069	19.1555	43.3668	.4575
9.0000	35.7576	20.7005	41.3173	.5248
10.0000	32.3207	21.9626	39.0767	.5968
11.0000	28.6217	22.9192	36.6673	.6752
12.0000	24.6877	23.5504	34.1189	.7618
13.0000	20.5471	23.8386	31.4716	.8594

FIGURE 7-4 (cont.)

OM REAL	OM IMAG	GR + RADIM	GI + RADIM
1.000	0.	-18.33878732	-98.35989571
1.307	.541	-35.42846918	-66.54965591
1.473	.911	-35.66267061	-48.90717983
1.622	1.169	-32.92311192	-39.80612516
1.762	1.376	-30.30980539	-34.05883455
3.000	0.	-1.35976274	-33.45416689
3.419	.555	-5.99139506	-29.72544479
3.707	1.122	-9.08221734	-25.99602365
3.920	1.624	-10.84757888	-22.70292568
4.099	2.049	-11.54850972	-20.03336453
5.000	0.	-.00022192	-18.90171933
5.451	.540	-2.03622216	-17.64584374
5.809	1.119	-3.75803775	-16.28397965
6.095	1.688	-5.07429743	-14.92240572
6.330	2.220	-6.01989067	-13.64264572
7.000	0.	.24439156	-12.19061434
7.464	.530	-.95016365	-11.54961872
7.861	1.101	-2.03529790	-10.87913442
8.196	1.682	-2.97444546	-10.19178843
8.481	2.252	-3.75720891	-9.50764668
9.000	0.	.19990624	-8.14504623
9.472	.525	-.62619440	-7.75948763
9.890	1.086	-1.40095861	-7.36975020
10.258	1.665	-2.10781932	-6.97051781
10.581	2.245	-2.73760936	-6.56600744
11.000	0.	.03440140	-5.34818542
11.477	.521	-.59403431	-5.09569544
11.910	1.074	-1.19384781	-4.84761500
12.300	1.647	-1.75602128	-4.59509265
12.650	2.229	-2.27468616	-4.33813322
13.000	0.	-.18033493	-3.26229548
13.481	.518	-.68816631	-3.08503622
13.924	1.065	-1.17801630	-2.91548795
14.330	1.632	-1.64481352	-2.74449623
14.701	2.211	-2.08493969	-2.57095474
15.000	0.	-.39088345	-1.63298841
15.483	.516	-.81956053	-1.49375515
15.934	1.058	-1.23586872	-1.36650102
16.352	1.619	-1.63717850	-1.23950838
16.739	2.194	-2.02126980	-1.11118117
17.000	0.	-.55722022	-.31403939
17.485	.514	-.92762703	-.18677346
17.941	1.052	-1.29200929	-.07921662
18.369	1.608	-1.64626738	.02734733
18.768	2.178	-1.98902506	.13440918
19.000	0.	-.65103935	.78138889
19.487	.512	-.97062717	.91504874
19.948	1.047	-1.29554090	1.01993085
20.382	1.599	-1.61414784	1.12436602
20.792	2.165	-1.92586088	1.22958593

FIGURE 7-5 This is a stability calculation (like figure 7-2) for the filter synthesized in figure 7-4.

```

printf .tape. 5
W 2130.5
00010 1 5 1 0
00020 133374.6
00030 00.00
00040 -00.20 -00.20 -54.90 -104.81 -179.72
00050 04.07
00060 19.55
00070 00.00
00080 00.00
R .150+1.016

```

```

loadgo tot rat trns egval
W 2146.3
EXECUTION.

```

RAD	RFR	RFI	SIZE	ANGLE
1.000	.035	.193	.196	1.393
2.000	.018	.090	.092	1.379
3.000	.012	.054	.055	1.357
4.000	.007	.035	.036	1.384
5.000	.001	.024	.024	1.527
6.000	-.005	.018	.018	1.844
7.000	-.011	.015	.019	2.190
8.000	-.016	.017	.023	2.340
9.000	-.018	.021	.028	2.301
10.000	-.016	.026	.031	2.113
11.000	-.005	.031	.031	1.734
12.000	.017	.029	.034	1.029
13.000	.055	.012	.056	.220
14.000	.113	-.031	.117	-.272
15.000	.205	-.119	.237	-.527
16.000	.398	-.263	.477	-.584
17.000	.853	-.246	.888	-.281
18.000	.899	.260	.936	.282
19.000	.603	.302	.674	.464
20.000	.457	.191	.495	.396

```

EXIT CALLED. PM MAY BE TAKEN.
R 10.516+.866

```

FIGURE 7-6 Results of calculation to determine reflection coefficients for filter synthesized in figure 7-4.

## Chapter 8

### OBLIQUE WAVES

Consider two-dimensional inviscid, incompressible fluid motions in a semi-infinite channel of depth  $h$  as shown in fig.(2-1). The velocity potential must satisfy

$$\frac{\partial^2 \phi}{\partial x^2} + \frac{\partial^2 \phi}{\partial y^2} = \nabla^2 \phi = 0 \quad (8-1)$$

The boundary condition at the bottom of the tank is

$$\left. \frac{\partial \phi}{\partial y} \right|_{y=-h} = 0 \quad (8-2)$$

The conditions imposed at the remaining boundaries depend on the particular problem being considered.

The most common solution to equation (8-1) satisfying (8-2) is of the form:

$$\phi = A \cosh \alpha(y+h) e^{i(\alpha x \pm \omega t)} \quad (8-3)$$

where  $A$  is an arbitrary complex constant and the real part of the above expression corresponds to the physical solution.

Another solution is

$$\phi = A \cos \alpha(y+h) e^{\alpha x \pm i \omega t} \quad (8-4)$$

Examples of both of the above solutions appear in chapter 4.

Solutions of the type of equation (8-3) can be thought of as  $x$  directed

waves where this means the plus or minus x axis corresponds to the direction of propagation if the wave is a traveling wave. If the wave is a standing wave the direction of pure sinusoidal spatial dependence is the x axis. Similarly solutions of the type of equation (8-4) are y directed waves.

Now consider an  $(x', y')$  coordinate system rotated an angle  $\theta$  from the  $(x, y)$  system.  $\theta$  is called the obliqueness angle.

$$x' = x \cos \theta + y \sin \theta$$

$$y' = -x \sin \theta + y \cos \theta$$

An  $x'$  directed wave which satisfies (8-1) is:

$$\phi = A e^{[i(k \cos \theta + y \alpha \sin \theta)]} e^{[\alpha x \sin \theta - \alpha y \cos \theta]} e^{-i \omega t} \quad (8-5)$$

Regrouping terms gives

$$\phi = A e^{[x(i \alpha \cos \theta + \alpha \sin \theta) + y(i \alpha \sin \theta - \alpha \cos \theta) - i \omega t]} \quad (8-6)$$

This wave does not satisfy the lower boundary condition (equation 8-2) but the sum of such a wave and a wave with an obliqueness angle of  $-\theta$  can satisfy the lower boundary condition. The direction of  $y'$  in which the waves attenuate is chosen such that the potential remains bounded as  $x \rightarrow -\infty$ . This is done so the results can be applied to the semi-infinite channel which is theoretically investigated in this work. In general, the proper signs are dictated by the physics of the problem.

Consider

$$\begin{aligned} \phi = & A e^{[x(i\alpha \cos \theta + \alpha \sin \theta) + y(i\alpha \sin \theta - \alpha \cos \theta) - i\omega t]} \\ & + B e^{[x(i\alpha \cos \theta + \alpha \sin \theta) + y(i\alpha \sin \theta + \alpha \cos \theta) - i\omega t} \end{aligned} \quad (8-7)$$

Let,

$$-i\alpha \sin \theta + \alpha \cos \theta = f \quad (8-8)$$

Then,

$$i\alpha \cos \theta + \alpha \sin \theta = if \quad (8-9)$$

$$\phi = A e^{ifx - fy - i\omega t} + B e^{ifx + fy - i\omega t} \quad (8-10)$$

$$\begin{aligned} \phi_y|_{y=h} &= -A f e^{(ifx + fh - i\omega t)} + B f e^{(ifx - fh - i\omega t)} \\ &= f e^{(ifx - i\omega t)} [-A e^{fh} + B e^{-fh}] \end{aligned} \quad (8-11)$$

The lower boundary condition (equation 8-2) is satisfied if:

$$B = A e^{2fh} \quad (8-12)$$

Thus, the sum of two oblique waves at opposite obliqueness angles provides a solution to equation (8-1) satisfying the lower boundary condition.

Next, equation (8-12) is incorporated in equation (8-10) where

$$\begin{aligned} A e^{2fh} &= A' \\ \phi &= A' [e^{ifx - f(y+h) - i\omega t} + e^{ifx + f(y+h) - i\omega t}] \\ &= A' \cosh f y \cosh f h e^{i(fx - \omega t)} \end{aligned} \quad (8-13)$$

Note that the form of equation (8-13) is identical to that of equation (8-3). However equation (8-13) is a wave with a complex wave

number. Waves of this type must be used to satisfy the inhomogeneous free surface condition for some second order waves as exemplified in the solution for  $\phi_{nh_2}$  in chapter 5.

Pairs of oblique waves can also be used to satisfy the homogeneous first order surface condition for unstable or decaying waves. In order to demonstrate this we seek solutions of equation (8-1) satisfying the lower boundary condition (8-2) and the usual linearized free surface condition,

$$\phi_{tt} + g\phi_y \Big|_{y=0} = 0 \quad (8-14)$$

where the solution has the form

$$\phi = X(x) Y(y) T(t) \quad (8-15)$$

The functions X, Y and T may be complex and the real part of their product is the physical function  $\phi$ . For such a solution, the free surface condition is

$$Y(\omega) T'' + g Y'(\omega) T = 0 \quad (8-16)$$

or

$$T = A e^{i\sqrt{\frac{gY'(\omega)t}{Y(\omega)}}} + B e^{-i\sqrt{\frac{gY'(\omega)t}{Y(\omega)}}} \quad (8-17)$$

If the quantity  $g \frac{Y'(0)}{Y(0)}$  is positive, the time dependence is sinusoidal.

This corresponds to usual standing or progressive waves. If the quantity

$g \frac{Y'(0)}{Y(0)}$  is negative or complex, decaying and/or increasing (unstable)

waves are possible. For example, the potential of equation (8-13)

yields for  $g \frac{Y'(0)}{Y(0)}$  the value of  $(fg) \tanh(fh)$  which can be

negative or complex for complex values of  $f$ . The preceding discussion is

intended to give an introduction and some physical understanding of the

problems to be considered more formally now. The general problems en-

countered are the initial value problem and problems of the so-called

"sinusoidal steady state" at frequency  $\omega$ . Problems utilizing real values

of  $\omega$  are the wavemaker problem and the wave absorber problem. Imaginary

values of  $\omega$  are encountered in considerations of the stability of various

terminations at the end of a channel which can remove or add energy to

the fluid.

Formal Derivations of the Eigenfunctions for waves of fixed or Variable Amplitude

The linear problem is solved for frictionless, irrotational incompressible flow so that

$$\vec{v} = \nabla \phi \tag{8-18}$$

and  $\nabla^2 \phi = 0 \tag{8-19}$

The boundary conditions are:

$$\frac{\partial \phi}{\partial y} = 0 \quad \text{at} \quad y = -h \quad (8-20)$$

$$\phi_{ctt} + g \phi_y = 0 \quad \text{at} \quad y = 0 \quad (8-21)$$

$$\nabla \phi < \infty \quad \text{at} \quad x = -\infty \quad (8-22)$$

At  $x = 0$ , the boundary condition depends on the termination at this location which is left arbitrary at this time.

Eigenfunctions of equation (8-18) are sought in the form:

$$\phi_0 = \text{Re} \{ F(x) G(y) e^{-i\omega t} \} \quad (8-23)$$

For these eigenfunctions equation (8-21) becomes

$$-\omega^2 G + g G' = 0 \quad (8-24)$$

In equation (8-23)  $F$  and  $G$  may be complex functions and  $\omega$  may be a complex variable.

Substitution of equation (8-23) in equation (8-19) yields

$$\frac{F''}{F} + \frac{G''}{G} = 0 \quad (8-25)$$

which requires

$$\frac{F''}{F} = -f^2 \quad (8-26)$$

$$\frac{G''}{G} = f^2 \quad (8-27)$$

$f$  is a complex variable.

The solutions to equation (8-25) are:

$$F = e^{ifx} \quad (8-28)$$

and

$$F = e^{-ifx} \quad (8-29)$$

These solutions place limits on  $\text{Im}(f)$ . If equation (8-28) is used,  $\text{Im}(f) \leq 0$  to satisfy the boundary condition (8-22) and if equation (8-29) is used  $\text{Im}(f) \geq 0$ . The solution to equation (8-27) which satisfies the boundary condition (8-20) is:

$$\zeta = \cosh f(y+h) \quad (8-30)$$

The free surface condition (8-24) is satisfied if:

$$\omega^2 = fg \tanh fh \quad (8-31)$$

For any value of  $\omega$ , there are an infinite number of values of  $f$  which satisfy the above equation.

$$\text{Let } Z = fh \quad (8-32)$$

Then, equation (8-31) is equivalent to

$$\frac{\omega^2 h}{g} = Z \tanh Z \quad (8-33)$$

$$\text{Let } w(Z) = Z \tanh Z \quad (8-34)$$

$$\text{where } Z = \alpha + i\beta \quad (8-35)$$

A fundamental region in  $Z$  for  $Z \tanh Z$  is  $0 \leq \beta \leq \frac{1}{2}\pi$ ,  $-\infty < \alpha < \infty$

This strip maps onto the entire  $w$  plane. Similarly

$$n - \frac{1}{2}\pi < \beta \leq n + \frac{1}{2}\pi, \quad -\infty < \alpha < \infty$$

are fundamental regions in  $Z$  for non-negative integer  $n$ . Negative

integer values of  $n$  also give fundamental regions as does the strip

$-\frac{1}{2}\pi \leq \beta \leq 0, -\infty < \alpha < \infty$  . For a definite problem with a definite choice of equation (8-28) or (8-29) only eigenfunctions associated with one of the two sets of fundamental regions those with positive  $\beta$ , or those with negative  $\beta$  satisfy the boundary condition of boundedness at  $x = -\infty$  . Equation (8-34) and therefore equation (8-33) have solutions in each fundamental region. Each successive value of  $n$  from zero to infinity yields a solution  $f$  having a greater imaginary part than the preceding solution. It should be noted that equation (8-33) is identical to that used for fixed amplitude waves except for the fact that now  $f$  is complex.

To proceed further, a definite termination at  $x = 0$  must be considered. To retain in similarity with the remainder of this work, a paddle hinged at  $y = -P$  with a solid wall below the paddle will be considered.

Normal modes for a hinged paddle termination.

For a linear device of the type considered in the remainder of this work the paddle angle is equal to the filtered wave height as measured a distance  $d$  from the paddle. The filter frequency response is taken as

$$\frac{\theta}{\pi} \Big|_{x=-d} = \mathcal{H}(-\omega) \tag{8-36}$$

where  $\omega$  may be complex.

A normal mode of the tank is defined as a function satisfying all the boundary conditions and having a fixed  $\omega$ . A normal mode can be written as

$$\phi_n = \sum_{n=1}^{\infty} A_n F_n(x) G_n(y) e^{-i\omega t} \quad (8-37)$$

Each  $F_n$  and  $G_n$  have the form of equation (8-28) or (8-28) and (8-30) with  $f_n$  given by equation (8-31) and  $n$  corresponding to the  $n^{\text{th}}$  fundamental region as described in the preceding section. The  $A_n$ 's are constants to be determined.

$$\phi_n = \sum_{n=1}^{\infty} A_n \cosh f_n (y+h) e^{i(\pm f_n x - \omega t)} \quad (8-38)$$

$$\phi_{nx} \Big|_{x=0} = \sum_{n=1}^{\infty} \pm i f_n A_n \cosh f_n (y+h) e^{-i\omega t} \quad (8-39)$$

From chapters 3 and 4 the relationship between  $\phi_x$  at  $x = 0$  and  $\theta$  is

$$\phi_x \Big|_{x=0} = \begin{cases} -i\omega B e^{-i\omega t (y+\beta)} & y \geq -\beta \\ 0 & y < -\beta \end{cases} \quad (8-40)$$

$$\theta = B e^{-i\omega t} \quad (8-41)$$

Combining equations (8-39) and (8-40) gives

$$\sum \pm i f_n A_n \cosh f_n (y+h) = \begin{cases} -i\omega B (y+\beta) & y \geq -\beta \\ 0 & y < -\beta \end{cases} \quad (8-42)$$

The formulae for the integrals  $I_1$  and  $I_2$  of chapter 4 are valid for complex  $\alpha_0$  and will be called  $I_{1n}$  and  $I_{2n}$  when  $f_n$  replaces  $\alpha_0$

$$\text{Hence, } A_n = \frac{\omega B \bar{I}_{2n}}{f_n \bar{I}_{1n}} \quad (8-43)$$

The problem just examined of finding the normal modes of a hinged paddle termination is a non self-adjoint boundary value problem. The eigenfunctions automatically satisfy the boundary conditions at  $y = 0$ ,  $y = -h$  and  $x = -\infty$ . In order that the series of eigenfunctions satisfy the boundary condition at  $x = 0$ , the  $x$  derivative of the series must converge to the  $x$  directed velocity of the termination in some sense.

The non-self adjointness comes about because of the complex value of  $\omega^2$  in equation (8-24). It is known by Coddington and Levinson (8) that in problems of this type the eigenfunctions form a complete, but non-orthogonal set. Completeness is demonstrated in the sense that the integral of the error squared over the termination at  $x = 0$  can be made as small as desired by using a sufficient number of terms in the expansion. Calling the eigenfunctions  $G_i(y)$ , the non-orthogonality means that

$$\int_{-h}^0 G_i(y) G_j^*(y) dy \neq 0 \text{ for } i \neq j$$

Therefore, the usual method for determining the coefficients in a self adjoint problem would fail in this case. However for the particular problem at hand

$$\int_{-h}^0 G_i(y) G_j(y) dy = 0 \quad \text{for } i \neq j$$

So the coefficients can be easily determined and are given by equation (8-43).

It is shown in chapter 11 that if certain restrictions on the nature of the wave absorbing system function at very low and very high frequencies are met the complete solution to the initial value problem in a semi-infinite tank can be represented by an integral over a set of eigenfunctions of fixed amplitude.

If one wishes to solve the initial value problem for a finite tank the solution will have to be represented by a sum of normal modes for such a tank with complex frequencies.

Restrictions on the sign of  $\omega^2$

Consider positive going travelling waves which propagate towards the termination at  $x = 0$ . For such waves the eigenfunctions have the form:

$$\phi_e = A \cosh f(y+h) e^{i(fx - \omega t)} \quad (8-44)$$

The sign of  $\text{Re}(\omega)$  is arbitrary inasmuch as the physical potential is the real part of equation (8-44). To avoid ambiguity the sign of  $\text{Re}(\omega)$  is taken as positive.

$$\text{Re}(\omega) > 0 \quad (8-45)$$

Then positive going waves require that

$$\text{Re}(f) > 0 \quad (8-46)$$

For boundedness at  $x = -\infty$

$$\text{Im}(f) \leq 0 \quad (8-47)$$

The relation between  $f$  and  $\omega$  is given by equation (8-33)

$$\frac{\omega^2 h}{g} = Z \tanh Z \quad (8-33)$$

where

$$Z = fh \quad (8-32)$$

Let

$$Z = (\alpha + i\beta) \quad (8-35)$$

Since  $h$  is positive equations (8-46) and (8-47) require that

$$\alpha = \text{Re}(Z) > 0 \quad (8-48)$$

$$\beta = \text{Im}(Z) \leq 0 \quad (8-49)$$

$$Z \tanh Z = \frac{\left( \frac{\alpha \tanh \alpha}{\cos^2 \beta} - \frac{\beta \tan \beta}{\cosh^2 \alpha} \right) + i \left( \frac{\beta \tanh \alpha}{\cos^2 \beta} + \frac{\alpha \tan \beta}{\cosh^2 \alpha} \right)}{1 + \tanh^2 \alpha \tan^2 \beta}$$

(8-50)

Lemma 1

For positive going waves of the form of equation (8-44) which are bounded at  $x = -\infty$ ,  $\text{Im}(\omega^2) \leq 0$

Proof. If  $\text{Im}(Z \tanh Z) \leq 0$ ,  $\text{Im}(\omega^2) \leq 0$  (8-51)  
from equation (8-33).

$$1 + \tanh^2 \alpha \tan^2 \beta > 0 \quad (8-52)$$

Hence  $\text{Im}(Z \tanh Z) \leq 0$  if  $\frac{\beta \tanh \alpha}{\cos^2 \beta} + \frac{\alpha \tan \beta}{\cosh^2 \alpha} \leq 0$  (8-53)

$$\frac{\beta \tanh \alpha}{\cos^2 \beta} \leq 0 \quad \text{for } \alpha > 0, \beta \leq 0 \quad (8-54)$$

Now consider two cases, Case A in which  $\frac{\alpha \tan \beta}{\cosh^2 \alpha} \leq 0$  and Case B in which  $\frac{\alpha \tan \beta}{\cosh^2 \alpha} > 0$ . Case B implies  $\tan \beta < 0$ . Case A; Here  $\text{Im}(\omega^2)$  is the sum of two quantities each of which is  $\leq 0$  so for this case the

lemma is true.

Case B.

$$\frac{\beta \operatorname{tanh} \alpha}{\cos^2 \beta} + \frac{\alpha \tan \beta}{\cosh^2 \alpha} = \operatorname{tanh} \alpha \left( \frac{\beta}{\cos^2 \beta} + \tan \beta \cdot \frac{\alpha}{\sinh \alpha \cosh \alpha} \right) \quad (8-55)$$

$$\frac{\alpha}{\sinh \alpha \cosh \alpha} < 1 \quad (8-56)$$

Therefore,  $\operatorname{Im}(Z \operatorname{tanh} Z) \leq \operatorname{tanh} \alpha \left( \frac{\beta}{\cos^2 \beta} + \tan \beta \right) \quad (8-57)$

Use of the identity  $\frac{1}{\cos^2 \beta} = 1 + \tan^2 \beta \quad (8-58)$

gives  $\frac{\operatorname{Im}(Z \operatorname{tanh} Z)}{\operatorname{tanh} \alpha} \leq \beta(1 + \tan^2 \beta) + \tan \beta \quad (8-59)$

Since  $\tan \beta \leq 0$  and  $\beta \leq 0$ ,

$$\beta < -\frac{\pi}{2} \quad (8-60)$$

Since  $1 \leq 1 + \tan^2 \beta$

and  $\tan^2 \beta \leq 1 + \tan^2 \beta$

the two following inequalities hold

$$\frac{\operatorname{Im}(Z \operatorname{tanh} Z)}{\operatorname{tanh} \alpha} < -\frac{\pi}{2} + \tan \beta \quad (8-61)$$

$$\frac{\operatorname{Im}(Z \operatorname{tanh} Z)}{\operatorname{tanh} \alpha} < |\tan \beta| \left( -\frac{\pi}{2} |\tan \beta| - 1 \right) \quad (8-62)$$

Either  $|\tan \beta| \leq 1$  or  $|\tan \beta| > 1$ ,

If  $|\tan \beta| \leq 1$  equation (8-61) shows  $\text{Im}(z \tanh z) < \tanh \alpha (-\frac{\pi}{2} + 1) < 0$

If  $|\tan \beta| > 1$ , equation (8-62) shows that

$$\text{Im}(z \tanh z) < -\frac{\pi}{2} \epsilon \tanh \alpha \quad (8-63) \quad \text{where } \epsilon > 0$$

This proves lemma 1.

Lemma 2.

$$0 \geq \text{Arg } \omega > -\frac{\pi}{2}$$

Proof  $0 \geq \text{Arg } \omega^2 > \pi \quad (8-64) \quad \text{from Lemma 1}$

$$\text{Arg } \sqrt{\omega^2}$$

has the two values

$$\frac{1}{2} \text{Arg } \omega^2$$

$$\text{and } -\pi + \frac{1}{2} \text{Arg } \omega^2$$

From equations (8-64)

$$0 \geq \frac{1}{2} \text{Arg } \omega^2 > -\frac{\pi}{2} \quad (8-65)$$

$$-\pi \geq (-\pi + \frac{1}{2} \text{Arg } \omega^2) > -\frac{3}{2} \pi \quad (8-66)$$

Thus the value of  $\sqrt{\omega^2}$  having the argument  $-\pi + \frac{1}{2} \text{Arg } \omega^2$  has

a negative real part which is not permitted by equation (8-45). Therefore

$$\text{Arg } \omega = \frac{1}{2} \text{Arg } \omega^2 \quad (8-67)$$

so  $0 \geq \text{Arg } \omega > -\frac{\pi}{2} \quad (8-68)$

which proves Lemma 2.

Theorem 1

Waves with a bounded amplitude at  $x = -\infty$  and which propagate towards the channel termination at  $x = 0$  must have a fixed or exponentially decaying amplitude with respect to time, independent of the details of the termination. Their amplitude cannot increase with time.

Proof: The time dependence of the waves is:

$$e^{i\omega t} = e^{-i\omega_r t + \omega_i t} \quad (8-69)$$

where

$$\omega = \omega_r + i \omega_i \quad (8-70)$$

$$\omega_i \leq 0 \text{ by lemma 2.}$$

Hence  $e^{\omega_i t}$  decays with increasing positive time.

Theorem 2.

Waves with a bounded amplitude at  $x = -\infty$  and which propagate away from the termination at  $x = 0$  must have a fixed or exponentially increasing amplitude with respect to time independent of the details of the termination. These waves cannot decay with time.

The counterparts to Lemmas 1 and 2 needed to prove theorem 2 can be proven in the same manner as Lemmas 1 and 2.

## Chapter 9

### The Stability of Linear Active Wave Absorbers

In general, a linear active water wave absorber will measure some signal, pass this signal through a linear filter, and move the tank termination in some mode with a magnitude that is proportional to the filter output. In the case of the absorber considered in detail in this work, the measured signal is the wave height some distance from the paddle and the mode of paddle motion which is made proportional to the filter output is the paddle angle. The system function of the filter is some approximation to that function which would absorb all waves according to linear theory.

In order that an active wave absorber be a usable device, it must be stable with respect to negative going waves. It will necessarily be stable with respect to positive going waves by theorem 1 of chapter eight which shows that the amplitude of positive going waves cannot increase with time. However, if the tank and termination have any normal modes with negative going waves, these waves will be unstable or at best neutrally stable by theorem 2 of chapter 8. The stability of a hinged paddle absorber for negative going waves will now be examined.

For a normal mode with negative going waves

$$\phi_n = \sum A_n \cosh f_n (y+h) e^{i(f_n y - \omega t)} \quad (9-1)$$

$$\text{with } \operatorname{Re} f_n > 0 \quad (9-2)$$

$$\operatorname{Re} \omega > 0 \quad (9-3)$$

The upper boundary condition gives the relationship between  $\omega$  and  $f_n$ .

$$\omega^2 = f_n g \tanh f_n h \quad (9-4)$$

Within each fundamental region for  $f_n$  (see chapter 8),  $f_n$  is a continuous function of  $\omega^2$ . The  $f_n$ 's for a given value of  $\omega^2$  can be found as follows.

First, find the  $f_n$ 's for

$$f_n g \tanh f_n h = \text{Re}(\omega^2) \quad (9-5)$$

This is done in chapter 4 to determine the system function for a linear wave absorber. Then let  $\text{Im}(\omega^2)$  go from zero to the desired value and trace the path of each  $f_n$  in the complex plane from its value at  $\text{Im}(\omega^2) = 0$  to its value at the desired value of  $\text{Im}(\omega^2)$ . A normal mode for the channel is given by equation (8-38). The  $A_n$ 's are given by equation (8-43) with the minus sign

$$A_n = - \frac{\omega B \tilde{I}_{2n}}{f_n I_{1n}} \quad (9-6)$$

where  $\theta = B e^{-i\omega t} \quad (8-41)$

The wave amplitude can be determined from equation (2-22), which is the kinematic boundary condition

$$\phi_y |_{y=0} = \eta c \quad (2-22)$$

This gives

$$\eta = \sum_{n=1}^{\infty} -\frac{1}{i\omega} f_n A_n \sinh f_n h e^{i(f_n x - \omega t)} \quad (9-7)$$

From equations (8-41) and (9-7),

$$X_k(\omega) = \frac{\theta}{\eta|_{x=d}} = \frac{1}{\sum_{n=1}^{\infty} -i \frac{I_{2n}}{I_{1n}} \sinh f_n k e^{i f_n d}}$$

The wave absorbing filter has a value of  $\frac{\theta}{\eta|_{x=d}}$  given by  $H_e(\omega)$ .

Any complex values of  $\omega$  for which  $H_e(\omega)$  equals  $H_n(\omega)$  constitutes a possible unstable radian frequency of the complete electro-hydrodynamical system. The electric filter should be designed so that its response at frequencies above the range of interest is small to avoid possible instabilities at these frequencies. In order to determine whether or not a possible instability exists in the frequency range of interest, the complex frequency plane must be searched to see if there are any unstable points. This is done by the computer program STABI. Sample outputs from STABI are shown in figures 7-2 and 7-5. STABI uses the subroutines DRVTV, TRNS AND RAT.

DRVTV is used to compute the derivative of a function which is zero at an eigenvalue. This derivative is needed by STABI to find the eigenvalues (f's) for complex  $\omega$  which is done by an extension of Newton's method to complex numbers. TRNS computes the real and imaginary parts, size and angle of the following functions of a complex variable: EXP, SINH, COSH and TANH. RAT computes the complex value of the filter response which is a rational function of S and therefore of  $\omega$  since

$$(i\omega)^* = S \quad (9-8)$$

Fig. (7-2) shows the output from STABI where

$\text{Re}(\omega)$  is labeled OM Real

$\text{Im}(\omega)$  is labeled OM Imag

$\text{Re}[\mathcal{H}_e(\omega) - \mathcal{H}_r(\omega)]$  is labeled GR + RADIM

$\text{Im}[\mathcal{H}_e(\omega) - \mathcal{H}_r(\omega)]$  is labeled GI + RADIM

The preceding theory for stability in a semi-infinite channel does not indicate one type of instability which can occur in a finite tank. Consider a finite channel with an absorbing system at one end and a solid wall at the other end. A possible instability exists if at any frequency the reflection coefficient exceeds unity. A small wave incident on the absorber would result in a larger reflected wave. This wave would be completely reflected by the solid wall and travel back to the absorbing end of the tank. If this wave at the absorber has a phase relative to the initial reflected wave phase within a certain range an increase in the amplitude of the negative going wave would result and an instability would exist. The stability theory of a finite tank with standing waves could be carried out in a straightforward fashion, but in order to insure stability in a finite tank for an absorber which is stable in an infinite tank it is only necessary to make sure that the reflection coefficient remains small up to frequencies where the viscous dissipation is large. To be more explicit, the reflection coefficient multiplied by the viscous attenuation coefficient for a wave travelling twice the length of the tank should be less than unity.

## Chapter 10

### DETERMINATION OF THE REFLECTION COEFFICIENT

#### Theory

When the tank is operating in the "sinusoidal steady state" the wave height due to the traveling waves can be written as

$$\eta_{travel} = a [\cos(\alpha_0 x - \omega t) + e \cos(\alpha x + \omega t + \delta)] \quad (10-1)$$

The total wave height will be the sum of  $\eta_{travel}$  and the local non-travelling waves at the ends of the tank. The local waves attenuate very rapidly with distance from the ends of the tank. Calculation has shown that at the ends of the tank the local waves can have amplitudes as large as 1/10 of the travelling wave amplitude, but at a position one wavelength from the end of the tank they have amplitudes less than 1/5000 of the travelling wave amplitude. Since measurements were not taken near the ends of the tank, the local waves can be neglected in the measurements.

When a travelling wave is generated by the wavemaker (primary wave) a part of it is reflected by the absorber. This reflected wave is almost totally reflected by the wavemaker and at this point it is called a secondary incident wave by Ursell, Dean and Yu (2). A part of this wave is then reflected by the absorber, etc. Ursell, Dean and Yu carried out the determination of the formulae for the reflection coefficient by considering primary and secondary incident and reflected waves. They did this because they were interested in eventually determining the amplitude of the primary incident wave. However, in the present case it is more

convenient to lump all the incident waves into one, and all the reflected waves into one as indicated by equation (10-1). Then  $\epsilon$  (in equation 10-1) is the reflection coefficient. Since the first term in equation (10-1) represents a positive going wave with some wavelength  $\lambda$  and some speed  $v$ , and the second term represents a negative going wave with the same wavelength and wave speed; there will be some points in the tank where the amplitudes of the two waves add and some points where the amplitudes subtract. In fact, since the speed of approach of one wave with respect to the other is  $2V$  the distance from one point in the tank where the amplitudes add to the next point where the amplitudes add is  $\lambda/2$ .

At a point in the tank where the amplitude is maximum,

$$\eta_{max} = a(1+\epsilon) \quad (10-2)$$

At a point in the tank where the amplitude is minimum,

$$\eta_{min} = a(1-\epsilon) \quad (10-3)$$

Hence,

$$\epsilon = \frac{\eta_{max} - \eta_{min}}{\eta_{max} + \eta_{min}} \quad (10-4)$$

This is the same formula that was obtained by Ursell, Dean and Yu (2).

Since the system function of the wave absorbing system is not exactly equal to the system function needed for complete absorption, a theoretical value for the reflection coefficient is determined here.

Let the wave absorber system function from surface elevation at  $x = -d$  to paddle angle be denoted by  $H_e(\omega)$

$$\mathcal{H}_e(\omega) = \frac{\theta}{\eta|_{x=-d}} \quad (10-5)$$

Let the relation between paddle angle and surface elevation at  $x = -d$  which is required by the hydrodynamics of the system be denoted by  $H_h(\omega)$

$$\mathcal{H}_h(\omega) = \frac{\theta}{\eta|_{x=-d}} \quad (10-6)$$

The reflection coefficient will then be determined by the relation

$$\mathcal{H}_e(\omega) = \mathcal{H}_h(\omega) \quad (10-7)$$

The notation of chapter 4 will be used in the determination of  $H_h(\omega)$  except that here a negative going wave is denoted by  $\text{Re} [e^{i(-\alpha_0 x - \omega t)}]$  whereas in chapter 4 it is denoted by  $\text{Re} (e^{i(\alpha_0 x + \omega t)})$

$$\begin{aligned} \phi = & A \cosh \alpha_0 (y+h) e^{i(\alpha_0 x - \omega t)} + A' \cosh \alpha_0 (y+h) e^{i(-\alpha_0 x - \omega t)} \\ & + \sum_{n=1}^{\infty} A_n \cos \alpha_n (y+h) e^{\alpha_n x} e^{-i\omega t} \end{aligned} \quad (10-8)$$

$$\begin{aligned} \phi_y|_{y=0} = \eta_t = & A \alpha_0 \sinh \alpha_0 h e^{i(\alpha_0 x - \omega t)} + A' \alpha_0 \sinh \alpha_0 h e^{i(-\alpha_0 x - \omega t)} \\ & + \sum_{n=1}^{\infty} \alpha_n A_n \sin \alpha_n h e^{\alpha_n x} e^{-i\omega t} \end{aligned}$$

$$\begin{aligned} \eta = \frac{\alpha_0}{-i\omega} A \sinh \alpha_0 h e^{i(\alpha_0 x - \omega t)} & + \frac{\alpha_0}{-i\omega} A' \sinh \alpha_0 h e^{i(-\alpha_0 x - \omega t)} \\ & + \sum_{n=1}^{\infty} \frac{\alpha_n A_n}{i\omega} \sin \alpha_n h e^{\alpha_n x} e^{-i\omega t} \end{aligned} \quad (10-9)$$

$$(10-10)$$

As in chapter 4, let

$$A_n = i b_n \quad (10-11)$$

$$\theta = B e^{-i\omega t} \quad (10-12)$$

$$\dot{\theta} = -i\omega B e^{-i\omega t} \quad (10-13)$$

$$\left. \frac{\theta}{\eta} \right|_{x=d} = \frac{B}{i \frac{\alpha_0}{\omega} \sinh \alpha_0 h (A e^{-i\alpha_0 d} + A' e^{i\alpha_0 d}) + \sum \frac{\alpha_n b_n}{\omega} \sin \alpha_n h e^{-\alpha_n d}} \quad (10-14)$$

The coefficients, A, A' and the b<sub>n</sub>'s are determined as in chapter 4. This gives:

$$B = -\frac{\alpha_0}{\omega} \frac{\tilde{I}_1}{\tilde{I}_2} (A - A') \quad (10-15)$$

$$b_n = \frac{\alpha_0}{\alpha_n} \frac{\tilde{I}_{4n}}{\tilde{I}_{3n}} \frac{\tilde{I}_1}{\tilde{I}_2} (A - A') \quad (10-16)$$

where the I's are also determined in chapter 4.

Let  $A = 1$  (10-17)

Then A' equals the reflection coefficient

$$R_e(\omega) = \left. \frac{\theta}{\eta} \right|_{x=d} = \frac{-\frac{\alpha_0}{\omega} \frac{\tilde{I}_1}{\tilde{I}_2} (1 - A')}{i \frac{\alpha_0}{\omega} \sinh \alpha_0 h (e^{-i\alpha_0 d} + A' e^{i\alpha_0 d}) + \sum \frac{\alpha_n}{\omega} \frac{\alpha_0}{\alpha_n} \frac{\tilde{I}_{4n}}{\tilde{I}_{3n}} \frac{\tilde{I}_1}{\tilde{I}_2} (1 - A') \sin \alpha_n h e^{-\alpha_n d}} \quad (10-18)$$

Let  $R_e(\omega) = R_r + i R_i$  (10-19)

$$A' = \frac{(H_r + iH_i) \left( i \sin \alpha h e^{-\alpha d} + \sum_{n=1}^{\infty} \frac{I_{2n}}{I_{2n}} \frac{I_2}{I_2} \sin \alpha_n h e^{-\alpha_n d} \right) + \frac{I_2}{I_2}}{\frac{I_2}{I_2} - (H_r + iH_i) \left( i \sin \alpha h e^{\alpha d} - \sum_{n=1}^{\infty} \frac{I_{2n}}{I_{2n}} \frac{I_2}{I_2} \sin \alpha_n h e^{-\alpha_n d} \right)} \quad (10-20)$$

The values of  $A'$  for various frequencies when  $H_e(\omega)$  is given by the rational function determined by the computer program IMERG are determined by the computer program TOT. The computer program TOTEX evaluates (10-20) when  $H_e(\omega)$  is given by a table of measured values.

#### Experiments With the Wave Absorber

The following experiment was performed.

The wavemaker was set at a fixed stroke and a fixed frequency. A wave height measuring probe was attached to a carriage mounted atop the tank which was towed down the tank at a speed which was very small compared to the wave speed. The electronic circuitry associated with the wave probe is the same type as the circuitry associated with the wave probe in the wave absorbing system (appendix C). The output signal from this wave measuring probe was sent through a low pass filter and then to a chart recorder which recorded the wave height at the probe. The low pass filter was set to a cutoff frequency of 1.5 times wave frequency. At large amplitudes there were significant second harmonic waves in the tank due to the non-linearities in the hydrodynamics and in the absorbing system. The filter eliminated the second harmonic from the records. The wave height pattern was, according to the preceding discussion, an oscillating pattern

inside an oscillating envelope. The experiment is depicted in figure (10-1).

A sample record is shown in figure (10-2). From these records values of  $\eta_{max}$  and  $\eta_{min}$  were determined and were used to calculate the reflection coefficient. These results are shown in table (10-1) and figure (10-3). Figure (10-4) shows the calculated magnitude and angle of the system function of the servomechanism and electronic filter. This function was measured in the experiment now described and depicted in figure (10-5). The output from a low frequency sine wave generator was simultaneously connected to the absorbing filter input and one channel of the two channel paper recorder. The servomechanism feedback pot output voltage, which varies linearly with paddle angle to first order in paddle angle, was connected to the second recorder channel. From the recordings made by this system, the magnitude and phase relations between input voltage and paddle angle were determined and are shown in figure 10-4 together with the calculated values of these quantities. Within the range of frequencies for which the wave filter was designed (3 radians/sec to 13 radians/sec) the measured magnitude of the transfer function is within 3 percent of the calculated value and has an RMS deviation of less than one percent. The measured phase is within .045 radians of the calculated phase with an RMS deviation of less than .03 radians. Figure 10-3 shows a curve of the reflection coefficient computed by TOTEX as well as the values of the reflection coefficient found in the experiment described above.

The difference between theoretical and experimental values of the reflection coefficient is one percent or less for most experimental points. The major exception to this occurs for a wave radian frequency of 9.25 radians/sec. Visual observations at the time of the experiment showed that shortly after the wavemaker was turned on the absorber motion was sinusoidal, but after some time had elapsed a rather large second harmonic component of paddle motion existed. This resulted in waves of twice the wavemaker frequency. The amplitude of these higher frequency waves was comparable to that of the lower frequency waves generated by the wavemaker. Examination of figure 10-3 shows that at 18.5 radians/second (second harmonic frequency) the reflection coefficient is 1.6. The only reason why the finite length tank is not unstable at some high frequencies is that the wave attenuates considerably in traversing the length of the tank twice. Because of the large reflection coefficient at 18.5 radians per second and the inherent non-linearities in the hydrodynamics and the servo-mechanism the large second harmonic wave forms when the fundamental radian frequency is 9.25 radians per second. The effect of the second harmonic paddle motion upon the first harmonic motion due to non-linearities in the servo-mechanism seems to be the most likely reason why an 8 percent reflection coefficient of the fundamental wave was measured although the theoretical reflection coefficient is 4 percent.

<u>RADIAN FREQUENCY</u>	<u>THEORETICAL REFLECTION COEFFICIENT</u>	<u>EXPERIMENTAL REFLECTION COEFFICIENT</u>
3.13	0.05	0.07
3.93	0.01	0.03
4.94	0.03	0.03
6.04	0.05	0.05
7.06	0.06	0.05
8.38	0.05	0.06
9.24	0.04	0.08
11.63	0.06	0.07
12.57	0.06	0.06

TABLE 10-1 Reflection Coefficients. The theoretical values are based on the measured system characteristics. These theoretical values were determined by the computer program TOTEX. The experimental value at any frequency is the average of all measurements taken at that frequency.

loadgo ratio  
W 1824.5  
EXECUTION.

RAD	ALP	RATIO	RATIO/LAMBDA
1.9845	.5000	.1049	.0083
3.8551	1.0000	.2138	.0340
5.5353	1.5000	.3293	.0786
6.9990	2.0000	.4513	.1437
8.2585	2.5000	.5770	.2296
9.3450	3.0000	.7017	.3351
10.2937	3.5000	.8203	.4569
11.1361	4.0000	.9288	.5913
11.8971	4.5000	1.0251	.7342
12.5955	5.0000	1.1089	.8824
13.2454	5.5000	1.1810	1.0338
13.8566	6.0000	1.2428	1.1868
14.4365	6.5000	1.2960	1.3407
14.9903	7.0000	1.3422	1.4953
15.5220	7.5000	1.3825	1.6503
16.0346	8.0000	1.4181	1.8056
16.5302	8.5000	1.4498	1.9613
17.0108	9.0000	1.4783	2.1175
17.4778	9.5000	1.5040	2.2740
17.9324	10.0000	1.5273	2.4308
18.3756	10.5000	1.5486	2.5880
18.8082	11.0000	1.5682	2.7455
19.2310	11.5000	1.5862	2.9032
19.6447	12.0000	1.6028	3.0612
20.0499	12.5000	1.6182	3.2194

TABLE 10-2 The Relationships Between Radian Frequency (RAD), Circular Wave Number (ALP), Wave Height/Wavemaker Stroke (RATIO) and the ratio of (RATIO/Wavelength). To obtain the wave height, multiply the wavemaker stroke by RATIO. To obtain the ratio of wave height/wavelength, multiply the wavemaker stroke by the appropriate number in the column labeled RATIO/LAMBDA. This table is based on a water depth of 5" (0.4167') and a wavemaker which is hinged  $\frac{1}{2}$ " above the bottom of the channel. The wavemaker stroke is taken at the waterline.

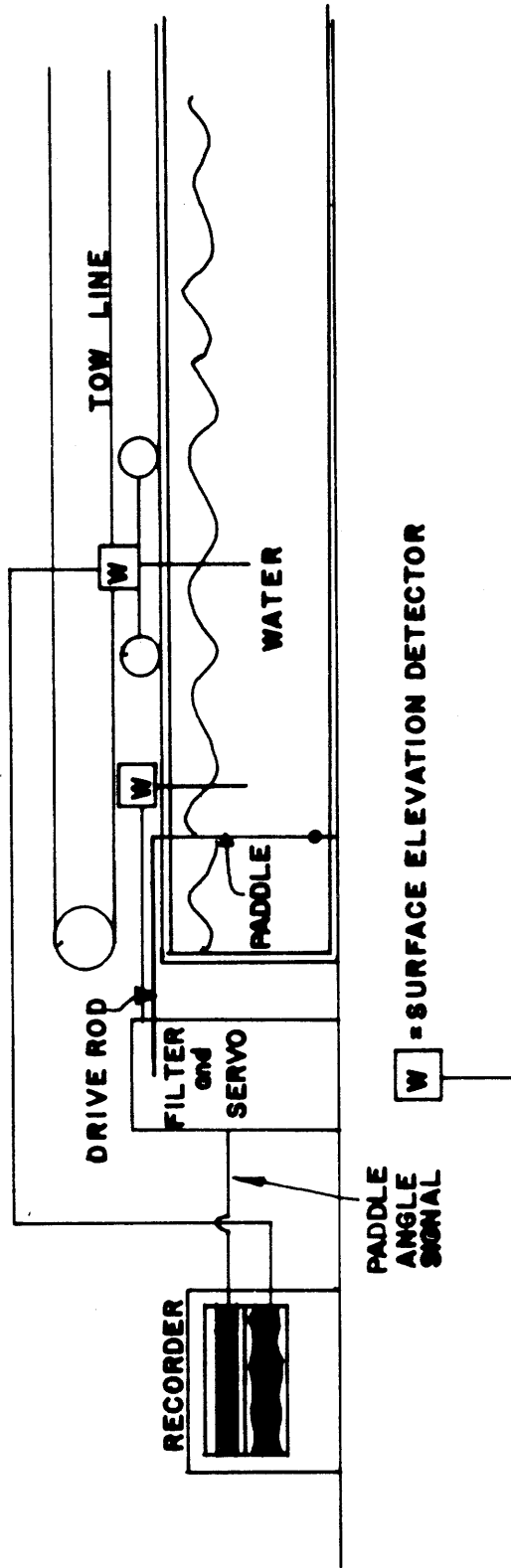
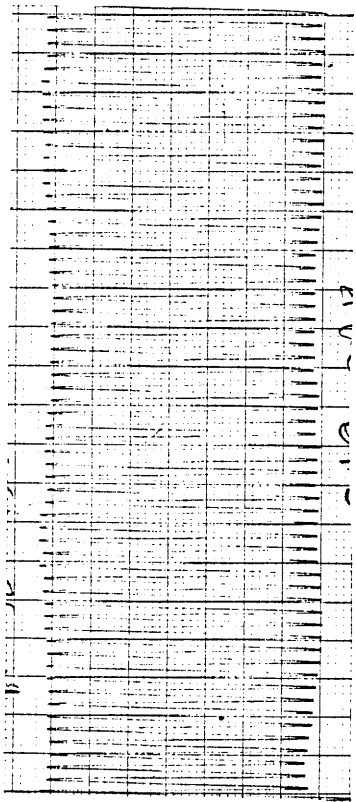
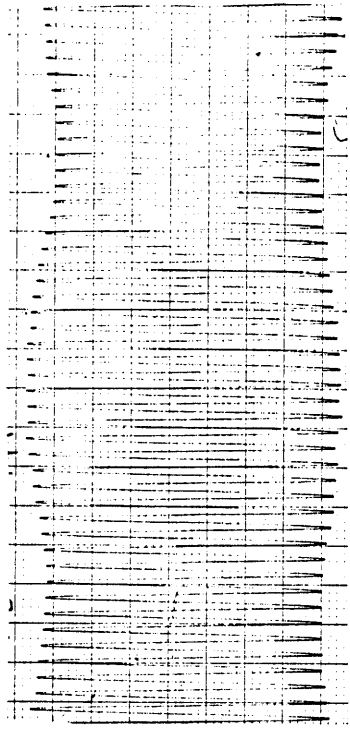


FIGURE 10-1 This depicts the experimental arrangement for measuring reflection coefficients. The wavemaker is far to the right.



(For this record the reflection coefficient is 3.5%)



(For this record the reflection coefficient is 9.3%)

FIGURE 10-2 Sample records from the reflection coefficient measuring experiment.

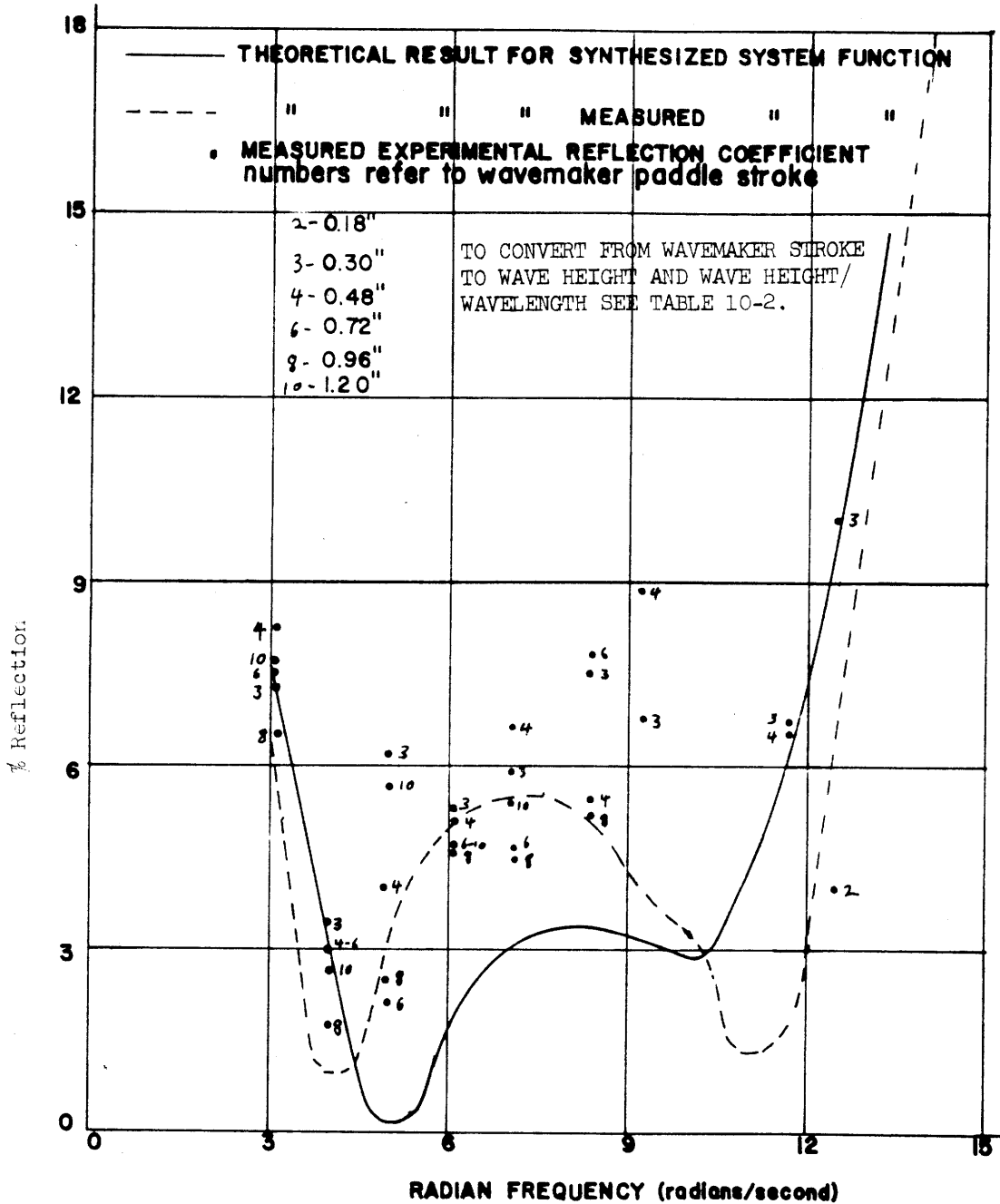


FIGURE 10-3 Theoretical and experimental reflection coefficients

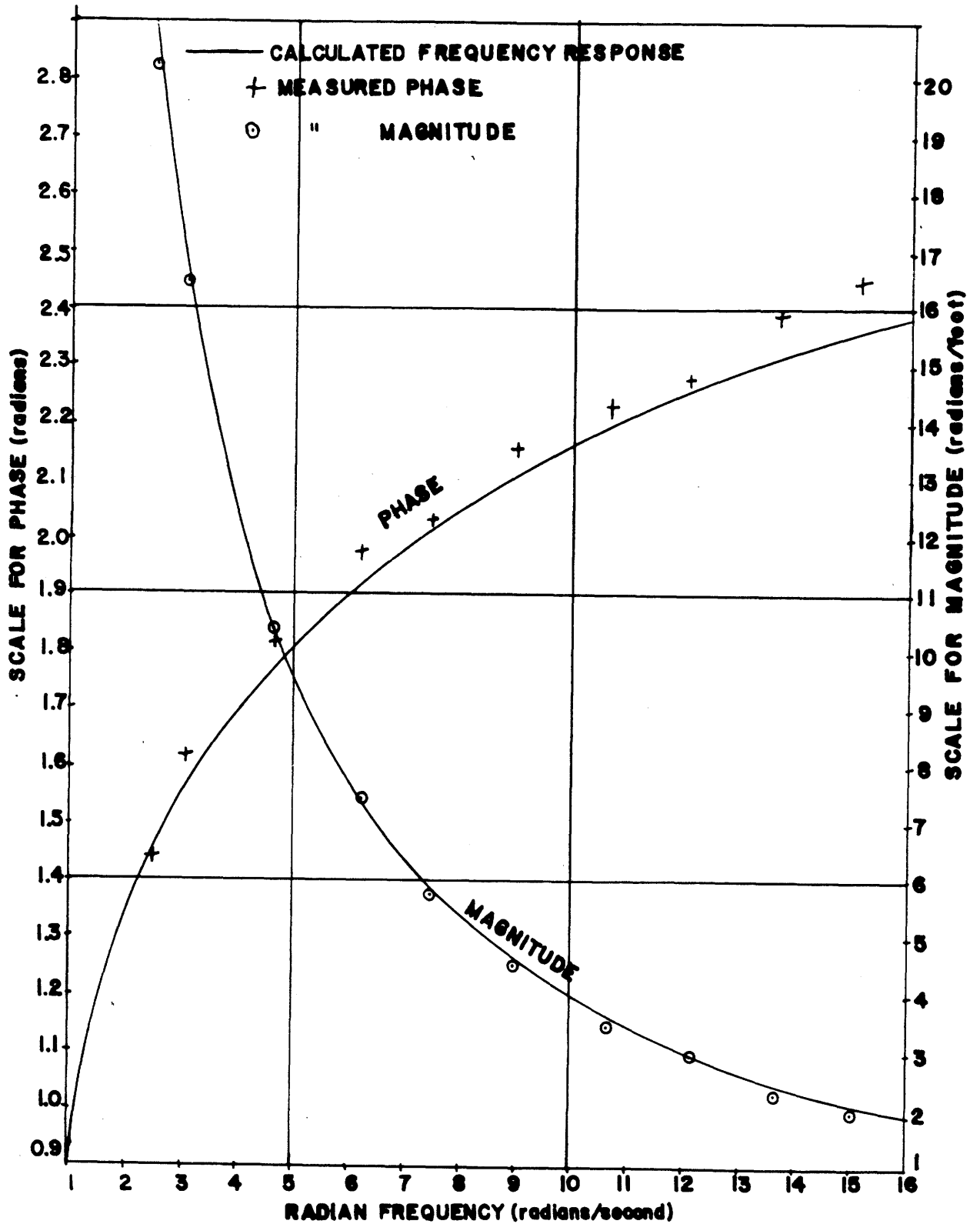


FIGURE 10-4 Calculated and measured values for the frequency response of the absorbing system.



Chapter 11  
ABSORPTION OF WAVE PULSES

Introduction

This chapter deals with the absorption of a wave pulse by a linear wave absorber. The theoretical problem is then a consideration of the initial value problem according to linear theory (first order). Since the solution for a sinusoidal incident wave exists (see chapter 4) it seems reasonable, at first glance, to expect that any square integrable initial condition could be represented by an integral over the normal modes of the tank and that the resulting solution would be well behaved. However, this is not the case in general because of two types of singularities in the problem. The first type of singularity can come about if the value of  $\eta$  or  $\eta_t$  for any eigenfunction is zero at  $t = 0$ . The second type of singularity comes about because for a unit eigenfunction of wave elevation or surface velocity, as  $\omega \rightarrow 0$  the amplitude of the associated paddle angle eigenfunction can become infinite. As will be shown subsequently, each of these singularities can be avoided by placing certain restrictions on the transfer function from wave height at the measuring probe to paddle angle.

Theory

The notation of chapter 10 will be used in this development. The problem considered here will be for a given initial surface elevation which is square integrable and no initial surface velocity. The problem for given initial surface velocity and no initial surface elevation can be

treated in a similar way to the problem treated here. Since the theory used is linear, the solutions for initial elevation and initial velocity can be added to achieve the solution for given values of initial elevation and velocity.

Let

$$A'(\alpha_0) = K(\alpha_0) A(\alpha_0) \quad (11-1)$$

K can be determined from the system function of the absorber (see chapter 10)

Let the initial surface elevation be given by  $\psi(x)$

$$\eta(x, 0) = \psi(x) \quad (11-2)$$

The purpose here is to determine the conditions under which the surface elevation,  $\eta(x, t)$ , can be represented by an integral over the eigenfunctions of surface elevation; i.e., to determine when the following representation is valid:

$$\eta(x, t) = \int_0^{\infty} g(\alpha_0) \left\{ \frac{\alpha_0}{-i\omega(\alpha_0)} A(\alpha_0) \sinh \alpha_0 h e^{i(\alpha_0 x - \omega t)} + \frac{\alpha_0}{-i\omega(\alpha_0)} A'(\alpha_0) \sinh \alpha_0 h e^{i(-\alpha_0 x - \omega t)} + \sum \frac{\alpha_n(\alpha_0) A_n(\alpha_0)}{i\omega(\alpha_0)} \sin[\alpha_n(\alpha_0) h] e^{[\alpha_n(\alpha_0) x] - i\omega(\alpha_0) t} \right\} d\alpha_0$$

(11-3)

$$\eta(x,0) = \int_0^{\infty} g(\alpha_0) \left\{ \frac{\alpha_0}{-i\omega(\alpha_0)} [A(\alpha_0) - \overline{A'(\alpha_0)}] \sinh \alpha_0 h e^{i\alpha_0 x} + \sum \frac{\alpha_n(\alpha_0) A_n(\alpha_0)}{i\omega(\alpha_0)} \sin[\alpha_n(\alpha_0)h] e^{[\alpha_n(\alpha_0)x]} \right\} d\alpha_0 \quad (11-4)$$

The normalization of the eigenfunctions will be taken such that:

$$\frac{\alpha_0}{-i\omega(\alpha_0)} [A(\alpha_0) - \overline{A'(\alpha_0)}] \sinh \alpha_0 h = 1 \quad (11-5)$$

Solving for A in equation (11-5) and using equation (11-1) gives:

$$A = - \frac{i\omega(\alpha_0)}{\alpha_0} \frac{1}{\sinh \alpha_0 h} \frac{\bar{K}-1}{|K|^2-1} \quad (11-6)$$

It is shown in chapter 10 that

$$A_n = i \frac{\alpha_0}{\alpha_n} \frac{\bar{I}_{1n}}{I_{3n}} \frac{\bar{I}_1}{I_2} (A - A')$$

where the A's are functions of  $\alpha_0$ .

From equations (11-1) and (11-6),

$$(A - A') = \frac{\bar{K}-K}{|K|^2-1} \frac{-i\omega(\alpha_0)}{\alpha_0 \sinh \alpha_0 h} \quad (11-7)$$

Let

$$\frac{\bar{K}-K}{|K|^2-1} = U(\alpha_0) \quad (11-8)$$

Hence

$$A_n = \frac{\omega(\alpha_0)}{\alpha_n} \frac{\bar{I}_{1n}}{I_{1n}} \frac{\bar{I}_2}{I_2} \frac{U(\alpha_0)}{\sinh \alpha_0 h} \quad (11-9)$$

It should be noted that there are possible singularities in  $A_n$  at any value of  $\alpha_0$  for which  $|K(\alpha_0)| = 1$  and at  $\alpha_0 = 0$ .

Now consider equation (11-4) and make use of the normalization (11-5), equation (11-9), for the  $A_n$ 's and equation (11-2).

$$\psi(x) = \int_0^{\infty} g(\alpha_0) \{ e^{i\alpha_0 x} + g(\alpha_0, x) \} d\alpha_0 \quad (11-10)$$

where

$$g(\alpha_0, x) = \sum_{n=1}^{\infty} \frac{1}{i} \frac{U(\alpha_0)}{\sinh \alpha_0 h} \frac{\bar{I}_2}{I_2} \frac{\bar{I}_{1n}}{I_{1n}} \sin[\alpha_n(\alpha_0)k] e^{[\alpha_n(\alpha_0)x]} \quad (11-11)$$

Equation (11-10) is an integral equation of the first kind. Very little useful general information exists for conditions needed for the existence of solutions for such equations. However, an integral equation of the second kind can be obtained by taking the Fourier transform from  $x$  to  $\beta$  of equation (11-10). For the present problem the integration limits for Fourier transforms are  $(-\infty, 0]$  in  $x$  and  $[0, \infty)$  in  $\beta$ .

Let

$$\int_{-\infty}^0 \psi(x) e^{-i\beta x} dx = \Psi(\beta) \quad (11-12)$$

and

$$\int_{-\infty}^{\infty} g(\alpha_0, x) e^{-i\beta x} dx = Q(\alpha_0, \beta) \quad (11-13)$$

Since the paddle velocity is a continuous function of  $y$ , the series for  $q$  converges uniformly to a function of  $x$ ; so the order of summation and integration in equation (11-13) can be reversed giving:

$$Q(\alpha_0, \beta) = \sum_{n=1}^{\infty} \frac{1}{i} \frac{U(\alpha_0)}{\sinh \alpha_0 h} \frac{I_2}{I_2} \frac{I_{4n}}{I_{3n}} \sin[\alpha_n(\alpha_0)h] \frac{1}{\alpha_n(\alpha_0) + i\beta} \quad (11-14)$$

The terms in the sum for  $Q(\alpha_0, \beta)$  behave as  $\frac{1}{n}$  for large  $n$  except as  $\alpha_0$  goes to zero in which case they behave as  $\frac{1}{n^3}$ . Therefore the series converges uniformly for all  $\alpha_0$  and  $\beta$  in  $[0, \infty)$  so in any subsequent integrals, the sum can be integrated term by term if this is necessary.

The Fourier transform of equation (11-10) is:

$$\Psi(\beta) = g(\beta) + \int_0^{\infty} g(\alpha_0) Q(\alpha_0, \beta) d\alpha_0 \quad (11-15)$$

It is shown in most treatises on Fredholm Integral Equations of the second kind (for example, see Mikhlin, Ref. 9) that a solution to equation (11-15) exists if:

$$C_1 = \int_0^{\infty} \int_0^{\infty} |Q(\alpha_0, \beta)|^2 d\beta d\alpha_0 < \infty \quad (11-16)$$

and

$$C_2 = \int_0^{\infty} |Q(\alpha_0, \beta)|^2 d\alpha_0 < \infty \quad (11-17)$$

Moreover the solution is unique if there are no non-trivial solutions to the homogeneous equation.

$$0 = g(\beta) + \int_0^{\infty} g(\alpha_0) Q(\alpha_0, \beta) d\alpha_0 \quad (11-18)$$

If a solution to equation (11-18) exists then it represents a solution to the problem with the water at rest at  $t = 0$ . The non-existence of non-trivial solutions to equation (11-18) is a criterion of stability. Therefore, if a solution to equation (11-15) exists, it is unique if the absorber is stable.

In order to determine when equations (11-16) and (11-17) hold, an upper bound on  $|Q(\alpha_0, \beta)|^2$  will be determined first. This upper bound will be called  $Q_m(\alpha_0, \beta)^2$ . The expressions for  $I_1$ ,  $I_2$ ,  $I_{3n}$  and  $I_{4n}$  are taken from chapter 4.

$$|Q(\alpha_0, \beta)|^2 < \sum \frac{|H(\alpha_0)|^2 \frac{h^2}{4} \left( \frac{1}{\sinh \alpha_0 h} + \frac{1}{\alpha_0 h} \cosh \alpha_0 h \right)^2}{\left\{ \frac{\rho}{\alpha_0} \sinh \alpha_0 h + \frac{1}{\alpha_0^2} [\cosh \alpha_0 (h-\beta) - \cosh \alpha_0 h] \right\}^2} .$$

$$\left\{ \frac{\frac{\rho}{\alpha_n} + \frac{2}{\alpha_n^2}}{\frac{1}{2} \left[ \frac{1}{2\alpha_n} \sin 2\alpha_n h + h \right]} \right\}^2 \frac{1}{\alpha_n^2 + \beta^2}$$

(11-19)

The equation for the  $\alpha_n$ 's, (4-11), shows that:

$$\alpha_n > \frac{\pi}{2h} \quad (11-20)$$

Therefore

$$|Q(\alpha_0, \beta)|^2 < \frac{|U(\alpha_0)|^2 \frac{h^2}{4} \left( \frac{1}{\sinh \alpha_0 h} + \frac{1}{\alpha_0 h} \cosh \alpha_0 h \right)^2}{\left\{ \frac{\beta}{\alpha_0} \sinh \alpha_0 h + \frac{1}{\alpha_0^2} [\cosh \alpha_0 (h-\beta) - \cosh \alpha_0 h] \right\}^2} \cdot$$

$$\sum_{n=1}^{\infty} \left\{ \frac{\frac{2\beta}{\alpha_n} + \frac{4}{\alpha_n^2}}{h(1-\frac{\beta}{\alpha_n})} \right\}^2 \frac{1}{\alpha_n^2 + \beta^2} \equiv |Q_m(\alpha_0, \beta)|^2 \quad (11-21)$$

$$C_1 < \int_0^{\infty} \int_0^{\infty} |Q_m(\alpha_0, \beta)|^2 d\beta d\alpha_0 \equiv C_{1m} \quad (11-22)$$

$$C_2 < \int_0^{\infty} |Q_m(\alpha_0, \beta)|^2 d\alpha_0 \quad (11-23)$$

The integral over  $\beta$  in the expression for  $C_{1m}$  can be carried out by quadrature leaving:

$$C_{1m} = \int_0^{\infty} \frac{u(\alpha_0) \frac{k^2}{4} \left( \frac{1}{\sinh \alpha_0 h} + \frac{1}{\alpha_0 h} \cosh \alpha_0 h \right)^2}{\left\{ \frac{\rho}{\alpha_0} \sinh \alpha_0 h + \frac{1}{\alpha_0^2} [\cosh \alpha_0 (h-\rho) - \cosh \alpha_0 h] \right\}^2} \cdot \sum_{n=1}^{\infty} \left\{ \frac{\left( \frac{2\rho}{\alpha_n} + \frac{4}{\alpha_n^2} \right)^2}{k \left( 1 - \frac{1}{\pi} \right)} \right\}^2 \frac{\pi}{2\alpha_n^2} d\alpha_0$$

(11-24)

The series in equation (11-24) converges to a finite number. Let this number be S. At this point it is clear that if  $C_{1m} < \infty$ , then  $C_{2m} < \infty$ . Therefore, a unique solution to equation (11-15) exists if

$$C_{1m} = S \int_0^{\infty} \frac{|u(\alpha_0)|^2 \frac{k^2}{4} \left( \frac{1}{\sinh \alpha_0 h} + \frac{1}{\alpha_0 h} \cosh \alpha_0 h \right)^2}{\left\{ \frac{\rho}{\alpha_0} \sinh \alpha_0 h + \frac{1}{\alpha_0^2} [\cosh \alpha_0 (h-\rho) - \cosh \alpha_0 h] \right\}^2} d\alpha_0 < \infty$$

(11-25)

Apart from the factor  $|u(\alpha_0)|^2$  there are two possible singularities in the expression for  $C_{1m}$ ; these being the possible singularity in the integrand at  $\alpha_0 = 0$  and the infinite integration limit.

$$\text{As } \alpha_0 \rightarrow 0 \text{ the integrand behaves like } \frac{1}{\alpha_0^2} |u(\alpha_0)|^2 \quad (11-26)$$

$$\text{As } \alpha_0 \rightarrow \infty \text{ the integrand behaves like } \alpha_0^2 |u(\alpha_0)|^2 \quad (11-27)$$

Therefore, if all the singularities in  $|u(\alpha_0)|^2$  are properly integrable,

$C_{1m} < \infty$  if:

$$|u(\alpha_0)| \underset{\alpha_0 \rightarrow 0}{\sim} \alpha_0^{f_1}, \quad f_1 > \frac{1}{2} \quad (11-28)$$

and

$$|u(\alpha_0)| \underset{\alpha_0 \rightarrow \infty}{\sim} \frac{1}{\alpha_0^{f_2}}, \quad f_2 > \frac{3}{2} \quad (11-29)$$

The conditions (11-28) and (11-29) as well as the condition that  $|u(\alpha_0)|^2$  is properly integrable over  $[0, \infty)$  form a set of sufficient conditions for equation (11-15) to be a valid representation for the solution to the initial value problem. The restriction (11-28) is needed because for unit wave amplitude the paddle stroke goes to infinity as the frequency goes to zero. The restriction (11-29) is needed to insure bounded energy in the local, non-travelling waves.

In theory, any wave pulse can be absorbed by a perfect absorber since  $u(\alpha_0)$  is identically zero for a perfect absorber. However, unless the low frequency energy in the pulse goes to zero rapidly enough as  $\omega \rightarrow 0$ , the paddle amplitude will become infinite invalidating the assumption of small motion.

### Experiment

In view of the preceding theoretical development, a wave absorber should absorb almost all of that part of a wave pulse whose spectrum lies in the frequency range for which the reflection coefficient of the absorbing system is small compared to unity. In order to confirm this result the following qualitative experiment was performed.

A wave measuring probe was fixed in the center of the tank and the wavemaker was given a pulse that would produce a wave pulse whose spectrum

had a measurable amount of energy in the range of  $\omega = 0.8$  to  $\omega = 20$  radians per second. The range for which the wave absorber gives a small reflection coefficient is from  $\omega = 3$  to  $\omega = 13$  radians per second. A recording of the measured wave elevation for this experiment appears in figure (11-1). As a control, the experiment was repeated for the absorber replaced by a 10 degree sloping beach and again for a solid immovable wall at  $x = 0$ . In each case the water started at rest and the wave pulses were identical. The surface elevation recording for the pulse with the sloping beach appears as figure (11-2) and the recording for the pulse with a solid wall appears as figure (11-3).

The recording made with the wave absorber in use (figure 11-1) has some interesting features. Considerable reflected wave energy is observable at frequencies outside the range of wave frequencies the system was designed to absorb (3 to 13 radians per second). These frequencies should be reflected for the absorbing system function which was used and the broad band pulse (0.8 to 20 radians/sec) was used to allow an experimental confirmation of this fact. Figure (11-1) also contains a recording of paddle angle vs time and the comparatively large paddle motion at low frequencies compared to the low frequency wave elevation is one of the salient features of the figure. This is a graphic example of the reason for the possible low frequency singularity described in the theoretical subchapter of this chapter.

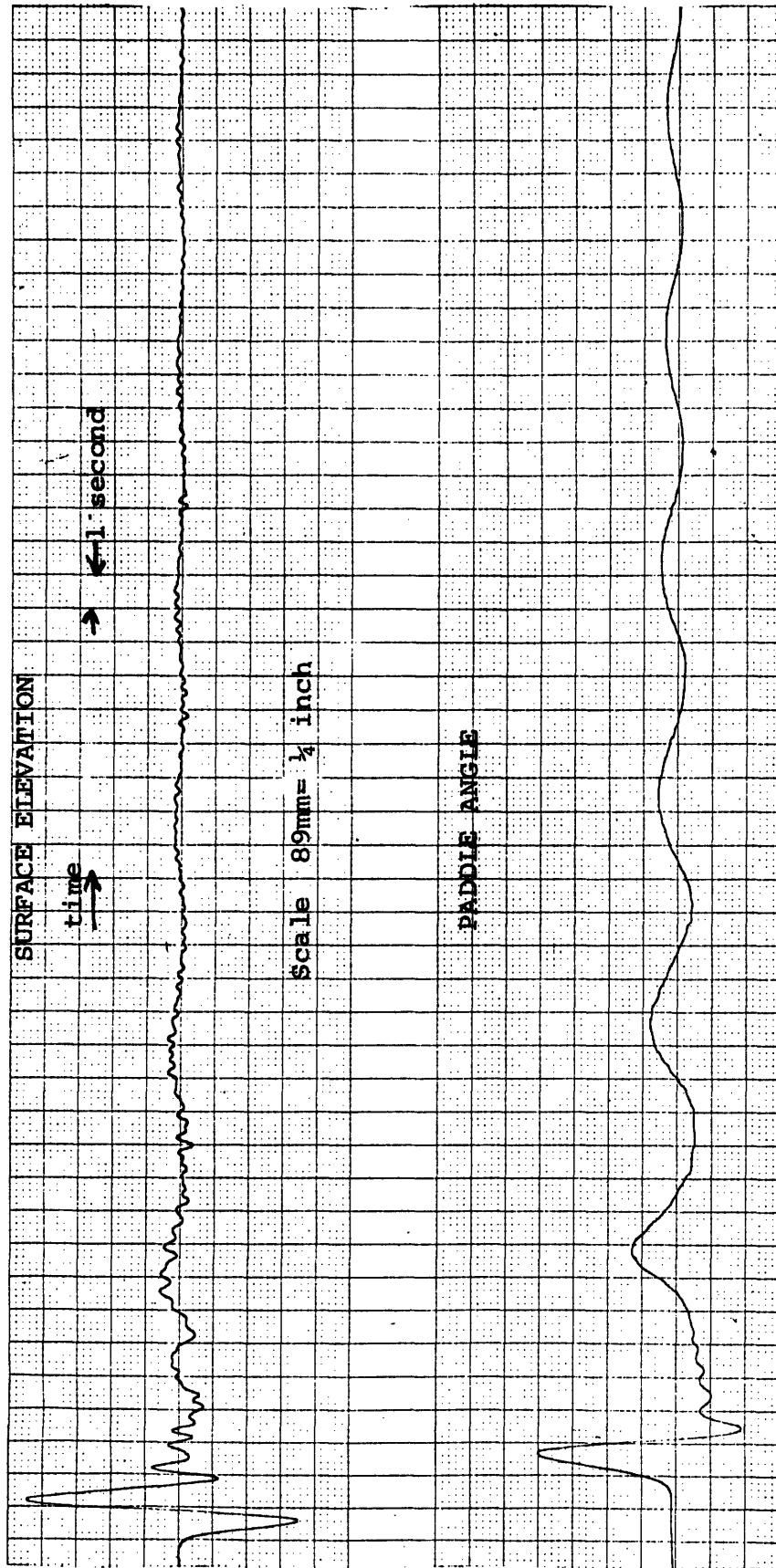


FIGURE 11-1 Paddle angle vrs. time and surface elevation at a fixed point vrs. time for a wave pulse with the wave absorber in operation.

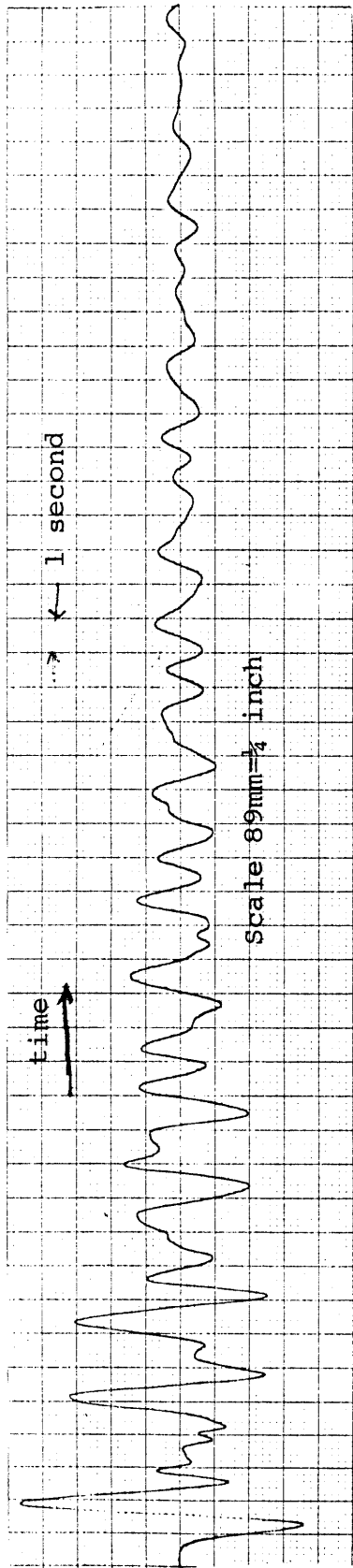


FIGURE 11-2 Surface elevation vrs. time for the same pulse used for figure 11-1, but here the wave absorber is replaced by a 10° sloping beach.

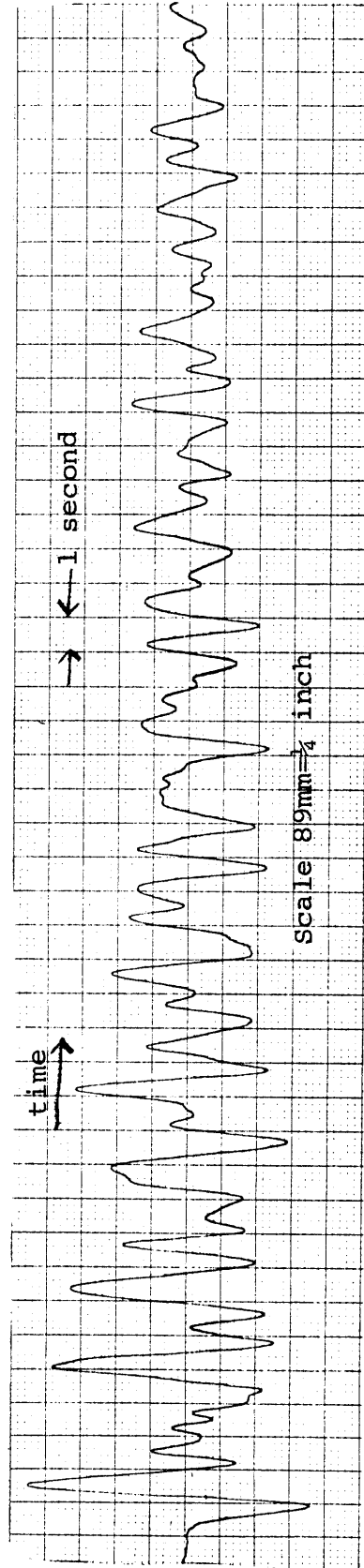


FIGURE 11-3 Surface elevation vrs. time for the same pulse used in figure 11-1, but here the wave absorber is replaced by a solid vertical wall.

## Chapter 12

### DISCUSSION OF THEORETICAL AND EXPERIMENTAL WAVE ABSORBER RESULTS

The theoretical results of chapters 4 and 10 indicate that complete absorption is theoretically possible at any wave frequency for which the absorbing system is stable with respect to negative going waves. Roughly speaking, an absorbing filter will be stable for all frequencies less than the frequency for which the distance from the absorber to the wave sensing element is equal to one quarter of a wavelength. This effect is described as follows. For very long waves, the character of the wave at the sensing element is almost the same as the character of the wave at the absorber. In order to absorb waves, the absorbing paddle velocity is approximately in phase with the fluid velocity in the incident wave, this velocity being approximately in phase with the surface elevation. Thus, for very long waves the absorbing paddle has a maximum forward (toward positive  $x$ ) velocity when the surface elevation at the probe is maximum. As the incident wavelength is decreased, the absorbing paddle velocity lags the wave elevation at the sensing probe to account for the time it takes for the wave crest to travel from the probe to the paddle. When the wavelength is four times the distance from the probe to the paddle, the phase lag is approximately 90 degrees. The word "approximately" keeps coming up because of effects of the local, non-travelling waves. Now consider the stability of the absorber for very long waves. Say the absorber attains a small velocity in the negative  $x$  direction creating a wave crest at the absorber and at the wave probe. For long waves (low frequencies) the absorbing system has the characteristic that when there

is a crest at the sensing probe the absorbing paddle is moving at maximum velocity in the positive x direction. Thus there is a negative hydrodynamic feedback signal which stabilizes the paddle at low frequencies. Such is not the case when the distance from the absorber to the probe is one quarter of a wavelength. If the absorbing paddle obtains a velocity in the negative x direction and makes a wave whose wavelength is four times the distance from absorber to probe, the wave crest reaches the probe one quarter of a period later than the time of maximum magnitude of the negative paddle velocity. At this frequency the absorbing system causes the paddle to have a maximum positive velocity one quarter of a period later than the time of maximum wave elevation at the probe, or one half a period later than the largest negative paddle velocity. Also, the relationship between wave amplitude and paddle stroke is the same for a wavemaker as it is for a wave absorber and hence the magnitude of the positive feedback is unity. These are the exact criteria for self-sustained oscillation.

In practice, the magnitude of the absorbing system function from wave elevation to paddle angle should start dropping below the theoretical value for 100 percent absorption at frequencies somewhat below the critical frequency (frequency for which the wavelength is four times the probe to paddle distance), say 15 percent below this value. This is desirable so that the small unavoidable deviations of the system function from its value for complete absorption will not cause instability and also so that any negative going waves that get started will decay quickly. The critical

frequency can be raised by using a more sophisticated wave detection scheme. If the activating signal is taken as the sum of the signals from two separate probes and a filter is built to operate on this input signal to give paddle angle, the critical frequency is that frequency whose associated wavelength is four times the longitudinal separation of the wave height probes.

The theory developed in chapter 8 of oblique waves and waves with complex eigenvalues is useful in dealing with waves where energy is added or removed at a boundary and with some waves satisfying a non-homogeneous surface condition such as those second order waves which result from the non-linear interaction of a travelling first order wave and a bound first order wave which is considered in chapter 5. At the time of the writing of chapter 5, the theory of waves with complex eigenvalues was not developed. Use of the method of complex eigenvalues would simplify some of the cumbersome expressions of this section.

The comparison between theory and experiment for the compliant wave absorber is excellent. As is shown in chapter 10 the measured reflection coefficient is within one percent of the value computed from the measured filter characteristics except for a few isolated instances. Therefore, it is reasonable to conclude that the reflection coefficient can be made as small as the calculated reflection coefficient for the absorbing system function used down to reflection coefficients somewhat less than one percent. The calculated reflection coefficient can be made as small as desired.

However, the smaller the value of the desired reflection coefficient, the more sophisticated is the needed absorbing filter.

The results on the absorption of wave pulses show that pulses can be effectively absorbed with a fairly simple electric filter such as that used in the experiments. Of course more effective absorption can be achieved with a more sophisticated electric filter. The absorber performs over a wide amplitude range and is effective for much smaller waves than for which a sloping beach is effective. This occurs because a sloping beach depends on non-linear effects for its operation and small waves are predominantly linear.

Initially it was anticipated that the absorbing system would be a device which would give the paddle the needed impedance (complex ratio of moment to paddle angle as a function of frequency) to absorb waves over a broad frequency range. Since this would be an energy absorbing device for all frequencies it would necessarily be stable so no stability analysis would be needed. However, the theoretical impedance for such a device (equation 4-32) has poles at all frequencies for which:

$$\alpha_0 = \frac{(n - \frac{1}{2})\pi}{l} \quad (12-1)$$

$\alpha_0$  is the circular wave number,  $l$  is the distance from the paddle to the end wall of the tank and  $n$  is any integer.

At these frequencies, which are the natural frequencies for the body of fluid between the paddle and the solid end wall of the tank, the moment on the paddle becomes infinite in theory. From a practical standpoint it

would be impossible to make such a device operate satisfactorily. First of all very small errors would result in very large paddle angles thus causing destruction of the apparatus. Also, at or near resonant frequencies the linear theory is very wrong so absorption would not be achieved. An interesting possibility is to use a paddle with no water in the space behind it. With small clearances between the paddle and the side and bottom walls there would be some small leakage which could be pumped back into the bottom of the tank. The currents due to the leakage and the pumping could be made negligibly small.

## Chapter 13

### INVESTIGATION OF THE RELATIONSHIP BETWEEN PRESSURE AND SURFACE ELEVATION

#### Introduction

A very convenient signal to use to activate a wave absorber is the pressure measured at a solid boundary of a tank. A pressure tap in a side wall can be located closer to an absorbing paddle without being interfered with by the paddle than can a wave height probe. A pressure tap is less susceptible to damage than a wave height probe and a pressure tap signal is not affected by menisci and free surface dirt. The theoretical relationship between the stroke of a wavemaker and the amplitude of resulting waves was experimentally verified by Ursell, Dean and Yu( 2 ). Hence it was expected that a wave absorber activated by the wave height would yield good performance. Such an expectation would exist for an absorber activated by a pressure tap if it were known that the theoretical relationship between the pressure and the wave height was valid. For this reason an investigation between the pressure at a solid boundary and the wave height was carried out.

#### Theory

Consider a semi-infinite channel of depth  $h$  extending from  $x = -\infty$  to  $x = 0$  with a solid wall at  $x = 0$ . For two dimensional waves whose amplitude is uniform in time and which satisfy all the boundary conditions (see chapters 2 and 4).

$$\phi = A_0 \cos \alpha_0 x \cosh \alpha_0 (y + h) e^{-i\omega t} \quad (13-1)$$

$$\text{where } \omega^2 = \alpha_0 g \tanh \alpha_0 h \quad (13-2)$$

Standing waves are required by the boundary condition at  $x = 0$ .

From the linearized form of Bernoulli's equation

$$P_{total} = -\rho [gy + \phi_t] \quad (13-3)$$

denoting the time varying part by  $P(t)$ ,

$$P(t) = -\rho \phi_t \quad (13-4)$$

$$P(t) \Big|_{y=y'} = i\rho \omega A_0 \cos \alpha_0 x \cosh \alpha_0 (y'+h) e^{-i\omega t} \quad (13-5)$$

The free surface kinematic condition ( $\phi_y|_{y=0} = \eta_t$  (2-22)) gives,

$$\eta = \frac{\alpha_0 A_0}{-i\omega} \cos \alpha_0 x \sinh \alpha_0 h e^{-i\omega t} \quad (13-6)$$

The experiment performed was to determine the ratio of the pressure measured at  $x = 0$  and at some depth, divided by the wave amplitude measured at  $x = -d$ . The variables were the depth of the pressure tap, the wave amplitude and the wave frequency.

$$\frac{P \Big|_{x=0, y=y'}}{\eta \Big|_{x=-d}} = \rho \frac{\omega^2}{\alpha_0} \frac{\cosh \alpha_0 (y'+h)}{\sinh \alpha_0 h \cos \alpha_0 d} \quad (13-7)$$

This function was evaluated by means of the computer program REFLEC, the output of which appears as table 13-1. The extreme left hand column of this table gives  $y'$  and the uppermost row of the table gives the radian frequency. This table is calculated for  $h = 0.4167$  feet (5 inches) and  $d = 0.0833$  feet (1 inch).

## Experiments

For this experiment, the wave absorbing paddle at  $x = 0$  was replaced by an immovable wall containing a column of pressure taps along its centerline as shown in figure 13-1. The wave height probe (Appendix C) was mounted one inch (0.0833 ft) downstream of the end wall and about two inches to the side of the tank centerline to avoid interfering with the pressure measurements which were taken on the tank centerline. Experiments were performed for pressure measurements at depths of 0.03125, 0.06250, 0.09375, 0.12500, 0.15625, 0.18750, 0.21875, 0.25000 and 0.28125 feet (every  $3/8$  inches).

The wave height probe was calibrated by moving it up and down by fixed amounts in still water and comparing the change in probe height with recorder pen deflection. The pressure transducer was calibrated by connecting its input to a vessel of water and moving the vessel up and down by fixed amounts and comparing the change in vessel level with recorder pen deflection.

In the experiments the wavemaker was turned on and allowed to run until a constant amplitude standing wave developed. Then the wave height and the pressure were simultaneously recorded on a two channel recorder (Appendix D). The pressure transducer is a Sanborn Model 268B. This transducer is very sensitive to noise so the recorder filtering described in Appendix D and extreme care in avoiding vibration were necessary to obtain a clean signal. The experiments were carried out for a range of radian frequencies from 2 to 20 radians per second and a range of wave-maker strokes from 0.2 to 2.0 inches.

Figures (13-2) through (13-10) show the results of this experiment. Each figure corresponds to a given pressure tap depth. The ordinate of each graph is the ratio of wave pressure to wave amplitude and the abscissa is the radian frequency. The theoretical functions computed by REFLEC are shown in these figures as a solid line and the experimental results are shown as points.

#### Discussion of Experimental Results

Examination of figures (13-2) through (13-10) shows that the experimental results have an average value within two percent of the theoretical value with a standard deviation of about two percent except for a few of the results for the smallest wavemaker stroke and the largest pressure tap depth at the higher frequencies. For these erroneous points the magnitude of the measured pressure was about 1/500 PSI so the error could be due to noise, hysteresis in the transducer or error in the attenuation resistors in the recorder amplifiers. There does not appear to be any significant relation between the measured value of the pressure/height ratio and wave amplitude over the range of wave amplitudes used in this experiment. Because of this fact and the very good agreement between theory and experiment, the small observed error is probably due to calibration error. The agreement between theory and experiment indicates that it would most likely be feasible to activate a wave absorber with a pressure signal. However, since such a signal would probably come from a tap in a side wall, it is deemed advisable to measure the pressure/wave height ratio for a few

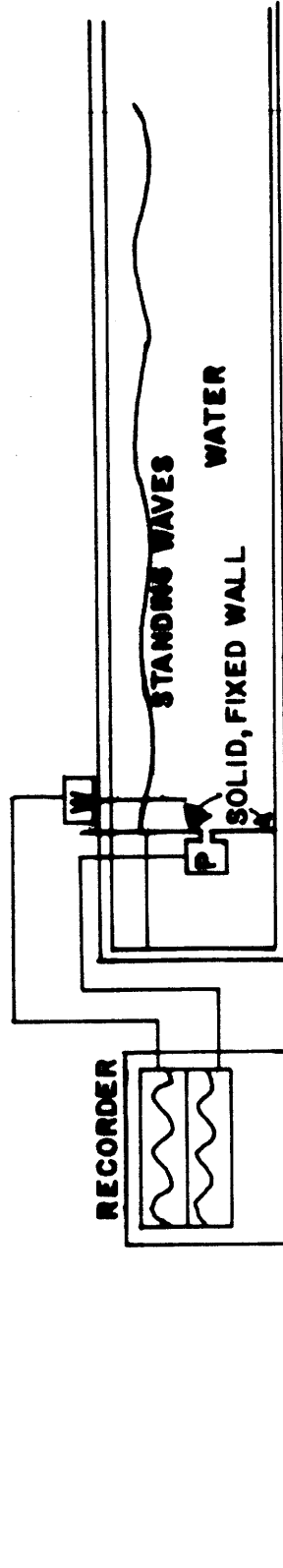
values of wave height and wave frequency with a pressure tap in a side wall. This would determine whether or not there is a significant effect on the ratio from the boundary layer at the side wall. There most likely is no such significant effect, but one does not know this for sure until the experiment is performed.

print .tape. 6  
W 1301.9

.TAPE. 6 - M2213 2966 - CTR1H2 - MAY 11, 1965 - 1302.0

OMEGA DEPTH	2.000	4.000	6.000	8.000	10.000	12.000	14.000	16.000	18.000	20.000
-.03125	62.223	61.734	60.971	60.040	59.146	58.672	59.234	61.758	67.895	81.750
-.06250	62.008	60.876	59.050	56.647	53.895	51.184	49.077	48.253	49.693	55.684
-.09375	61.811	60.094	57.310	53.610	49.278	44.783	40.738	37.735	36.384	37.933
-.12500	61.633	59.387	55.748	50.911	45.241	39.332	33.908	29.554	26.656	25.847
-.15625	61.473	58.755	54.357	48.531	41.738	34.716	28.333	23.201	19.551	17.620
-.18750	61.331	58.196	53.135	46.455	38.725	30.837	23.808	18.285	14.372	12.023
-.21875	61.207	57.710	52.076	44.672	36.169	27.612	20.165	14.501	10.607	8.223
-.25000	61.102	57.296	51.178	43.170	34.039	24.974	17.268	11.615	7.887	5.650
-.28125	61.015	56.954	50.438	41.938	32.310	22.865	15.011	9.448	5.943	3.921
-.31250	60.945	56.684	49.854	40.971	30.962	21.242	13.310	7.865	4.584	2.777
-.34375	60.894	56.484	49.424	40.260	29.978	20.070	12.102	6.770	3.676	2.048
-.37500	60.861	56.354	49.146	39.803	29.347	19.324	11.342	6.093	3.130	1.625

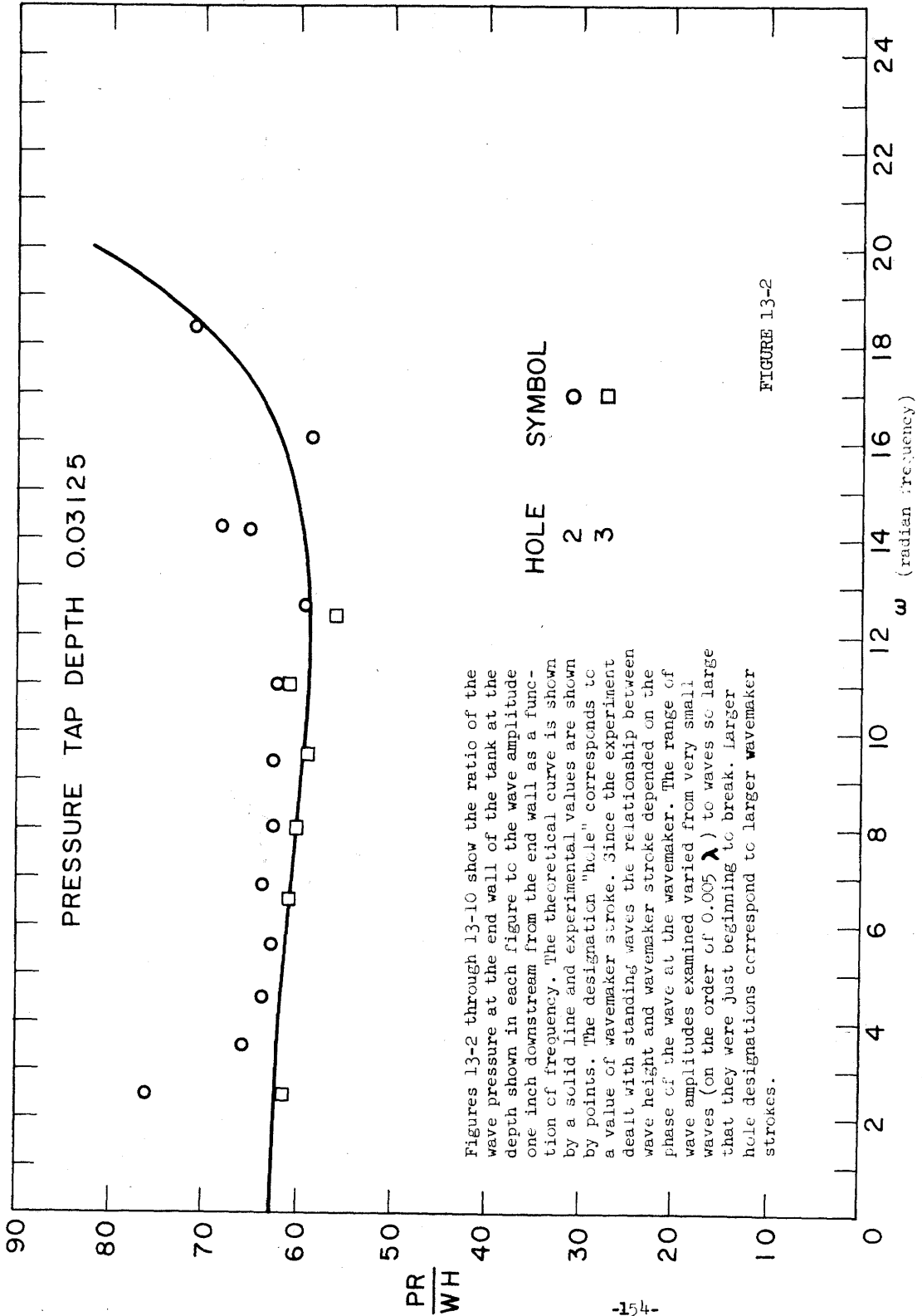
TABLE 13-1 Theoretical values of the ratio of wave pressure to wave height as a function of radian frequency and depth of the pressure tap.



**W** = SURFACE ELEVATION DETECTOR

**P** = PRESSURE TRANSDUCER

FIGURE 13-1 This depicts the experiment for measuring the relationship between pressure and wave height.



Figures 13-2 through 13-10 show the ratio of the wave pressure at the end wall of the tank at the depth shown in each figure to the wave amplitude one inch downstream from the end wall as a function of frequency. The theoretical curve is shown by a solid line and experimental values are shown by points. The designation "hole" corresponds to a value of wavemaker stroke. Since the experiment dealt with standing waves the relationship between wave height and wavemaker stroke depended on the phase of the wave at the wavemaker. The range of wave amplitudes examined varied from very small waves (on the order of  $0.005 \lambda$ ) to waves so large that they were just beginning to break. Larger hole designations correspond to larger wavemaker strokes.

FIGURE 13-2

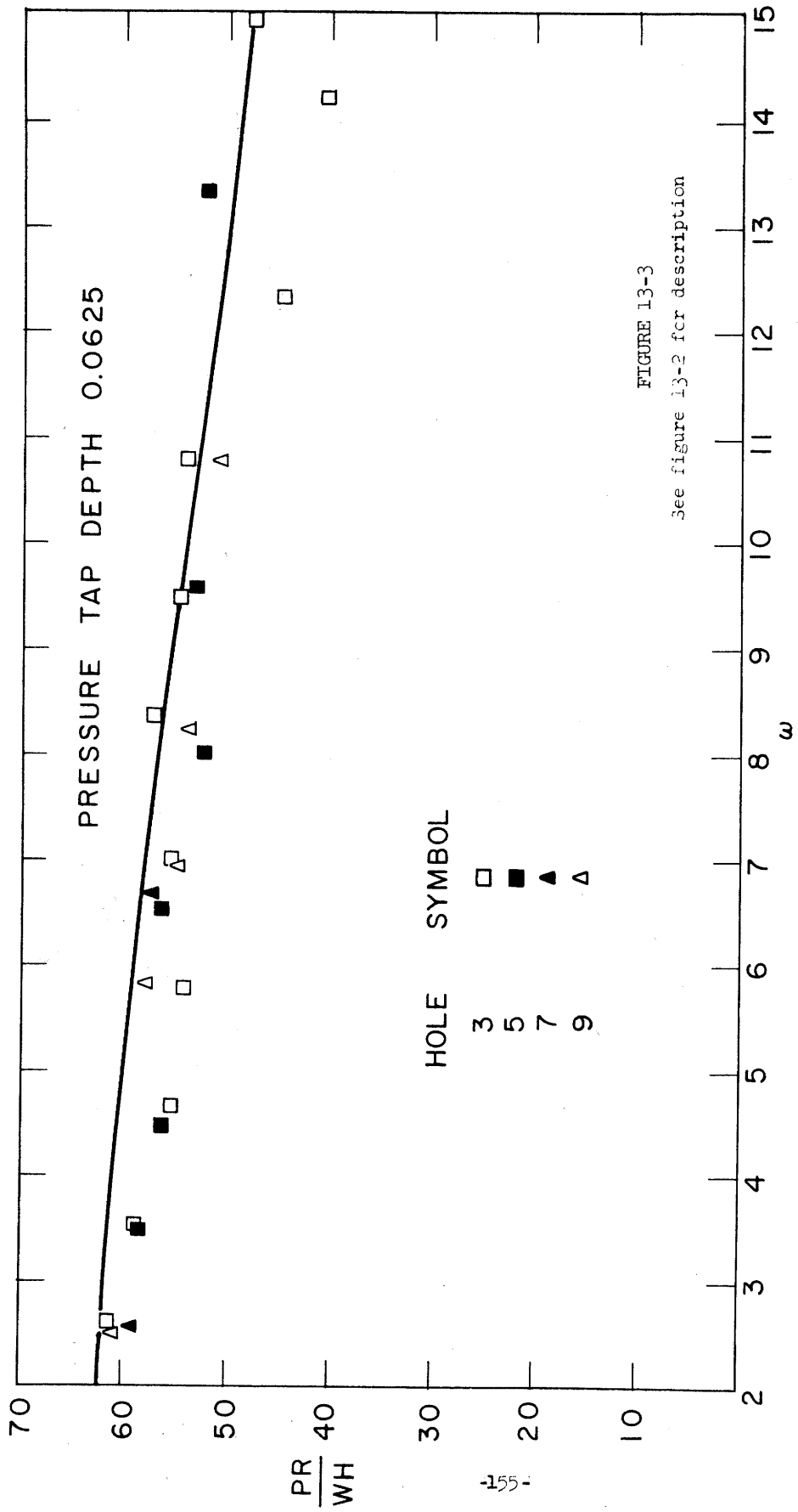


FIGURE 13-3

See figure 13-2 for description

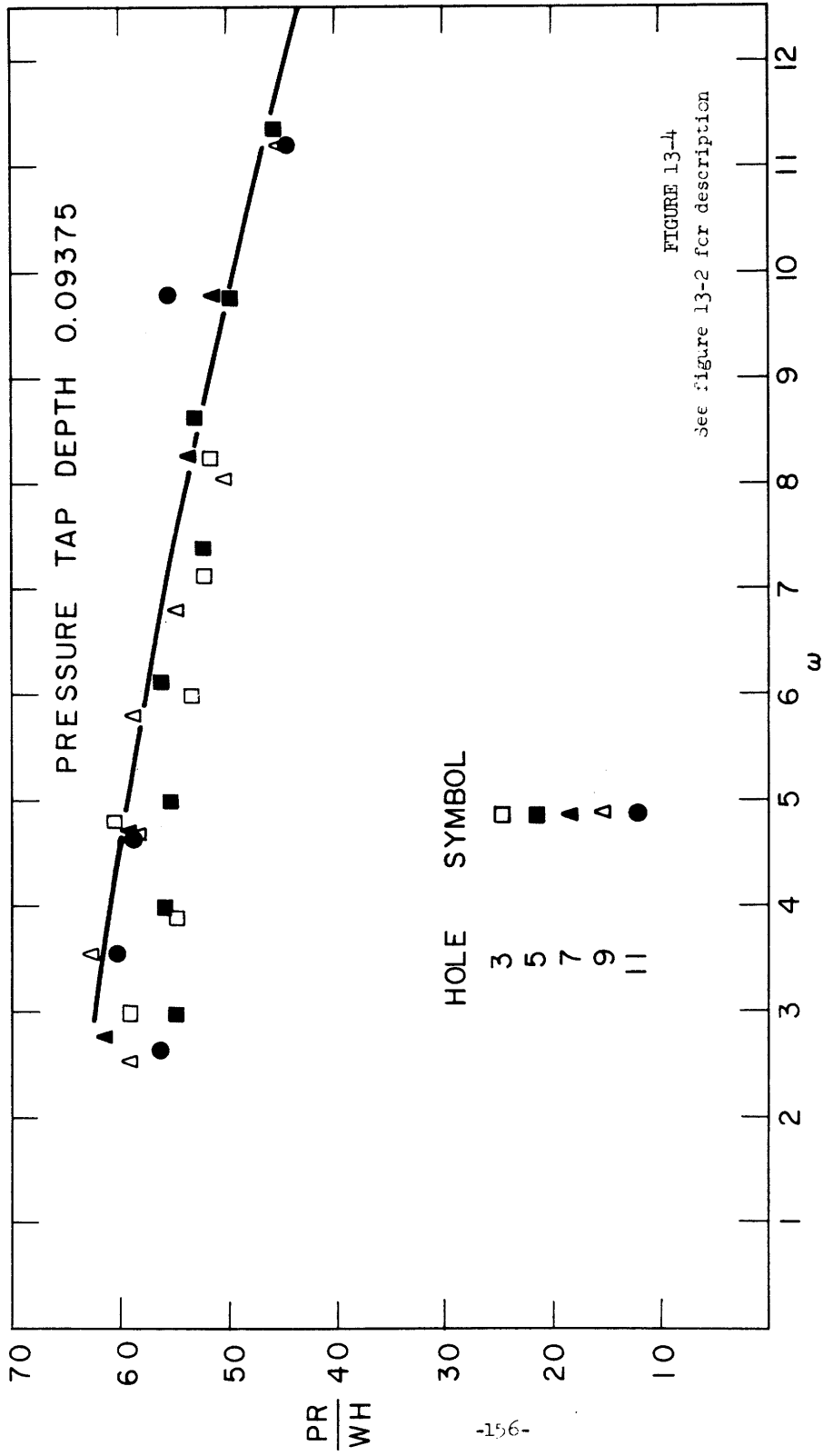


FIGURE 13-4

See figure 13-2 for description

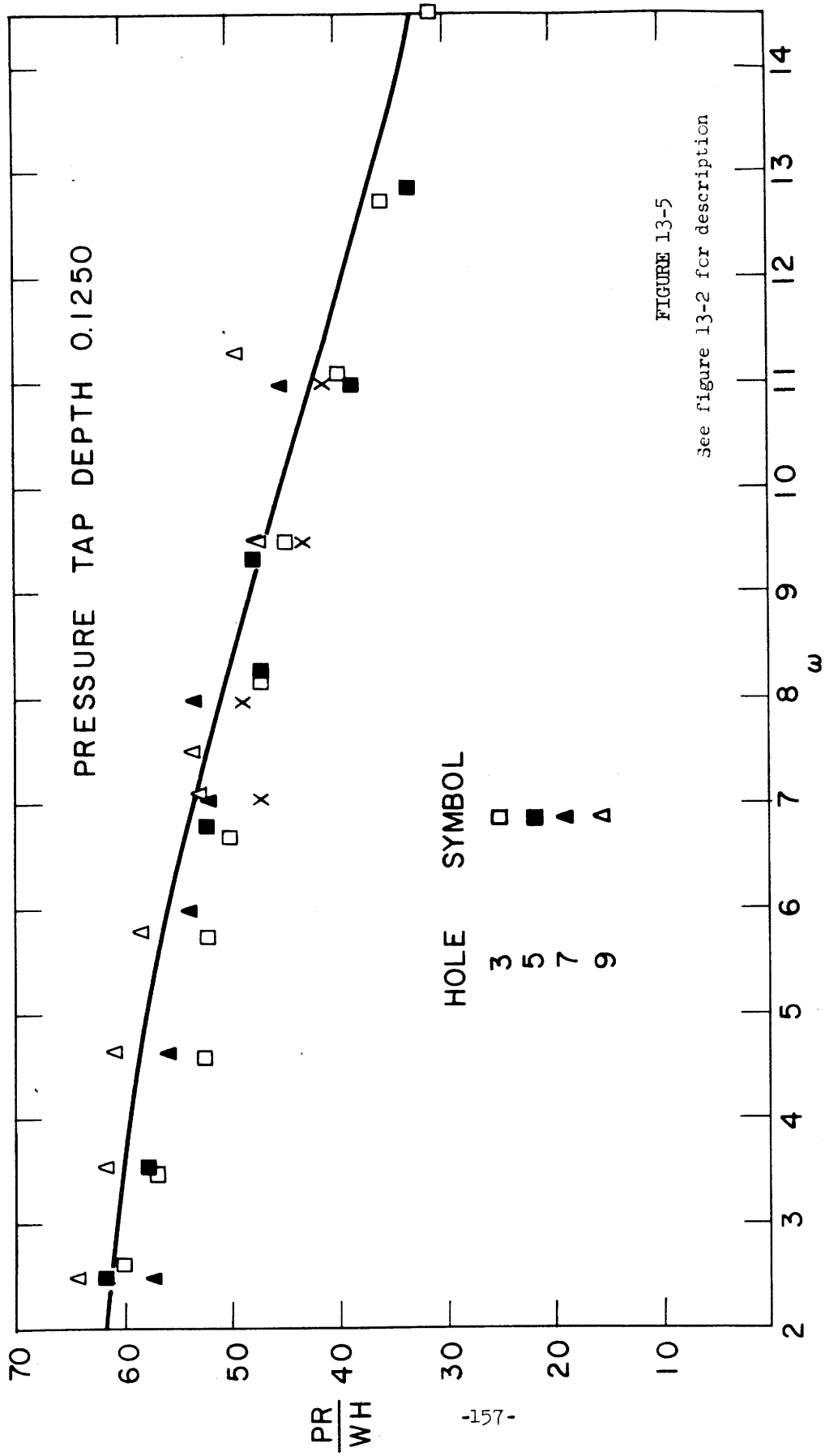


FIGURE 13-5

See figure 13-2 for description

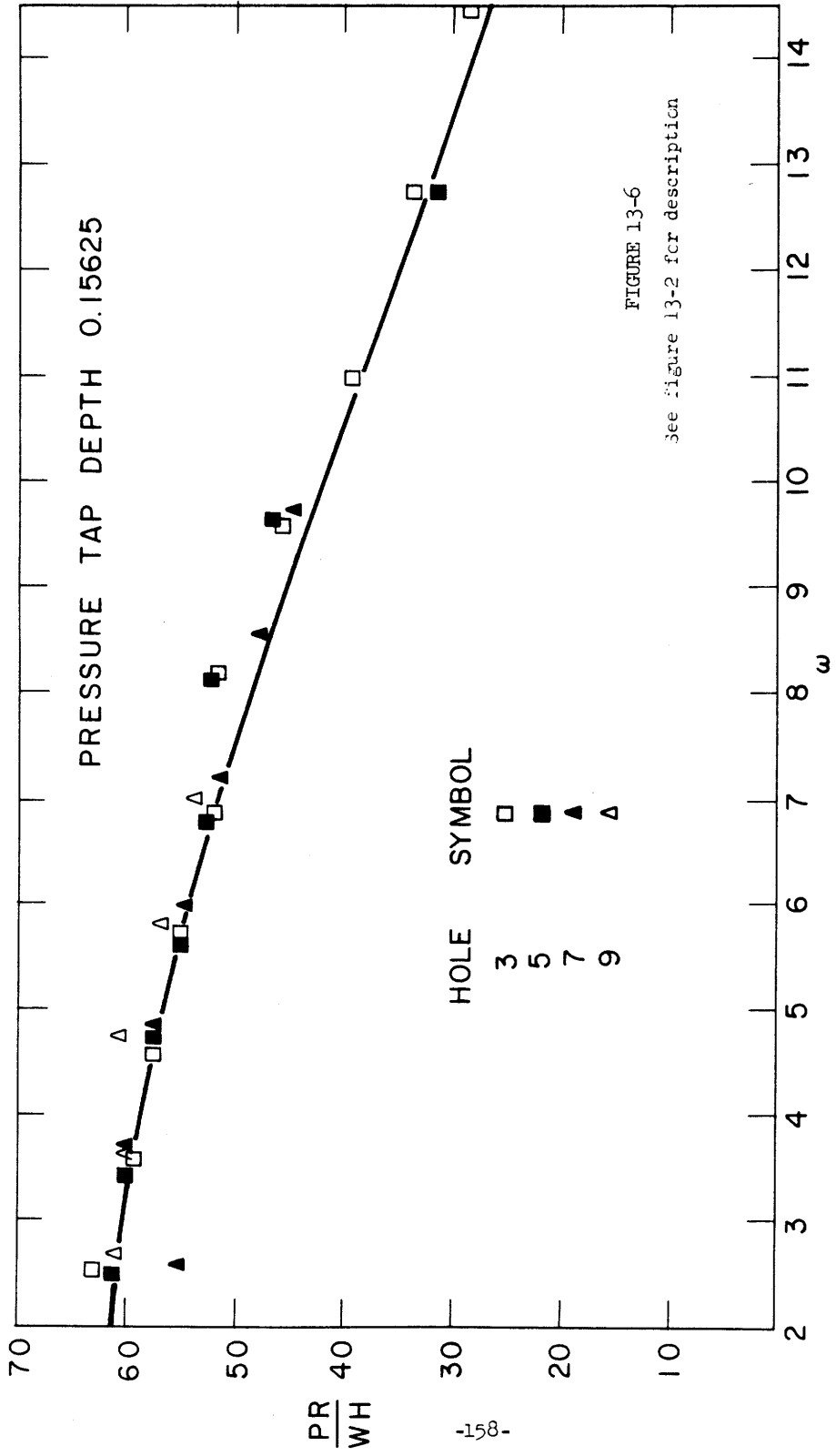


FIGURE 13-6

See figure 13-2 for description

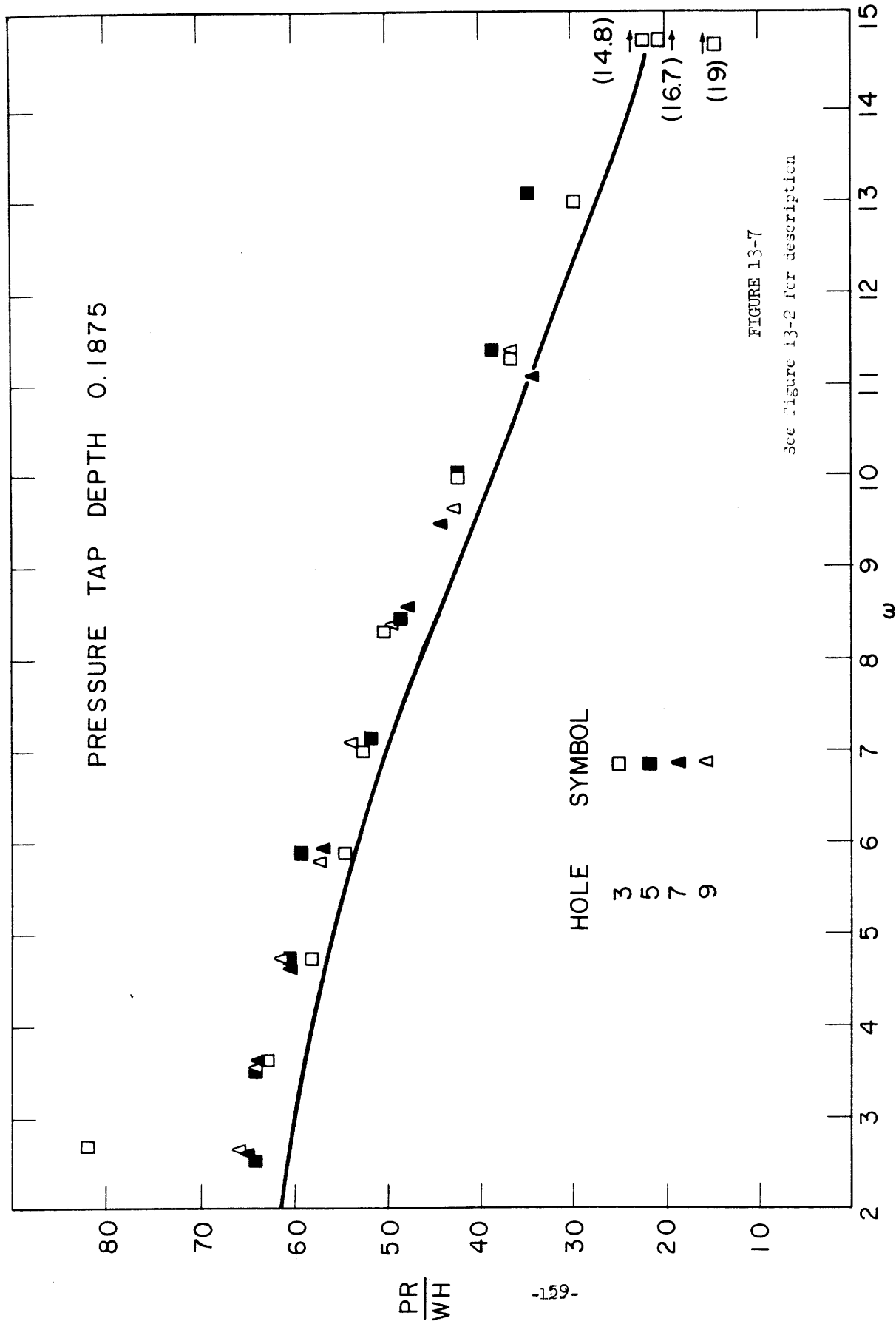


FIGURE 13-7

See Figure 13-2 for description

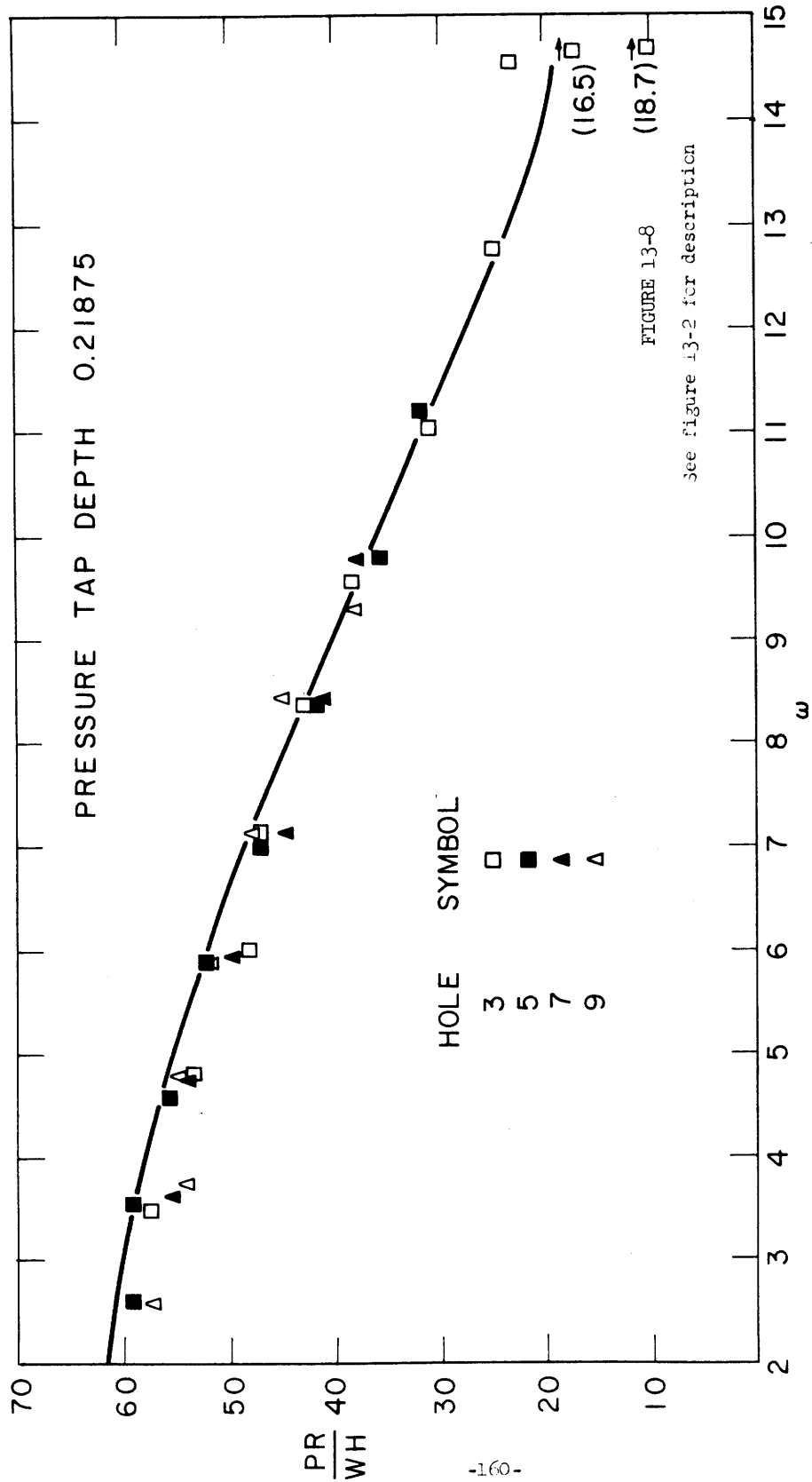


FIGURE 13-8

See figure 13-2 for description

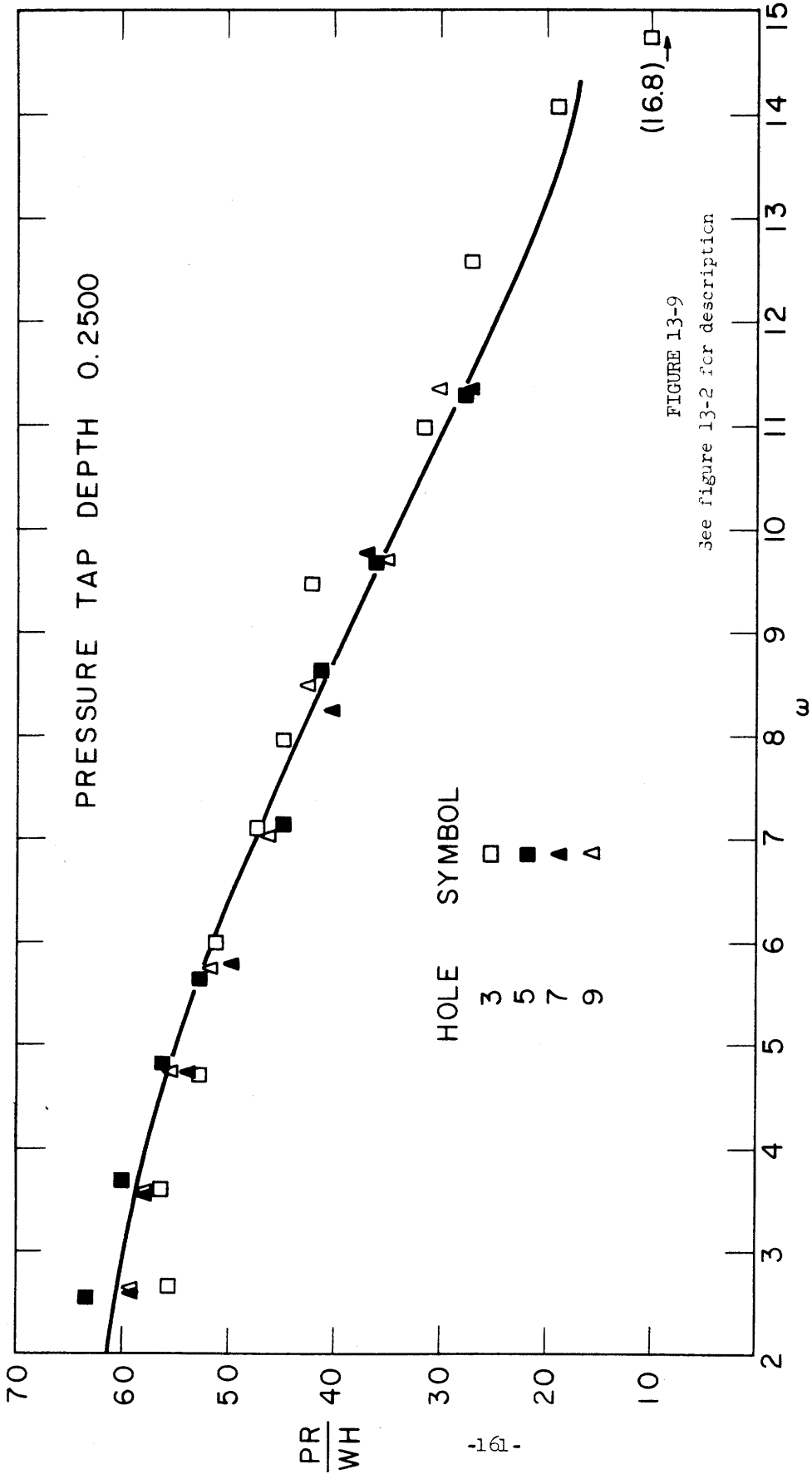


FIGURE 13-9

See figure 13-2 for description

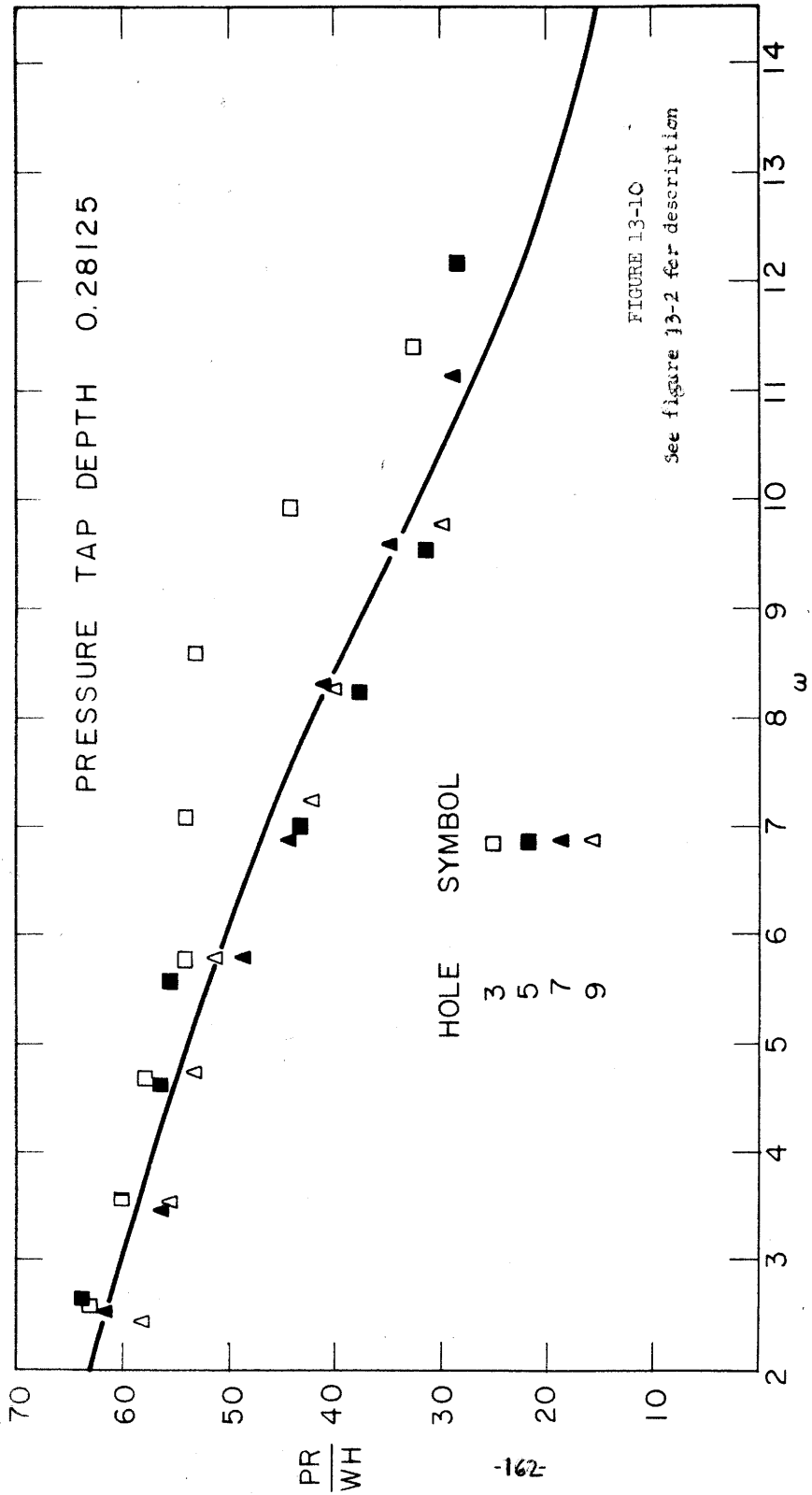


FIGURE 13-10

See figure 13-2 for description

## Chapter 14

### CONCLUSIONS

The agreement between theory and experiment for the reflection coefficient of a moving wave absorber and for the ratio of pressure to amplitude in standing waves has been found to be within two percent of the measured quantity for almost all of the measured quantities and usually the deviation is less than one percent. In the case of the pressure measurements there is a two percent standard deviation of the measured quantities due to calibration uncertainty. The deviation of experimental results from theory shows no definite trend; sometimes experimental results slightly exceed theory and sometimes they fall slightly short of theory. Thus it is reasonable to conclude that the characteristic quantities given by linear theory are correct within limits of less than one percent for small waves. Ursell, Dean and Yu (2) found a deviation of three percent between theory and experiment for the relationship between wave height and stroke of a piston type wavemaker and concluded that the deviation was mostly due to experimental problems and the theory really gave a better approximation to the truth than 97 percent. In light of the present work, their conclusion seems to be correct.

The agreement between theory and experiment for the linear wave absorber is sufficiently good to provide experimental confirmation of the theory. No experiments have been carried out as yet with a non-linear absorber.

Some experimental confirmation has been given to the stability theory. The first absorbing system was constructed prior to considerations of stability. In operation it was found to be unstable. Later, calculations showed this system was theoretically unstable.

## REFERENCES

- 1) Baumann, H., "Ein Wellentilger für Modell-Seegangversuche", Jarbuch der Schiffbautechnischen Gesellschaft, No. 48, 1954, pp. 165-174.
- 2) Ursell, F., Dean, R. G., and Yu, Y.S., "Forced Small-Amplitude Water Waves; A Comparison of Theory and Experiment," M.I.T. Hydrodynamics Laboratory Technical Report No. 29, 1958.
- 3) Havelock, T. H., "Forced Surface Waves on Water," Philosophical Magazine, No. 7, Vol. 8, 1929, pp. 569-576.
- 4) Thomas, G. B., Calculus and Analytic Geometry, Addison-Wesley Publishing Co., Cambridge, Mass. 1956, pp. 403-406.
- 5) Guillemin, E. A., Introductory Circuit Theory, John Wiley and Sons, New York, 1953.
- 6) Guillemin, E. A., The Mathematics of Circuit Analysis, John Wiley and Sons, New York, 1953.
- 7) Linvill, J. G., "The Selection of Network Functions to Approximate Prescribed Frequency Characteristics," M.I.T. Research Laboratory of Electronics Technical Report No. 145, March 14, 1950.
- 8) Coddington, E. A., and Levinson, N., Theory of Ordinary Differential Equations, McGraw-Hill Book Company, New York, 1955. pp. 298-313.
- 9) Mikhlin, S.G., Linear Integral Equations, Hindustan Publishing Corp. (India), Delhi, 1960, pp. 1-74.
- 10) Corbato, F. J., Daggett, M.M., Daley, R.C., Creasy, R. J., Hellwig, J.D., Orenstein, R. H., Korn, L. K., The Compatible Time Sharing System, A Programmers Guide, The M.I.T. Press, Cambridge, Mass., 1963.
- 11) Zimmermann, H. J., and Mason, S.J., Electronic Circuit Theory, John Wiley and Sons, Inc., New York, 1960, pp. 127-128.
- 12) Lukasik, S. J., and Grosch, C. E., "Pressure Velocity Correlations in Ocean Swell," Journal of Geophysical Research, Vol. 68, No. 20, Oct. 1963, pp. 5689-5699.

## Appendix A

### DESIGN AND CONSTRUCTION OF THE EXPERIMENTAL WAVE TANK

A drawing of the tank used for this experiment appears as figure A-1. As shown in the figure, the tank is fitted with paddles at both ends and has aligning brackets near the paddles as well as every twelve inches along the sides. As a result of the numerous aligning brackets and careful construction the tank does not deviate more than 0.005 inches from the rectangular parallelepiped it approximates. The tank is 8 inches deep, 12 inches wide and 11.04 feet long, being 10 feet between paddles. The tank was operated with a water depth of 5 inches. There are plates with tapped holes on the overhangs of the tank which are used to hold equipment. With the tank properly aligned and with small clearances between the paddles and the walls (0.005 inches), excellent two dimensional waves were obtained by moving one of the paddles. When the tank was improperly aligned, modes with transverse nodes sometimes appeared, so proper alignment is important if a good experiment is to be attained.

The material used for the tank structure is 6061-T6 aluminum which was anodized after fabrication, but before assembly.

The attachment of the sides of the tank to the bottom was done with bolts and epoxy resin to avoid the possible warping that might occur in welding.



## Appendix B

### DESIGN OF THE WAVE ABSORBING FILTER

#### Introduction

In chapter 7 a means for synthesizing a wave absorbing system function was set out and two filters were synthesized, one being more complicated and having a lower mean reflection coefficient than the other. In this section, the circuit design of each of these filters is carried out.

Although it is theoretically possible to design the synthesized filters with wholly passive elements, this is impractical because of the very large capacitances and inductances which would be needed for filters operating at water wave frequencies. Therefore, active circuits have been designed, the active elements being operational amplifiers. In order to acquaint any reader, who is unfamiliar with operational amplifiers, with these devices a short description of their operational usage follows.

#### The Operational Usage of Operational Amplifiers

Figure (B-1) shows the symbol which is used to represent an operational amplifier.

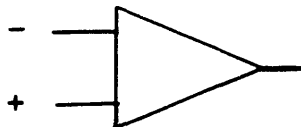


Figure B-1

The line labeled + is the positive, or plus, input; the line labeled - is the negative, or minus, input; and the line at the extreme right is the output. The operational amplifier itself is an extremely high gain amplifier.

At the present time, 1965, the gain of typical, readily available amplifiers varies from  $10^4$  to  $10^8$  depending on the exact type of amplifier. The output voltage of the amplifier is equal to the difference in voltage at negative and positive inputs multiplied by the gain. In almost all applications some form of feedback is applied between the output and one of the inputs. For any normal operating output voltage, the differential input voltage will be very small. The internal resistance between the input terminals is quite high, varying between  $10^4$  and  $10^8$  ohms, depending on the amplifier. The internal resistance from either input terminal to ground is very high, typically varying from  $10^7$  to  $10^9$  ohms. Owing to the small differential voltage and the large input resistance, the input current is very small in normal operation. Because of the forementioned facts, a very accurate design approximation is obtained by assuming that the input current is zero and the differential input voltage is zero.

As a simple example, consider the amplifier circuit of figure (B-2).

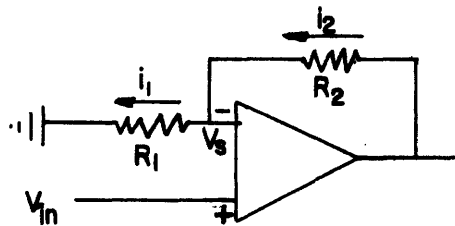


Figure B-2

Since the differential input voltage is zero,

$$V_s = V_{in} \quad (B-1)$$

By Ohm's Law

$$i_1 = \frac{V_s}{R_1} \quad (B-2)$$

Since the input current at either input is zero (in this case the minus input point is under consideration) Kirchoff's current law gives

$$i_2 = i_1 \quad (B-3)$$

Hence

$$\frac{V_{out} - V_{in}}{R_2} = \frac{V_{in}}{R_1} \quad (B-4)$$

or

$$V_{out} = V_{in} \left(1 + \frac{R_2}{R_1}\right) \quad (B-5)$$

Thus the circuit of figure B-2 is an amplifier with a gain of

$$\left(1 + \frac{R_2}{R_1}\right).$$

As a more complicated example, consider the very general linear circuit of figure (B-3) where the Z's represent complex impedances.

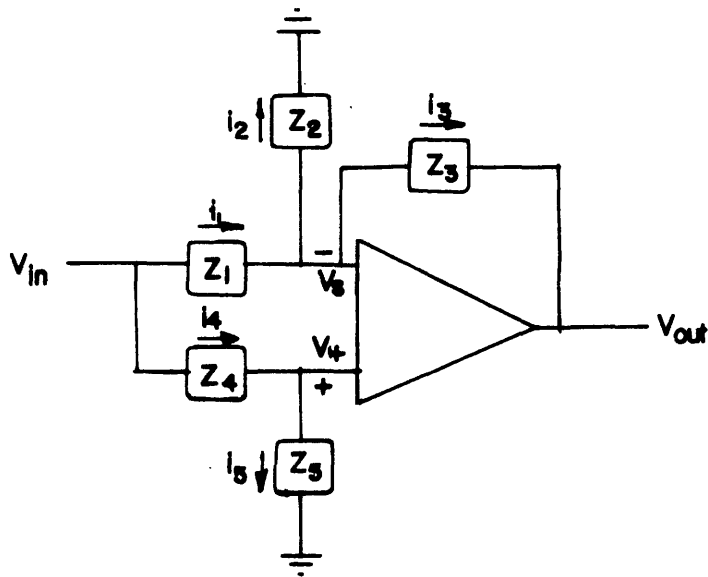


Figure B-3

It should be noted here that the designer must take into account the effect of the input impedance of the circuit of figure (B-3) on the circuit applying  $V_{in}$ .

Since no current enters the operational amplifier at plus input

$$i_4 = i_5 \quad (B-6)$$

and

$$V_+ = V_{in} \frac{Z_5}{Z_4 + Z_5} \quad (B-7)$$

Since there is zero differential input voltage on the operational

amplifier

$$V_s = V_+ \quad (B-8)$$

or

$$V_s = \frac{Z_5}{Z_4 + Z_5} \quad (B-9)$$

By Ohm's Law

$$i_2 = \frac{V_s}{Z_2} = V_{in} \frac{Z_5}{Z_2(Z_4 + Z_5)} \quad (B-10)$$

$$i_1 = \frac{V_{in} - V_s}{Z_1} = \frac{V_{in}}{Z_1} \left( \frac{Z_4}{Z_4 + Z_5} \right) \quad (B-11)$$

By Kirchoff's Current Law

$$i_3 = i_1 - i_2 = \frac{V_{in}}{(Z_4 + Z_5)} \left( \frac{Z_5}{Z_2} - \frac{Z_4}{Z_1} \right) \quad (B-12)$$

Then, by Ohm's Law

$$\frac{V_{out} - V_s}{Z_3} = \frac{V_{in}}{(Z_4 + Z_5)} \left( \frac{Z_5}{Z_2} - \frac{Z_4}{Z_1} \right) \quad (B-13)$$

or

$$V_{out} = V_{in} \frac{Z_3}{Z_4 + Z_5} \left[ Z_5 \left( \frac{1}{Z_2} + \frac{1}{Z_3} \right) - \frac{Z_4}{Z_1} \right] \quad (B-14)$$

Thus figure (B-3) represents a linear filter with the transfer function:

$$T = \frac{Z_3}{Z_4 + Z_5} \left[ Z_5 \left( \frac{1}{Z_2} + \frac{1}{Z_3} \right) - \frac{Z_4}{Z_1} \right] \quad (\text{B-15})$$

The Servomechanism Control Circuit

A diagram of the wave absorbing system appears as figure (B-4). The paddle is activated by a 60 cycle a-c servo motor which is driven by a power amplifier, this amplifier being driven by a chopper whose input is a d-c control signal. A d-c feedback signal is provided by a potentiometer which is geared to the servo motor. The output of the potentiometer is proportional to the paddle angle within a linearized approximation valid for small paddle angles. The mechanical gearing is shown in figure (B-5). The d-c control signal is supplied by an operational amplifier connected as shown in figure (B-6). The mechanical characteristics of the servo

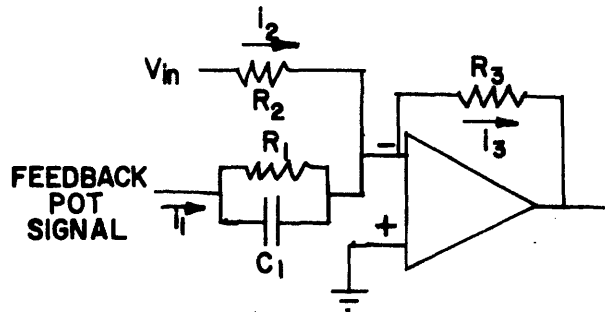


Figure B-6

motor can be described in a general way by stating that the control voltage can be obtained by some operation on the paddle angle. The output voltage of the operational amplifier, and consequently the control voltage to the servo motor, is proportional to  $i_3$  in figure (B-6) and

$$i_3 = i_1 + i_2 \quad (B-16)$$

$$i_2 = \frac{V_{in}}{R_2} \quad (B-17)$$

$$i_1 = V_P \left( \frac{1 + R_1 C_1 S}{R_1} \right) \quad (B-18)$$

where  $V_P$  is the feedback potentiometer voltage and

$$V_P = K_1 \theta \quad (B-19)$$

$\theta$  being the paddle angle.

$$i_3 = \frac{V_{in}}{R_2} + K_1 \theta \left( \frac{1 + R_1 C_1 S}{R_1} \right) \quad (B-21)$$

Call the input control voltage to the servo motor  $V_m$ .

$$V_m = Op(\theta) = K_2 \frac{V_{in}}{R_2} + K_1 \theta \left( \frac{1 + R_1 C_1 S}{R_1} \right) \quad (B-22)$$

$K_2$  is equal to  $R_3$  times the gain in the circuitry between the operational amplifier output and the servo motor input. The proper operation of the type of servomechanism used here requires that  $K_2$  be sufficiently large

that equation (B-22) is well approximated by

$$\frac{V_{in}}{R_2} + K_1 \theta \left( \frac{1 + R_1 C_1 S}{R_1} \right) = 0 \quad (B-23)$$

Then

$$\theta = -V_{in} \frac{R_1}{K_1 R_2 (1 + R_1 C_1 S)} \quad (B-24)$$

Hence the transfer function from input volts to paddle angle has a pole at

$$S = - \frac{1}{R_1 C_1} \quad (B-25)$$

#### Design of the Simpler Wave Absorbing Filter

The system function for this filter is obtained from figure (7-1).

This function is:

$$H_1(s) = 927.23 \frac{s(s + 50.45)}{(s+0.4)(s+0.4)(s+10.72)(s+82.67)} \quad (B-26)$$

The zero at  $S = 0$  and the double pole at  $S = 0.4$  constitute the pre-filtering done by the computer program BHN and the remaining poles and zero are located by the computer program IMERG. Details of this work are explained in chapter 7. A pole-zero plot for this filter appears in figure B-7. The process for designing such a filter is as follows. First, a filter with a set of nominal values for the various circuit elements is

designed. For the filter designed here only resistors and capacitors are used for the circuit elements. Then the capacitors are obtained and their capacitance is measured. This capacitance usually differs from the nominal value, so the needed values for the resistors are altered to keep the correct positions of the poles and zeros. This sequence is followed because the usual tolerance of capacity of readily available capacitors is 10 percent, and one percent resistors are readily available.

Inasmuch as the simpler filter was built and used, the values of the circuit elements used in the filter will be given here. The filter is built in three stages. The first stage contains the zero at  $S = 0$ , the pole at  $S = -10.72$  and one of the poles at  $S = -0.4$ . The second stage contains the zero at  $S = -50.45$  and the second of the poles at  $S = -0.4$ . The third stage is the servo mechanism feedback amplifier which contains the pole at  $S = -82.67$ . The circuit elements used gives positions of the poles and zeros which are very close to the desired values.

The circuits used here are a specialization of figure (B-3) with  $Z_2 = \infty$ ,  $Z_5 = 0$  and  $Z_4 = \infty$ .

For this circuit

$$T = \frac{V_{out}}{V_{in}} = - \frac{Z_3}{Z_1} \quad (B-27)$$

The first stage is shown in figure (B-8).

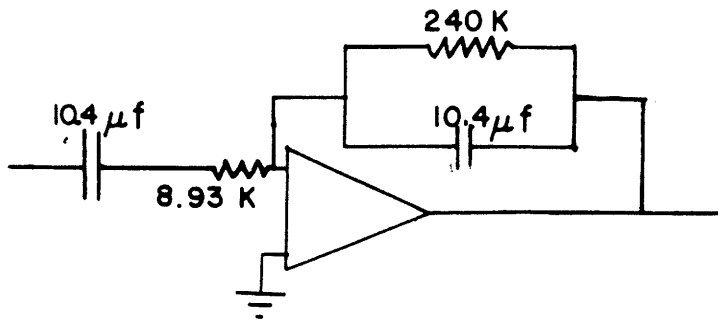


Figure B-8

For this circuit,

$$Z_1 = \frac{s+10.75}{11.2 \times 10^5 s} \quad (\text{B-28})$$

$$Z_3 = 96.1 \times 10^3 \frac{1}{s+0.4} \quad (\text{B-29})$$

Hence

$$T_{11} = 10.75 \frac{s}{(s+0.4)(s+10.75)} \quad (\text{B-30})$$

The second stage is shown in figure (B-9)

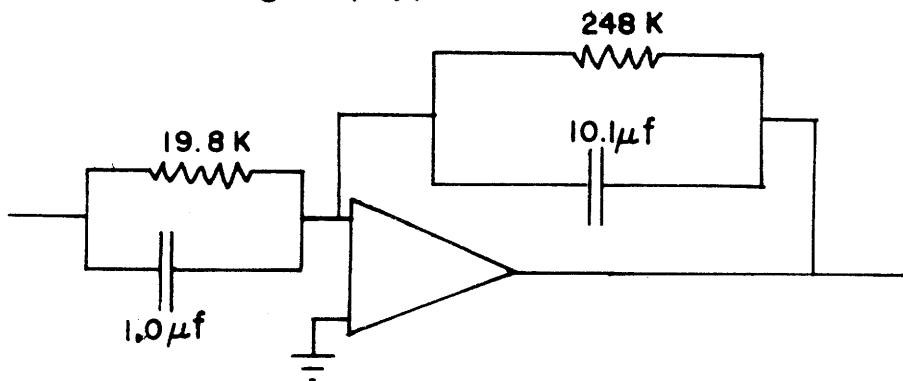


Figure B-9

$$Z_1 = \frac{10^6}{s+50.5} \quad (\text{B-31})$$

$$Z_3 = \frac{98.9 \times 10^3}{s+0.4} \quad (\text{B-32})$$

Hence,

$$T_{12} = 0.248 \frac{s+50.5}{s+0.4} \quad (\text{B-33})$$

The third stage is the servomechanism feedback amplifier which is shown in figure (B-6).

Referring to this figure,

$$R_1 = 24.2 \times 10^3 \Omega$$

$$C_1 = 5 \times 10^{-7} \text{ f}$$

This gives a transfer function from volts to paddle angle of

$$T_{13} = K \frac{1}{s+82.67} \quad (\text{B-34})$$

where K is a constant to be adjusted so that the overall gain is correct.

The complete system function is  $T_1$ .

$$T_1 = T_{11} T_{12} T_{13} = 2.665 K \frac{s(s+50.5)}{(s+0.4)(s+0.4)(s+10.75)(s+82.67)} \quad (\text{B-35})$$

It is desired that  $T_1 = H_1(s)$  given by equation (B-26). Hence

$$K = 348 \quad (\text{B-36})$$

K can be adjusted by adjusting  $R_3$  in figure (B-6). In order to determine the correct value of  $R_3$  first try any reasonable value and experimentally measure the d-c relationship between  $V_{in}$  (fig. B-4) and the paddle angle.

The desired ratio at d-c is given by equations (B-35) and (B-36).

$$\left. \frac{\theta}{V_{in}} \right|_{dc} = \frac{K}{82.67} = 4.21 \quad (B-37)$$

Then the correct value of  $R_3$  is the inserted value multiplied by

$$\frac{4.21}{(\text{measured value of } (\theta/V_{in})_{dc})}$$

#### Design of the More Complicated Wave Absorbing Filter

The system function for this filter is obtained from figure (7-4).

This function is

$$H_2(s) = \frac{1.334 \times 10^5 s [s - (4.07 + j119.96)] [s - (4.07 - j119.96)]}{(s + 0.2)(s + 0.2)(s + 54.90)(s + 104.81)(s + 179.72)} \quad (B-38)$$

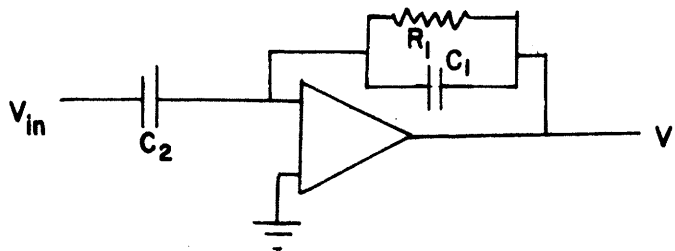
As was the case with the simpler filter, one of the poles will be contained in the servomechanism feedback loop. Experiments with the servomechanism have shown that it will operate satisfactorily with a pole at  $s = -54.90$  so this pole will be inserted in its feedback loop.  $H_2(s)$  contains a conjugate pair of zeros in the right half of the S-plane. This could be obtained by use of the generalized circuit of figure (B-3), by a

twin-tee input circuit (see Guillemin, ref. 6), or by a "brute force" technique which will be described subsequently. Actually the twin-tee circuit is a form of figure (B-3) where  $Z_1$  is the impedance of the twin-tee. There are other forms of figure (B-3) yielding zeros in the right half of the S-plane but for the positions of the complex zeros in  $H_2(s)$ , these circuits subtract two large currents to get a small resulting current which could result in a large total error caused by a small percentage error in one resistor. The twin-tee gives an undesirable pole and an undesirable zero as well as the two desired zeros and one desired pole. Therefore the following brute force technique is recommended. Multiplying together the bracketed factors of equation (B-38) gives:

$$H_2(s) = \frac{1.334 \times 10^5 s [s^2 - 8.14s + 561]}{(s+0.2)(s+0.2)(s+54.90)(s+104.81)(s+179.72)} \quad (B-39)$$

The factor in the square brackets contains the two right half plane zeros. In short, this factor will be obtained by adding 561 to  $s^2$  and subtracting 8.14s. The system function S represents a differentiator, and  $S^2$  represents a double differentiator. These system functions amplify high frequency noise. Although high frequency noise is attenuated by the complete system function (there are more poles than zeros) it is important to make sure that there is a minimum of high frequency noise at all stages of the filter to prevent saturating the amplifiers which would result in non-linear operation.

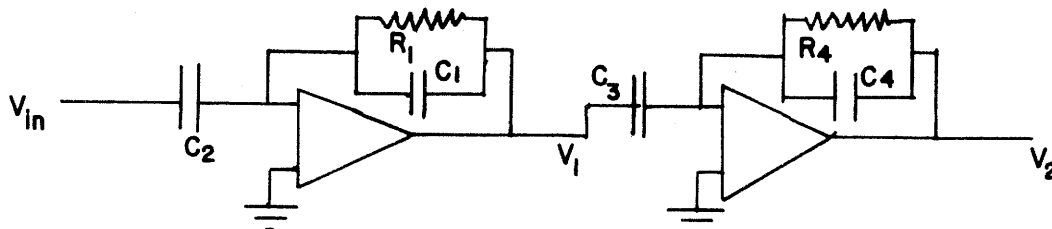
First consider the circuit of figure (B-10).



$$V_1 = - \frac{R_1 C_2 S}{1 + R_1 C_1 S} V_{in} \quad (B-40)$$

Figure B-10

Next consider the circuit of figure (B-11) which is the circuit of figure (B-10) cascaded with another modified differentiator.



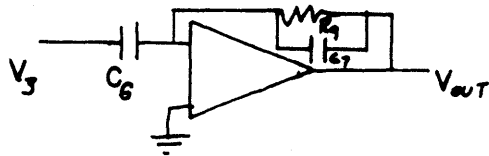
$$V_2 = V_{in} \frac{R_1 C_2 R_4 C_4 S^2}{(1 + R_1 C_1 S)(1 + R_4 C_4 S)} \quad (B-41)$$

Figure B-11

Now the bracketed quantity in equation (B-39) along with three of the poles can be obtained by the circuit of figure (B-12).



Then cascade the circuit of figure (B-12) with one having a zero at  $S = 0$  and a pole at  $S = -0.2$  as shown in figure (B-13).



$$\frac{1}{R_7 C_7} = 0.2 \quad (\text{B-49})$$

Figure B-13

Then,

$$V_{out} = \text{constant } H_2(s) \quad (\text{B-50})$$

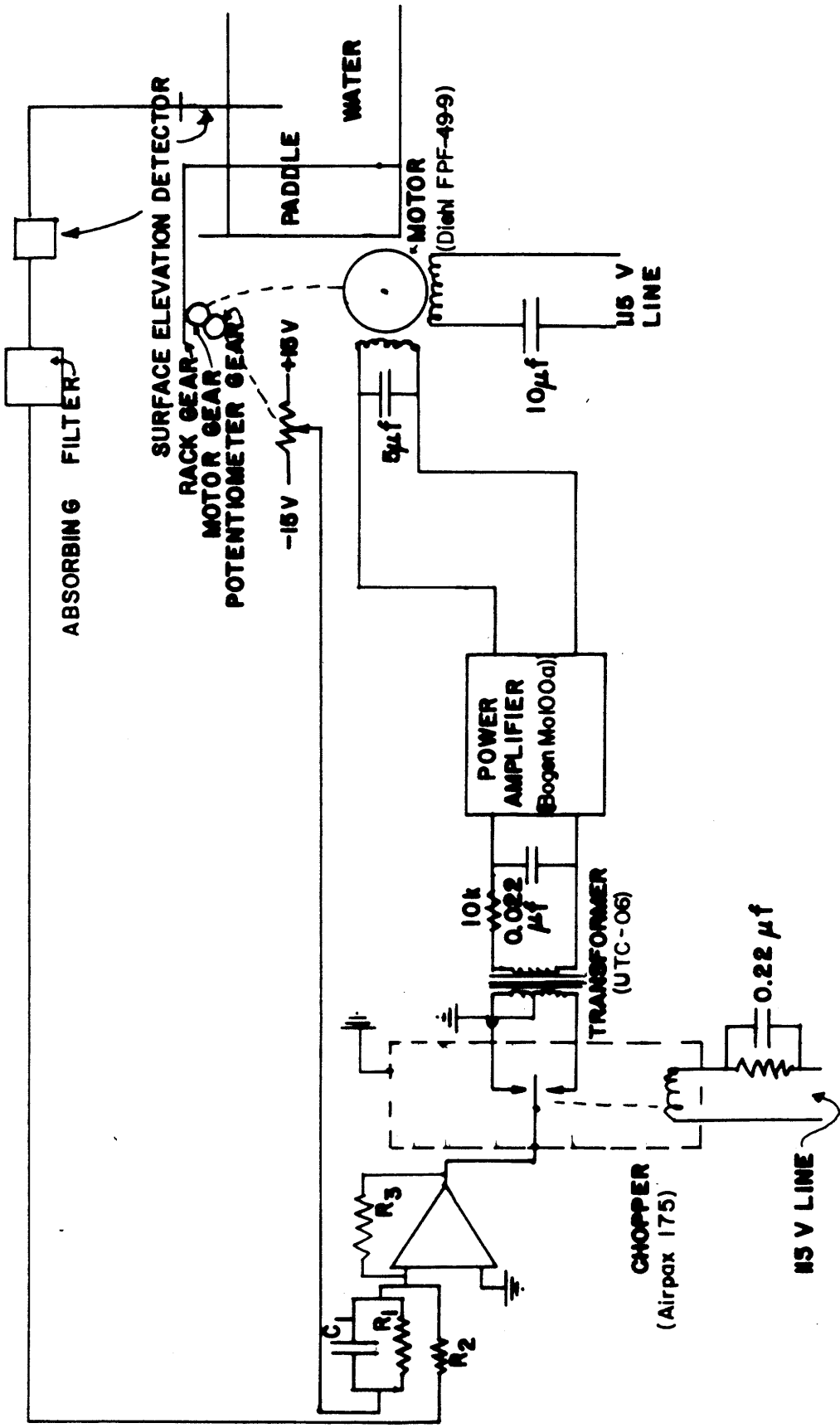


FIGURE B-4 Diagram of the Wave Absorbing System. The Absorbing Filter is treated in detail in Appendix B. The Surface elevation Detector is treated in detail in Appendix C.

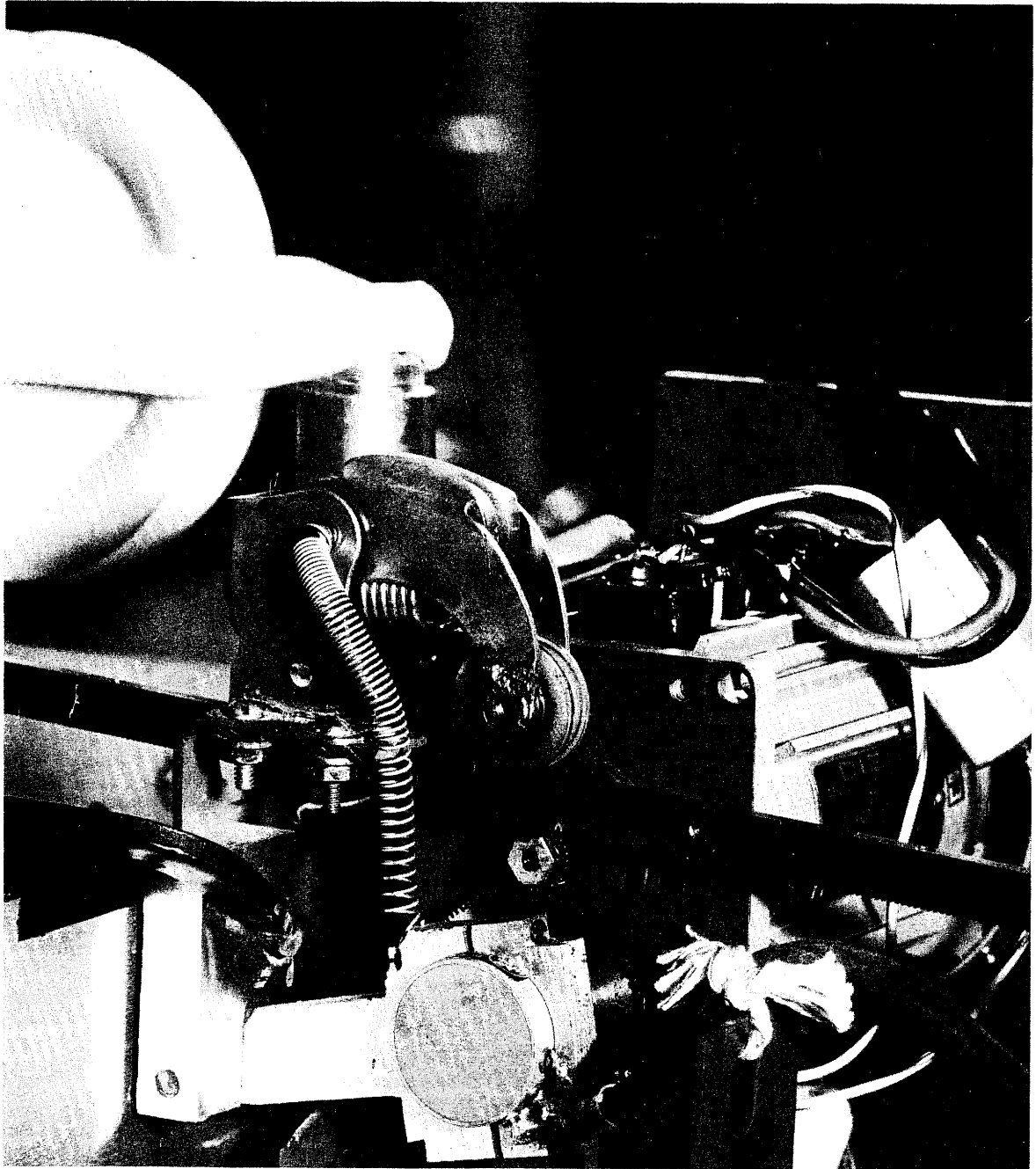


FIGURE B-5 This shows the gearing between the motor, the paddle drive rack and the feedback potentiometer. Note the springs used to prevent backlash.

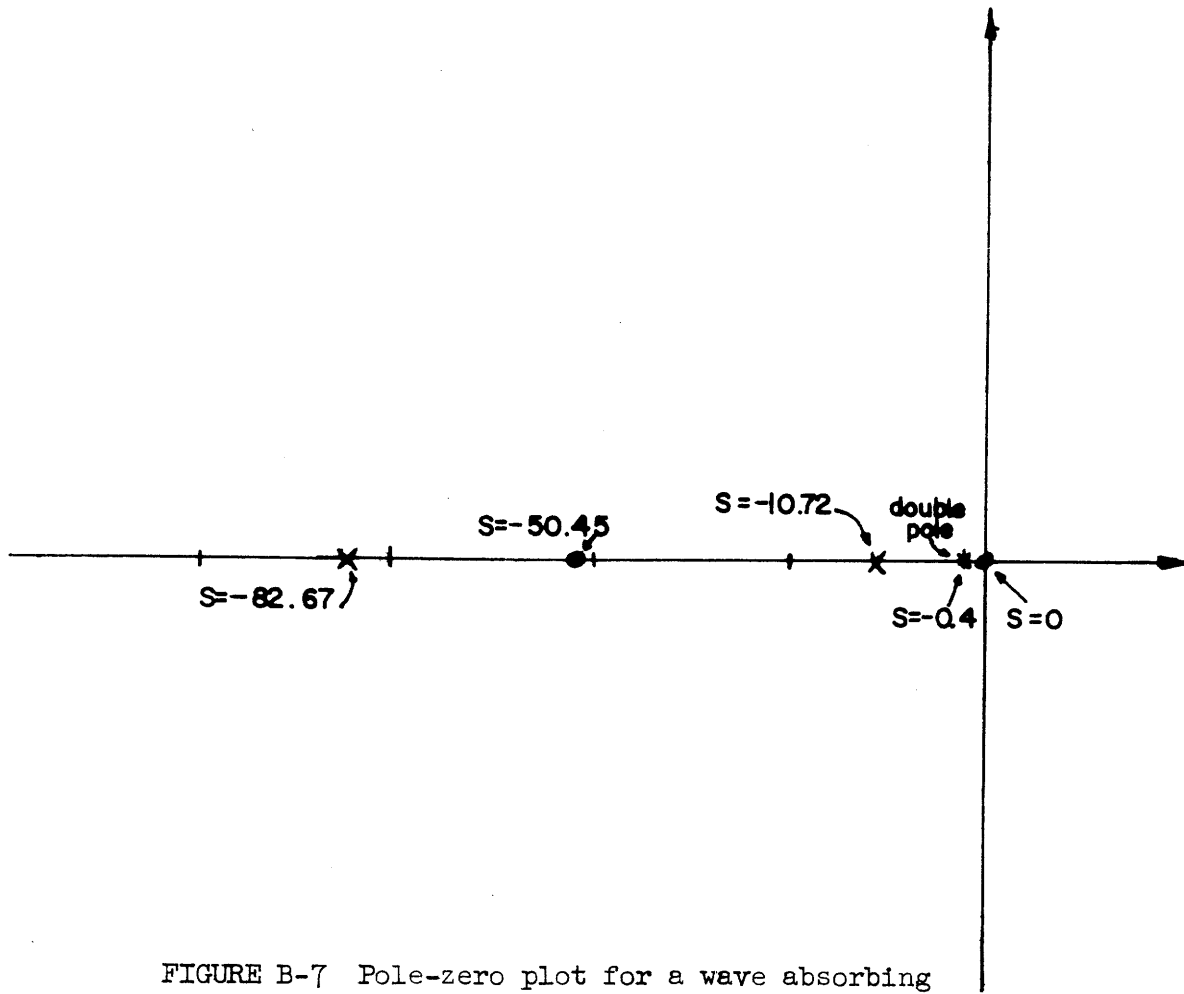


FIGURE B-7 Pole-zero plot for a wave absorbing system function which was built and tested.

## Appendix C

### WAVE HEIGHT TO VOLTAGE TRANSDUCER

An electrical voltage proportional to the wave height having an error of less than 1/10 percent in the slope of the response function, ( $\frac{\text{Volts Output}}{\text{foot of wave height}}$ ), was produced by a modulated temperature stabilized differential oscillator. A description of how this device operates follows:

Two identical 1 mc oscillators are built on a single circuit board. Each pair of components (one for each oscillator) is matched and the layout of components for one oscillator is symmetrical to the layout of components for the other oscillator. By this scheme, when the circuit is enclosed in a case having a high thermal conductivity, the temperature, although possibly changing with time, and varying with positions in the case, is the same on a given component of one oscillator as the temperature on the identical component of the other oscillator. This follows from the fact that all points on the case have the same temperature. Hence, the frequency drift of each oscillator is identical. In addition, the oscillators are designed to have a very small temperature drift. Air core inductors, glass insulation capacitors and low drift transistors are used for all components which affect the oscillator frequency. The frequency of one of the oscillators is modulated by a capacitance wave height probe. The difference frequency between the two oscillator frequencies is detected by means of an A-M detection diode and an L-C low-pass filter. The difference frequency between the two oscillators is amplified and clipped at

an upper and a lower value by means of a zener diode. The clipped signal then goes to a capacitor-diode network which gives out a charge proportional to the peak to peak voltage of the clipped wave on every cycle of wave. This pulsating charge goes into a low-pass filter whose output is a voltage proportional to the wave height. The peak to peak voltage of the clipped wave is temperature dependent owing to the temperature dependent characteristics of the zener diode. To cancel out this effect, the factor of proportionality between charge out the diode-capacitor network per cycle and the peak to peak voltage was made temperature dependent by using temperature dependent capacitors in the network. The capacitors and zener diode were chosen so that the temperature dependent effects would cancel each other in the final output voltage.

The capacitance probe itself is a 0.047 inch diameter 9 inch long piece of spring tempered monel wire covered with a teflon sleeve with a 0.005 inch wall thickness. The immersed end of the probe is sealed off with a hard thermoplastic wax. If the probe were stationary as the fluid level moved up and down a considerable error in the measured surface elevation would be introduced because the fluid meniscus at the probe would invert as the direction of vertical fluid velocity inverts. This effect causes an error because the wave height transducer measures the capacitance between the center conductor of the probe and the layer of water immediately adjacent to the probe. The teflon sleeve on the probe serves as the dielectric insulator. To avoid this problem, the capacitance probe is mounted on a loudspeaker driver and oscillated through a double amplitude

of about 3/32 inches at a frequency of 120 cycles per second. Thus, if whenever the wave height signal is used it is passed through a low pass filter having a very small response at 120 cps, the signal at any time is "averaged" over all phases of the miniscus position.

A schematic diagram of the transducer appears as figure C-1 and this diagram is now explained.

The oscillator circuit associated with inductor  $L_2$  is the oscillator whose frequency is modulated by the wave elevation. The oscillator circuit associated with inductor  $L_1$  is the reference oscillator. The 5.1K resistor and the 1N541 diode between the two oscillators form the detection circuit so that the sum and difference frequencies of the two oscillators appear across the 5.1K resistor. The filter formed by  $L_3$ ,  $L_4$ , the 510  $\mu$  f capacitor and the 2.7  $\mu$  f capacitor allows only the difference frequency of the two oscillators to appear at its output. The first amplifier stage, centered on the first 2N466 transistor, is an emitter follower stage used so that the second 2N466 transistor amplifier stage does not load down the filter output. This second stage is a common emitter amplifier whose output is clipped top and bottom by the 1N757 zener diode. The circuitry following the zener diode is a frequency detector which gives a voltage at the collector of the 2N267 transistor that is proportional to the input frequency of the clipped wave. The basis of its operation can be found in ref. 11. The 2N213A amplifier stage is an emitter follower used to obtain a low impedance output.

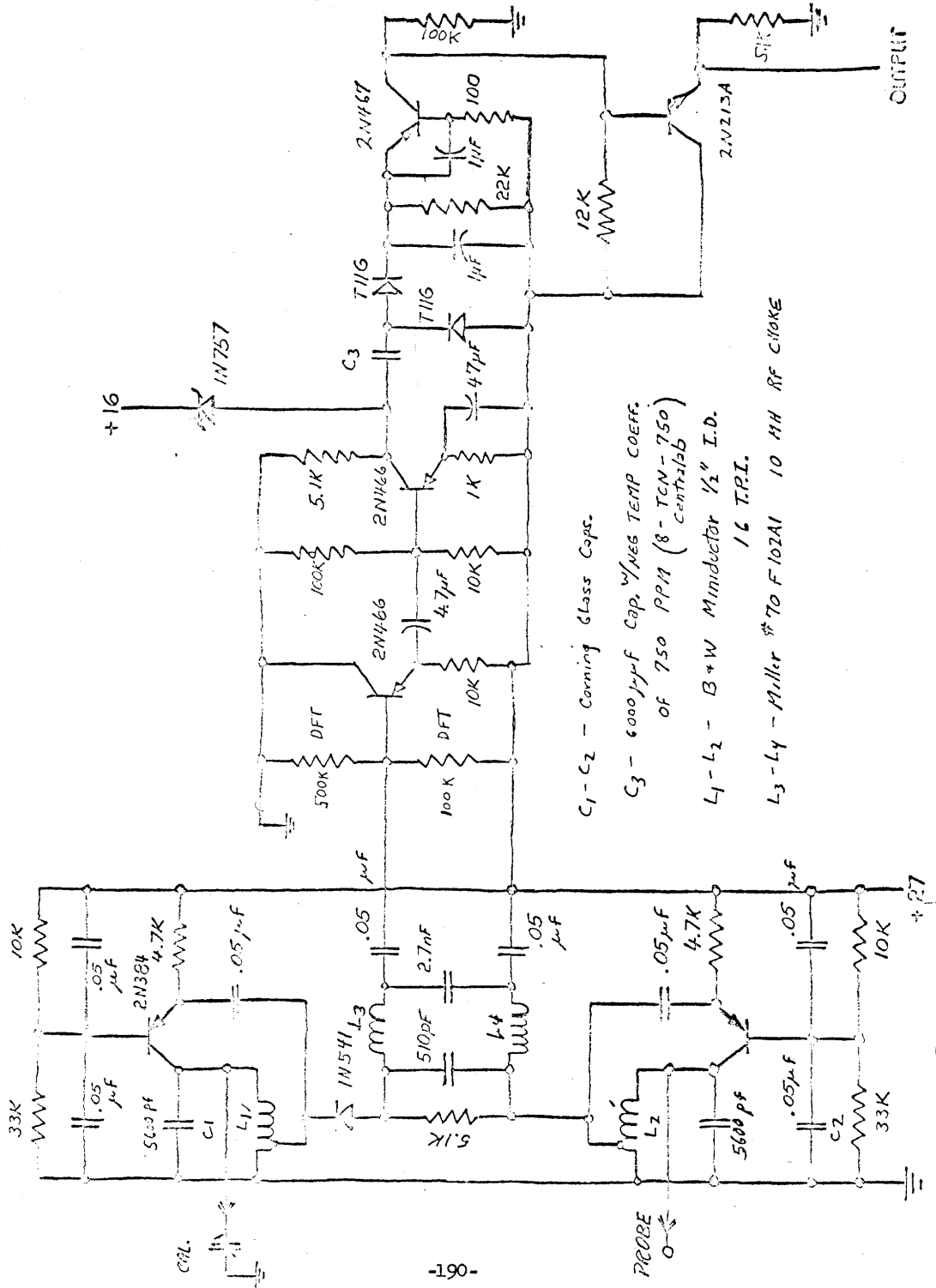


FIGURE C-1 Schematic diagram of the surface elevation to voltage transducer.

## Appendix D

### ALTERATIONS TO THE CHART RECORDER

All chart recordings taken during experiments in this project were made on a Sanborn Model 297 two channel recording system. This recording system has a very wide frequency response, being only 3 dB down at 125 cycles per second. For the experiments conducted in this project it was desirable to cut off the frequency response well below 125 cycles per second. This is so because the 120 cps from the capacitance probe vibrator appears as noise in the wave height signal. When pressure measurements are made the vibrator 120 cps and motor noise appear as noise on the pressure signal and quite a lot of motor noise around 25 cps comes from the gear train of the wavemaker which is picked up by the pressure transducer. The desired cutoff was accomplished by adding two capacitors to the Sanborn plug in element E78 as shown in figure D-1. These two capacitors filter the signal to the pen amplifier by the following transfer function:

$$T = \frac{1}{(1 + 0.0275(\omega))(1 + 0.01875(\omega))}$$

A graph of  $T$  vs  $\omega$  appears as figure D-2.

This transfer function has some attenuation and phase shift in the range of wave frequencies of interest which is from 0.025 to 3.0 cps. However, in the experiments done in this work, only ratios of measured quantities and relative phase shifts between two measured signals are considered. By adding identical filters to both recorder channels, no error is introduced in these measurements.

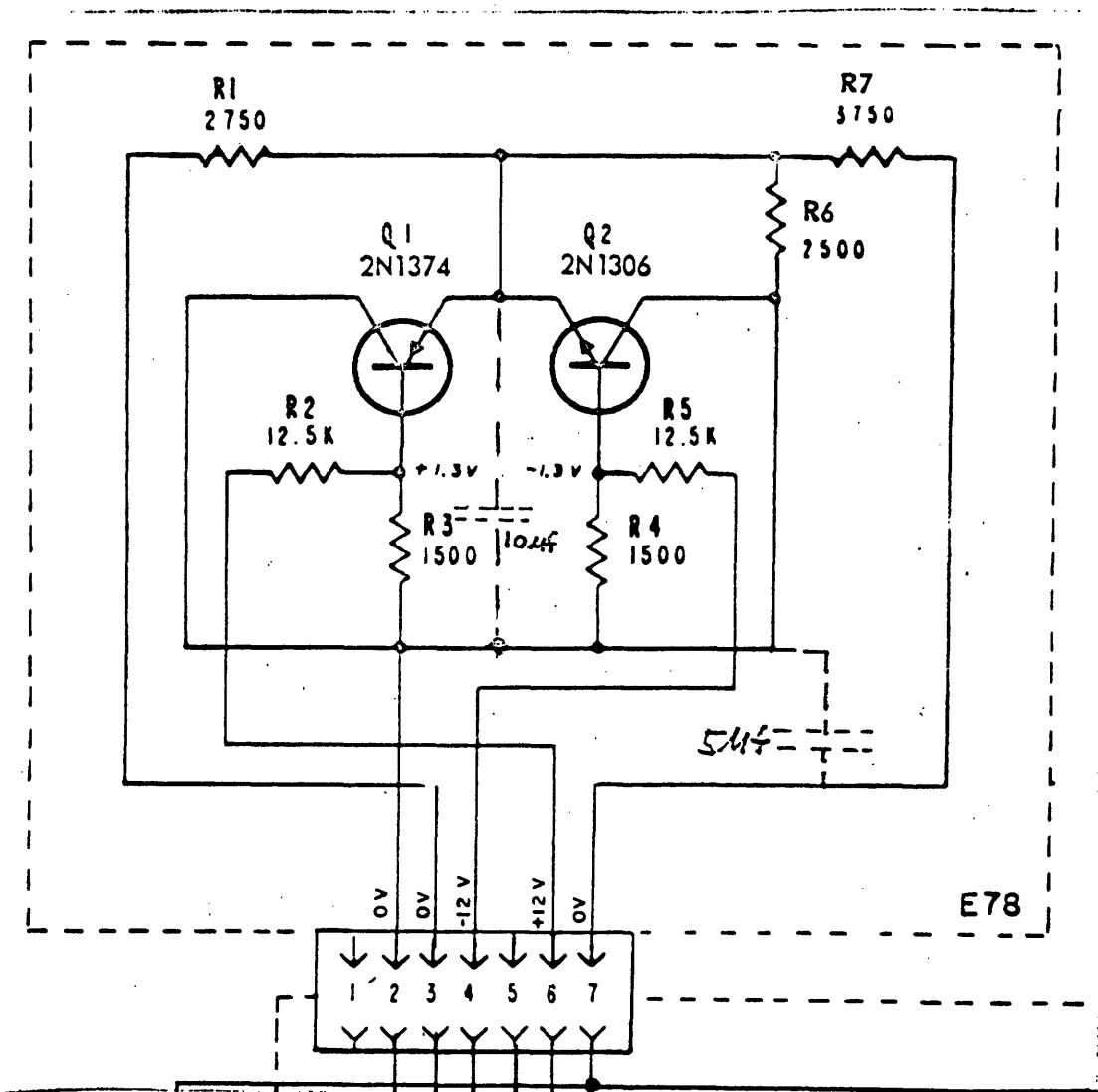


FIGURE D-1 Alterations to electronics of Sanborn Model 297 recorder to produce rolloff characteristic shown in figure D-2. Alterations are shown as dotted lines. (Reprinted by permission of Sanborn, Div. Hewlett-Packard Corp.)

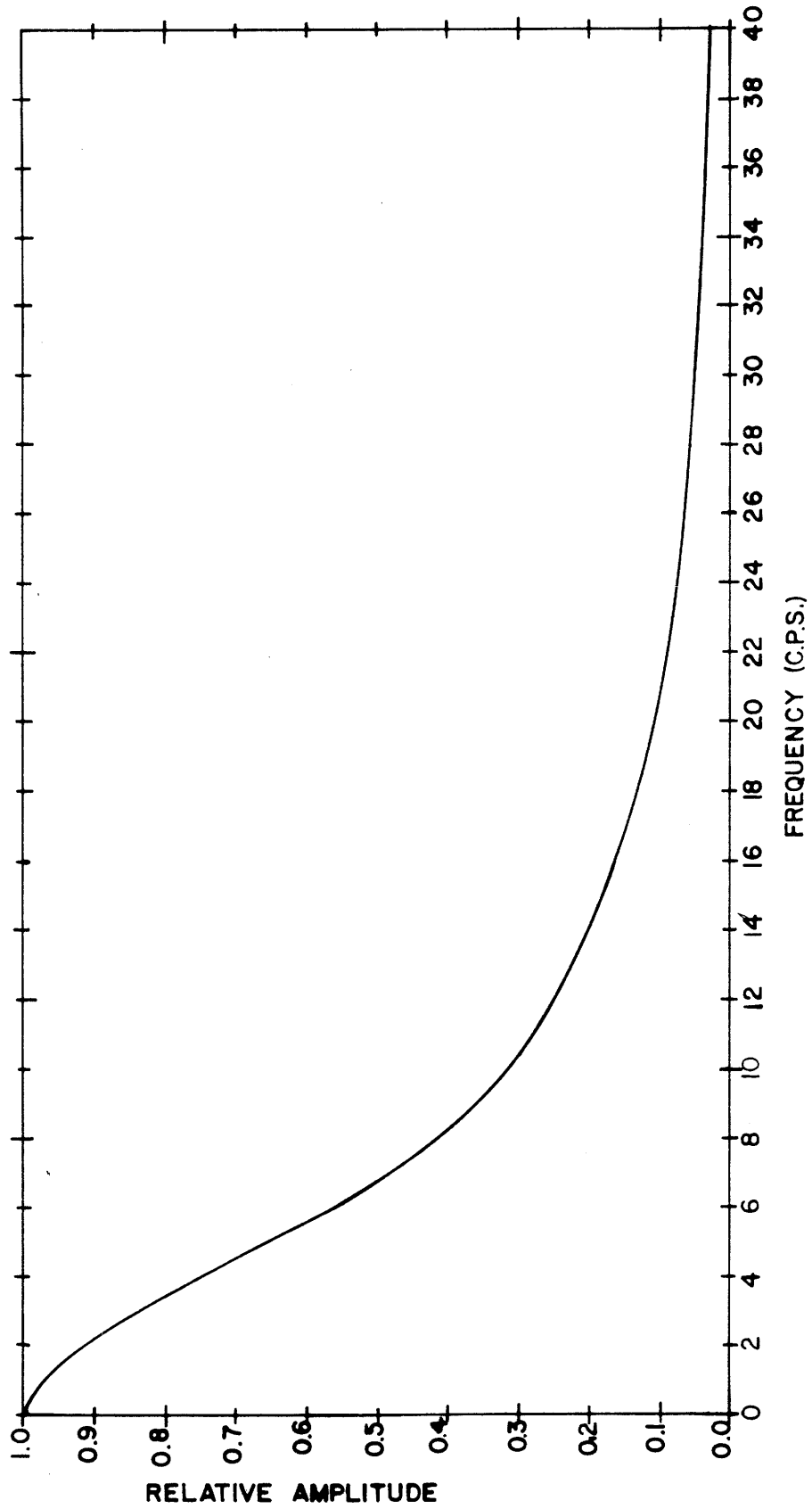


FIGURE D-2 Frequency response of altered paper chart recorder.

Appendix E

INTEGRAL TABLES

$$\tilde{I}_1^{(1)} = \int_{-h}^0 \cosh^2 \alpha_0 (y+h) dy = \frac{h}{2} \left[ 1 + \frac{1}{2\alpha_0 h} \sinh 2\alpha_0 h \right]$$

$$\tilde{I}_2^{(2)} = \int_{-p}^0 (y+p) \cosh \alpha_0 (y+h) dy = \frac{p}{\alpha_0} \sinh \alpha_0 h + \frac{1}{\alpha_0^2} (\cosh \alpha_0 (h-p) - \cosh \alpha_0 h)$$

$$\tilde{I}_{3n}^{(1)} = \int_{-h}^0 \cosh^2 \alpha_n (y+h) dy = \frac{1}{2} \left[ \frac{1}{2\alpha_n} \sinh 2\alpha_n h + h \right]$$

$$\tilde{I}_{4n}^{(1)} = \int_{-p}^0 (y+p) \cos \alpha_n (y+h) dy = \frac{p}{\alpha_n} \sin \alpha_n h + \frac{1}{\alpha_n^2} [\cos \alpha_n h - \cos \alpha_n (h-p)]$$

$$\tilde{I}_1^{(2)} = \int_{-p}^0 (y+p) \cosh \gamma_0 (y+h) dy = \frac{p}{\gamma_0} \sinh \gamma_0 h + \frac{1}{\gamma_0^2} (\cosh \gamma_0 (h-p) - \cosh \gamma_0 h)$$

$$\tilde{I}_2^{(2)} = \int_{-h}^0 \sinh \alpha_0 (y+h) \cosh \gamma_0 (y+h) dy = \frac{1}{2(\alpha_0^2 - \gamma_0^2)} \left[ (\alpha_0 - \gamma_0) \cosh (\alpha_0 + \gamma_0) h + (\alpha_0 + \gamma_0) \cosh (\alpha_0 - \gamma_0) h - 2\alpha_0 \right]$$

$$\tilde{I}_3^{(2)} = \int_{-p}^0 (y+p) \cosh \alpha_0 (y+h) \cosh \gamma_0 (y+h) dy = \frac{1}{2} \left[ \frac{1}{(\alpha_0 + \gamma_0)^2} (\alpha_0 + \gamma_0) h \sinh (\alpha_0 + \gamma_0) h - \cosh (\alpha_0 + \gamma_0) h + 1 + \frac{1}{(\alpha_0 - \gamma_0)^2} (\alpha_0 - \gamma_0) h \sinh (\alpha_0 - \gamma_0) h - \cosh (\alpha_0 - \gamma_0) h + 1 \right]$$

$$\tilde{L}_{4n}^{(2)} = \int_{-h}^0 \sin \alpha_n (y+h) \cosh \gamma_0 (y+h) dy = \frac{1}{\alpha_0^2 + \gamma_0^2} \left[ \gamma_0 \sin \alpha_n h \sinh \gamma_0 h - \alpha_n \cos \alpha_n h \cosh \gamma_0 h + \alpha_n \right]$$

$$\tilde{L}_{5n}^{(2)} = \int_{-p}^0 (y+p) \cos \alpha_n (y+h) \cosh \gamma_0 (y+h) dy = \left\{ [\gamma_0^2 - \alpha_n^2] \cdot \right. \\ \left. [-\cosh \gamma_0 h \cos \alpha_n h + \cosh \gamma_0 (h-p) \cos \alpha_n (h-p)] \right. \\ \left. + 2\gamma_0 \alpha_n [-\sinh \gamma_0 h \sin \alpha_n h + \sinh \gamma_0 (h-p) \sin \alpha_n (h-p)] \right. \\ \left. + p[\gamma_0^2 + \alpha_n^2] [\gamma_0 \sinh \gamma_0 h \cos \alpha_n h + \alpha_n \sin \alpha_n h \cosh \gamma_0 h] \right\}$$

$$\tilde{L}_{6n}^{(2)} = \int_{-h}^0 e^{-\beta_n y} \cosh \gamma_0 (y+h) dy = \frac{1}{2} \frac{e^{\beta_n h}}{\beta_n + \gamma_0} (1 - e^{-h(\beta_n + \gamma_0)}) + \frac{1}{2} \frac{e^{-\beta_n h}}{\beta_n - \gamma_0} (1 - e^{-h(\beta_n - \gamma_0)})$$

$$\tilde{L}_{7n}^{(2)} = \int_{-h}^0 e^{-\beta_n y} \cosh \gamma_0 (y+h) dy = \frac{1}{2} \frac{e^{\gamma_0 h}}{(-\beta_n + \gamma_0)} (1 - e^{-h(-\beta_n + \gamma_0)}) \\ + \frac{1}{2} \frac{e^{-\gamma_0 h}}{(-\beta_n - \gamma_0)} (1 - e^{-h(-\beta_n - \gamma_0)})$$

$$\tilde{L}_8^{(2)} = \int_{-h}^0 \cosh 2\alpha_0 (y+h) \cosh \gamma_0 (y+h) dy =$$

$$\frac{\sinh 3\gamma_0 h}{6\gamma_0} - \frac{\sinh \gamma_0 h}{2\gamma_0}$$

$$\begin{aligned} \tilde{I}_{9n}^{(2)} &= \int_{-h}^0 \cos \alpha_{mn}(y+h) \cosh \gamma_0(y+h) dy = \\ & \frac{1}{\alpha_{mn}^2 + \gamma_0^2} [\alpha_{mn} \sin \alpha_{mn} h \cosh \gamma_0 h - \gamma_0 \cos \alpha_{mn} h \sinh \gamma_0 h] \end{aligned}$$

$$\tilde{I}_{10n}^{(2)} = \int_{-h}^0 \cos^2 \gamma_n(y+h) dy = \frac{1}{2\gamma_n} \left[ \gamma_n h + \frac{1}{2} \sin 2\gamma_n h \right]$$

$$\tilde{I}_{11n}^{(2)} = \int_{-p}^0 (y+p) \cos \gamma_n(y+h) dy = \frac{p}{\gamma_n} \sin \gamma_n h + \frac{1}{\gamma_n^2} [\cos \gamma_n h - \cos \gamma_n(h-p)]$$

$$\tilde{I}_{12n}^{(2)} = \int_{-h}^0 \sinh \alpha_0(y+h) \cos \gamma_n(y+h) dy = \frac{1}{\alpha_0^2 + \gamma_n^2} [\alpha_0 \cosh \alpha_0 h \cos \gamma_n h - \gamma_n \sinh \alpha_0 h \sin \gamma_n h - \alpha_0]$$

$$\tilde{I}_{13n}^{(2)} = \int_{-p}^0 (y+p) \cosh \alpha_0(y+h) \cos \gamma_n(y+h) dy =$$

$$\frac{1}{(\alpha_0^2 + \gamma_n^2)^2} [(\alpha_0^2 - \gamma_n^2) (-\cosh \alpha_0 h \cos \gamma_n h + \cosh \alpha_0(h-p) \cos \gamma_n(h-p))$$

$$+ 2\alpha_0 \gamma_n (-\sinh \gamma_0 h \sin \alpha_n h + \sinh \alpha_0(h-p) \sin \gamma_n(h-p))$$

$$+ p(\alpha_0^2 + \gamma_n^2) (\alpha_0 \sinh \alpha_0 h \cos \gamma_n h + \gamma_n \sin \gamma_n h \cosh \alpha_0 h)]$$

$$\begin{aligned} \tilde{I}_{14j}^{(2)} &= \int_{-h}^0 \sin \alpha_j (y+h) \cos \gamma_n (y+h) dy \\ &= \frac{-1}{2(\alpha_j^2 - \gamma_n^2)} \left[ (\alpha_j + \gamma_n) \cos (\alpha_j - \gamma_n)h + (\alpha_j - \gamma_n) \cos (\alpha_j + \gamma_n)h - \alpha_j \right] \end{aligned}$$

$$\begin{aligned} \tilde{I}_{15j}^{(2)} &= \int_{-p}^0 (y+p) \cos \alpha_j (y+h) \cos \gamma_n (y+h) dy = \\ &\frac{(h-\frac{p}{2})}{\alpha_j + \gamma_n} \sin (\alpha_j + \gamma_n)h + \frac{(h-\frac{p}{2})}{\alpha_j - \gamma_n} \sin (\alpha_j - \gamma_n)h \\ &- \frac{(h-p)}{\alpha_j + \gamma_n} \sin (\alpha_j + \gamma_n)(h-p) - \frac{(h-p)}{\alpha_j - \gamma_n} \sin (\alpha_j - \gamma_n)(h-p) \\ &+ \frac{1}{(\alpha_j + \gamma_n)^2} \cos (\alpha_j + \gamma_n)h + \frac{1}{(\alpha_j - \gamma_n)^2} \cos (\alpha_j - \gamma_n)h \\ &- \frac{1}{(\alpha_j + \gamma_n)^2} \cos (\alpha_j + \gamma_n)(h-p) - \frac{1}{(\alpha_j - \gamma_n)^2} \cos (\alpha_j - \gamma_n)(h-p) \end{aligned}$$

$$\tilde{I}_{16j}^{(2)} = \int_{-h}^0 e^{\beta_j y} \cos \gamma_n (y+h) dy = \frac{\beta_j \cos \gamma_n h + \gamma_n \sin \gamma_n h - \beta_j e^{-\beta_j h}}{(\beta_j^2 + \gamma_n^2)}$$

$$\tilde{I}_{17j}^{(2)} = \int_{-h}^0 e^{-\beta_j y} \cos \gamma_n (y+h) dy = \frac{1}{\beta_j^2 + \gamma_n^2} \left[ -\beta_j \cos \gamma_n h + \gamma_n \sin \gamma_n h + \beta_j e^{\beta_j h} \right]$$

$$\begin{aligned} \tilde{I}_{18n}^{(2)} &= \int_{-h}^0 \cosh 2\alpha_0 (y+h) \cos \gamma_n (y+h) dy = \\ &\frac{1}{(4\alpha_0^2 - \gamma_n^2)} \left[ 2\alpha_0 \sinh 2\alpha_0 h \cos \gamma_n h - \gamma_n \cosh 2\alpha_0 h \sin \gamma_n h \right] \end{aligned}$$

$$\int_{19njk}^{(2)} = \int_{-h}^0 \cos \alpha_{jk} (y+h) \cos \gamma_n (y+h) dy =$$

$$\frac{1}{2(\alpha_{jk}^2 - \gamma_n^2)} \left[ (\alpha_{jk} + \gamma_n) \sin(\alpha_{jk} - \gamma_n)h + (\alpha_{jk} - \gamma_n) \sin(\alpha_{jk} + \gamma_n)h \right]$$

$$\int_{20n}^{(2)} = \int_{-h}^0 \sinh \alpha_0 (y+h) \cos \frac{n\pi y}{h} dy = \frac{(-1)^n}{\alpha_0^2 + \left(\frac{n\pi}{h}\right)^2} \left[ \alpha_0 \cosh \alpha_0 h - \alpha_0 \right]$$

$$\int_{21n}^{(2)} = \int_{-p}^0 (y+p) \cosh \alpha_0 (y+h) \cos \frac{n\pi y}{h} dy = \frac{e^{\alpha_0 h}}{2\left(\alpha_0^2 + \frac{n^2 \pi^2}{h^2}\right)^2} \cdot$$

$$\left\{ \alpha_0^2 - \frac{n^2 \pi^2}{h^2} + e^{\alpha_0 p} \left[ \left(\alpha_0^2 - \frac{n^2 \pi^2}{h^2}\right) (\beta \alpha_0 - 1) + 2\alpha_0 \frac{n^2 \pi^2}{h^2} \right] \cos \frac{n\pi p}{h} \right.$$

$$\left. + e^{\alpha_0 p} \left[ 2\alpha_0 \frac{n\pi}{h} (\beta \alpha_0 - 1) - \frac{n\pi}{h} \left(\alpha_0^2 - \frac{n^2 \pi^2}{h^2}\right) \right] \sin \frac{n\pi p}{h} \right\}$$

$$+ \frac{e^{-\alpha_0 h}}{\alpha_0^2 + \frac{n^2 \pi^2}{h^2}} \left\{ \alpha_0^2 + \frac{n^2 \pi^2}{h^2} + e^{-\alpha_0 p} \left[ \left(\alpha_0^2 - \frac{n^2 \pi^2}{h^2}\right) (-\beta \alpha_0 - 1) - 2\alpha_0 \frac{n^2 \pi^2}{h^2} \right] \cos \frac{n\pi p}{h} \right.$$

$$\left. + e^{-\alpha_0 p} \left[ -2\alpha_0 \frac{n\pi}{h} (-\beta \alpha_0 - 1) - \frac{n\pi}{h} \left(\alpha_0^2 - \frac{n^2 \pi^2}{h^2}\right) \right] \sin \frac{n\pi p}{h} \right\}$$

$$\int_{22n}^{(2)} = \int_{-h}^0 e^{\beta_j y} \cos \frac{n\pi y}{h} dy = \frac{\beta_j}{\beta_j^2 + \left(\frac{n\pi}{h}\right)^2} \left[ 1 - (-1)^n e^{-\beta_j h} \right]$$

$$\int_{23n}^{(2)} = \int_{-h}^0 e^{-\beta_j y} \cos \frac{n\pi y}{h} dy = \frac{\beta_j}{(\beta_j)^2 + \left(\frac{n\pi}{h}\right)^2} \left[ 1 - (-1)^n e^{\beta_j h} \right]$$

$$\int_{24}^{(2)} = \int_{-h}^0 \cosh^2 \gamma_0 (y+h) dy = \frac{\sinh \gamma_0 h}{4} + \frac{\gamma_0 h}{2}$$

$$\tilde{L}_{25mn}^{(2)} = \int_{-h}^0 \cos \alpha'_{mn}(y+h) \cosh \gamma_0(y+h) dy =$$

$$\frac{1}{\gamma_0^2 - \alpha'^2_{mn}} \left[ \gamma_0 \sinh \gamma_0 h \cos \alpha'_{mn} h - \alpha'_{mn} \cosh \gamma_0 h \sin \alpha'_{mn} h \right]$$

$$\tilde{L}_{26njk}^{(2)} = \int_{-h}^0 \cos \alpha'_{jk}(y+h) \cos \gamma_n(y+h) dy =$$

$$\frac{1}{2(\alpha'^2_{jk} - \gamma_n^2)} \left[ (\alpha'_{jk} + \gamma_n) \sin(\alpha'_{jk} - \gamma_n) h + (\alpha'_{jk} - \gamma_n) \sin(\alpha'_{jk} + \gamma_n) h \right]$$

## APPENDIX F

### DESCRIPTIONS AND LISTINGS OF COMPUTER PROGRAMS

#### Introduction

All of the computer programs which follow were written to be executed via the compatible Time-Sharing System from a remote console connected to the IBM 7094 computer at M.I.T. (ref.10). This is a rather unique computation facility at the present time and had it not been available, the amount of work done in the time that was available on the task reported here would necessarily have been considerably less than was done. Other programs than those listed and described here were prepared and used in various stages of the research. Only those programs used in obtaining the reported results are considered to be of sufficient general interest to report here. Subroutines in the CTSS systems can and often do, have two or more names. The filing name is the name used to talk about the program and the name used to manipulate the storage of the program to and from the disc and the computer memory. The logical name is the name used to call the subroutine from another program.

The following program descriptions are not intended to inform a reader, who is unfamiliar with these programs, of sufficient details so we can use them; but rather as an introduction to the interested reader of what the programs can do and as a reference for one who has gained some familiarity with the programs and their use.



COMPUTER PROGRAM EGVAL

This program is a subroutine used to compute the various eigenvalues for a normal mode of real radian frequency  $\omega$ . For each frequency the subroutine finds  $\alpha_0$  which is given implicitly by the formula

$$\frac{\omega^2}{\alpha_0 g + \frac{3}{\rho} \alpha_0^3} = \tanh \alpha_0 h \quad (6-10)$$

and the first K  $\alpha_n$ 's which are given by the formula

$$\frac{\omega^2}{\alpha_n g + \frac{3}{\rho} \alpha_n^3} = -\tan \alpha_n h \quad (6-9)$$

This process is carried out for values of the radian frequency of RADO, RADO + RADS, RADO + 2 RADS... until the value of the radian frequency exceeds RADF within the following qualification. If a value of the radian frequency is less than RADF, Egval will find the eigenvalues for this value plus RADS before returning control to the calling program. The computed values of  $\alpha_0$  are stored in a one-dimensional array called ALPO(J) where J = 1 corresponds to a radian frequency of RADO, J = 2 corresponds to RADO + RADS, etc. The  $\alpha_n$ 's are stored in a two dimensional array called ALP(J,N) where the J's correspond to the radian frequency just like they do for ALPO and the N's correspond to the number of the eigenvalue, N = 1 corresponds to the lowest eigenvalue of (6-9) etc.

The eigenvalues are found by Newton's method. In finding the value of  $\alpha_0$ , the initial guess is

$$\alpha_{0 \text{ guess}} = \sqrt{\omega^2 / gh}$$

In this case the value of the initial guess is not very important because

$\frac{\omega^3}{\alpha_0 g + \mathcal{I} \alpha_0^3} - \tan \alpha_0 h$  is monotonic in  $\alpha_0$ . Whenever the change in

value of  $\alpha_0$  from one iteration to the next is less than 0.00025 of the iterated value of  $\alpha_0$ , the iterated value is taken as the correct value. The set of statements from 210 to 330 in the program listing are the instructions for finding  $\alpha_0$ .

The initial guess for  $\alpha_n$  is very important because

$$\frac{\omega^2}{\alpha_n g + \mathcal{I} \alpha_n^3} + \tan \alpha_n h$$

is not monotonic  $\alpha_n$ . It is essential when determining the  $n^{\text{th}}$  root that the iterated value stay on the  $n^{\text{th}}$  branch of the tangent. This can be assured by making sure that the initial guess for the  $n^{\text{th}}$  root is on the  $n^{\text{th}}$  branch of the tangent and that the guess is an underestimate for the value of the root. Then (as can be seen in figure ) each successive iterated value will be an underestimate of the true value, but a closer approximation than the preceding iterated value. For the present work a workable value for the initial guess has been found to be

$$\alpha_n(\text{guess}) = (n - 0.48) \frac{\pi}{h}$$

Since  $\tan x$  takes on all real values as  $x$  changes by  $\pi$ , the change in  $\alpha_n$  as the  $n^{\text{th}}$  branch of the tangent varies over its entire range is  $\frac{\pi}{h}$ . The iterated value of  $\alpha_n$  is taken as correct when the change in the iterated value from one iteration to the next is less than  $\frac{1}{4000h}$ . The set of statements from 340 to 520 in the program listing are the instructions for finding the  $\alpha_n$ 's.

All input and output for this subroutine is done via common storage with a program that performs the input-output operations.

The logical name for EGVAL is EIGVAL.

EGVAL

```

EXTERNAL FUNCTION MTR00010
ENTRY TO EIGVAL. MTR00020
DIMENSION ETR(100),ETI(100),HPR(100),HPI(100) MTR00030
VECTORVALUESQQ0002 = 000002 ,1, 000040 MTR00040
VECTORVALUESQQ0003 = 000002 ,1, 000040 MTR00050
VECTORVALUESQQ0004 = 000002 ,1, 000040 MTR00060
VECTORVALUESQQ0005 = 000002 ,1, 000040 MTR00070
DIMENSION ALPO(100),B1(100),CNO(100),TOR(100),TOI(100),HR(1 MTR00080
100),HI(100),ALP( 004000, QQ0002),CN( 004000, QQ0003 MTR00090
1),CB( 004000, QQ0004),T( 004000, QQ0005) MTR00100
PROGRAM COMMON ALPO,ALP,B1,CB,CNO,CN,TOR,TOI,T,HR,HI,RADO, MTR00110
1RADF,RADS,H,P,QL,RO,G,TEN,PI,R,ETR,ETI,HPR,HPI,K MTR00120
INTERNAL FUNCTION SINH .( QQ0006)=0.5*(EXP .( QQ0006 MTR00130
1)-EXP .( - QQ0006)) MTR00140
INTERNAL FUNCTION COSH .( QQ0007)=0.5*(EXP .( QQ0007 MTR00150
1)+EXP .( - QQ0007)) MTR00160
PI=3.1415927 MTR00170
RAD=RADO-RADS MTR00180
T'H QQ0009, FOR J=1,1, J .G. 100 MTR00190
RAD=RAD+RAUS MTR00200
AA=SQRT.(RAD*RAD/(G*H)) MTR00210
A1=COSH.(AA*H) MTR00220
A2=TEN*(AA.P.2)/RO MTR00230
A3=AA*(G+A2) MTR00240
FU=TANH.(AA*H)-RAD*RAD/A3 MTR00250
A=(H/A1)/A1+RAD*RAD*(G+3.0*A2)/(A3*A3) MTR00260
AAA=AA-FU/A MTR00270
RATIO=.ABS.(FU/(A*AAA)) MTR00280
W'R (RATIO-0.00025) .G. 0.0,TRANSFER TO QQ0011 MTR00290
TRANSFER TO QQ0012 MTR00300
QQ0010 AA=AAA MTR00310
TRANSFER TO QQ0010 MTR00320
QQ0012 ALPO(J)=AAA MTR00330
T'H QQ0013, FOR N=1,1, N.G. K MTR00340
PIH=PI/H MTR00350
AA=N*PIH-0.480*PIH MTR00360
QQ0014 A1=COS.(AA*H) MTR00370
A2=TEN*(AA .P.2)/RO MTR00380
A3=AA*(G-A2) MTR00390
A4=TAN.(AA*H) MTR00400
A5=RAD*RAD/A3 MTR00410
FU=A4+A5 MTR00420
A6=H/(A1*A1) MTR00430
A7=RAD*RAD*(G-3.0*A2)/(A3*A3) MTR00440
A=A6-A7 MTR00450
AAA=AA-FU/A MTR00460
RATIO=.ABS.(FU*H/A) MTR00470
W'R (RATIO-0.00025) .G. 0.0,TRANSFER TO QQ0015 MTR00480
TRANSFER TO QQ0013 MTR00490
QQ0015 AA=AAA MTR00500
TRANSFER TO QQ0014 MTR00510
QQ0013 ALP(J,N)=AAA MTR00520
W'R (RADF-RAD) .G. 0.0,TRANSFER TO QQ0016 MTR00530

```

QQ0016  
QQ0009  
QQ0017

TRANSFER TO QQ0017  
CONTINUE  
CONTINUE  
CONTINUE  
INTEGER QQ0002, J, N, K  
FUNCTION RETURN  
END OF FUNCTION

MTR00540  
MTR00550  
MTR00560  
MTR00570  
MTR00580  
MTR00590  
MTR00600

## COMPUTER PROGRAM BHN

BHN is the main control program used for determining the characteristics of a wave absorber and for designing such an absorber. BHN calls EGVAl to obtain the eigenvalues and calls IMERG to aid in the design of the electric filter.

The following quantities are inputs to BHN

H = calm water depth

P = depth of paddle pivot point

QL = length of space containing water behind the paddle.

This is a vestige from the time when a previous version of BHN was used to compute  $H_m(\omega)$  the angular amplitude to moment response for a wave absorbing paddle.

RO = water density 1.94 slugs/ft.<sup>3</sup>

G = acceleration due to gravity = 32.2 ft/sec<sup>2</sup>

TEN = water surface tension 0.0050 lbs/ft

R = downstream distance from the paddle to the actuating wave height probe.

RADO = lowest radian frequency for which the computation is carried out.

RADF = highest radian frequency for which the computation is carried out.

RADS = radian frequency increments between values of radian frequency at which the computation is carried out.

K is the index of the highest eigenvalue computed. For each radian frequency at which the computation is performed the eigenvalues which are determined (by EGVAl) are:  $\alpha_0, \alpha_1, \alpha_2 \dots \alpha_K$ . Also the various

series which are derived in chapter 4 which have the form  $\sum_{n=1}^{\infty} a_n$  are truncated to  $\sum_{n=1}^K a_n$

AP equals the magnitude of the position of two real poles in that S plane for the prefilter (described in chapter 7.) in the absorbing system function. The program statements from 340 to 580 are the instructions for evaluating equation (4-35) which gives the system function for an ideal absorber. The statements numbered from 590 to 650 perform the prefiltering which was described in chapter 7.

The system function of the prefilter is

$$H_p(s) = \frac{s}{(s+a)(s+a)}$$

BHN prints out the real and imaginary parts, size and angle of the ideal wave absorbing system function as well as the size and angle of the system function of a filter which when cascaded with the prefilter will give the ideal system function (system function for complete absorption).

The statement numbered 720 transfers control to the program IMERG whose logical name is HURAT.

```

HPR(J)=B1(J)*ETR(J)/DNM
HPI(J)=-B1(J)*ETI(J)/DNM
SIZE=(HPR(J)*HPR(J)+HPI(J)*HPI(J)) .P.0.5
ANGLE=ATAN.(HPI(J)/HPR(J))
W'R HPR(J) .L. 0.0,ANGLE =ANGLE+3.14159
A=AP
SIGZ=((A*A-RAD*RAD).P.2+4.*A*A*RAD*RAD).P.0.5/RAD
AN=ATAN.(RAD*RAD-A*A)/(2.0*RAD*A)
S(J)=SIZE*.IGZ
AN=ANGLE-AN+6.28318
N=AN/6.28318
ANT(J)=AN-N*6.28318
PRINT FORMAT QQ0015,RAD,HPR(J),HPI(J),SIZE,ANGLE,
IS(J),ANT(J)
WHENEVER (RADF-RAD) .G.0, TRANSFER TO QQ0012
TRANSFER TO QQ0016
CONTINUE
CONTINUE
EXECUTE HURAT.(S,ANT,RADO,RADS,RADF)
V'S QQ0015=$(7F10.3)$
INTEGLR J , N , K
E'M

```

```

MTR00540
MTR00550
MTR00560
MTR00570
MTR00580
MTR00590
MTR00600
MTR00610
MTR00620
MTR00630
MTR00640
MTR00650
MTR00660
MTR00670
MTR00680
MTR00690
MTR00700
MTR00710
MTR00720
MTR00730
MTR00740
MTR00750

```

```

QQ0012
QQ0016

```

BHN

```
DIMENSION LTR(100),ETI(100),HPR(100),HPI(100) MTR00010
DIMENSION S(100),AN(100) MTR00020
VECTORVALUESQQ0002 = 000002 ,1, 000040 MTR00030
VECTORVALUESQQ0003 = 000002 ,1, 000040 MTR00040
VECTORVALUESQQ0004 = 000002 ,1, 000040 MTR00050
VECTORVALUESQQ0005 = 000002 ,1, 000040 MTR00060
DIMENSION ALPO(100),B1(100),CNO(100),LOR(100),LOI(100),HR(1 MTR00070
100),HI(100),ALP( 004000, QQ0002),CN( 004000, 'QQ0003 MTR00080
1),CB( 004000, QQ0004),T( 004000, QQ0005) MTR00090
PROGRAM COMMON ALPO,ALP,B1,CB,CNO,CI,TOR,TUI,T,TR,HI,RADU,MTR00100
1RADF,RADS,H,P,QL,R,G,TEN,PI,R,EIR,ETI,HPR,HPI,K MTR00110
INTERNAL FUNCTION SINH .( QQ0006)=0.5*(EXP .( QQ0006 MTR00120
1)-EXP .( - QQ0006)) MTR00130
INTERNAL FUNCTION CUSH .( QQ0007)=0.5*(EXP .( QQ0007 MTR00140
1)+EXP .( - QQ0007)) MTR00150
READ BCD TAPE 4 , QQ0008, H , P MTR00160
1, QL , RU , G , TEN , R MTR00170
READ BCD TAPE 4 , QQ0009, RADU , RADF MTR00180
1, RADS MTR00190
READ BCD TAPE 4 , QQ0010, K MTR00200
VECTOR VALUES QQ0008 = $( 7F8.4)$ MTR00210
VECTOR VALUES QQ0009 = $( 3F6.2)$ MTR00220
VECTOR VALUES QQ0010 = $( 12)$ MTR00230
EXECUTE EIGVAL .( 0) MTR00240
PRINT ONLINEFCRMAT QQ0011 MTR00250
V'SQQ0011=$(7H RAD,7X,3HHPR,7X,3HHPI,7X,4HSIZE, MTR00260
15X,3HANGLE,8X,2HSF,7X,4HANGF)$ MTR00270
RAD=RADO-RADS MTR00280
READ BCD TAPE 4, FORA,AP MTR00290
V'S FORA=$(F7.3)$ MTR00300
THROUGH QQ0012 ,FOR J = 1 ,1, J .G. MTR00310
1100 MTR00320
RAD=RAD+RADS MTR00330
A=ALPO(J) MTR00340
ETR(J)=A*SINH.(A*H)*SIN.(A*R) MTR00350
ETI(J)=A*SINH.(A*H)*COS.(A*R) MTR00360
AA=0.5*H+0.25*SINH.( 2.0*A*H)/A MTR00370
AAA=P*SINH.(A*H)/A+(COSH.(A*(H-P))-COSH.(A MTR00380
1*H))/(A*AA) MTR00390
B1(J)=-A*AA/(RAD*AAA) MTR00400
THROUGH QQ0013 ,FOR N = 1 ,1, N .G. MTR00410
1K MTR00420
A=ALP(J,N) MTR00430
AA=0.5*H+.25*SIN .( 2.0*A*H)/A MTR00440
AAA=P*SIN .( A*H)/A+(COS .( A*H)-COS .( A*(H-P) MTR00450
1))/(A*AA) MTR00460
CB(J,N)=-RAD*B1(J)*AAA/(A*AA) MTR00470
ETR(J)=ETR(J)+A*CB(J,N)*SIN.(A*H)*EXP.(-A*R) MTR00480
T(J,N)=(-CB(J,N)+CN(J,N))*CUSH .( A*QL))*AAA MTR00490
HR(J)=HR(J)*A MTR00500
ETR(J)=ETR(J)/RAD MTR00510
ETI(J)=ETI(J)/RAD MTR00520
DNM=ETR(J)*ETR(J)+ETI(J)*ETI(J) MTR00530
```

QQ0013

COMPUTER PROGRAMS EP, SCP, SCS, SCA, THP, and THSA

The computer program EP is used to obtain the real part, the imaginary part, the magnitude or the angle of the exponential function;

$$f = e^{(A+iB)} .$$

The logical functions contained in EP are:

$$\text{EPR.}(A,B) = \text{Re}(e^{(A+iB)}) = e^A \cos B$$

$$\text{EPI.}(A,B) = \text{Im}(e^{(A+iB)})$$

$$\text{EPS.}(A,B) = |e^{(A+iB)}| = e^A$$

$$\text{EPA.}(A,B) = \text{Arg}(e^{(A+iB)}) = B \text{ modulo } 2\pi$$

The program SCP is used to find the real or imaginary part of  $\text{SINH}(A + iB)$  or  $\text{COSH}(A + iB)$ . The logical functions contained in SCP are:

$$\text{SHR}(A,B) = \text{Re } \sinh(A + iB)$$

$$\text{SHI}(A,B) = \text{Im } \sinh(A + iB)$$

$$\text{CHR}(A,B) = \text{Re } \cosh(A + iB)$$

$$\text{CHI}(A,B) = \text{Im } \cosh(A + iB)$$

The program SCS is used to obtain the magnitude of  $\sinh(A + iB)$  or  $\cosh(A + iB)$ . The logical functions contained in SCS are:

$$\text{SHS}(A + iB) = \sinh(A + iB)$$

$$\text{CHS}(A + iB) = \cosh(A + iB)$$

The program SCA is used to find the argument of  $\sinh(A + iB)$  or  $\cosh(A + iB)$ . The logical functions contained in SCA are:

$$\text{SHA}(A,B) = \text{ARG } \sinh(A + iB)$$

$$\text{CHA}(A,B) = \text{ARG } \cosh(A + iB)$$

The program THP is used to obtain the real or imaginary part of  $\tanh(A + iB)$ . The logical functions contained in THP are:

$$\text{THR}(A,B) = \text{Re } \tanh(A + iB)$$

$$\text{THI}(A,B) = \text{Im } \tanh(A + iB)$$

The program THSA is used to find the magnitude or angle of  $\tanh(A + iB)$ . The logical functions contained in THSA are:

THS. (A,B) = tanh (A + iB)

THA. (A,B) = ARG tanh (A + iB)

For convenience the binary compilations of EP, SCP, SCS, SCA, THP, and THSA are lumped into the single disc file called TRNS.

EP, SCP, SCS, SCA, THP, and THSA

EXTERNAL FUNCTION (A,B)		00010
INTEGER N		00020
ENTRY TO EPR.		00030
F=EXP.(A)*COS.(B)		00040
FUNCTION RETURN F		00050
ENTRY TO EPI.		00060
F=EXP.(A)*SIN.(B)		00070
FUNCTION RETURN F		00080
ENTRY TO EPS.	EP	00090
F=EXP.(A)		00100
FUNCTION RETURN F		00110
ENTRY TO EPA.		00120
N=B/6.28318		00130
F=B-6.28318*N		00140
FUNCTION RETURN F		00150
END OF FUNCTION		00160
EXTERNAL FUNCTION (A,B)		00010
ENTRY TO SHR.		00020
F=0.5*(EPR.(A,B)-EPR.(-A,-B))		00030
FUNCTION RETURN F		00040
ENTRY TO SHI.	SCP	00050
F=0.5*(EPI.(A,B)-EPI.(-A,-B))		00060
FUNCTION RETURN F		00070
ENTRY TO CHR.		00080
F=0.5*(EPR.(A,B)+EPR.(-A,-B))		00090
FUNCTION RETURN F		00100
ENTRY TO CHI.		00110
F=C.5*(EPI.(A,B)+EPI.(-A,-B))		00120
FUNCTION RETURN F		00130
END OF FUNCTION		00140
EXTERNAL FUNCTION (A,B)		00010
ENTRY TO SHS.		00020
F=(SHR.(A,B).P.2+SHI.(A,B).P.2).P. 0.5	SCS	00030
FUNCTION RETURN F		00040
ENTRY TO CHS.		00050
F=(CHR.(A,B).P.2+CHI.(A,B).P.2).P. 0.5		00060
FUNCTION RETURN F		00070
END OF FUNCTION		00080

EXTERNAL FUNCTION (A,B)		00010
ENTRY TO SHA.		00020
F=ASIN.(SHJ.(A,B)/SHS.(A,B))		00030
W'R SHR.(A,B) .L. 0.0,F=3.14159-F		00040
FUNCTION RETURN F		00050
ENTRY TO CHA.		00060
F=ASIN.(CHI.(A,B)/CHS.(A,B))	SCA	00070
W'R CHR.(A,B) .L. 0.0,F=3.14159-F		00080
FUNCTION RETURN F		00090
END OF FUNCTION		00100
EXTERNAL FUNCTION (A,B)		00010
ENTRY TO THR.		00020
F=THS.(A,B)*COS.(THA.(A,B))		00030
FUNCTION RETURN F	THP	00040
ENTRY TO THI.		00050
F=THS.(A,B)*SIN.(THA.(A,B))		00060
FUNCTION RETURN F		00070
END OF FUNCTION		00080
EXTERNAL FUNCTION (A,B)		00010
ENTRY TO THS.		00020
W'R A .G. 20.0		00030
F=1.0		00040
OR WHENEVER A .L. -20.0		00050
F=1.0		00060
OTHERWISE	THSA	00070
F=SHS.(A,B)/CHS.(A,B)		00080
E'L		00090
FUNCTION RETURN F		00100
ENTRY TO THA.		00110
W'R A .G. 20.0		00120
F=0.0		00130
OR WHENEVER A .L. -20.0		00140
F=3.14159		00150
OTHERWISE		00160
F=SHA.(A,B)-CHA.(A,B)		00170
E'L		00180
FUNCTION RETURN F		00190
END OF FUNCTION		00200

## COMPUTER PROGRAMS RATR AND RATC

RATR is a subroutine used in finding the size and angle of a real pole or zero in a rational function. The term to be evaluated has the form:

$$h_p(s) = (s - s_c)$$

where  $s = \sigma + i\omega$  and  $s_c$  is the position of the real pole or zero.

Thus

$$h_p(s) = [(\sigma - s_c) + i\omega]$$

In RATR  $\sigma$  is called RI and  $\omega$  is called R.

The magnitude of  $h(s)$  is given by the logical function FM. (R, RI, SC) and the angle of  $h(s)$  is given by the logical function AGR. (R, RI, SC) RATC is a

subroutine used in finding the contributions to the size and angle of a rational function from a conjugate pair of poles or zeros. Here the term to be evaluated is:

$$h_c(s) = (s - s_0)(s - s_0^*)$$

where

$$s = \sigma + i\omega = RI + iR$$

and

$$s_0 = s_c + iR_c$$

The magnitude of  $h_c(s)$  is given by the logical function F2. (R, RI, RC, SC) and the angle of  $h_c(s)$  is given by the logical function AGC, (R, RI, RC, SC).

RATR and RATC

EXTERNAL FUNCTION (R,RI,SC)	00010
ENTRY TOAGR.	00020
AR=RI-SC	00030
W'R .ABS.(R/10000.0).G. .ABS.(AR)	00040
ANG=1.57079	00050
W'R AR .E. 0.0,ANG=.ABS.(R)*ANG/R	RATR 00060
O'E	00070
ANG=ATAN.(R/AR)	00080
E'L	00090
W'R AR .L. 0.0,ANG=ANG+3.14159	00100
FUNCTION RETURN ANG	00110
ENTRY TO FM.	00120
T=SQRT.((RI-SC)*(RI-SC)+R*R)	00130
FUNCTION RETURN T	00140
END OF FUNCTION	00150

EXTERNAL FUNCTION (R,RI,RC,SC)	00010
ENTRY TO AGC.	00020
AR=(RI-SC)*(RI-SC)-(R*R-RC*RC)	00030
AI=2.0*R*(RI-SC)	00040
W'R .ABS.(AI/10000.0).G. .ABS.(AR)	RATC 00050
ANG=1.57079	00060
W'R AR .E. 0.0,ANG=.ABS.(AI)*ANG/AI	00070
O'E	00080
ANG=ATAN.(AI/AR)	00090
E'L	00100
W'R AR .L. 0.0, ANG=ANG+3.14159	00110
FUNCTION RETURN ANG	00120
ENTRY TO F2.	00130
AR=(RI-SC)*(RI-SC)-(R*R-RC*RC)	00140
AI=2.0*R*(RI-SC)	00150
T=SQRT.(AR*AR+AI*AI)	00160
FUNCTION RETURN T	00170
END OF FUNCTION	00180

COMPUTER PROGRAMS STABI AND DRVTV

The program STABI is used to investigate the stability of a wave absorbing system with respect to negative going waves. The theory associated with this investigation is described in chapter 9 . STABI evaluates

$H_e(\omega) - H_g(\omega)$  (see chapter 9) for any specified complex value of  $\omega$ .

The inputs to STABI are:

H, P, RO, G, TEN, R, RAD, RADF and RADS as described in the description of the computer program BHN.

SIM and BIM control the imaginary parts of  $\omega$  at which  $H_e(\omega) - H_g(\omega)$  is evaluated. At any value  $v$  of  $\text{Re}(\omega)$ ,  $[H_e(\omega) - H_g(\omega)]$  is evaluated at the following points of the complex  $\omega$  plane

$$\left\{ |r^2 + 2n \cdot \text{SIM} \cdot r|^{\frac{1}{2}} \right\} e^{i \frac{1}{2} \tan^{-1} \left( \frac{2n \cdot \text{SIM}}{r} \right)}$$

where  $n = 1, 2, \dots$  until  $n$  exceeds  $\text{BIM}/\text{SIM}$ .

For small values of SIM the points in the complex plane are approximately  $v, v, + i \text{SIM}, v + i \cdot 2 \cdot \text{SIM}, \text{etc.}$

NZR = number of real zeros of  $h_e(s)$

NPR = number of real poles

NZC = number of pairs of conjugate zeros

NPC = number of pairs of conjugate poles

HH = multiplicative constant in  $h(s)$  where  $h_e(s) = K \frac{(s-a)(s-b)\dots}{(s-d)(s-e)\dots}$

DZ's are positions of the real zeros as in IMERG

DP's are positions of the real poles as in IMERG

ZER's real parts of the positions of the complex zeros as in IMERG

ZEI's are imaginary parts of the positions of the complex zeros as in IMERG

PR's are real parts of the positions of the complex poles as in IMERG

PI's are imaginary parts of the positions of the complex poles as in IMERG

K is the number of terms in the eigenfunction series for the potential  
as in BHN.

The output from STABI is written on the "pseudo tape" disc file, TAPE.  
10 (see CTSS Manual, Ref.10) which can be subsequently printed by a console  
command. At each complex radian frequency at which the computation is  
performed the output quantities are:

$$Re(\omega), Im(\omega), Re[\mathcal{H}_e(\omega) - \mathcal{H}_g(\omega)], \text{ and} \\ Im[\mathcal{H}_e(\omega) - \mathcal{H}_g(\omega)]$$

An operational description of STABI follows. First, a subsection of  
STABI which is exactly the same as the operational section of EGVAL finds  
the eigenvalues at real values of  $\omega$  equal to RADO, RADO + RADS, RADO + 2  
RADS, etc. The equation for the complex eigenvalues is (chapter 8 )

$$\frac{\omega^2}{fg} - \cosh fh = 0 \quad (8-31)$$

where the solutions  $f$  are the eigenvalues.

Let  $fh = Z$  (8-32)

Then,  $\frac{\omega^2 h}{g} - Z \tanh Z = 0$  (8-33)

Hence the eigenvalues can be determined from the roots of the function

$$g(Z) = \frac{\omega^2 k}{g} - Z \tanh Z$$

where  $\omega$  and  $Z$  are complex numbers.

Newton's method for finding the roots of a function can be extended to analytic functions of a complex variable.  $q(Z)$  is analytic except for the poles at  $(n - \frac{1}{2})\pi i$ . The evaluation of  $H_e(\omega) - H_g(\omega)$  is carried out at values of  $\text{Re}(\omega^2)$  equal to  $(\text{RADO})^2$ ,  $(\text{RADO} + \text{RADS})^2$ , etc. For these values of  $\text{Re}(\omega^2)$  and  $\text{Im}(\omega^2) = 0$  the roots of  $q(Z)$  are known. For a fixed value of  $\text{Re}(\omega^2)$ ,  $\text{Im}(\omega^2)$  is set at

$$\hat{\text{Im}}(\omega^2) = 2 \cdot \text{SIM} \cdot \sqrt{\text{Re}(\omega^2)}$$

For this value of  $\omega^2$  the roots of  $q(Z)$  are found by the extended form of Newton's method using for initial guesses the roots for  $\text{Im}(\omega^2) = 0$ . Then the imaginary part of  $\omega^2$  is set at

$$\hat{\text{Im}}(\omega^2) = 4 \cdot \text{SIM} \cdot \sqrt{\text{Re}(\omega^2)}$$

and the roots are determined where the initial guesses are the roots for  $\text{Im}(\omega^2)$  equal to the previously computed value.

The process is continued for values of  $\text{Im}(\omega^2)$  given by

$$\hat{\text{Im}}(\omega^2) = 2n \cdot \text{SIM} \cdot \sqrt{\text{Re}(\omega^2)}$$

where the initial guesses for the roots are the computed roots at

$$\hat{\text{Im}}(\omega^2) = 2 \cdot (n-1) \cdot \text{SIM} \cdot \sqrt{\text{Re}(\omega^2)}$$

After this is done for all the desired values of  $n$ ,  $\text{Re}(\omega^2)$  is changed and the process is repeated.

Newton's Method of finding roots requires the derivative of the function whose roots are to be found (see Thomas, Ref. 4), in the extended form, Newton's Method requires the real and imaginary parts of the derivative

of  $q(Z)$ . These values are determined by the subroutine DRVTV. Operationally, these values are obtained by STABI.in function form as  $DVR.(FR(M), FI(M))$  and  $DVI.(FR(M), FI(M))$ , DVR.is the real part of the derivative and DVI. is the imaginary part of the derivative evaluated at  $Re(Z) = FR(M)$ ,  $Im(Z)=FI(M)$ . Outputs from STABI.appear in figures 7-2 and 7-5 .

## STABI

printf stabi mad

W 1447.0

```

00010      DIMENSION DR(100),DI(100),DS(100),DA(100),ZR(100),ZI(100)
00020      DIMENSION FR(100),FI(100),ALPO(100),ALP(4000,DIM)
00030      DIMENSION DZ(6),DP(6),ZER(6),ZEI(6),PR(6),PI(6)
00040      V'S DIM=2,41,40
00050      INTEGER KR,KI,LI,LO,I,J,K,L,M,N,JJ
00060      INTEGER NZR,NPR,NZC,NPC
00070      INTERNAL FUNCTION
00080      ENTRY TO MA.
00090      AA=0.0
00100      W'R HH .L. 0.0,AA=3.14159
00110      SLA=.ABS.(HH)
00120      T'H T2, FOR JJ=1,1, JJ .G. NZR
00130      V'S TST=$(1H 12)$
00140      SLA=SLA*FM.(-RAD,RADIM,DZ(JJ))
00150 T2      AA=AA+AGR.(-RAD,RADIM,DZ(JJ))
00160      T'H T3, FOR JJ=1,1, JJ .G. NPR
00170      SLA=SLA/FM.(-RAD,RADIM,DP(JJ))
00180 T3      AA=AA-AGR.(-RAD,RADIM,DP(JJ))
00190      T'H T4, FOR JJ=1,1, JJ .G. NZC
00200      SLA=SLA*F2.(-RAD,RADIM,ZEI(JJ),ZER(JJ))
00210 T4      AA=AA+AGC.(-RAD,RADIM,ZEI(JJ),ZER(JJ))
00220      T'H T5, FOR JJ=1,1, JJ .G. NPC
00230      SLA=SLA/F2.(-RAD,RADIM,PI(JJ),PR(JJ))
00240 T5      AA=AA-AGC.(-RAD,RADIM,PI(JJ),PR(JJ))
00250      N=AA/6.28318
00260      W'R AA .L. 0.0, N=N-1
00270      AA=AA-N*6.28318
00280      FRR=SLA*COS.(AA)
00290      FRI=SLA*SIN.(AA)
00300      FUNCTION RETURN
00310      END OF FUNCTION
00320      INTERNAL FUNCTION
00330      ENTRY TO VAL.
00340      NI=0.0
00350      NR=0.0
00360      T'H SUMI, FOR L=0,1, L .G. K
00370      VR=FR(L)/H
00380      VI=FI(L)/H
00390      DEN=VR*VR+VI*VI
00400      BR=VR*H
00410      BI=VI*H
00420      CR=VR*(H-P)
00430      CI=VI*(H-P)
00440      I1R=.5*H+.25*(VR*SHR.(2.*BR,2.*BI)+VI*SHI.(2.*BR,2.*BI))
00450      1/DEN
00460      I1I=.25*(VR*SHI.(2.*BR,2.*BI)-VI*SHR.(2.*BR,2.*BI))/DEN
00470      I3R=P*SHR.(BR,BI)+(VR*(CHR.(CR,CI)-CHR.(BR,BI))
00480      1+VI*(CHI.(CR,CI)-CHI.(BR,BI))/DEN

```

STABI (cont.)

```

00490      I3I=P*SHI.(BR,BI)+(VR*(CHI.(CR,CI)-CHI.(BR,BI))
00500      I-VI*(CHR.(CR,CI)-CHR.(BR,BI))/DEN
00510      I1R=I1R*1.0 E-15
00520      I1I=I1I*1.0 E-15
00530      I3R=I3R*1.0 E-15
00540      I3I=I3I*1.0 E-15
00550      DEN=I1R*I1R+I1I*I1I
00560      INR=(I1R*I3R+I1I*I3I)/DEN
00570      INI=(I1R*I3I-I1I*I3R)/DEN
00580      DEN=VR*VR+VI*VI
00590      X=(INR*VR+INI*VI)/DEN
00600      Y=(INI*VR-INR*VI)/DEN
00610      DDR=-D*VI
00620      DDI=D*VR
00630      S=SHR.(BR,BI)*EPR.(DDR,DDI)-SHI.(BR,BI)*EPI.(DDR,DDI)
00640      T=SHI.(BR,BI)*EPR.(DDR,DDI)+SHR.(BR,BI)*EPI.(DDR,DDI)
00650      NR=NR+X*S-Y*T
00660 SUMI  NI=NI+X*T+S*Y
00670      EXECUTE MA.
00680      DEN=NR*NR+NI*NI
00690      NRR=-NI/DEN
00695      NII=-NR/DEN
00700      ZPR=NRR-FRR
00710      ZPI=NII-FRI
00720      WRITE BCD TAPE LO,FFB,RAD,RADIM,ZPR,ZPI
00730      V'S FFB=$(1H 2F9.3,2F17.8)$
00740      FUNCTION RETURN
00750      END OF FUNCTION
00760      LI=9
00770      LO=10
00780      READ BCD TAPE LI,FORA,H,P,RO,G,TEN,R
00790      V'S FORA=$(6F8.4)$
00800      READ BCD TAPE LI,FORJ,RADO,RADF,RADS,BIM,SIM
00810      V'S FORJ=$(5F6.2)$
00820      V'S FORK=$(F20.9)$
00830      V'S FORL=$(9F8.2)$
00840      V'S FORGG=$(4I3)$
00850      READ BCD TAPE 5, FORGG,NZR,NPR,NZC,NPC
00860      READ BCD TAPES, FORK,HH
00870      READ BCD TAPE 5, FORL,DZ(1)...DZ(NZR)
00880      READ BCD TAPE 5, FORL,DP(1)...DP(NPR)
00890      READ BCD TAPE 5, FORL,ZER(1)...ZER(NZC)
00900      READ BCD TAPE 5, FORL,ZEI(1)...ZEI(NZC)
00910      READ BCD TAPE 5, FORL,PR(1)...PR(NPC)
00920      READ BCD TAPE 5, FORL,PI(1)...PI(NPC)
00930      P=P*1.0
00940      D=R
00950      CN=H/G
00960      CNN=CN*CN
00970      READ BCD TAPE LI,FORB,K
00980      V'S FORB=$(I2)$
00990      INTERNAL FUNCTION SINH .(      QQ0006)=0.5*(EXP .(      QQ0006
01000      1)-EXP .(      -      QQ0006))

```

## STABI (cont.)

```

01010 INTERNAL FUNCTION COSH .( QQ0007)=0.5*(EXP .( QQ0007
01020 1)+EXP .( - QQ0007))
01030 PI=3.1415927
01040 RAD=RADO-RADS
01050 T'H QQ0009, FOR J=1,1, J .G. 100
01060 RAD=RAD+RADS
01070 AA=SQRT.(RAD*RAD/(G*H))
01080 QQ0010 A1=COSH.(AA*H)
01090 A2=TEN*(AA.P.2)/RO
01100 A3=AA*(G+A2)
01110 FU=TANH.(AA*H)-RAD*RAD/A3
01120 A=(H/A1)/A1+RAD*RAD*(G+3.0*A2)/(A3*A3)
01130 AAA=AA-FU/A
01140 RATIO=.ABS.(FU/(A*AAA))
01150 W'R (RATIO-.001) .G. 0.0,TRANSFER TO QQ0011
01160 TRANSFER TO QQ0012
01170 QQ0011 AA=AAA
01180 TRANSFER TO QQ0010
01190 QQ0012 ALPO(J)=AAA
01200 T'H QQ0013, FOR N=1,1, N.G. K
01210 PIH=PI/H
01220 AA=N*PIH-0.480*PIH
01230 QQ0014 A1=COS.(AA*H)
01240 A2=TEN*(AA .P.2)/RO
01250 A3=AA*(G-A2)
01260 A4=TAN.(AA*H)
01270 A5=RAD*RAD/A3
01280 FU=A4+A5
01290 A6=H/(A1*A1)
01300 A7=RAD*RAD*(G-3.0*A2)/(A3*A3)
01310 A=A6-A7
01320 AAA=AA-FU/A
01330 RATIO=.ABS.(FU/(A*H))
01340 W'R (RATIO-.001) .G . 0.0,TRANSFER TO QQ0015
01350 TRANSFER TO QQ0013
01360 QQ0015 AA=AAA
01370 TRANSFER TO QQ0014
01380 QQ0013 ALP(J,N)=AAA
01390 W'R (RADF-RAD) .G. 0.0,TRANSFER TO QQ0016
01400 TRANSFER TO QQ0017
01410 QQ0016 CONTINUE
01420 QQ0009 CONTINUE
01430 QQ0017 CONTINUE
01440 KR=(RADF-RADO)/RADS+1
01450 KI=BIM/SIM
01460 WRITE BCD TAPE LO, FFA
01470 V'S FFA=$(8H OM REAL,4X,7HOM IMAG,7X,10HGR + RADIM,7X,
01480 110HGI + RADIM)$
01490 T'H TH1, FOR J=1,1, J .G. KR
01495 RAD=RADO+(J-1)*RADS
01500 A=RAD*RAD
01510 SIMM=2.0*SIM*SQRT.(A)
01520 FI(0)=0.0

```

STABI (cont.)

```

01530      FR(0)=ALPO(J)*H
01540      DI(0)=DVI.(FR(0),0.0)
01550      DR(0)=DVR.(FR(0),0.0)
01560      T'H TH2, FOR M=1,1, M .G. K
01570      FI(M)=ALP(J,M)*H
01580 TH2   FR(M)=0.0
01590      AIM=0.0
01600      RADIM=0.0
01610      EXECUTE VAL.
01620      V'S FORR=$(1H )$
01630      V'S FORD=$(23H IMAGINARY PART OF F*F=F6.2)$
01640      T'H TH3, FOR I=1,1, I .G. KI
01650      AIM=AIM+SIMM
01660      MAG=SQRT.(A+AIM)
01670      ANG=0.5*ATAN.(AIM/A)
01680      W'R A .L. 0.0, ANG=-ANG
01690      RAD=MAG*COS.(ANG)
01700      RADIM=MAG*SIN.(ANG)
01710      T'H TH4, FOR M=0,1, M .G. K
01720      N=0
01730 TR1   AI=THI.(FR(M),FI(M))
01740      AR=THR.(FR(M),FI(M))
01750      ZR(M)=A*CN-(FR(M)*AR-FI(M)*AI)
01760      ZI(M)=AIM*CN-(FR(M)*AI+FI(M)*AR)
01770      DIST=.ABS.(FI(M)-(M-0.5)*3.14159)
01780      W'R DIST .G. 1.57079, DIST=1.57079
01790      CNNN=MAG*MAG*CNN/500.0
01800      W'R (ZR(M).P.2+ZI(M).P.2).L.CNNN,TRANSFER TO TR2
01810      N=N+1
01820      W'R N .G. 50, TRANSFER TO TR3
01830      DR(M)=DVR.(FR(M),FI(M))
01840      DI(M)=DVI.(FR(M),FI(M))
01850      DEN=DR(M)*DR(M)+DI(M)*DI(M)
01860      FR(M)=FR(M)-(ZR(M)*DR(M)+ZI(M)*DI(M))/DEN
01870      CGT=(ZI(M)*DR(M)-ZR(M)*DI(M))/DEN
01880      W'R .ABS.(CGT).G.0.5*DIST,CGT=0.5*CGT*DIST/.ABS.(CGT)
01890      FI(M)=FI(M)-CGT
01900      TRANSFER TO TR1
01910 TR3   CONTINUE
01920 TR2   CONTINUE
01930 TH4   CONTINUE
01940      EXECUTE VAL.
01950 TH3   CONTINUE
01960 TH1   CONTINUE
01970      V'S FORG=$(22H NO CONVERGENCE FOR M=12)$
01980      END OF PROGRAM
R 4.850+2.183

```

DRVTY

EXTERNAL FUNCTION (A,B)	00010
INTERNAL FUNCTION	00020
ENTRY TO PRELIM.	00030
C=THR.(A,B)	00040
CC=THI.(A,B)	00050
D=((A*A+B*B).P.0.5)/(CHS.(A,B).P.2)	00060
W'R .ABS.(B).G.(1000.0*.ABS.(A))	00070
ANN=1.57070	00080
OTHERWISE	00090
ANN=ATAN.(B/A)	00100
E'L	00110
W'R A.L.0.0,ANN=ANN+3.14159	00120
AN=ANN-2.0*CHA.(A,B)	00130
FUNCTION RETURN	00135
E'N	00140
E'O DVR.	00150
EXECUTE PRELIM.	00160
F=-C-D*COS.(AN)	00170
F'N F	00180
ENTRY TO DVI.	00190
EXECUTE PRELIM.	00200
F=-CC-D*SIN.(AN)	00210
F'N F	00220
ENTRY TO DVS.	00230
EXECUTE PRELIM.	00240
F=((C+D*COS.(AN)).P.2+(CC+D*SIN.(AN)).P.2).P.0.5	00250
F'N F	00260
E'O DVA.	00270
EXECUTE PRELIM.	00280
PR=-C-D*COS.(AN)	00290
PI=-CC-D*SIN.(AN)	00300
W'R .ABS.PI .G.(1000.0*.ABS.(PR))	00310
F=3.14159	00320
OTHERWISE	00330
F=ATAN.(PI/PR)	00340
E'L	00350
W'R PR .L. 0.0, F=F+3.14159	00360
F'N F	00370
E'N	00380

## COMPUTER PROGRAMS TOT AND TOTEX

TOT evaluates equation (0-20) to obtain theoretical values for the reflection coefficient when  $H_e(\omega)$  is given by a rational function.

TOTEX evaluates equation (0-20) to obtain values for the reflection coefficient when the values of magnitude and phase of  $H_e(\omega)$  are listed within the program. TOTEX determines the theoretical values for the reflection coefficient when the listed values of  $H_e$  are those which are measured experimentally.

Both TOT and TOTEX take input from the pseudo-tape disc file. TAPE.4 (see CTSS Manual, Ref. 10). These input quantities which are some of the input quantities that STABI takes from TAPE.4 (see the description of STABI for an explanation of these quantities) are H, P, RO, G, TEN, R, RADO, RADS, RADF, and K.

TOT needs the information about the rational function. This information is taken from TAPE.5 and is the same as the information STABI takes from TAPE.5 (see the description of STABI for an explanation of this information). The quantities taken from TAPE.5 are: NZR, NPR, NZC, NPC, HH, DZ, DP, ZER, ZEI, PR and PI.

Output from TOT, or TOTEX, is written on TAPE.10 for subsequent printout. Sample printouts appear in figures 7-3 and 7-6.

## COMPUTER PROGRAM REFLEC

REFLEC evaluates equation (13-7). All needed information is internal to the program. Output is written on the pseudo-tape disc file (see CTSS Manual, Ref. 10) TAPE 6 for subsequent printing. A printout from REFLEC appears in table 13-1.

TOT

```

DIMENSION ETR(100),ETI(100),HPR(100),HPI(100) MTR00010
DIMENSION S(100),ANI(100) MTR00020
DIMENSION DZ(6),DP(6),ZER(6),ZEI(6),PR(6),PI(6) MTR00030
VECTORVALUESQQ0002 = 000002 ,1, 000040 MTR00040
VECTORVALUESQQ0003 = 000002 ,1, 000040 MTR00050
VECTORVALUESQQ0004 = 000002 ,1, 000040 MTR00060
VECTORVALUESQQ0005 = 000002 ,1, 000040 MTR00070
DIMENSION ALPO(100),B1(100),CNO(100),TOR(100),TOI(100),HR(100) MTR00080
100),HI(100),ALP( 004000, QQ0002),CN( 004000, QQ0003 MTR00090
1),CB( 004000, 700004),T( 004000, QQ0005) MTR00100
PROGRAM COMMON ALPO,ALP,B1,CB,CNO,CN,TOR,TOI,T,HR,HI,RADO,MTR00110
1RADF,RADS,H,P,QL,RO,G,TEN,PI,R,ETR,ETI,HPR,HPI,K MTR00120
INTERNAL FUNCTION SINH .( QQ0006)=0.5*(EXP .( QQ0006 MTR00130
1)-EXP .( - QQ0006)) MTR00140
INTERNAL FUNCTION COSH .( QQ0007)=0.5*(EXP .( QQ0007 MTR00150
1)+EXP .(-QQ0007)) MTR00160
V'S FORK=$(F20.9)$ MTR00170
V'S FORL=$(9F8.2)$ MTR00180
V'S FORGG=$(4I3)$ MTR00190
READ BCD TAPE 5, FORGG,NZR,NPR,NZC,NPC MTR00200
READ BCD TAPE 5, FORK,HH MTR00210
READ BCD TAPE 5,FORL,DZ(1)...DZ(NZR) MTR00220
READ BCD TAPE 5, FORL,DP(1)...DP(NPR) MTR00230
READ BCD TAPE 5, FORL,ZER(1)...ZER(NZC) MTR00240
READ BCD TAPE 5,FORL,ZEI(1)...ZEI(NZC) MTR00250
READ BCD TAPE 5, FJRL,PR(1)...PR(NPC) MTR00260
READ BCD TAPE 5, FORL,PI(1)...PI(NPC) MTR00270
READ BCD TAPE 4 , QQ0008, H , P MTR00280
1, QL , RU , G , TEN , R MTR00290
READ BCD TAPE 4 , QQ0009, RADO , RADF MTR00300
1, RADS MTR00310
READ BCD TAPE 4 , QQ0010, K MTR00320
VECTOR VALUES QQ0008 = $( 7F8.4)$ MTR00330
VECTOR VALUES QQ0009 = $( 3F6.2)$ MTR00340
VECTOR VALUES 700010 = $( I2)$ MTR00350
INTERNAL FUNCTION MTR00360
ENTRY TO MA. MTR00370
AA=0.0 MTR00380
W'R HH .L. 0.0,AA=3.14159 MTR00390
SLA=.ABS.(HH) MTR00400
T'H T2, FOR JJ=1,1, JJ .G. NZR MTR00410
V'S TST=$(1H I2)$ MTR00420
SLA=SLA*FM.(-RAD,RADIM,DZ(JJ)) MTR00430
AA=AA+AGR.(-RAD,RADIM,DZ(JJ)) MTR00440
T'H T3, FOR JJ=1,1, JJ .G. NPR MTR00450
SLA=SLA/FM.(-RAD,RADIM,DP(JJ)) MTR00460
AA=AA-AGR.(-RAD,RADIM,DP(JJ)) MTR00470
T'H T4, FOR JJ=1,1, JJ .G. NZC MTR00480
SLA=SLA*F2.(-RAD,RADIM,ZEI(JJ),ZER(JJ)) MTR00490
AA=AA+AGC.(-RAD,RADIM,ZEI(JJ),ZER(JJ)) MTR00500
T'H T5, FOR JJ=1,1, JJ .G. NPC MTR00510
SLA=SLA/F2.(-RAD,RADIM,PI(JJ),PR(JJ)) MTR00520
AA=AA-AGC.(-RAD,RADIM,PI(JJ),PR(JJ)) MTR00530

```

## TOT(cont.)

```

N=AA/6.28318
W'R AA .L. 0.0, N=N-1
AA=AA-N*6.28318
FRR=SLA*COS.(AA)
FRI=SLA*SIN.(AA)
FUNCTION RETURN
END OF FUNCTION
RADIM=0.0
EXECUTE EIGVAL .( 0)
PRINT ONLINEFORMAT QQ0011
V'S QQ0011=(10H RAD,7X,3HRFR,7X,3HRFI,7X,4H=IZE,
15X,5SHANGLE,2X,8HFTR SIZE,1X,9HFTR ANGLE)$
RAD=RADO-RADS
THROUGH QQ0012 ,FOR J = 1 ,1, J .G.
1100
RAD=RAD+RADS
A=ALPO(J)
RR=SINH.(A*H)*SIN.(A*R)
RI=SINH.(A*H)*COS.(A*R)
AA=0.5*H+0.25*SINH.( 2.0*A*H)/A
AAA=P*SINH.(A*H)/A+(COSH.(A*(H-P))-COSH.(A
1*H))/(A*A)
B1(J)=AA/AAA
S=0.0
THROUGH QQ0013 ,FOR N = 1 ,1, N .G.
1K
A=ALP(J,N)
AA=0.5*H+.25*SIN .( 2.0*A*H)/A
AAA=P*SIN .( A*H)/A+(CUS .( A*H)-CUS .( A*(H-P)
1))/(A*A)
CB(J,N)=AAA/AA
S=S+CB(J,N)*B1(J)*SIN.(A*H)*EXP.(-A*R)
EXECUTE MA.
HR(J)=FRR
HI(J)=FRI
FRS=SQRT.(FRR*FRR+FRI*FRI)
FRANG=ATAN.(FRI/FRR)
W'R FRR .L. 0.0, FRANG=3.14159+FRANG
PNR=S+RR
PNI=RI
QNR=HR(J)*PNR-HI(J)*PNI+B1(J)
QNI=HR(J)*PNI+HI(J)*PNR
PDR=-RR-S
PDI=RI
DR=B1(J)-HR(J)*PDR+HI(J)*PDI
DI=-HR(J)*PDI-HI(J)*PDR
DEN=DR*DR+DI*DI
ETR(J)=(QNR*DR+QNI*DI)/DEN
ETI(J)=(QNI*DR-QNR*DI)/DEN
HPR(J)=ETR(J)
HPI(J)=ETI(J)
SIZE=(HPR(J)*HPR(J)+HPI(J)*HPI(J)) .P.0.5
ANGLE=ATAN.(HPI(J)/HPR(J))
W'R HPR(J) .L. 0.0,ANGLE =ANGLE+3.14159
N=ANGLE/6.28318

```

```

MTR00540
MTR00550
MTR00560
MTR00570
MTR00580
MTR00590
MTR00600
MTR00610
MTR00620
MTR00630
MTR00640
MTR00650
MTR00660
MTR00670
MTR00680
MTR00690
MTR00700
MTR00710
MTR00720
MTR00730
MTR00740
MTR00750
MTR00760
MTR00770
MTR00780
MTR00790
MTR00800
MTR00810
MTR00820
MTR00830
MTR00840
MTR00850
MTR00860
MTR00870
MTR00880
MTR00890
MTR00900
MTR00910
MTR00920
MTR00930
MTR00940
MTR00950
MTR00960
MTR00970
MTR00980
MTR00990
MTR01000
MTR01010
MTR01020
MTR01030
MTR01040
MTR01050
MTR01060
MTR01070
MTR01080

```

QQ0013

TOT(cont.)

	ANGLE=ANGLL-6.28318*N	MTR01090
	PIT QQ0015,RAD,HPR(J),HPI(J),SIZE,ANGLE,FRS,FRANG	MTR01100
	WHENEVER (RADF-RAD) .G.O, TRANSFER TO QQ0012	MTR01110
	TRANSFER TO QQ0016	MTR01120
	INTEGER JJ,NZR,NPR,NZC,NPC	MTR01130
QQ0012	CONTINUE	MTR01140
QQ0016	CONTINUE	MTR01150
	VIS QQ0015=\$(1H 7F10.3)\$	MTR01160
	INTEGER J , N , K	MTR01170
	E*M	MTR01180

TOTEX

```

DIMENSION C(50) MTR00005
DIMENSION ETR(100),ETI(100),HPR(100),HPI(100) MTR00010
DIMENSION S(100),ANT(100) MTR00020
DIMENSION DZ(6),DP(6),ZER(6),ZEI(6),PR(6),PI(6) MTR00030
VECTORVALUESQQ0002 = 000002 ,1, 000040 MTR00040
VECTORVALUESQQ0003 = 000002 ,1, 000040 MTR00050
VECTORVALUESQQ0004 = 000002 ,1, 000040 MTR00060
VECTORVALUESQQ0005 = 000002 ,1, 000040 MTR00070
DIMENSION ALPO(100),B1(100),CNO(100),TOR(100),TOI(100),HR(1 MTR00080
100),HI(100),ALP( 004000, QQ0002),CN( 004000, QQ0003 MTR00090
1),CB( 004000, QQ0004),T( 004000, QQ0005) MTR00100
PROGRAM COMMON ALPO,ALP,B1,CB,CNO,CN,TOR,TOI,T,HR,HI,RADO,MTR00110
1RADF,RADS,H,P,QL,RO,G,TEN,PI,R,ETR,ETI,HPR,HPI,K MTR00120
INTERNAL FUNCTION SINH .( QQ0006)=0.5*(EXP .( QQ0006 MTR00130
1)-EXP .( - QQ0006)) MTR00140
INTERNAL FUNCTION CUSH .( QQ0007)=0.5*(EXP .( QQ0007 MTR00150
1)+EXP.(-QQ0007)) MTR00160
S(1)=50.00 MTR00170
S(2)=25.00 MTR00180
S(3)=16.30 MTR00190
S(4)=12.10 MTR00200
S(5)=9.45 MTR00210
S(6)=7.60 MTR00220
S(7)=6.25 MTR00230
S(8)=5.20 MTR00240
S(9)=4.45 MTR00250
S(10)=3.80 MTR00260
S(11)=3.26 MTR00270
S(12)=3.00 MTR00271
S(13)=2.40 MTR00272
S(14)=2.10 MTR00273
S(15)=1.95 MTR00274
READ BCD TAPE 4, QQ0008,H,P MTR00280
1, QL , RO , G , TEN , R MTR00290
READ BCD TAPE 4 , QQ0009, RADO , RADF MTR00300
1, RADS MTR00310
READ BCD TAPE 4 , QQ0010, K MTR00320
VECTOR VALUES QQ0008 = $( 7F8.4)$ MTR00330
VECTOR VALUES QQ0009 = $( 3F6.2)$ MTR00340
VECTOR VALUES QQ0010 = $( 12)$ MTR00350
C(1)=0.20 MTR00360
C(2)=1.10 MTR00370
C(3)=1.59 MTR00380
C(4)=1.76 MTR00390
C(5)=1.87 MTR00400
C(6)=1.96 MTR00410
C(7)=2.03 MTR00420
C(8)=2.09 MTR00430
C(9)=2.14 MTR00440
C(10)=2.20 MTR00450
C(11)=2.23 MTR00460
C(12)=2.27 MTR00470
C(13)=2.35 MTR00480

```

TOTEX(cont.)

```

C(14)=2.39
C(15)=2.44
RADIM=0.0
EXECUTE EIGVAL .( 0)
PRINT ONLINEFORMAT QQ0011
V'S QQ0011=(10H RAD,7X,3HRFR,7X,3HRF1,7X,4H SIZE,
15X,5HANGLE,2X,8HFTR SIZE,1X,9HFTR ANGLE)
RAD=RADO-RADS
THROUGH QQ0012 ,FOR J = 1 ,1, J .G.
1100
RAD=RAD+RADS
A=ALPO(J)
RR=SINH.(A*H)*SIN.(A*R)
RI=SINH.(A*H)*COS.(A*R)
AA=0.5*H+0.25*SINH.( 2.0*A*H)/A
AAA=P*SINH.(A*H)/A+(COSH.(A*(H-P))-COSH.(A
1*H))/(A*A)
B1(J)=AA/AAA
S=0.0
THROUGH QQ0013 ,FOR N = 1 ,1, N .G.
1K
A=ALP(J,N)
AA=0.5*H+.25*SIN .( 2.0*A*H)/A
AAA=P*SIN .( A*H)/A+(COS .( A*H)-COS .( A*(H-P)
1))/A*A)
CB(J,N)=AAA/AA
S=S+CB(J,N)*B1(J)*SIN.(A*H)*EXP.(-A*R)
HR(J)=S(J)*COS.(C(J))
HI(J)=S(J)*SIN.(C(J))
FRS=SQRT.(FRR*FRR+FRI*FRI)
FRANG=ATAN.(FRI/FRR)
W'R FRR .L. 0.0, FRANG=3.14159+FRANG
PNR=S+RR
PNI=RI
QNR=HR(J)*PNR-HI(J)*PNI+B1(J)
QNI=HR(J)*PNI+HI(J)*PNR
PDR=-RR-S
PDI=RI
DR=B1(J)-HR(J)*PDR+HI(J)*PDI
DI=-HR(J)*PDI-HI(J)*PDR
DEN=DR*DR+DI*DI
ETR(J)=(QNI*DR+QNI*DI)/DEN
ETI(J)=(QNI*DR-QNR*DI)/DEN
HPR(J)=ETR(J)
HPI(J)=ETI(J)
SIZE=(HPR(J)*HPR(J)+HPI(J)*HPI(J)) .P.0.5
ANGLE=ATAN.(HPI(J)/HPR(J))
W'R HPR(J) .L. 0.0, ANGLE =ANGLE+3.14159
N=ANGLE/6.28318
ANGLE=ANGLE-3.28318*N
P'IT QQ0015,RAD,HPR(J),HPI(J),SIZE,ANGLE,FRS,FRANG
WHENEVER (RADF-RAD) .G.0, TRANSFER TO QQ0014
TRANSFER TO QQ0016
INTEGER JJ,NZR,NPR,NZC,NPC
CONTINUE

```

QQCJ13

QQ0012

MTR00490  
MTR00500  
MTR00610  
MTR00620  
MTR00630  
MTR00640  
MTR00650  
MTR00660  
MTR00670  
MTR00680  
MTR00690  
MTR00700  
MTR00710  
MTR00720  
MTR00730  
MTR00740  
MTR00750  
MTR00760  
MTR00770  
MTR00780  
MTR00790  
MTR00800  
MTR00810  
MTR00820  
MTR00830  
MTR00840  
MTR00850  
MTR00860  
MTR00880  
MTR00890  
MTR00900  
MTR00910  
MTR00920  
MTR00930  
MTR00940  
MTR00950  
MTR00960  
MTR00970  
MTR00980  
MTR00990  
MTR01000  
MTR01010  
MTR01020  
MTR01030  
MTR01040  
MTR01050  
MTR01060  
MTR01070  
MTR01080  
MTR01090  
MTR01100  
MTR01110  
MTR01120  
MTR01130  
MTR01140

TOTEX(cont.)

QQ0016 CONTINUE  
V'S QQ0015=\$(1H 7F10.3)\$  
INTEGER J , N , K  
E'M

MTR01150  
MTR01160  
MTR01170  
MTR01180

## APPENDIX G

# COMPUTER-AIDED DESIGN PROCEDURE FOR THE SYNTHESIS OF A RATIONAL SYSTEM FUNCTION WHICH APPROXIMATES PRESCRIBED FREQUENCY CHARACTERISTICS

### Introduction

When one wishes to design an electric filter whose system function is to approximate a prescribed function, it is convenient to first approximate the prescribed function by a rational function because of the connection between rational functions and linear circuits. The procedure described here utilizes both man and computing machine; the man for his intuition and ability to consider many factors simultaneously, and the computing machine for its ability to perform high speed computation.

To begin the procedure the designer examines the prescribed function and chooses a rational function to approximate it, within a multiplicative constant. He can do this conveniently by making a pole-zero plot while examining the rate of change of magnitude and phase of the prescribed function with respect to a change in frequency. Then the designer communicates the number of poles and zeros he has chosen and their positions to a computer. The procedure was developed for use on a time-sharing system so the communication was through a typewriter console in this case. Communication through punched cards could also be used, but this would result in a slower procedure. Magnitude and phase characteristics of the prescribed function must also be stored in the computer. Then the

computer program IMERG performs a relaxation scheme, moving the poles and zeros about in the complex plane in a methodical way in order to cause the rational function to be a better approximation to the prescribed function. Here the "degree of goodness" of the approximation is based on minimization of the mean square error. At various stages of the computation the mean square error is printed out so the designer knows how the scheme is progressing. Also, after the designer becomes familiar with the way the scheme proceeds, he can tell how good his initial choice of a rational function was. If he decides his choice was a poor one, he can stop the computation, if he is using a time sharing system, and makes a new initial choice.

After the process of moving the poles and zeros about is completed the new positions of the poles and zeros are printed out as well as the frequency response of the synthesized system function. Then the designer looks over the results and decides if they are satisfactory or what changes in his initial choice should be made if they are not satisfactory.

A description of the computer program IMERG follows and following this a sample synthesis is carried out. In the Compatible Time-Sharing System for which this procedure was prepared, subroutines can have two names, a filing name and a logical name. The filing name is used to access the program through console commands and the logical name is the name of the entry point of the subroutine. The logical name is used in calling sequences. The logical name of Imerg is HURAT.

## COMPUTER PROGRAM IMERG

IMERG performs a relaxation scheme for locating the poles and zeros of a rational system function which is supposed to be a good approximation to a given function. This program is in the form of a subroutine with the argument list (S,A, RO, RS, RF). The logical name is HURAT.(S,A,RO,RS,RF). S is the name of the one dimensional array of the values of the magnitude of the given function which is to be approximated. A is the name of the one dimensional array of the values of the angle of the given function which is to be approximated. The values of the radian frequency which are considered are RO, RO + RS, RO + 2RS, etc. until the value RF is exceeded. The values of S and A for  $\omega = RO$  must be in locations S(1) and A(1). Similarly, the values of S and A for  $\omega = RO + RS$  must be in locations S(2) and A(2), etc.

In addition to the information in the argument list, IMERG takes input from the pseudo tape file (see CTSS Reference Manual, Ref.10). Tape 5. The quantities in this input list (statements 1100 to 1200) are described below.

NZR = number of real zeros in the filter

NPR = number of real poles in the filter

NZC = number of conjugate pairs of complex zeros in the filter

NPC = number of conjugate pairs of complex poles in the filter

The rational function which is to approximate the given function has the form:

$$H_R(s) = H \frac{(s-a)(s-b)(s-c)\dots}{(s-d)(s-e)(s-f)\dots} \quad (G-1)$$

where:

H = multiplicative constant. The value of H given as input is entirely inconsequential.

DZ(1) ... DZ(NZR) are the positions of the real zeros on the real axis.

DP(1)... DP(NPR) are the positions of the real poles on the real axis.

The program keeps all poles on or to the left of the line in the S plane

$\text{Re}(S) = -0.1$ .

The input values of DP should all be less than -0.1 or else the program will automatically change the values to -0.1.

ZR(1) ... ZR(NZC) are the real parts of the positions of the NZC pairs of conjugate zeros.

ZI(1) ... ZI(NPC) are the imaginary parts of the positions of NZC of the complex zeros. The remaining NZC complex zeros are initially placed at locations having as imaginary parts the negative of the ZI's.

PR(1)...PR(NPC) are the real parts of the positions of the NPC pairs of conjugate poles. The preceding discussion about keeping the DP's less than -0.1 applies to the PR's also.

PI(1)...PI(NPC) are the imaginary parts of the locations of NPC of the complex poles. The remaining NPC poles are initially placed at locations having as imaginary parts the negative of the PI's.

The root mean square value of the magnitude of the given function is computed, stored (it is called SOM by the program) and divided into the elements of S in order to normalize the RMS value of the given function to unity. The normalization to unity is convenient because, for errors in angle of less than one half of a radian, the mean square error due to a unit error in angle (measured in radians) is approximately the same as the mean square error due to a unit error in magnitude of the system function.

IMERG contains an internal subprogram called MA. This subprogram determines the size and angle of the approximating rational function at the frequencies under consideration for the locations the poles and zeros have when it (MA.) is called. MA. automatically adjusts H so that the approximating rational function has an RMS value of unity, MA. also determines the mean square error of the approximating function with respect to the given function where the errors in magnitude and angle are weighted equally in the error determination. The name given to the mean square error by the program is ESI.

After normalizing the given function (statements 1230 to 1290) IMERG executes MA. to determine the initial mean square error (MSE) and stores the value of this error as BB (statements 1300 and 1310) Then H is replaced by -H and the MSE is again determined (1320 and 1330). The sign of

H is then set to the one yielding the smaller MSE (1340 to 1370).

The program will eventually try to reduce the MSE by moving the poles and zeros. The size of the movement is arbitrary and will first be  $0.9 \times SF$ . SF is initialized in statement 1380. The arbitrary value 2.0 is convenient for the range of frequencies used in this work. Typically SF should be set at about 20 percent of the center of the frequency range of interest.

IMERG next moves the poles and zeros in a methodical way to reduce the MSE. The moving is done by the two internal subprograms MOS and MOC. MOS is used to move poles and zeros in the direction of the real axis and MOC is used to move poles and zeros in the direction of the imaginary axis. The only difference in these two subprograms is that MOS tests to see if the real part of a pole is moved to a value greater than  $-0.1$  and if it is, the real part is moved to  $-0.1$ . MOS or MOC moves the pole or zero by  $.001 + SF$  along the direction appropriate to the subprogram and then returns the pole or zero to its original position. If the movement of the pole or zero reduces the MSE, the pole or zero is moved in the direction it was first moved by the amount of SF at the time of computation. If the movement increases this MSE the pole or zero is moved in the direction opposite to the direction it was first moved by the amount of SF at the time of computation. The MSE is calculated at the new position and if it is reduced from its previous value the pole or zero is left at the new position. If the MSE is increased from its previous value, the pole or zero is moved back to its original position. The statements numbered from 1420 to 1520 perform the above procedure on all poles and zeros (doing it in each of

two directions for complex poles and zeros) for 44 values of SF each value being 90 percent of the previous value. After going through its steps with each value of SF, the MSE is printed out so the filter designer knows how the scheme is progressing.

After the pole and zero moving is completed, IMERG prints out the new locations of poles and zeros, the normalized MSE and the value of H needed to get the actual, non-normalized system function. Then the real and imaginary parts, sizes and angles of the system functions are printed out. A sample output from IMERG appears in figure (G-1).

IMERG is based on a driving function of the form  $e^{-i\omega t}$ . The designer must realize this since for this driving function,  $i$  represents a phase lag, not a phase lead.

	EXTERNAL FUNCTION (S,A,RO,RS,RF)	00010
	ENTRY TO HURAT.	00020
	DIMENSION B(2000,DIM),SL(100),SLA(100),AA(100),X(20)	00030
	DIMENSION DZ(6),DP(6),ZR(6),ZI(6),PR(6),PI(6)	00040
	V*S DIM=2,I,20	00050
	INTERNAL FUNCTION (R,RC,SC)	00060
	ENTRY TO F2.	00070
	T=((RC*RC+SC*SC-R*R).P.2+4.*SC*SC*R*R).P. 0.5	00080
	FUNCTION RETURN T	00090
	ENTRY TO F1.	00100
	T=(SC*SC+(R-RC)*(R-RC)).P. 0.5	00110
	FUNCTION RETURN T	00120
	END OF FUNCTION	00130
	INTERNAL FUNCTION (R,RC,SC)	00140
	ENTRY TO AGC.	00150
	YT=RC*RC+SC*SC-R*R	00160
	W'R (.ABS.(2.*R*SC/10000.)) .G. .ABS.(YT)	00170
	T=-R*SC/(.ABS.(-R*SC))	00180
	ANG=1.57079*T	00190
	O'E	00200
	ANG=ATAN.(-2.*R*SC/(RC*RC+SC*SC-R*R))	00210
	W'R (RC*RC+SC*SC-R*R) .L. 0.0, ANG=ANG+3.14159	00220
	E'L	00230
	FUNCTION RETURN ANG	00240
	ENTRY TO AGR.	00250
	W'R .ABS.(R/10000.) .G. .ABS.(SC)	00260
	ANG=1.57079	00270
	W'R SC .E. 0.0, ANG=.ABS.(R)*ANG/R	00280
	O'E	00290
	ANG=ATAN.(R/(-SC))	00300
	E'L	00310
	W'R (-SC) .L. 0.0, ANG=ANG+3.14159	00320
	FUNCTION RETURN ANG	00330
	END OF FUNCTION	00340
	INTERNAL FUNCTION	00350
	ENTRY TO MA.	00360
	SM=0.0	00370
	ESI=0.0	00380
	R=-(RO-RS)	00390
	T'H T1, FOR I=1,1, I.G.K	00400
	R=R-RS	00410
	AA(I)=0.0	00420
	W'R H .L. 0.0, AA(I)=3.14159	00430
	SLA(I)=.ABS.(H)	00440
	T'H T2, FOR J=1,1, J.G.NZR	00450
T2	SLA(I)=SLA(I)*FM.(R+0.,DZ(J))	00460
	AA(I)=AA(I)+AGR.(R+0.,DZ(J))	00470
	T'H T3, FOR J=1,1, J .G. NPR	00480
	SLA(I)=SLA(I)/FM.(R+0.,DP(J))	00490
T3	AA(I)=AA(I)-AGR.(R+0.,DP(J))	00500
	T'H T4, FOR J=1,1, J.G.NZC	00510
	SLA(I)=SLA(I)*F2.(R,ZI(J),ZR(J))	00520
T4	AA(I)=AA(I)+AGC.(R,ZI(J),ZR(J))	00530

	TH I5, FOR J=1,1, J .G. NPC	00490
	SLA(I)=SLA(I)/F2.(R,PI(J),PR(J))	00500
I5	AA(I)=AA(I)-AGC.(R,PI(J),PR(J))	00510
	N=AA(I)/6.28318	00520
	W'R AA(I) .L. 0.0, N=N-1	00530
	AA(I)=AA(I)-N*6.28318	00540
T1	SM=SM+SLA(I).P.2	00550
	SM=(SM/K).P. 0.5	00560
	TH TH3, FOR I=1,1, I .G. K	00570
	SLA(I)=SLA(I)/SM	00580
	EA=.ABS.(A(I)-AA(I))	00590
	W'R EA .G. 3.14159,EA=6.28318-EA	00600
	ES=S(I)-SLA(I)	00610
TH3	ESI=ESI+EA*EA+ES*ES	00620
	ESI=ESI/(2.0*K)	00630
	H=H/SM	00640
	FUNCTION RETURN	00650
	END OF FUNCTION	00660
	INTERNAL FNCTION (D,M,NE)	00670
	INTEGER M,NE,IL	00680
	ENTRY TO MOS.	00690
	D(M)=D(M)+0.001*SF	00700
	EXECUTE MA.	00710
	D(M)=D(M)-(.001*SF	00720
	W'R ESI .G. BB,SF=-SF	00730
	SF=SF*0.999	00740
	D(M)=D(M)+SF	00750
	W'R ((D(M).G.-.1).AND.((NE.E.2).OR.(NE.E.4)))	00760
	AQ=D(M)-SF	00770
	D(M)=-0.1	00780
	EXECUTE MA.	00790
	W'R ESI .G. BB	00800
	D(M)=AQ	00810
	EXECUTE MA.	00820
	BB=ESI	00830
	E'L	00840
	FUNCTION RETURN	00850
	E'L	00860
	EXECUTE MA.	00870
	W'R ESI .G. BB	00880
	D(M)=D(M)-SF	00890
	EXECUTE MA.	00900
	E'L	00910
	BB=ESI	00920
	FUNCTION RETURN	00930
	ENTRY TO MOC.	00940
	D(M)=D(M)+0.001*SF	00950
	EXECUTE MA.	00960
	W'R ESI .G. BB, SF=-SF	00970
	SF=SF*0.999	00980
	D(M)=D(M)+SF	00990
	EXECUTE MA.	01000
	W'R ESI .G. BB	01010
	D(M)=D(M)-SF	01020
	EXECUTE MA.	01030

	E* L	01040
	BB=ESI	01050
	FUNCTION RETURN	01060
	END OF FUNCTION	01070
	INTEGER NZR,NPR,NZC,NPC,NZ2,NP2,KK,IL,NE,M,N,MM	01080
	INTEGER I,J,K,L,LL	01090
	READ BCD TAPE 5, FORG,NZR,NPR,NZC,NPC	01100
	V'S FORG=\$(4I3)\$	01110
	READ BCD TAPE 5, FORA,H	01120
	READ BCD TAPE 5, FORB,DZ(1)...DZ(NZR)	01130
	READ BCD TAPE 5, FORB,DP(1)...DP(NPR)	01140
	READ BCD TAPE 5, FORB,ZR(1)...ZR(NZC)	01150
	READ BCD TAPE 5, FORB,ZI(1)...ZI(NZC)	01160
	READ BCD TAPE 5, FORB,PR(1)...PR(NPC)	01170
	READ BCD TAPE 5, FORB,PI(1)...PI(NPC)	01180
	V'S FORA=\$(F20.9)\$	01190
	V'S FORB=\$(9F8.2)\$	01200
	K=(RF-RO)/RS+1	01210
	V'S FORZ=\$(1H F 11.5)\$	01220
	SOM=0.0	01230
TH1	T*H TH1, FOR I=1,1, I.G.K	01240
	SOM=SOM+S(I)*S(I)	01250
	SOM=(SOM/K).P.0.5	01260
	H=H/SOM	01270
TH2	T*H TH2, FOR I=1,1, I.G. K	01280
	S(I)=S(I)/SOM	01290
	EXECUTE MA.	01300
	BB=ESI	01310
	H=-H	01320
	EXECUTE MA.	01330
	W'R ESI .G. BB	01340
	H=-H	01350
	EXECUTE MA.	01360
	E* L	01370
	SF=2.0	01380
	T*H T10, FOR LL=1,1,LL.G.44	01390
	SF=0.9*SF	01400
	P*T FORZ,ESI	01410
	BB=ESI	01420
T7	T*H T7, FOR L=1,1, L .G. NZR	01430
	EXECUTE MOS.(DZ,L,1)	01440
T8	T*H T8, FOR L=1,1, L .G. NPR	01450
	EXECUTE MOS.(DP,L,2)	01460
	T*H T9, FOR L=1,1, L.G. NZC	01470
	EXECUTE MOC.(ZI,L,3)	01480
T9	EXECUTE MOS.(ZR,L,3)	01490
	T*H T10, FOR L=1,1, L .G. NPC	01500
	EXECUTE MOC.(PI,L,4)	01510
T10	EXECUTE MOS.(PR,L,4)	01520
	H=H*SOM	01530
	P*T FORR	01540
	PRINT RESULTS H	01550
	PRINT FORMAT FORR	01560
	PRINT COMMENTS\$ REAL ZEROS\$	01570
	PRINT RESULTS DZ(1)...DZ(NZR)	01580

PRINT FORMAT FORR	01590
PRINT COMMENT \$ REAL POLES\$	01600
PRINT RESULTS DP(1)...DP(NPR)	01610
PRINT FORMAT FORR	01620
PRINT COMMENT \$ COMPLEX ZEROS\$	01630
PRINT COMMENT \$ REAL PART\$	01635
PRINT RESULTS ZR(1)...ZR(NZC)	01640
PRINT FORMAT FORR	01650
PRINT COMMENT \$ IMAGINARY PARTS	01655
PRINT RESULTS ZI(1)...ZI(NZC)	01660
PRINT FORMAT FORR	01670
PRINT COMMENT \$ COMPLEX POLES\$	01680
PRINT COMMENT \$ REAL PART\$	01685
PRINT RESULTS PR(1)...PR(NPC)	01690
PRINT FORMAT FORR	01700
PRINT COMMENT \$ IMAGINARY PARTS	01705
PRINT RESULTS PI(1)...PI(NPC)	01710
PRINT FORMAT FORR	01720
PRINT FORMAT FORI,ESI	01730
PRINT FORMAT FORR	01740
PRINT COMMENT \$ FILTER FREQUENCY RESPONSE\$	01750
PRINT FORMAT FORD	01760
V'S FORI=\$(18H NORMALIZED ERROR=F8.5)\$	01770
V'S FORD=\$(1H ,4X,3HRAD,7X,3HHPR,7X,3HHPI,	01780
16X,4HSIZE,6X,5HANGLE)\$	01790
T'H TH14,FORI=1,1, I.G.K	01800
R=RO+RS*(I-1)	01810
SLA(I)=SLA(I)*SOM	01820
HPR=SLA(I)*COS.(AA(I))	01830
HPI=SLA(I)*SIN.(AA(I))	01840
PRINT FORMAT FORE,R,HPR,HPI,SLA(I),AA(I)	01850
V'S FORE=\$(1H 5F10.4)\$	01860
V'S FORR=\$(1H)\$	01870
END OF FUNCTION	01880
	01890

TH14

12

### Sample Synthesis

Assume that the prescribed function which is to be approximated by rational function is given by table F-1.

<u>Radian Frequency</u>	<u>Magnitude</u>	<u>Angle</u>
3	50.9	0.24
4	49.7	0.25
5	48.3	0.28
6	46.6	0.31
7	44.7	0.36
8	42.7	0.42
9	40.6	0.48
10	38.5	0.57
11	36.4	0.67
12	34.6	0.78
13	33.2	0.91

The computer program MASTER, which follows, is the controlling program for the design process. Since this process is to be carried out from a typewriter console it is as easy to make the prescribed function a part of MASTER as it is to read it as data.

PROGRAM MASTER

DIMENSION M(20),A(20)	00010
INTEGER K	00020
RADO=3.0	00030
RADF=13.0	00040
RADS=1.0	00050
M(1)=50.9	00060
A(1)=0.24	00070
M(2)=49.7	00080
A(2)=0.25	00090
M(3)=48.3	00100
A(3)=0.28	00110
M(4)=46.6	00120
A(4)=0.31	00130
M(5)=44.7	00140
A(5)=0.36	00150
M(6)=42.7	00160
A(6)=0.42	00170
M(7)=40.6	00180
A(7)=0.48	00190
M(8)=38.5	00200
A(8)=0.57	00210
M(9)=36.4	00220
A(9)=0.67	00230
M(10)=34.6	00240
A(10)=0.78	00250
M(11)=33.2	00260
A(11)=0.91	00270
PRINT COMMENT \$      PRESCRIBED FUNCTIONS	00280
P:T FORA	00290
V:S FORA=\$(8H      RAD,6X,9HMAGNITUDE,2X,5HANGLE)\$	00300
T:H THA, FOR K=1,1, K .G. 11	00310
RAD=RADO+(K-1)*RACS	00320
P:T FORB, RAD,M(K),A(K)	00330
V:S FORB=\$(1H 3F10.3)\$	00340
EXECUTE HURAT.(M,A,RADO,RADS,RADF)	00350
END OF PROGRAM	00360

1HA

Examination of the prescribed function shows that its magnitude diminishes with increasing frequency and its phase lags with increasing frequency (remember that the assumed driving function is  $e^{-i\omega t}$ ). Therefore a reasonable initial choice for the filter is a single pole which is located a distance on the negative real axis of the S-plane from the origin about equal to the magnitude of the center frequency range. In this case the initial choice for the pole position is -10.0. The filter data is written on the pseudo-tape file .TAPE. 5. The program MASTER with the Subroutine IMERG is then executed. The printout appears in figure G-1.



H = 695.730072

REAL ZEROS  
- DUMMY VARIABLE BLOCK

.000000E 00    -.000000E 00

REAL POLES  
- DUMMY VARIABLE BLOCK

-1.412309E 01

COMPLEX ZEROS  
REAL PART  
- DUMMY VARIABLE BLOCK

0                    0

IMAGINARY PART  
- DUMMY VARIABLE BLOCK

0                    0

COMPLEX POLES  
REAL PART  
- DUMMY VARIABLE BLOCK

.000000E 00    -.000000E 00

IMAGINARY PART  
- DUMMY VARIABLE BLOCK

.000000E 00    -.000000E 00

NORMALIZED ERROR= .00459

FILTER FREQUENCY RESPONSE

RAD	HPR	HPI	SIZE	ANGLE
3.0000	47.1351	10.0123	48.1868	.2093
4.0000	45.6038	12.9161	47.3975	.2760
5.0000	43.7752	15.4978	46.4376	.3403
6.0000	41.7302	17.7285	45.3399	.4017
7.0000	39.5468	19.6011	44.1378	.4602
8.0000	37.2952	21.1258	42.8630	.5154
9.0000	35.0346	22.3259	41.5436	.5674
10.0000	32.8117	23.2327	40.2041	.6161
11.0000	30.6616	23.8813	38.8645	.6617
12.0000	28.6083	24.3077	37.5406	.7043
13.0000	26.6672	24.5466	36.2447	.7440

EXIT CALLED. PM MAY BE TAKEN.  
R 11.333+5.200

FIGURE G-1 (cont.)

As a better approximation, a filter with a pair of conjugate zeros will be synthesized. The filter probably needs more poles than zeros so it will be given three real zeros. More poles than zeros is a good design process to avoid high frequency noise. Figure G-2 shows the result of this choice. The mean square error of the chosen filter is 0.00209 which means that it was a very good choice to begin with. IMERG reduces the mean square error to 0.00086 (on a function normalized to unity).

```

input .tape. 5
W 1339.4
00010 0 3 1 0
00020 5.0
00030 0.0
00040 -50.00 -100.00 -175.00
00050 05.00
00060 20.00
00070 00.00
00080 00.00
00090
M file .tape. 5
W 1340.6
R 1.366+3.100

```

```

loadgo master imerg
W 1340.8
EXECUTION.

```

PRESCRIBED FUNCTION		
RAD	MAGNITUDE	ANGLE
3.000	50.900	.240
4.000	49.700	.250
5.000	48.300	.280
6.000	46.600	.310
7.000	44.700	.360
8.000	42.700	.420
9.000	40.600	.480
10.000	38.500	.570
11.000	36.400	.670
12.000	34.600	.780
13.000	33.200	.910
.00209		
.00144		
.00140		
.00139	.00088	
.00139	.00087	
.00139	.00087	
.00139	.00087	
.00139	.00087	
.00139	.00087	
.00115	.00087	
.00100	.00087	
.00097	.00087	
.00095	.00087	
.00094	.00086	
.00094	.00086	
.00093	.00086	
.00093	.00086	
.00093	.00086	
.00093	.00086	
.00093	.00086	
.00092	.00086	
.00091	.00086	
.00090	.00086	
.00090	.00086	
.00089		
.00089		
.00089		
.00088		
.00088		

FIGURE G -2 Filter with one pair of conjugate zeros and three real poles.

(continued)

H = 1.337010E 05

REAL ZEROS  
- DUMMY VARIABLE BLOCK  
    .000000E 00   -.000000E 00

REAL POLES  
- DUMMY VARIABLE BLOCK  
    -5.351484E 01   -1.052622E 02   -1.842701E 02

COMPLEX ZEROS  
  REAL PART  
- DUMMY VARIABLE BLOCK  
    4.059374E 00

  IMAGINARY PART  
- DUMMY VARIABLE BLOCK  
    1.957211E 01

COMPLEX POLES  
  REAL PART  
- DUMMY VARIABLE BLOCK  
    .000000E 00   -.000000E 00

  IMAGINARY PART  
- DUMMY VARIABLE BLOCK  
    .000000E 00   -.000000E 00

NORMALIZED ERROR= .00086

FILTER FREQUENCY RESPONSE

RAD	HPR	HPI	SIZE	ANGLE
3.0000	49.6288	8.1648	50.2959	.1631
4.0000	48.2170	10.7196	49.3942	.2188
5.0000	46.4213	13.1335	48.2434	.2757
6.0000	44.2558	15.3736	46.8500	.3343
7.0000	41.7376	17.4088	45.2227	.3952
8.0000	38.8864	19.2098	43.3724	.4588
9.0000	35.7242	20.7492	41.3128	.5262
10.0000	32.2752	22.0022	39.0613	.5983
11.0000	28.5656	22.9461	36.6404	.6767
12.0000	24.6231	23.5611	34.0796	.7634
13.0000	20.4766	23.8299	31.4190	.8609

EXIT CALLED. PM MAY BE TAKEN.  
R 37.883+6.233

FIGURE G-2 (cont.)